ISSN 1007-9327 (print)
ISSN 2219-2840 (online)

World Journal of *Gastroenterology*

World J Gastroenterol 2020 January 14; 26(2): 109-265

Published by Baishideng Publishing Group Inc

World Journal of Gastroenterology

Contents

Weekly Volume 26 Number 2 January 14, 2020

REVIEW

ORIGINAL ARTICLE

Basic Study

Retrospective Cohort Study

Observational Study

SYSTEMATIC REVIEW

META-ANALYSIS

Contents

World Journal of Gastroenterology

Volume 26 Number 2 January 14, 2020

NAME OF JOURNAL

World Journal of Gastroenterology

ISSN

ISSN 1007-9327 (print) ISSN 2219-2840 (online)

LAUNCH DATE

October 1, 1995

FREQUENCY

Weekly

EDITORS-IN-CHIEF

Subrata Ghosh, Andrzej S Tarnawski

EDITORIAL BOARD MEMBERS

http://www.wjgnet.com/1007-9327/editorialboard.htm

EDITORIAL OFFICE

Ze-Mao Gong, Director

PUBLICATION DATE

January 14, 2020

INSTRUCTIONS TO AUTHORS

https://www.wjgnet.com/bpg/gerinfo/204

GUIDELINES FOR ETHICS DOCUMENTS

https://www.wjgnet.com/bpg/GerInfo/287

GUIDELINES FOR NON-NATIVE SPEAKERS OF ENGLISH

https://www.wjgnet.com/bpg/gerinfo/240

PUBLICATION MISCONDUCT

https://www.wjgnet.com/bpg/gerinfo/208

ARTICLE PROCESSING CHARGE

https://www.wjgnet.com/bpg/gerinfo/242

STEPS FOR SUBMITTING MANUSCRIPTS

https://www.wjgnet.com/bpg/GerInfo/239

ONLINE SUBMISSION

https://www.f6publishing.com

World Journal of Gastroenterology

Submit a Manuscript: https://www.f6publishing.com

World J Gastroenterol 2020 January 14; 26(2): 109-133

DOI: 10.3748/wjg.v26.i2.109

ISSN 1007-9327 (print) ISSN 2219-2840 (online)

REVIEW

Inflammation and fibrosis in chronic liver diseases including non-alcoholic fatty liver disease and hepatitis C

Sudeep Tanwar, Freya Rhodes, Ankur Srivastava, Paul M Trembling, William M Rosenberg

ORCID number: Sudeep Tanwar (0000-0002-4203-7771); Freya Rhodes (0000-0002-6884-6235); Ankur Srivastava (0000-0002-3963-265X); Paul M Trembling (0000-0002-5016-4607); William M Rosenberg (0000-0002-2732-2304).

Author contributions: All authors equally contributed to this paper with conception, literature review, analysis, drafting, critical revision, editing and approval of the final version.

Conflict-of-interest statement: Authors declare no conflict of interests for this article.

Manuscript source: Invited manuscript

Received: September 26, 2019
Peer-review started: September 26, 2019
First decision: November 4, 2019
Revised: December 17, 2019
Accepted: January 1, 2020

Sudeep Tanwar, Freya Rhodes, Ankur Srivastava, Paul M Trembling, William M Rosenberg, UCL Institute for Liver and Digestive Health, Division of Medicine, University College London, Royal Free Campus, Hampstead, London NW3 2PF United Kingdom

Sudeep Tanwar, Department of Gastroenterology, Whipps Cross University Hospital, Barts Health NHS Trust, Leytonstone, London E11 1NR, United Kingdom

Corresponding author: Sudeep Tanwar, MBBS, MRCP(UK), FRCP, FEBGH, PhD, Consultant Gastroenterologist and Hepatologist, Department of Gastroenterology, Whipps Cross University Hospital, Barts Health NHS Trust, Leytonstone, London E11 1NR, United Kingdom. sudeep.tanwar@nhs.net

Abstract

At present chronic liver disease (CLD), the third commonest cause of premature death in the United Kingdom is detected late, when interventions are ineffective, resulting in considerable morbidity and mortality. Injury to the liver, the largest solid organ in the body, leads to a cascade of inflammatory events. Chronic inflammation leads to the activation of hepatic stellate cells that undergo trans-differentiation to become myofibroblasts, the main extra-cellular matrix producing cells in the liver; over time increased extra-cellular matrix production results in the formation of liver fibrosis. Although fibrogenesis may be viewed as having evolved as a "wound healing" process that preserves tissue integrity, sustained chronic fibrosis can become pathogenic culminating in CLD, cirrhosis and its associated complications. As the reference standard for detecting liver fibrosis, liver biopsy, is invasive and has an associated morbidity, the diagnostic assessment of CLD by non-invasive testing is attractive. Accordingly, in this review the mechanisms by which liver inflammation and fibrosis develop in chronic liver diseases are explored to identify appropriate and meaningful diagnostic targets for clinical practice. Due to differing disease prevalence and treatment efficacy, disease specific diagnostic targets are required to optimally manage individual CLDs such as non-alcoholic fatty liver disease and chronic hepatitis C infection. To facilitate this, a review of the pathogenesis of both conditions is also conducted. Finally, the evidence for hepatic fibrosis regression and the mechanisms by which this occurs are discussed, including the current use of antifibrotic therapy.

Key words: Liver inflammation; Fibrosis; Cirrhosis; Non-alcoholic fatty liver disease; Chronic hepatitis C; Chronic liver disease; Anti-fibrotic; Biomarker

Article in press: January 1, 2020
Published online: January 14, 2020

P-Reviewer: Su CC, Tarantino G
S-Editor: Ma L
L-Editor: A
E-Editor: Zhang YL

Core tip: Only by having a comprehensive understanding of the pathophysiology of chronic liver disease can appropriate and meaningful diagnostic targets for research studies be identified. For clinicians who are not engaged in laboratory research this also requires a revision of basic anatomy, physiology and immunology. In this review article we have attempted to go "back to basics" to enable liver specific pathophysiology to be contextualised thereby allowing clinicians who are not engaged in laboratory practice to engage in translational research.

Citation: Tanwar S, Rhodes F, Srivastava A, Trembling PM, Rosenberg WM. Inflammation and fibrosis in chronic liver diseases including non-alcoholic fatty liver disease and hepatitis C. *World J Gastroenterol* 2020; 26(2): 109-133
URL: https://www.wjgnet.com/1007-9327/full/v26/i2/109.htm
DOI: https://dx.doi.org/10.3748/wjg.v26.i2.109

STRUCTURE AND FUNCTION OF THE LIVER

The liver is the largest solid organ in the body and has a median weight of 1.6 kg and 1.4 kg in adult males and females respectively[1]. The liver receives 75% of its blood supply *via* the portal vein and 25% *via* the hepatic arterial system. The portal vein carries blood from the entire capillary system of the digestive tract, spleen, pancreas and gallbladder. The hepatic artery is the second major branch of the celiac axis. The venous drainage of the liver is *via* the hepatic veins which open into the superior vena cava (Figure 1). The liver can be divided into eight functional segments or "lobules" based upon blood supply and biliary drainage. Hepatic lobules are comprised of a central hepatic vein and peripheral portal tracts that contain the final tributaries of the bile ducts (bile ductule), portal vein (portal venule) and hepatic vein (hepatic venule). Blood is drained from the portal tracts to the central vein by specialised capillaries known as the hepatic sinusoids[2].

The sinusoids are lined by a fenestrated endothelial layer containing numerous microvilli[2]. This structural organisation facilitates exchange of solutes between the portal tracts and the hepatocytes through the space of Disse. Endothelial cells, Kupffer cells and hepatic stellate cells (HSC) lie in juxtaposition with the hepatic sinusoid (Figures 2 and 3). Kupffer cells are the resident macrophages of the liver and their major functions include the clearance of particles, immune complexes, senescent red blood cells and endotoxins. In addition, Kupffer cells have a role in the innate immune response and produce pro-inflammatory cytokines including interleukin 1 and 6, tumour necrosis factor-α (TNF-α) and interferons. HSCs are distributed throughout the liver and form the main perisinusoidal cell type with a diverse range of functions.

HEPATIC EXTRACELLULAR MATRIX

The extracellular matrix (ECM) is the array of macromolecules that forms the liver "scaffolding"[3]. In the normal liver, ECM contributes to approximately 0.5% of the total weight of the liver, comprising less than 3% of the area on cross sectional imaging[3]. Normal ECM is composed of collagens (types I, III, IV, V, VI, XIV and XVIII), elastin, structural glycoproteins (laminin, fibronectin, nidogen/enactin, tenascin, osteopontin, various acidic proteins), proteoglycans (heparan sulfate, syndecan, biglycan and decorin), and hyaluronic acid (a glycosaminoglycan)[4]. All 3 of the cell types (hepatocytes, endothelial cells, HSC) that surround the space of Disse produce matrix components.

FUNCTION OF THE LIVER

The liver has a number functions which in broad terms can be defined as "the regulation of the concentrations of solutes in the blood that affect the function of other organs"[1]. Through the uptake, metabolism and secretion of solutes, the liver

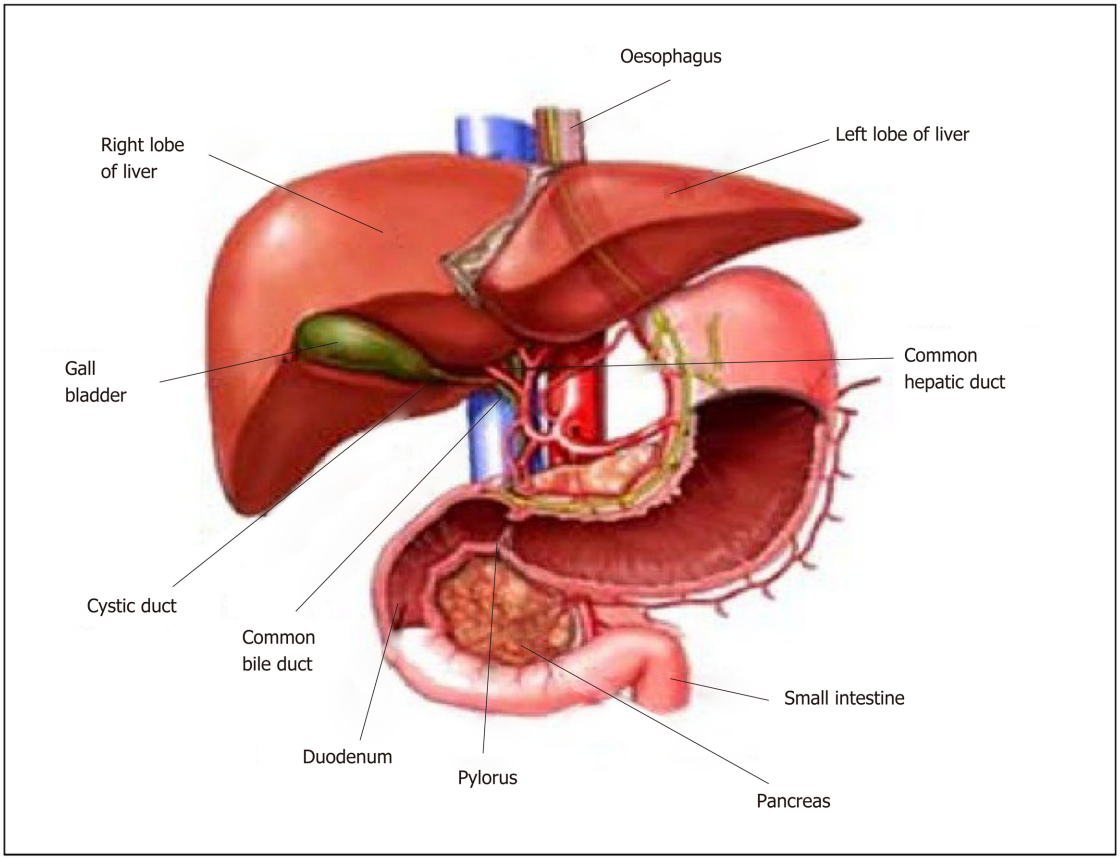

Figure 1 Anatomy of the liver and its macroscopic relationship to the intestinal tract and vasculature. Reproduced with permission of Creative Commons Attribution License from Ebaid *et al*[164].

performs an integral role in the metabolism of amino acids (for example transamination), carbohydrates (for example gluconeogenesis), lipids (for example lipid production), haemoglobin, bile salts, iron, copper, vitamins, ammonia and drugs. The liver is the major synthetic organ producing albumin, serum binding proteins (for example haptoglobin) and clotting factors. Furthermore, the liver is an important immunological site with functions such as cytokine signalling, antigen surveillance and immune tolerance.

HEPATIC INFLAMMATION IN RESPONSE TO CHRONIC INJURY

Whereas immune responses in CLD may contribute to the restoration of tissue function they may also lead to tissue injury. An overactive or exaggerated immune response, for example in non-alcoholic steatohepatitis (NASH) or chronic hepatitis C (CHC), can result in organ dysfunction by the replacement of hepatic parenchyma by scar tissue and by vascular architectural distortion. These immune responses are the subject of active investigation to not only extend understanding of the pathology of liver injury but to also identify diagnostic and therapeutic targets.

INNATE IMMUNE RESPONSE

Pattern recognition receptors (PRRs) are an essential part of the innate immune system that facilitate the detection of pathogens. The liver is enriched with both parenchymal liver cells and non-parenchymal liver cells that express PRRs. Hepatocytes express PRRs and are the main liver parenchymal cells. Non-parenchymal cells that express PRRs include liver sinusoidal endothelial cells (LSEC), HSC and bone marrow derived immune cells (Kupffer cells, and dendritic cells)[5]. PRR can be divided into 4 classes: Toll-like receptors (TLR), Nucleotide oligomerisation receptors (NLR), C-like lectin receptors and RIG-1 like receptors. PRR

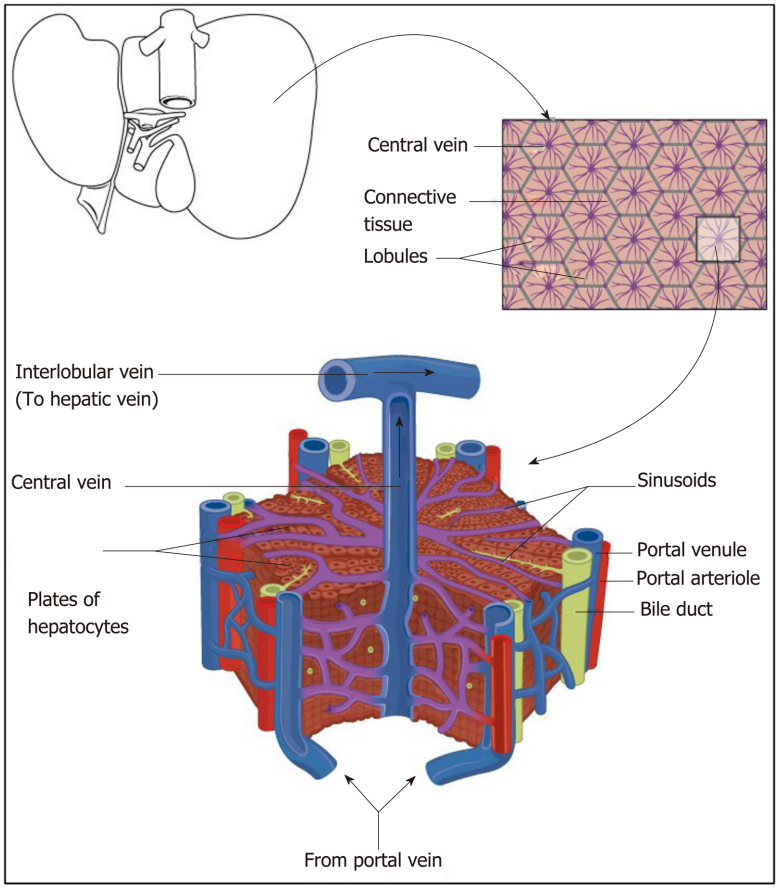

Figure 2 Schematic diagram representing the relationship of the macroscopic structure of the liver with the functional hepatic lobule with hepatic venules (blue), hepatic arteriole (red), bile ductules (yellow).
Reproduced with permission of Creative Commons Attribution License from Anatomy & Physiology textbook[165].

recognise conserved molecular structures called pathogen-associated molecular patterns that are pathogen specific. Of the 4 types of PRR, TLRs are the key sensor of the innate immune system for the recognition of pathogens[6] including viruses[7]. For example, TLR-3 is able to recognise viral dsRNA leading to the production of type 1 Interferons (IFN α or β)[8]. Three main pathways are activated by TLRs: Mitogen activated protein kinase pathway (ERK, p38 and JNK), nuclear factor κB pathway and interferon regulatory transcription factor pathway. Pro-inflammatory and anti-inflammatory cytokines can be induced following TLR stimulation. Inflammation is characterized by both the activation of innate immune cells and the production of pro-inflammatory cytokines such as IL-1α, IL-1β, and TNFα.

INNATE IMMUNE CELL RECRUITMENT TO SITES OF HEPATIC INFLAMMATION

Neutrophils (also known as neutrophilic granulocytes or polymorphonuclear leukocytes) infiltrate the site of injury within minutes in response to the injury itself following the release of damage-associated molecular patterns (DAMPS)[9] from damaged cells. Neutrophil recruitment peaks within hours[10]. Neutrophils are key effectors of the innate immune system with high phagocytic potential and possess a vast number of antimicrobial molecules. In addition to clearing pathogens, neutrophils may also exacerbate macrophage cytotoxicity and help promote a chronic inflammatory state[11].

Monocyte infiltration following tissue injury peaks between 24-48 h[12]. Recruited monocytes demonstrate a variety of functions including production of inflammatory mediators, clearance of neutrophils, ECM production and angiogenesis. In humans, 3 types of monocyte subsets have been identified: Classic ($CD14^{++}CD16^{-}$), intermediate ($CD14^{++}CD16^{+}$), and non-classic ($CD14^{++}CD16^{++}$)[13]. Furthermore, as derived from murine studies, monocytes can also be categorised into inflammatory ($CCR2^{hi}$,

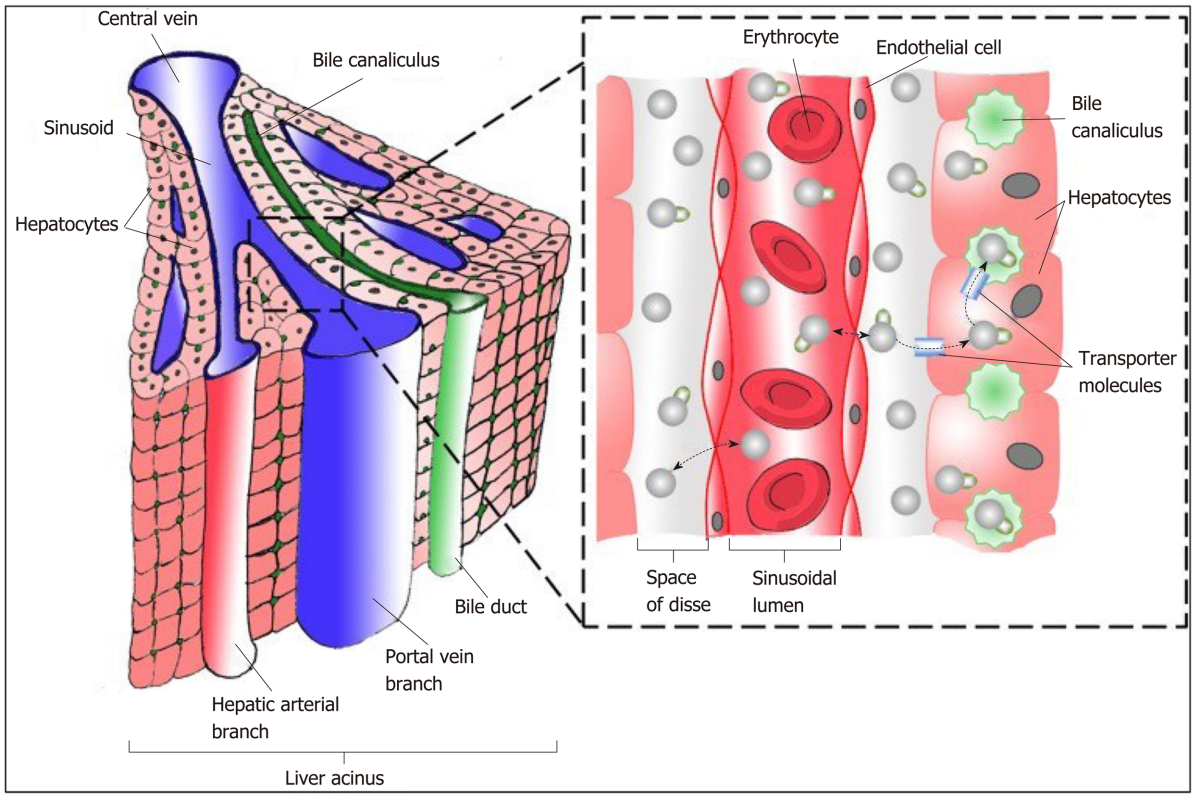

Figure 3 Schematic diagram representing functional hepatic acinus with hepatic venules (blue), hepatic arteriole (red), bile ductules (green) together with the relationship to the Space of Disse and the sinusoidal lumen. Reproduced with permission of Creative Commons Attribution License from Chouhan *et al*[166].

CX_3CR1^{lo}) and anti-inflammatory (CX_3CR1^{hi}, $CCR2^{lo}$) subtypes. Pro-inflammatory monocytes produce inflammatory cytokines and chemokines, produce proteases and facilitate clearance. Anti-inflammatory monocytes produce anti-inflammatory cytokines (IL-10), transforming growth factor-β (TGF-β), and vascular endothelial growth factor (VEGF) that promote resolution and restitution[14].

Kupffer cells are the resident macrophages of the liver[15]. In addition to detecting tissue injury, Kupffer cells can recruit inflammatory cells, promote tissue repair and remodelling. In addition, new populations of macrophages can be recruited following acute inflammation (emergency repopulation). Macrophages may be pro-inflammatory (classic M1 type) or anti-inflammatory (alternative M2 type) and their relative balance contributes to either injury or repair[16].

Platelets are metabolically and synthetically active cells that can produce many inflammatory cytokines and chemokines thus attracting neutrophils to sites of inflammation[17].

Natural killer T cells and natural killer (NK) cells (granular lymphocytes) can be thought of as being part of the innate immune system as they can kill target cells without priming[18]. NK cells can contribute to HSC clearance in a TNF-related apoptosis inducing ligand dependent manner[19].

ADAPTIVE IMMUNE RESPONSE TO HEPATIC INJURY

Both T (thymus) and B (bone marrow derived) lymphocytes mediate the adaptive immune response. Whereas T cells are involved in cell-mediated immunity, B cells are primarily responsible for humoral immunity. Regardless, the function of both T and B cells is to recognise "non self" antigens by generating specific responses to eliminate specific pathogens or cells expressing "non self" antigens[20].

T helper (CD4+) cells can activate other immune cells (including B cells), switch antibody classes, activate cytotoxic (CD8+) T cells and enhance macrophage phagocytosis. In response to cytokine stimulation, T helper cells can either assume a proinflammatory phenotype (Th1) or an anti-inflammatory phenotype (Th2). Th1 T cells secrete the inflammatory cytokines interferon-γ and TGF-β. Th2 T cells are characterised by the secretion of IL-4, IL-5 and IL-10. Proinflammatory M1 macrophages are induced by the release of interferon-γ by Th1 T cells.

In addition to Th1 and Th2 cells, Il-17 producing T helper cells (Th17) and regulatory T cells (Tregs) also function as effector T cells that are heavily involved in inflammation[21] and the development of liver fibrosis[22]. After activation Th17 cells secrete IL-17A, IL-17F, IL-21, IL-22, and TNFα, which promote tissue inflammation by induction of other proinflammatory cytokines and recruitment of leukocytes[23]. Treg cells are a unique subset of T-helper cells that control effector T-cell responses to prevent autoimmune reactions. Activated Treg suppress the development of functional immune reactions by the production of anti-inflammatory cytokines including IL-10 and TGFβ[24]. The transcription factors Foxp3, STAT5 and CD25 are expressed on the surface of Treg cells[25].

B cells secrete antibodies which provides humoral immunity within the adaptive immune system. In addition, B cells secrete cytokines and function as antigen presenting cells. All B cells express B cell receptors on their cell membrane. B cell receptors allow B cells to bind specific antigens which is followed by the production of antibodies. When naïve or memory B cells are activated by antigen, they proliferate and differentiate into effector B cells with the formation of large plasma cell representing the end stage of their maturation pathway.

CELL DEATH AND ONGOING INFLAMMATORY RESPONSE

Cell death can be categorised in several ways including non-inflammatory cell death (apoptosis) and inflammatory cell death (necrosis, pyroptosis and necroptosis). Regardless, the nature of the accompanying immune response is dependent on the signals liberated from dead cells. Apoptosis fails to generate an immune response as apoptotic cells retain membrane integrity. In addition, apoptotic cells also release factors that inhibit the recruitment and activation of neutrophils. By contrast, membrane integrity is disrupted during necrosis which results in the release of DAMPS[9]. Broadly, DAMPS are molecules that can activate inflammation. Necrosis also produces inflammatory signals by modifying extracellular matrix components including hyaluronic acid[26]. Moreover, necrosis can also result from programmed cell death pathways: Pyroptosis and necroptosis. Pyroptosis is initiated by inflammasome mediated activation of capsase-1 which results in lytic cell death and the production of the interleukins (IL) IL-1β and IL-18[27]. Necroptosis is activated by the presentation of "external death signals" to cells such as TNF, interferon receptor and selected TLR pathways[28]. Following activation by these signals, necroptosis involves inhibition of caspase-8 (promotes apoptosis), mixed-lineage kinase domain-like protein and RIP kinase family members 1 and RIP kinase family members 3.

INFLAMMASOME

Inflammasomes are an intracellular multiprotein scaffolding that are expressed in both parenchymal and non-parenchymal cells of the liver. Functionally, inflammasomes are both sensors and receptors of the innate immune system that can induce inflammation in response to pathogens and molecules derived from host proteins (DAMPs). In response to these "cellular danger signals" inflammasomes activate caspase-1 and release both IL-1β and IL-18[29].

PATHOPHYSIOLOGY OF LIVER FIBROSIS

Whereas the development of liver fibrosis itself is often a prerequisite for the morbidity associated with CLD it is important to highlight that fibrogenesis is also a part of the normal wound healing process in response to noxious stimuli.

Liver fibrosis is a structural change defined by an accumulation of ECM proteins such as collagen often triggered by chronic, sustained inflammation. The pattern of fibrosis deposition is dependent on the aetiology of liver injury. Pericellular and perisinusoidal fibrosis deposition in the centrilobular areas are characteristic of fibrosis related to NASH and alcohol related liver disease. By contrast, periportal fibrosis deposition is characteristic of autoimmune and viral liver diseases.

Regardless, it is important to recognise that maintenance of the liver matrix is a dynamic process in which deposition and resorption of matrix are balanced. In a steady physiologic state, both ongoing ECM deposition and removal are equal resulting in an unchanged amount of ECM[30]. At a cellular level, the HSC is recognised to be the most important cell lineage in the development of liver fibrosis. In its quiescent or resting state, the HSC is a lipid storing cell representing the body's

major location of Vitamin A. However, on activation the HSC undergoes transformation to become a myofibroblast capable of regulating matrix deposition and resorption whilst also possessing contractile properties. In addition to those derived from HSC, profibrogenic myofibroblasts can also be derived from portal fibroblasts, recruited bone marrow cells and epithelial cells (for example hepatocytes and cholangiocytes) that have undergone epithelial to mesenchymal transition[31]. HSC reside in the space of Disse and are the resident non-paranchymal cell type. Their embryonic origin is likely to be mesenchymal given that they produce α-smooth muscle actin when activated in addition to vimentin and desmin[32]. HSC themselves represent approximately 10% of the total liver cell number and 1.5% of the total liver cell volume[33]. The location of HSC within the space of Disse allows for direct (within 140μm) contact of the HSC with their other cell types including hepatocytes, endothelial cells and Kupfer cells[33] thus facilitating the intercellular transport of soluble mediators and cytokines. In addition to this intimate location within the space of Disse, intercellular communication between HSC and the neighbouring cells are also facilitated by their prominent dendritic cytoplasmic processes. Their contractility may contribute to the regulation of portal pressure[34]. When quiescent, the HSC serve as a reservoir for retinol (a precursor for vitamin A) and other lipid soluble compounds. Indeed, the presence of Vitamin A esters in cytoplasmic perinuclear lipid droplets is the characteristic microscopic feature of quiescent HSC. HSCs represent resting profibrogenic myofibroblasts which are a major constituent of the extracellular matrix in both the healthy and diseased liver. The phenotypic transformation of HSCs into profibrogenic myofibroblasts is associated with the acquisition of α-smooth muscle reactivity. The activation of HSC is comprised of 2 stages: Initiation and perpetuation.

HSC ACTIVATION

In response to liver injury, lipid peroxides and apoptotic bodies that accumulate in damaged hepatocytes initiate HSC activation in a process mediated by Fas and TNF-related apoptosis inducing ligand[35]. This activation process is initiated by profibrogenic cytokines (for example TGF-β), fibronectin, platelet derived growth factor (PDGF), reactive oxygen species (ROS) and apoptotic bodies derived from neighbouring cells, immune cells and platelets (Figures 4 and 5)[30]. Thereafter, HSC undergo characteristic phenotypic changes and resemble myofibroblasts[31].

HSC PERPETUATION

Following on from activation, the activated HSC enters the phase of perpetuation in which ECM is accumulated resulting in scar tissue formation (Figures 4 and 5). Tissue hypoxia, apoptosis and cell matrix interactions maintain ongoing HSC activation. HSC perpetuation is comprised of number of functional responses including proliferation, fibrogenesis, chemotaxis, contractility, matrix degradation, retinoid loss and cytokine expression.

Proliferation

HSC proliferate rapidly and gain a profibrogenic phenotype; this occurs primarily in response to both an increase in PDGF and PDGF responsivity[36,37]. Other mediators involved in HSC proliferation include TNFα, VEGF, thrombin and epidermal growth factor (EGF)[30].

Fibrogenesis

An accumulation of ECM (particularly collagen type I) occurs follows on from increased synthesis by activated myofibroblasts and decreased degradation. TGF-β1 is the main driver for ECM production by activated HSCs. Connective tissue growth factor (CTGF) also acts as a profibrogenic cytokine towards HSC.

Chemotaxis

HSCs migrate towards chemokines allowing cells to organise within regions of injury. Examples of chemokines toward which HSCs migrate to include PDGF, VEGF, Ang-1, TGF-β1, EGF, b-FGF, CCL2, CXR3 and CXR4[38]. In addition, tissue hypoxia enhances HSC migration with ROS activating extracellular signal-regulated kinase 1/2 (ERK) and JNK1/2 pathways.

Contraction

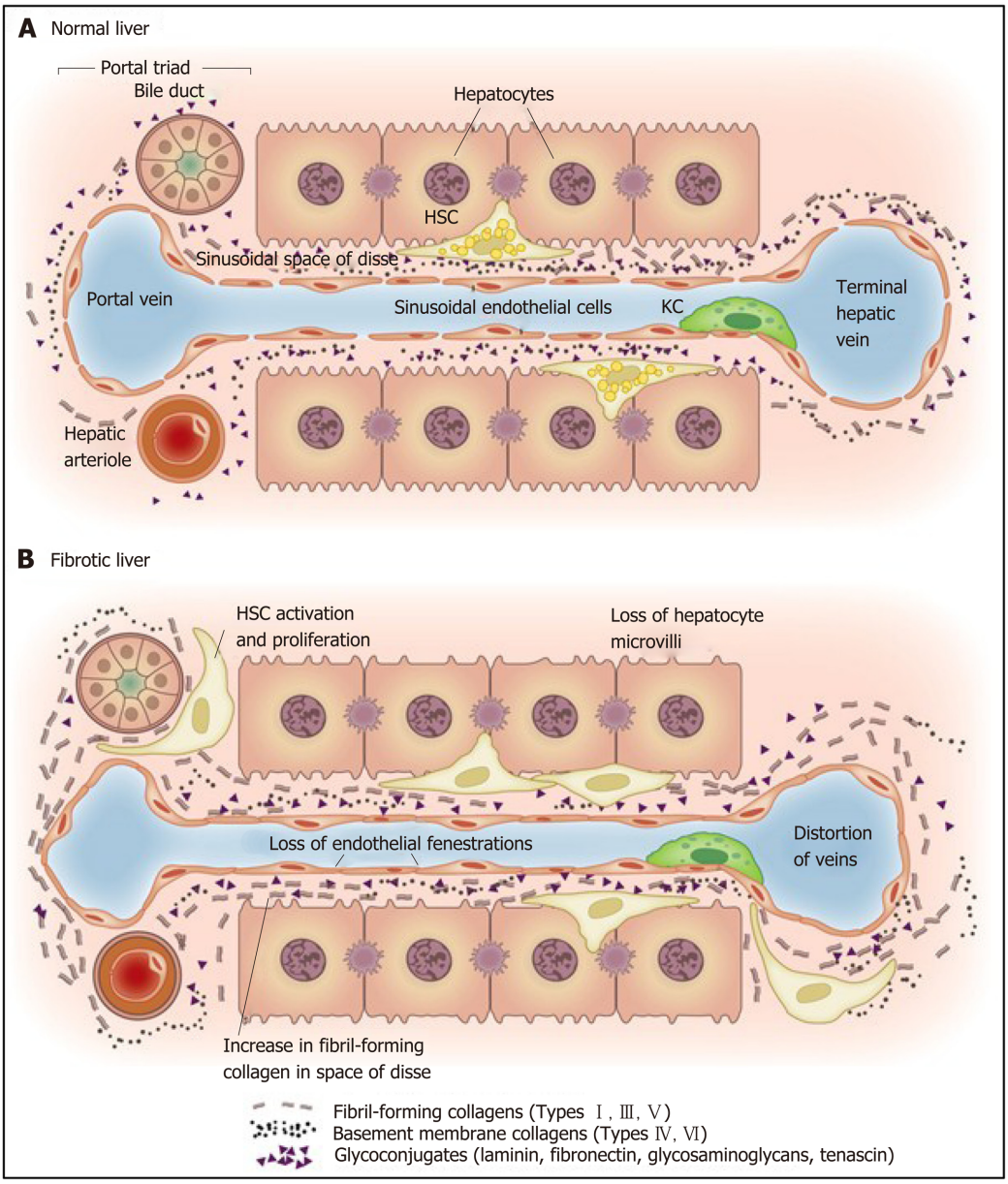

Figure 4 Matrix and cellular alteration in hepatic fibrosis. Normal liver parenchyma contains epithelial cells (hepatocytes) and nonparenchymal cells: fenestrated sinusoidal endothelium, hepatic stellate cells, and Kupffer cells. A: After injury, the stellate cells become activated and secrete large amounts of extracellular matrix (ECM); B: Deposition of ECM in the space of Disse leads to the loss of both endothelial fenestrations and hepatocyte microvilli. Reproduced with permission from Hernandez-Gea and Friedman[37]. HSC: Hepatic stellate cells; KC: Kupffer cells.

Hepatic sinusoidal remodelling occurs following HSC activation which is mediated by collagen matrix deposition, loss of fenestration and an increase in the number of contractile HSCs[39]. These events contribute in an increase in sinusoidal resistance; in the context of advanced fibrosis this can contribute to portal hypertension. Other factors that stimulate HSC contraction include nitrous oxide deficiency, ET-1, angiotensinogen II, eicosanoids, atrial naturetic peptide and somatostatin.

Retinoid loss

HSC activation is characterised by the loss of perinuclear retinoid droplets[40]. As described earlier HSC are the largest reserve of retinoids in the body and conversion of retinol into retinyl ester is a characteristic feature of HSC activation.

Matrix degradation

Matrix metalloproteinases (MMPs) are the are the main enzymes responsible for ECM degradation; the MMP activity is in turn regulated by tissue inhibitors of metalloproteinases (TIMPs). Both MMPs and TIMPs are produced by several liver cell populations including Kupffer cells, myofibroblasts and hepatocytes[41]. However, TIMPs are predominantly expressed by activated HSCs. The A Disintegrin and

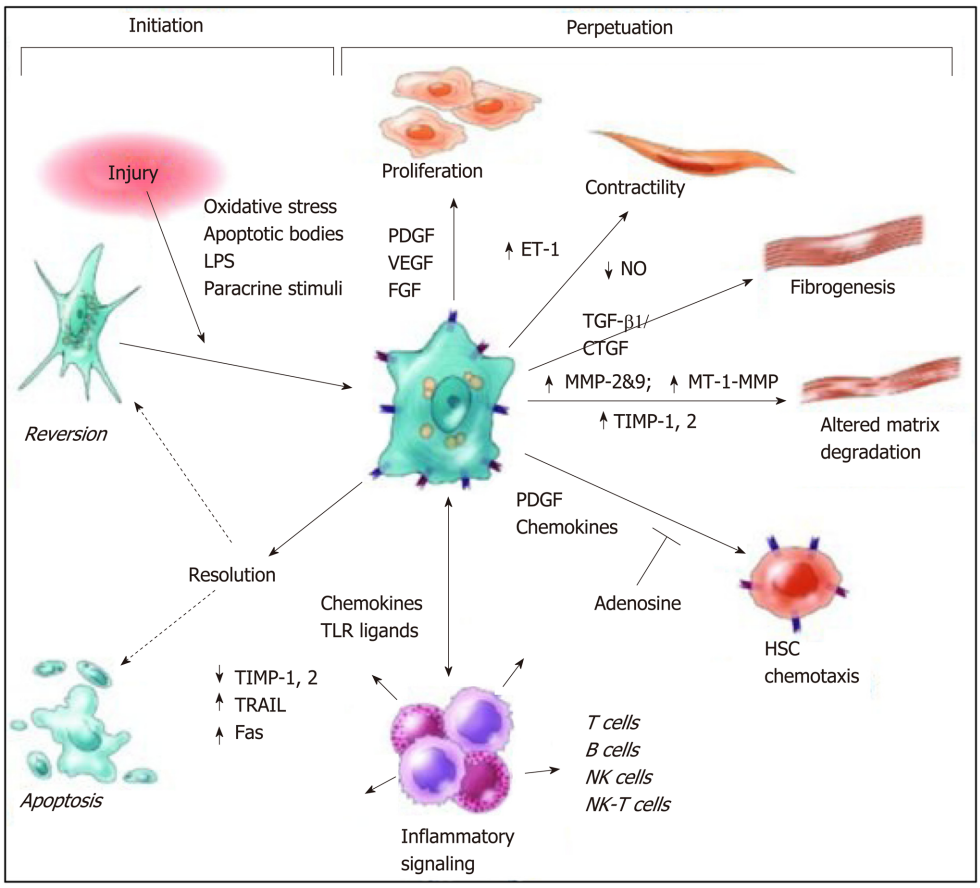

Figure 5 Pathways of hepatic stellate cell activation including those contributing to initiation and perpetuation. Initiation is provoked by soluble stimuli that include oxidant stress signals, apoptotic bodies, lipopolysaccharide, and cytokine stimuli from neighbouring cells. Perpetuation is characterised by specific phenotypic changes including proliferation, contractility, fibrogenesis, altered matrix degradation, chemotaxis, and cytokine signalling. Reproduced with permission from Friedman[30]. CTGF: Connective tissue growth factor; ET: Endothelin; FGF: Fibroblast growth factor; LPS: Lipopolysaccharide; MMP: Matrix metalloproteinase; MT-1: membrane type-1, NK: Natural killer, NO: Nitrous oxide; PDGF: Platelet derived growth factor; TIMP: Tissue inhibitor of metalloproteases; TGF: Transforming growth factor; TLR: Toll like receptor; TRAIL: Tumour necrosis factor-related apoptosis-inducing ligand; VEGF: Vascular endothelial growth factor.

Metallopoteinase-domain proteins form another stimulus for stellate cell collagen production *via* TGF-β activation[42].

Cytokine expression

HSCs express a vast array of chemokines that have been identified to recruit neutrophils, macrophages, NK/Natural killer T cells, dendritic cells and T cells. As a result, HSCs play an important role in immune cell infiltration.

PROGRESSION OF FIBROSIS IN CHRONIC LIVER DISEASES TO CIRRHOSIS

Cirrhosis can be defined as "the histological development of regenerative nodules surrounded by fibrous bands in response to chronic liver injury that leads to portal hypertension and end stage liver disease"[43]. Cirrhosis is a consequence of long standing excessive fibrogenesis resulting in encapsulation and/or replacement of injured liver parenchyma by a collagenous scar. Histologically, cirrhosis is characterized by fibrotic septa that link portal tracts with each other and central vein. This produces liver parenchyma that is composed of hepatocyte islands that are surrounded by fibrotic septa and devoid of a central vein. These changes result in an increase in intravascular resistance within the portal venous system and decreased hepatic perfusion. In addition, the development of cirrhosis confers a significant increase in the risk of developing hepatocellular carcinoma (incidence up to 30% over a 5 year period)[43]. Progression of fibrosis to cirrhosis is variable and is dependent on the cause of liver disease, environmental and host factors[43]. Cirrhosis is frequently asymptomatic and unsuspected until complications of liver disease present with include variceal bleeding, ascites, spontaneous bacterial peritonitis, encephalopathy

and death.

EXPLORING THE PATHOGENESIS OF INFLAMMATION AND FIBROSIS IN NAFLD

The pathogenesis of NASH is complex involving hepatic parenchymal and non-parenchymal cells together with immune cells. With regard to pathogenesis, a "two hit" hypothesis was first proposed in 1998[44]; this has subsequently been modified into "three hit"[45] and "multiple hit" hypotheses[46]. In the original "two hit" hypothesis, the development of insulin resistance results in excessive lipid accumulation within hepatocytes (the first hit). The first hit is followed by lipotoxic metabolite-induced mitochondrial dysfunction, oxidative stress and endoplasmic reticular (ER) stress which leads to hepatocyte death (the second hit). Under normal physiological circumstances, existing hepatocyte replication results in the replacement of dead hepatocytes. In NASH however, it is believed that progenitor cell replication is enhanced as hepatocyte replication is impaired. Although progenitor cell proliferation results in the replacement of dead hepatocytes it also results in hepatic stellate cell activation and fibrogenesis (the third hit). The "multiple hit" hypothesis describes further additional insults derived from other sites such as the GI tract (such as gut-derived endotoxins due to impaired gut permeability and stasis) and adipose tissue (adipokines). Moreover, the "multiple hit" hypothesis allows one to understand that the development of NASH is the result of a complex interplay between factors such as the genetic variation in immune balance and the influence of additional aetiologies such as alcohol consumption and obesity. Whereas several pathways (including direct lipotoxicity, inflammasome activation, toll-like receptor signalling, hedgehog signalling) have all been implicated in the pathogenesis of cellular inflammation in NASH, the final pathway appears to be the development of a profibrotic state.

EPIGENETIC AND GENETIC REGULATION IN NASH

Recent genome-wide association studies have identified several genes that confer an increased risk of NASH amongst individuals with NAFLD[47]. These include patatin-like phospholipase domain containing 3 (PNPLA3), transmembrane 6 superfamily member 2 (TM6SF2), farnesyl diphosphate farnesyl transferase 1 (FDFT1), EF-hand calcium binding domain 4B and glucokinase receptor. Of these identified genes, the most widely studied is the PNPLA3 gene located on chromosome 22. *PNPLA3* gene encodes a 481 amino acid protein that mediates triacylglycerol hydrolysis. In studies of Huh7 hepatoma cell line cells, *PNPLA3* variant p.I148M (rs738409 substitution of cytosine to guanine) was associated with reduced enzymatic activity of emulsified triglycerides following hydrolysis. Within clinical studies, the *PNPLA3* variant p.I148M has also been found to be associated with a high risk of NASH in adult[48], paediatric[49] and also lean patients[50].

In addition, genome-wide association studies have identified that epigenetics (a reversible phenomenon affecting gene expression) also appears to contribute to the pathogenesis of NASH. A study of rat liver tissues and high fat emulsion induced fatty liver identified that the expression of genes involved in apoptosis, biosynthesis and inflammation increase in NASH[51]. By contrast, these studies have revealed down-regulation of expression of genes involved in DNA damage response signal transduction, cholesterol biosynthesis and carbohydrate metabolism.

LIPOTOXIC HEPATOCYTE INJURY

The accumulation of excess free fatty acids (FFA) in hepatocytes results in the generation of toxic lipid metabolites. This process, lipotoxicity, is thought to be fundamental in the development of NASH. Following exposure to these toxic metabolites, injured hepatocytes appear enlarged and swollen in a process termed ballooning. In addition to steatosis and lobular inflammation, the presence of ballooning is an essential diagnostic criterion for the presence of histologic NASH[52].

The source of excess FFA is multifactorial and excess dietary intake is certainly a contributing factor. In addition, an increase in intrahepatic FFA can occur because of *de novo* lipogenesis, adipose lipolysis and impaired FFA oxidation. Under normal circumstances, hepatocytes store FFA as triglycerides and it is postulated that the conversion of FFA into triglycerides may be protective against lipotoxicity[53].

However, in the context of FFA excess, the conversion to tryglycerides becomes saturated and alternative highly toxic lipid metabolites are formed: Ceramides, diacylglycerols and lysophosphatidylcholine and oxidised cholesterol metabolites[54]. These toxic metabolites cause liver injury through the overproduction of ROS.

Two major mechanisms of oxidative stress in NASH have been identified. The first, direct cell injury, occurs when there is an imbalance between pro-oxidants and antioxidants. The second, indirect cell injury, occurs when damaging cellular pathways are activated such as those involving NF-κB. Increased production of ROS induces activation of NF-κB which regulates the production of pro-inflammatory cytokines such as interleukin-1β (IL-1β), TNFα and interleukin-6 (IL-6).

ER stress is activated by FFA induced oxidative stress and appears to be an important mechanism in the development of NASH[55]. Prolonged and severe ER stress can lead to cell death. Studies have identified that ER stress markers are elevated in NASH[56], and that ER stress can activate inflammatory pathways such as Jun-(N)-terminal Kinase (JNK) and NF-κB[57].

INFLAMMATORY AND IMMUNE MEDIATORS IN NAFLD

Analogous to other liver diseases, a variety of inflammatory and immunologic mechanisms contribute to NASH and NAFLD progression. These include innate immunity (neutrophils, macrophages, NK cells and NK T cells), adaptive immunity (T and B cells), inflammasome activation and the gut-liver axis[58].

GUT MICROBIOTA AND MACROPHAGES IN THE PATHOGENESIS OF NASH

As described above, the liver is exposed to low level endotoxaemia and antigenaemia *via* the portal vein. Thereafter, Kupffer cells are the principle cell type responsible for antigen and endotoxin clearance thus maintaining immune tolerance and homeostasis. This balance can, however, be impaired in the context of changes to gut flora, gut permeability and Kupffer cell responsivity. Studies have identified evidence for gut dysbiosis as a potential factor in the aetiology of NAFLD. Lower levels of *Bateriodetes* together with higher levels of *Prevotella* and *Porphoyromonas* have been identified in patients with NAFLD as compared to healthy controls[59]. Moreover, in mouse models, hepatic steatosis and inflammation driven by inflammasome mediated dysbiosis were associated with enhanced hepatic TNF-α expression[60]. In another study examining differences in gut microbiota between patients health subjects, obese patients and those with NASH, marked differences were identified in the composition of gut flora in either obese (without NASH) or obese (with NASH) patients as compared with healthy subjects[61]. Whereas the gut composition of patients with obese and NASH patients were more similar, there were significant differences in the concentrations of *Proteobacteria*, *Enterobacteriaceae*, and *Escherichia* species. Interestingly, whilst similar blood-ethanol concentrations were observed between healthy subjects and obese non-NASH patients, obese NASH patients exhibited significantly elevated blood ethanol levels. It was therefore hypothesised that elevated ethanol blood levels in patients with NASH may be the result of alcohol producing gut bacteria.

Macrophages may be proinflammatory (classic M1 type) or anti-inflammatory (alternative M2 type) and their relative balance contributes to either injury or repair[16]. In both mouse models and human subjects, an increase in M2 Kupffer cells was found to promote M1 Kupffer cell apoptosis which in turn was found to inhibit progression of NAFLD[62]. Toll-like receptor activation (particularly TLR4) is associated with macrophage mediated inflammation in NASH[63] and is associated with the release of IL-1β, TNFα and IL-6[64]. Studies have identified that both TLR4 inhibition and macrophage depletion reduces NAFLD progression in both animal and human liver biopsy studies[65,66]. In addition, liver macrophages transform into "foam cells" in NASH by internalising oxidised low-density lipoprotein (ox-LDL) resulting in storage of cholesterol and cholesterol crystals in enlarged lysosomes[67]. Studies in mice have revealed that inhibition of ox-LDL recognition and ox-LDL uptake into foam cells is associated with reduced hepatic histologic progression[68].

NEUTROPHILS IN THE PATHOGENESIS OF NASH

A number have studies have identified a possible role of neutrophils in the progression of NAFLD and NASH. Neutrophil infiltration is a common histologic finding in patients with NASH with neutrophils frequently surrounded steatotic hepatocytes, resembling the crown-like structures found in obese adipose tissue[69]. Moreover, patients with NASH and also advanced fibrosis related to NASH have been found to have a higher neutrophil-to-lymphocyte ratio than patients without either NASH or advanced fibrosis[70]. Human neutrophil peptides are proteins produced by neutrophils that induce cytokine and chemokine production under inflammatory conditions. Mouse studies have identified that human neutrophil peptides can enhance hepatic fibrosis in fatty liver by inducing hepatic stellate cell proliferation[71]. In addition, the deletion of elastase (a protease secreted by neutrophils) in high fat diet induced obese mice was found to improve hepatic histologic inflammation with reduced of neutrophil and macrophage infiltration[72].

T AND B LYMPHOCYTES IN THE PATHOGENESIS OF NASH

Recent studies have confirmed that the innate immune system appears to play an important role in the pathogenesis of NASH. Analysis of liver histology obtained from patients with NASH has identified that the inflammatory infiltrate in NASH is heavily enriched with both lymphocytes and macrophages[73]. Moreover, the inflammatory infiltrate at the portal tracts is composed predominantly of CD8+ lymphocytes[74]. Regulatory T cells play a critical role in regulating inflammatory processes in NASH. Th17 T cells functionally oppose regulatory T cells and produce IL-17. Elevated levels of IL-17 have been identified in patients with obesity[75]. In mouse studies, the neutralisation of IL-17 was found to reduce the severity of NASH, implicating IL-17 as a mediator of NASH and identifying this as a potential therapeutic target[76,77].

More recently, B cells have emerged as additional protagonists in the development of NASH[78]. Studies have identified that NASH is associated with the presence of circulating antibodies targeting neoantigens formed from the interaction between lipid peroxidation products and cellular proteins[79]. These IgG antibodies against malondialdehyde-derived products may be present in up to 60% of patients with NASH[80]. Furthermore, raised anti-malondialdehyde IgG titres have been identified in patients with severe histologic NASH and advanced fibrosis[38]. In both serum and adipose tissue, B cell levels have been found to increase markedly in mice fed a high fat diet[81]. Interestingly, whilst B cell deficient mice display exhibit reduced insulin resistance, the transfer of B cells or specific IgG (isolated from wild type mice fed a high fat diet) is able to induce insulin resistance.

IL-17 has also been identified as an important mediator in the development of atherosclerosis in NAFLD[82]. In a 2014 study, the severity of atherosclerosis was assessed in patients with ultrasound evidence of NAFLD and normal liver function tests using carotid intima-media thickness. Multiple regression identified that a raised intima-media thickness was predicted both by the IL-17-related chemokine eotaxin, intima-media thickness and the amount of visceral fat. These results support the hypothesis that visceral adipose tissue releases IL-17 which in turn induces smooth muscle eotaxin secretion in atherosclerotic lesions.

INTERFERON ALPHA AND GAMMA IN THE PATHOGENESIS OF NAFLD

The association between intramuscular triglycerides–as assessed by ultrasonography of skeletal muscles - and interferons in NAFLD was explored in a recent study[83]. As compared to healthy subjects, patients with NAFLD were found to have higher levels of interferon alpha 2 and lower levels of interferon gamma. Moreover, the severity of intramuscular triglyceride was found to be inversely proportional to interferon alpha 2 levels whereas interferon gamma levels were not associated with intramuscular triglycerides severity. These results suggest the interplay between these cytokines may be instrumental in the development of NAFLD.

INFLAMMASOME ACTIVATION IN THE PATHOGENESIS OF NASH

Several studies have identified that inflammasome activation contributes to the development of NASH and fibrosis in NAFLD. In both mouse and human studies, both pro-IL-1β and pro-IL-18 have been found to be markedly increased in NASH[84,85]. In addition, mice deficient of either NLRP3, IL1-α or IL-1β have been found to be from both from diet induced hepatic inflammation and fibrosis[85,86]. In a further mouse study, inhibition of caspase-1 was also able to prevent the development of diet induced NASH and fibrosis[87].

HSC ACTIVATION IN THE PATHOGENESIS OF NASH

Prior to the development of NASH, HSC are hypothesised to be in a quiescent state. Thereafter, the development of both lipotoxicity and steatohepatitis is followed by HSC activation which results in ongoing fibrogenesis. Hitherto, ongoing studies have attempted to elucidate the mechanism for HSC activation in NASH: Studies of human hepatocytes have identified that lipid metabolite accumulation increases TGF-β and impairs adiponectin-mediated induction of activin A[88].

The Notch single-pass transmembrane receptor signalling pathway has been implicated in HSC activation. In a recent study, Notch pathway components were found to be upregulated in TGF-β activated HSC and in fibrotic livers with inhibition of Notch signalling decreasing HSC activation[89].

The stress-activated protein kinases, c-Jun N-terminal kinase (JNK) and p38 have been identified to have distinct and opposed roles in rat HSC[90]. Whereas JNK was identified to promote HSC proliferation, P38 was identified to inhibit HSC proliferation.

Hedgehog pathway activation (sonic hedgehog) has been identified to corollate with the severity of histologic injury and fibrosis in human NAFLD biopsy samples[91].

EXPLORING THE PATHOGENESIS OF INFLAMMATION AND FIBROSIS IN CHC

HCV structure and replication

HCV is an enveloped, single stranded RNA molecule that is approximately 9600 nucleotides in length and encodes a polyprotein of approximately 3000 amino acids[92]. During HCV replication, the HCV polyprotein is cleaved by proteolytic enzymes into four structural and six non-structural proteins (Figure 6)[93]. New viral particles are assembled by the four structural proteins whilst the six non-structural proteins support viral replication. The post-translational processing of the non-structural proteins from the polypeptide is catalysed by the NS3 serine protease and cofactor NS4A. NS3/NS4A together complete the post translational processing of the NS proteins at the NS3/NS4A, NS4A/NS4B, NS4B/NS5A and NS5A/NS5B junctions[94]. These non-structural replicative products are then released and form a complex responsible for forming viral RNA.

The lack of a proof-reading capacity in the HCV RNA polymerase contributes to the extensive genetic variation within HCV isolates. Six major genotypes of HCV are recognised with numerous sub-types. Within an infected individual an HCV may exist as multiple quasi-species or minor genetic variants within a sub-type. The geographic distribution of HCV genotypes varies at an epidemiological level so that specific genotypes and sub-types are more common in certain countries.

Fifty five to 85% of individuals who develop acute HCV infection will develop CHC which is associated with progressive liver fibrosis and cirrhosis, portal hypertension, liver failure and hepatocellular carcinoma[95].

The primary goal of HCV treatment is to cure infection: Successfully treated patients may attain a sustain virologic response (SVR) which is considered tantamount to a "virological cure" (defined as the absence of HCV RNA 12-24 wk after the discontinuation of antiviral therapy). The attainment of SVR is typically associated with normalisation of liver function tests and either significant improvement or resolution of hepatic necroinflammation. In addition, this may also be associated with stabilisation or regression of liver fibrosis.

More recently, direct-acting antiviral (DAA) agents for the treatment of HCV have been developed that specifically target HCV viral replication. The development of DAA therapies is a consequence of the development of in-vitro HCV replication

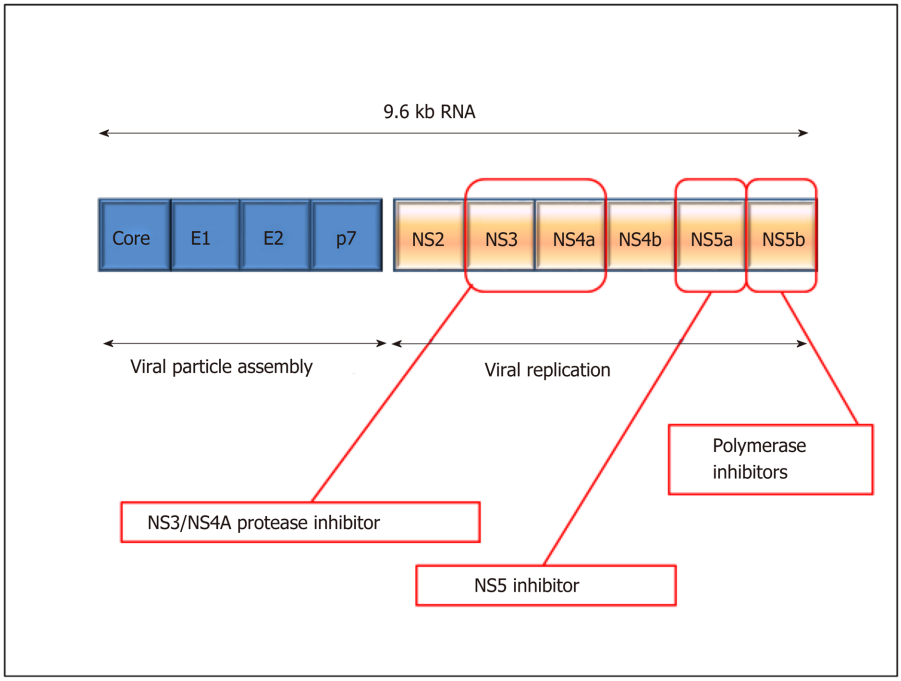

Figure 6 Depiction of hepatitis C virus genome structure and drug targets. NS: Non-structural.

models[96] including the HCV replicon system. DAA agents were discovered by screening for their ability to inhibit viral replication[97]. In addition, the replicon systems were used to select and characterise resistant mutations to specific DAAs and also assess replication fitness[98].

The introduction of DAA agents has led to HCV therapy in treatment regimens that are highly efficacious (SVR 95-100%), well tolerated and abbreviated even in difficult to treat populations such as those with advanced liver disease[99].

Despite these remarkable advances in the treatment of established infection, a vaccine for HCV is still in its infancy. Regardless, it is likely that both prophylactic and therapeutic vaccines will be developed over the next decade through a greater understanding of host immunological factors, cell culture systems and animal models.

TLRs and HCV

As described earlier, TLRs are an important component of virus-mediated innate immune responses; this has also been confirmed in HCV. TLR-3 has been found to mediate antiviral responses against HCV in hepatoma cells[100]. In addition to inducing the production of type I interferons, TLR-3 activation also induces type III interferon (IFN-λ/IL-28) production[101]. A recent study also identified that a pro-fibrogenic HSC phenotype is mediated by TLR-2 signalling pathway following HCV core and NS3 protein exposure[102].

Direct activation of fibrogenesis by HCV

The interaction between HSCs and HCV is now well established. Hepatocytes infected with HCV have been found to release several pro-fibrotic factors including TGF-β that modify the expression of several profibrogenic genes in HSCs[103]. HSC have also been identified to engulf apoptotic bodies derived from HCV infection-induced hepatocyte apoptosis; this process has been found to elicit a profibrogenic response[104]. There is also evidence that HSC and HCV directly communicate with each other[105,106]; there is evidence that this may be mediated through both the core and non-structural proteins directly. Studies have identified that the core protein can active pro-mitogenic intracellular pathways with HSC with the NS3 and NS5 proteins stimulating pro-inflammatory pathways *via* NF-κB and c-JNK[106]. In addition, the E2 structural protein has also been identified as profibrotic with MMP-2 activation occurring after binding to CD81 of HSC[105]. In HCV replicon models studies using rat and human HSCs, HCV replication has been followed by the activation of TGFβ1 and other profibrotic cytokines[103,107].

Indirect activation of fibrogenesis by HCV

Analogous to other liver diseases, the ongoing immune response to HCV infection results in ongoing fibrogenesis *via* the activation of HSC. The mediators involved in

the activation and proliferation of HSC include PDGF, TGFα, VEGF and activation of EGF receptor. Thereafter, several factors promote ECM production *via* TGF-β1 (stimulating collagen production *via* Smad signalling). Importantly, connective tissue growth factor (CTGF) and leptin also activate fibrogenesis *via* TGFβ1 signalling. Leptin also acts by suppressing proliferator-activated receptor γ (PPARγ). As described earlier, NF-κB signalling promotes a variety of chemotactic and mitogenic HSC effects.

REVERSIBILITY OF LIVER FIBROSIS

Fibrosis regression in CHC

Hitherto, treatment for chronic liver disease has been primarily aetiology specific in which the causative agent or factor has been eliminated or modified. The treatment of CHC is an excellent example of this in which successful antiviral therapy results in SVR which is tantamount to a virologic cure. The attainment of SVR abolishes ongoing liver injury and studies have confirmed that not only is fibrogenesis arrested but fibrosis reversal can also manifest[108-110].

Clinical regression of fibrosis in cirrhosis

Studies have identified that the potential for liver fibrosis regression may also be dependent on the duration of fibrosis and on several scar factors including scar composition, cellularity and spatial distribution[111]. Areas that may not be completely degraded include those that are acellular, rich in elastin and heavily cross-linked. Both animal and human studies have also identified that the regression of cirrhosis results in the transformation of cirrhotic micronodules into larger macronodules[111,112]. Furthermore, due to the significant vascular distortion, shunting and angiogenesis that is associated with cirrhosis, significant fibrosis regression in a previously cirrhotic liver may not result in portal pressure reduction[113].

Mechanisms for fibrosis regression

An understanding of the mechanisms that underlie fibrosis regression have led to the identification of antifibrotic targets and the developments of antifibrotic agents[114].

Studies have confirmed that rather than being a fixed entity, the hepatic scar is in a state of continuous dynamic flux with respect to its cellular and matrix composition. In keeping with fibrosis progression, both myofibroblasts and hepatic macrophages are key protagonists in the regression of fibrosis. MMPs are a group of proteolytic enzymes that are responsible for the degradation of extracellular matrix components. The MMP proteolytic activity is regulated by their potent specific inhibitors tissue inhibitors TIMPs as expressed by activated HSCs[115]. Moreover, the apoptosis of activated HSC may be inhibited by TIMPs.

In both animal models and human studies documenting fibrosis regression with scar degradation, TIMP levels decrease dramatically and MMP levels rise[111,115]. Thereafter, profibrogenic myofibroblasts are removed from the receding hepatic scar by apoptosis. In addition, recent studies have identified that hepatic macrophages are important regulators of ECM remodelling[116] highlighting the importance of specific macrophage subsets in either fibrogenesis or fibrosis regression (Ly-6C^{lo})[117].

HSCS AND FIBROSIS REGRESSION

As described earlier, HSCs play an important contribution to ECM remodelling in fibrosis evolution. Three mechanisms have been described through which HSCs can contribute to fibrosis regression: Apoptosis, senescence or quiescence.

HSC apoptosis

HSC apoptosis leads to a decrease in the number of activated HSCs and has been observed during fibrosis regression[118]. This results in a decrease in TIMP-1 expression and thus inhibiting MMP activity. Apoptosis can be initiated in HSCs *via* CD95L (Fas ligand), Bcl-2 and p53[119]. Moreover, apoptosis can be initiated by hepatocytes (*via* NGF)[120], NK cells (*via* TNF-related apoptosis inducing ligand and NKG2D)[19] and Kupffer cells (*via* capsase-9)[121].

HSC senescence

There is evidence that HSCs can enter a senescent phase adopting a more inflammatory but less fibrogenic phenotype[122]. Both in culture and *in vivo* there is evidence that HSC senescence is mediated by p53.

HSC quiescence

Studies have demonstrated that a large proportion (approximately 50%) of activated HSCs can revert to a quiescent phenotype[123,124]. What has also been demonstrated, however, is that quiescent HSCs have a lower threshold to enter an activated state than naïve HSCs. HSC quiescence is thought to be mediated by PPAR-γ.

TARGETS OF HSC MEDIATED ANTIFIBROTIC THERAPY

Reduction of the inflammatory/immune response or inhibition hepatocyte apoptosis/injury to avoid HSC activation.

Promotion of fibrosis regression by inhibiting scar formation; promotion of matrix degradation; inhibition HSC activation or stimulate HSC apoptosis/senescence/quiescence.

Inhibition of signalling pathways (extracellular and intracellular) that initiate and perpetuate HSCs

CLASSES OF ANTIFIBROTIC THERAPY

Treatments for liver fibrosis can be categorised into several ways. Antifibrotic treatment may target the underlying aetiology of liver disease specifically (for example in CHC). Conversely, antifibrotic treatments may act with a direct antifibrotic action in the absence of any effect on the underlying aetiology of liver disease. These may be established drugs licenced for other indications and rediscovered to investigate their potential antifibrotic effect (drug repositioning).

Type 1 interferons

In CHC, type 1 interferons were found to exhibit an antifibrotic effect in animal models[125,126] with a reduction in portal pressure[127] and significant histological improvement even in the absence of achieving SVR[128]. These observations were translated into the three large clinical trials that addressed the use of long term interferon in patients with advanced fibrosis[129-131]. All 3 trials identified that low maintenance dose of PEG-IFN did not improve outcomes in patients with compensated cirrhosis and CHC after a lead-in phase of PEG-IFN.

Activated myofibroblasts

Activated myofibroblasts can contribute to fibrosis regression by the release of proteolytic enzymes (mainly MMPs) that degrade ECM when subjected to favourable stimuli integrin receptor-mediated) in a process called "stress relaxation". Myofibroblast stress relaxation resulting in a reduction in fibrogenesis and portal hyper tension has been demonstrated in cirrhotic rats by inhibiting Rho kinase[132]. Myofibroblasts have also been targeted by liposomes loaded with siRNA-Loaded Cationic Nanohydrogel Particles[133].

Damaged hepatocytes

Myofibroblasts can become activated by the phagocytosis of apoptotic hepatocytes. Biliary fibrosis has been found to be ameliorated in mice by the inhibition of hepatocyte apoptosis using a pan-cases inhibitor or an antagonist of cathespin B (a lysosomal trigger of apoptosis)[134,135].

Biliary progenitors

The "ductular reaction" is classically seen in biliary fibrosis where biliary progenitor cells proliferate and secrete cytokines that promote HSC activation. In advanced fibrosis of "non-biliary" liver diseases, liver progenitor cell proliferation is also marked after the development of portal fibrosis. Several drugs targeting biliary progenitor cells have been used as antifibrotics including those inhibiting integrin αvβ6 (a receptor for fibronectin and tenascin-C)[136] and the hedgehog pathway[137,138].

LSECs

During perisinusoidal fibrosis, activated LSECs produce ECM and secrete fibrogenic cytokines. LSECs themselves are activated by angiogenic factors produced by myofibroblasts including VEGF and angiopoetin-1[139]. Polykinase inhibitors such as sunitinib and sorafenib are antiangiogenic and have been identified to ameliorate experimental liver fibrosis[39,140].

Monocytes

Monocytes are the precursors of myofibroblasts, macrophages and dendritic cells playing an important role in inflammation and fibrosis. The chemokine CXCL9 has been identified to inhibit fibrogenesis by activating the monocyte receptor CX3CR[141,142].

Lysyl oxidase (LOXL2)

The enzyme LOXL2 mediates ECM crosslinking of matrix proteins including collagen. Antifibrotic activity has been demonstrated using LOXL an experiment models of liver fibrosis[143]. Simtuzumab is a monoclonal antibody targeting LOX2 and is currently being evaluated in phase II trials in patients with NAFLD with and without cirrhosis.

TLRs

TLR activation promotes a proinflammatory environment and TLR3 and TLR4 are being investigated for their antifibrotic properties.

TREATMENTS AND THERAPIES FOR NASH

Numerous medications are currently being studied for the treatment of NASH and fibrosis related to NAFLD. Whereas many of these medications have been shown to be effective in improving liver histology, the magnitude of the treatment effect is at best modest and there may also be associated adverse events.

Diet and physical activity

Sustained weight loss of more than 10% has been identified to be effective at improving liver histology (inflammation and fibrosis)[144-146].

PPAR agonists

Perioxisome proliferator-activator receptors (PPARs) are nuclear receptors that are expressed in a variety of organs including the liver. There are 3 types of PPAR receptor: α, β/δ and γ. PPARs regular metabolic processes including oxidation and lipid transport. PPARα agonists (for example fibrates) have not shown significant histologic benefit in NAFLD. In a phase IIb study, the dual PPARα/δ agonist was found to increase resolution of histologic NASH[147]; phase III studies are currently being conducted. Thiazolidinediones (for example pioglitazone) are PPARγ agonists that commonly used to treat diabetes and act as insulin sensitisers. In patients with NAFLD, treatment with pioglitazone has been shown to improve liver histology[148-150]. There is however, a risk of weight gain and congestive heart failure with pioglitazone treatment.

Farnesoid X receptor bile acid axis

Farnesoid X receptor (FXR) is a bile acid intracellular receptor that both regulates bile acid synthesis and decreases hepatic gluconeogenesis[151]. Obeticholic acid is a synthetic bile acid derivative and an FXR agonist. In phase II studies treatment with Obeticholic acid significantly improved liver histology (NASH and fibrosis) in patients with NAFLD[152]. Side effects of Obeticholic acid include reversible pruritus and worsening lipid profile. Phase III trials of Obeticholic acid are currently being conducted. Other agents work *via* the FXR-bile acid are also under investigation (FGF-19 and NGM-282)

Lipid-altering agents

Aramchol is Stearoyl-CoA desaturase inhibitor that is currently being investigated in phase III studies for NASH. In a small phase II study Aramchol was associated with a decrease in hepatic fat content[153]. HMG-CoA reductase inhibitors (statins) are used extensively in both primary and secondary care for the treatment of hyperlipidaemia. There is evidence that statin use may improve liver histology (steatosis, steatohepatitis and fibrosis) in patients with NAFLD[154].

Incretin based therapies

Glucagon-like peptide 1 agonists such as liraglutide and exenatide are primarily used for the treatment of diabetes. Glucagon-like peptide 1 belongs to the incretin family of proteins and acts on the pancreas to cause beta-cell proliferation and enhance insulin biosynthesis. A meta-analysis of several studies identified that treatment with Glucagon-like peptide 1 agonist was associated with improved hepatic steatosis and fibrosis[155].

Agents targeting inflammation, cell injury and inflammation

Vitamin E is an antioxidant that has been shown in both paediatric and adult NAFLD studies to improve hepatic steatosis, inflammation and NASH but not hepatic fibrosis[156,157]. Pentoxyphilline is a methylxanthine derivative that modulates several cytokines including inhibiting TNFα. In a small study of 55 patients, as compared to placebo, patients with biopsy proven NASH treated with pentoxyphilline were found to have improved NAS scores and fibrosis scores[158]. Larger studies will be needed to confirm these findings.

CONCLUSION

As CLD often develops insidiously most CLD is diagnosed at the stage of cirrhosis when interventions are ineffective, resulting in considerable morbidity and mortality[159,160]. Standard "liver function tests" have poor sensitivity and specificity for the detection of liver fibrosis[161,162]. The reference standard for staging liver fibrosis remains the histological staging of a liver biopsy specimen. Liver biopsy itself, even in experienced centres, is associated with complications such as pain (20%), serious morbidity (0.6%) and even death (0.01%)[163]. Moreover, the accuracy and reliability liver biopsy is limited due to sampling error and both inter- and intra-observer variability. As such the reference standard for assessing liver disease is not practicable for the detection of liver injury amongst individuals at risk of CLD and instead a non-invasive approach is desirable.

Non-invasive alternatives to liver biopsy include imaging modalities and serum markers. Imaging modalities such as transient elastography have been developed to detect liver fibrosis by measuring the degree of liver stiffness. Whereas serum markers of fibrosis may not be entirely liver specific, liver stiffness itself is importantly an intrinsic physical property of liver tissue. On an individual patient basis however, it can be more time consuming to assess liver fibrosis using an imaging modality than by using a serum marker. Although scanning itself may take only a few minutes the procedure time may be prolonged due to factors such as patient positioning and patient compliance. By contrast, serum markers of fibrosis can be measured at the time of routine blood tests. Liver stiffness values can be influenced by a variety of factors including concurrent inflammation and recent food ingestion. Whereas imaging modalities are reliable clinical discriminators (for example advanced versus non-advanced fibrosis) they have a limited role in furthering our understanding of hepatic pathophysiology.

Only by having a comprehensive understanding of the pathophysiology of chronic liver disease can appropriate and meaningful diagnostic targets for research studies be identified. Regardless, for clinicians who are not engaged in laboratory research this also requires a revision of basic anatomy, physiology and immunology. In this review article we have attempted to go "back to basics" to enable liver specific pathophysiology to be contextualised.

Through an understanding of hepatic inflammation and matrix biology, candidate direct biomarkers have been successfully identified and validated for use in clinical practice with these studies complementing the indirect candidate biomarker approach that have also proved successful. Indeed, these approaches have been combined and there are now numerous examples of hybrid biomarker panels.

Regardless, clinically meaningful diagnostic targets can change dramatically in response to advances in therapy. This point is highlighted by our focus on both CHC and NAFLD. Whereas the treatment of NAFLD is still in its infancy, treatment for CHC has evolved from toxic interferon containing regimens to the abbreviated highly efficacious regimens of today. As such, whereas fibrosis stratification and CHC related fibrosis are no longer the priorities that they were perhaps a decade ago, the lessons learnt from these studies remain invaluable. Moreover, these studies continue to foster the development of antifibrotic therapies through both drug repositioning and the development of novel agents. Even after the successful eradication of CHC, therapies to accelerate fibrosis regression are needed for patients with cirrhosis as ongoing fibrotic reversal is slow and in some cases liver fibrosis can continue to progress.

By contrast to the treatment of CHC, therapies for NAFLD are still very much in their infancy. Notwithstanding, the development of novel agents targeting hepatic inflammation and fibrosis is now progressing at a rapid pace. Furthermore, we hope that we will soon embrace an era of personalised treatment of liver fibrosis and inflammation that can be accurately monitored by non-invasive biomarkers.

REFERENCES

1 **Bacon BR**, O'Grady JG. Comprehensive Clinical Hepatology. Elsevier. 2006
2 **Rosenberg W**, Baldrick T, Tanwar S. Liver Disease. Tietz textbook of clinical chemistry and molecular diagnostics. Missouri: Elsevier 2019; 699-722
3 **Bedossa P**, Paradis V. Liver extracellular matrix in health and disease. *J Pathol* 2003; **200**: 504-515 [PMID: 12845618 DOI: 10.1002/path.1397]
4 **Schuppan D**. Structure of the extracellular matrix in normal and fibrotic liver: collagens and glycoproteins. *Semin Liver Dis* 1990; **10**: 1-10 [PMID: 2186485 DOI: 10.1055/s-2008-1040452]
5 **Protzer U**, Maini MK, Knolle PA. Living in the liver: hepatic infections. *Nat Rev Immunol* 2012; **12**: 201-213 [PMID: 22362353 DOI: 10.1038/nri3169]
6 **Delneste Y**, Beauvillain C, Jeannin P. [Innate immunity: structure and function of TLRs]. *Med Sci (Paris)* 2007; **23**: 67-73 [PMID: 17212934 DOI: 10.1051/medsci/200723167]
7 **Kawai T**, Akira S. Innate immune recognition of viral infection. *Nat Immunol* 2006; **7**: 131-137 [PMID: 16424890 DOI: 10.1038/ni1303]
8 **Alexopoulou L**, Holt AC, Medzhitov R, Flavell RA. Recognition of double-stranded RNA and activation of NF-kappaB by Toll-like receptor 3. *Nature* 2001; **413**: 732-738 [PMID: 11607032 DOI: 10.1038/35099560]
9 **Kono H**, Rock KL. How dying cells alert the immune system to danger. *Nat Rev Immunol* 2008; **8**: 279-289 [PMID: 18340345 DOI: 10.1038/nri2215]
10 **McDonald B**, Pittman K, Menezes GB, Hirota SA, Slaba I, Waterhouse CC, Beck PL, Muruve DA, Kubes P. Intravascular danger signals guide neutrophils to sites of sterile inflammation. *Science* 2010; **330**: 362-366 [PMID: 20947763 DOI: 10.1126/science.1195491]
11 **Xu R**, Huang H, Zhang Z, Wang FS. The role of neutrophils in the development of liver diseases. *Cell Mol Immunol* 2014; **11**: 224-231 [PMID: 24633014 DOI: 10.1038/cmi.2014.2]
12 **Nahrendorf M**, Pittet MJ, Swirski FK. Monocytes: protagonists of infarct inflammation and repair after myocardial infarction. *Circulation* 2010; **121**: 2437-2445 [PMID: 20530020 DOI: 10.1161/CIRCULATIONAHA.109.916346]
13 **Geissmann F**, Manz MG, Jung S, Sieweke MH, Merad M, Ley K. Development of monocytes, macrophages, and dendritic cells. *Science* 2010; **327**: 656-661 [PMID: 20133564 DOI: 10.1126/science.1178331]
14 **Dal-Secco D**, Wang J, Zeng Z, Kolaczkowska E, Wong CH, Petri B, Ransohoff RM, Charo IF, Jenne CN, Kubes P. A dynamic spectrum of monocytes arising from the in situ reprogramming of CCR2+ monocytes at a site of sterile injury. *J Exp Med* 2015; **212**: 447-456 [PMID: 25800956 DOI: 10.1084/jem.20141539]
15 **Crispe IN**. The liver as a lymphoid organ. *Annu Rev Immunol* 2009; **27**: 147-163 [PMID: 19302037 DOI: 10.1146/annurev.immunol.021908.132629]
16 **Italiani P**, Boraschi D. From Monocytes to M1/M2 Macrophages: Phenotypical vs. Functional Differentiation. *Front Immunol* 2014; **5**: 514 [PMID: 25368618 DOI: 10.3389/fimmu.2014.00514]
17 **Rossaint J**, Zarbock A. Platelets in leucocyte recruitment and function. *Cardiovasc Res* 2015; **107**: 386-395 [PMID: 25712962 DOI: 10.1093/cvr/cvv048]
18 **Seino K**, Taniguchi M. Functionally distinct NKT cell subsets and subtypes. *J Exp Med* 2005; **202**: 1623-1626 [PMID: 16365145 DOI: 10.1084/jem.20051600]
19 **Radaeva S**, Sun R, Jaruga B, Nguyen VT, Tian Z, Gao B. Natural killer cells ameliorate liver fibrosis by killing activated stellate cells in NKG2D-dependent and tumor necrosis factor-related apoptosis-inducing ligand-dependent manners. *Gastroenterology* 2006; **130**: 435-452 [PMID: 16472598 DOI: 10.1053/j.gastro.2005.10.055]
20 **Romagnani S**. Type 1 T helper and type 2 T helper cells: functions, regulation and role in protection and disease. *Int J Clin Lab Res* 1991; **21**: 152-158 [PMID: 1687725]
21 **Harrington LE**, Hatton RD, Mangan PR, Turner H, Murphy TL, Murphy KM, Weaver CT. Interleukin 17-producing CD4+ effector T cells develop *via* a lineage distinct from the T helper type 1 and 2 lineages. *Nat Immunol* 2005; **6**: 1123-1132 [PMID: 16200070 DOI: 10.1038/ni1254]
22 **Sun HQ**, Zhang JY, Zhang H, Zou ZS, Wang FS, Jia JH. Increased Th17 cells contribute to disease progression in patients with HBV-associated liver cirrhosis. *J Viral Hepat* 2012; **19**: 396-403 [PMID: 22571901 DOI: 10.1111/j.1365-2893.2011.01561.x]
23 **Ouyang W**, Kolls JK, Zheng Y. The biological functions of T helper 17 cell effector cytokines in inflammation. *Immunity* 2008; **28**: 454-467 [PMID: 18400188 DOI: 10.1016/j.immuni.2008.03.004]
24 **Sakaguchi S**. Naturally arising CD4+ regulatory T cells for immunologic self-tolerance and negative control of immune responses. *Annu Rev Immunol* 2004; **22**: 531-562 [PMID: 15032588 DOI: 10.1146/annurev.immunol.21.120601.141122]
25 **Fontenot JD**, Gavin MA, Rudensky AY. Pillars Article: Foxp3 Programs the Development and Function of CD4+CD25+ Regulatory T Cells. Nat. Immunol. 2003. 4: 330-336. *J Immunol* 2017; **198**: 986-992 [PMID: 28115587]
26 **Scheibner KA**, Lutz MA, Boodoo S, Fenton MJ, Powell JD, Horton MR. Hyaluronan fragments act as an endogenous danger signal by engaging TLR2. *J Immunol* 2006; **177**: 1272-1281 [PMID: 16818787]
27 **Fernandes-Alnemri T**, Yu JW, Datta P, Wu J, Alnemri ES. AIM2 activates the inflammasome and cell death in response to cytoplasmic DNA. *Nature* 2009; **458**: 509-513 [PMID: 19158676 DOI: 10.1038/nature07710]
28 **Chan FK**, Luz NF, Moriwaki K. Programmed necrosis in the cross talk of cell death and inflammation. *Annu Rev Immunol* 2015; **33**: 79-106 [PMID: 25493335 DOI: 10.1146/annurev-immunol-032414-112248]
29 **Szabo G**, Csak T. Inflammasomes in liver diseases. *J Hepatol* 2012; **57**: 642-654 [PMID: 22634126 DOI: 10.1016/j.jhep.2012.03.035]
30 **Friedman SL**. Mechanisms of hepatic fibrogenesis. *Gastroenterology* 2008; **134**: 1655-1669 [PMID: 18471545 DOI: 10.1053/j.gastro.2008.03.003]
31 **Friedman SL**. Liver fibrosis: from mechanisms to treatment. *Gastroenterol Clin Biol* 2007; **31**: 812-814 [PMID: 18166858]
32 **Moreira RK**. Hepatic stellate cells and liver fibrosis. *Arch Pathol Lab Med* 2007; **131**: 1728-1734 [PMID: 17979495 DOI: 10.1043/1543-2165(2007)131[1728:HSCALF]2.0.CO;2]
33 **Giampieri MP**, Jezequel AM, Orlandi F. The lipocytes in normal human liver. A quantitative study. *Digestion* 1981; **22**: 165-169 [PMID: 7308589]
34 **Rockey DC**. Endothelial Dysfunction in Advanced Liver Disease. *The American Journal of the Medical Sciences* 2015; **349**: 6-16 [DOI: 10.1097/maj.0000000000000403]

35 **Canbay A**, Higuchi H, Bronk SF, Taniai M, Sebo TJ, Gores GJ. Fas enhances fibrogenesis in the bile duct ligated mouse: a link between apoptosis and fibrosis. *Gastroenterology* 2002; **123**: 1323-1330 [PMID: 12360492]

36 **Borkham-Kamphorst E**, van Roeyen CR, Ostendorf T, Floege J, Gressner AM, Weiskirchen R. Pro-fibrogenic potential of PDGF-D in liver fibrosis. *J Hepatol* 2007; **46**: 1064-1074 [PMID: 17397961 DOI: 10.1016/j.jhep.2007.01.029]

37 **Hernandez-Gea V**, Friedman SL. Pathogenesis of liver fibrosis. *Annu Rev Pathol* 2011; **6**: 425-456 [PMID: 21073339 DOI: 10.1146/annurev-pathol-011110-130246]

38 **Nobili V**, Parola M, Alisi A, Marra F, Piemonte F, Mombello C, Sutti S, Povero D, Maina V, Novo E, Albano E. Oxidative stress parameters in paediatric non-alcoholic fatty liver disease. *Int J Mol Med* 2010; **26**: 471-476 [PMID: 20818484]

39 **Thabut D**, Routray C, Lomberk G, Shergill U, Glaser K, Huebert R, Patel L, Masyuk T, Blechacz B, Vercnocke A, Ritman E, Ehman R, Urrutia R, Shah V. Complementary vascular and matrix regulatory pathways underlie the beneficial mechanism of action of sorafenib in liver fibrosis. *Hepatology* 2011; **54**: 573-585 [PMID: 21567441 DOI: 10.1002/hep.24427]

40 **Friedman SL**. Hepatic stellate cells: protean, multifunctional, and enigmatic cells of the liver. *Physiol Rev* 2008; **88**: 125-172 [PMID: 18195085 DOI: 10.1152/physrev.00013.2007]

41 **Knittel T**, Mehde M, Kobold D, Saile B, Dinter C, Ramadori G. Expression patterns of matrix metalloproteinases and their inhibitors in parenchymal and non-parenchymal cells of rat liver: regulation by TNF-alpha and TGF-beta1. *J Hepatol* 1999; **30**: 48-60 [PMID: 9927150]

42 **Bourd-Boittin K**, Bonnier D, Leyme A, Mari B, Tuffery P, Samson M, Ezan F, Baffet G, Theret N. Protease profiling of liver fibrosis reveals the ADAM metallopeptidase with thrombospondin type 1 motif, 1 as a central activator of transforming growth factor beta. *Hepatology* 2011; **54**: 2173-2184 [PMID: 21826695 DOI: 10.1002/hep.24598]

43 **Schuppan D**, Afdhal NH. Liver cirrhosis. *Lancet* 2008; **371**: 838-851 [PMID: 18328931 DOI: 10.1016/S0140-6736(08)60383-9]

44 **Day CP**, James OF. Hepatic steatosis: innocent bystander or guilty party? *Hepatology* 1998; **27**: 1463-1466 [PMID: 9620314 DOI: 10.1002/hep.510270601]

45 **Friedman SL**. Liver fibrosis in 2012: Convergent pathways that cause hepatic fibrosis in NASH. *Nat Rev Gastroenterol Hepatol* 2013; **10**: 71-72 [PMID: 23296246 DOI: 10.1038/nrgastro.2012.256]

46 **Tilg H**, Moschen AR. Evolution of inflammation in nonalcoholic fatty liver disease: the multiple parallel hits hypothesis. *Hepatology* 2010; **52**: 1836-1846 [PMID: 21038418 DOI: 10.1002/hep.24001]

47 **Speliotes EK**, Yerges-Armstrong LM, Wu J, Hernaez R, Kim LJ, Palmer CD, Gudnason V, Eiriksdottir G, Garcia ME, Launer LJ, Nalls MA, Clark JM, Mitchell BD, Shuldiner AR, Butler JL, Tomas M, Hoffmann U, Hwang SJ, Massaro JM, O'Donnell CJ, Sahani DV, Salomaa V, Schadt EE, Schwartz SM, Siscovick DS, NASH CRN, GIANT Consortium, MAGIC Investigators, Voight BF, Carr JJ, Feitosa MF, Harris TB, Fox CS, Smith AV, Kao WH, Hirschhorn JN, Borecki IB, GOLD Consortium. Genome-wide association analysis identifies variants associated with nonalcoholic fatty liver disease that have distinct effects on metabolic traits. *PLoS Genet* 2011; **7**: e1001324 [PMID: 21423719 DOI: 10.1371/journal.pgen.1001324]

48 **Xu R**, Tao A, Zhang S, Deng Y, Chen G. Association between patatin-like phospholipase domain containing 3 gene (PNPLA3) polymorphisms and nonalcoholic fatty liver disease: a HuGE review and meta-analysis. *Sci Rep* 2015; **5**: 9284 [PMID: 25791171 DOI: 10.1038/srep09284]

49 **Santoro N**, Kursawe R, D'Adamo E, Dykas DJ, Zhang CK, Bale AE, Calí AM, Narayan D, Shaw MM, Pierpont B, Savoye M, Lartaud D, Eldrich S, Cushman SW, Zhao H, Shulman GI, Caprio S. A common variant in the patatin-like phospholipase 3 gene (PNPLA3) is associated with fatty liver disease in obese children and adolescents. *Hepatology* 2010; **52**: 1281-1290 [PMID: 20803499 DOI: 10.1002/hep.23832]

50 **Feldman A**, Eder SK, Felder TK, Kedenko L, Paulweber B, Stadlmayr A, Huber-Schönauer U, Niederseer D, Stickel F, Auer S, Haschke-Becher E, Patsch W, Datz C, Aigner E. Clinical and Metabolic Characterization of Lean Caucasian Subjects With Non-alcoholic Fatty Liver. *Am J Gastroenterol* 2017; **112**: 102-110 [PMID: 27527746 DOI: 10.1038/ajg.2016.318]

51 **Xu C**, Wang G, Hao Y, Zhi J, Zhang L, Chang C. Correlation analysis between gene expression profile of rat liver tissues and high-fat emulsion-induced nonalcoholic fatty liver. *Dig Dis Sci* 2011; **56**: 2299-2308 [PMID: 21327921 DOI: 10.1007/s10620-011-1599-9]

52 **Brunt EM**, Kleiner DE, Wilson LA, Belt P, Neuschwander-Tetri BA; NASH Clinical Research Network (CRN). Nonalcoholic fatty liver disease (NAFLD) activity score and the histopathologic diagnosis in NAFLD: distinct clinicopathologic meanings. *Hepatology* 2011; **53**: 810-820 [PMID: 21319198 DOI: 10.1002/hep.24127]

53 **Li ZZ**, Berk M, McIntyre TM, Feldstein AE. Hepatic lipid partitioning and liver damage in nonalcoholic fatty liver disease: role of stearoyl-CoA desaturase. *J Biol Chem* 2009; **284**: 5637-5644 [PMID: 19119140 DOI: 10.1074/jbc.M807616200]

54 **Liu J**, Han L, Zhu L, Yu Y. Free fatty acids, not triglycerides, are associated with non-alcoholic liver injury progression in high fat diet induced obese rats. *Lipids Health Dis* 2016; **15**: 27 [PMID: 26868515 DOI: 10.1186/s12944-016-0194-7]

55 **Zhang XQ**, Xu CF, Yu CH, Chen WX, Li YM. Role of endoplasmic reticulum stress in the pathogenesis of nonalcoholic fatty liver disease. *World J Gastroenterol* 2014; **20**: 1768-1776 [PMID: 24587654 DOI: 10.3748/wjg.v20.i7.1768]

56 **Lake AD**, Novak P, Hardwick RN, Flores-Keown B, Zhao F, Klimecki WT, Cherrington NJ. The adaptive endoplasmic reticulum stress response to lipotoxicity in progressive human nonalcoholic fatty liver disease. *Toxicol Sci* 2014; **137**: 26-35 [PMID: 24097666 DOI: 10.1093/toxsci/kft230]

57 **Meakin PJ**, Chowdhry S, Sharma RS, Ashford FB, Walsh SV, McCrimmon RJ, Dinkova-Kostova AT, Dillon JF, Hayes JD, Ashford ML. Susceptibility of Nrf2-null mice to steatohepatitis and cirrhosis upon consumption of a high-fat diet is associated with oxidative stress, perturbation of the unfolded protein response, and disturbance in the expression of metabolic enzymes but not with insulin resistance. *Mol Cell Biol* 2014; **34**: 3305-3320 [PMID: 24958099 DOI: 10.1128/MCB.00677-14]

58 **Vonghia L**, Michielsen P, Francque S. Immunological mechanisms in the pathophysiology of non-alcoholic steatohepatitis. *Int J Mol Sci* 2013; **14**: 19867-19890 [PMID: 24084730 DOI: 10.3390/ijms141019867]

59 **Mouzaki M**, Comelli EM, Arendt BM, Bonengel J, Fung SK, Fischer SE, McGilvray ID, Allard JP. Intestinal microbiota in patients with nonalcoholic fatty liver disease. *Hepatology* 2013; **58**: 120-127 [PMID: 23401313 DOI: 10.1002/hep.26319]

60 **Henao-Mejia J**, Elinav E, Jin C, Hao L, Mehal WZ, Strowig T, Thaiss CA, Kau AL, Eisenbarth SC,

Jurczak MJ, Camporez JP, Shulman GI, Gordon JI, Hoffman HM, Flavell RA. Inflammasome-mediated dysbiosis regulates progression of NAFLD and obesity. *Nature* 2012; **482**: 179-185 [PMID: 22297845 DOI: 10.1038/nature10809]

61 **Zhu L**, Baker SS, Gill C, Liu W, Alkhouri R, Baker RD, Gill SR. Characterization of gut microbiomes in nonalcoholic steatohepatitis (NASH) patients: a connection between endogenous alcohol and NASH. *Hepatology* 2013; **57**: 601-609 [PMID: 23055155 DOI: 10.1002/hep.26093]

62 **Wan J**, Benkdane M, Teixeira-Clerc F, Bonnafous S, Louvet A, Lafdil F, Pecker F, Tran A, Gual P, Mallat A, Lotersztajn S, Pavoine C. M2 Kupffer cells promote M1 Kupffer cell apoptosis: a protective mechanism against alcoholic and nonalcoholic fatty liver disease. *Hepatology* 2014; **59**: 130-142 [PMID: 23832548 DOI: 10.1002/hep.26607]

63 **Wenfeng Z**, Yakun W, Di M, Jianping G, Chuanxin W, Chun H. Kupffer cells: increasingly significant role in nonalcoholic fatty liver disease. *Ann Hepatol* 2014; **13**: 489-495 [PMID: 25152980]

64 **Eguchi A**, Wree A, Feldstein AE. Biomarkers of liver cell death. *J Hepatol* 2014; **60**: 1063-1074 [PMID: 24412608 DOI: 10.1016/j.jhep.2013.12.026]

65 **Huang W**, Metlakunta A, Dedousis N, Zhang P, Sipula I, Dube JJ, Scott DK, O'Doherty RM. Depletion of liver Kupffer cells prevents the development of diet-induced hepatic steatosis and insulin resistance. *Diabetes* 2010; **59**: 347-357 [PMID: 19934001 DOI: 10.2337/db09-0016]

66 **Sharifnia T**, Antoun J, Verriere TG, Suarez G, Wattacheril J, Wilson KT, Peek RM, Abumrad NN, Flynn CR. Hepatic TLR4 signaling in obese NAFLD. *Am J Physiol Gastrointest Liver Physiol* 2015; **309**: G270-G278 [PMID: 26113297 DOI: 10.1152/ajpgi.00304.2014]

67 **Walenbergh SM**, Koek GH, Bieghs V, Shiri-Sverdlov R. Non-alcoholic steatohepatitis: the role of oxidized low-density lipoproteins. *J Hepatol* 2013; **58**: 801-810 [PMID: 23183522 DOI: 10.1016/j.jhep.2012.11.014]

68 **Bieghs V**, van Gorp PJ, Walenbergh SM, Gijbels MJ, Verheyen F, Buurman WA, Briles DE, Hofker MH, Binder CJ, Shiri-Sverdlov R. Specific immunization strategies against oxidized low-density lipoprotein: a novel way to reduce nonalcoholic steatohepatitis in mice. *Hepatology* 2012; **56**: 894-903 [PMID: 22334337 DOI: 10.1002/hep.25660]

69 **Rensen SS**, Slaats Y, Nijhuis J, Jans A, Bieghs V, Driessen A, Malle E, Greve JW, Buurman WA. Increased hepatic myeloperoxidase activity in obese subjects with nonalcoholic steatohepatitis. *Am J Pathol* 2009; **175**: 1473-1482 [PMID: 19729473 DOI: 10.2353/ajpath.2009.080999]

70 **Alkhouri N**, Morris-Stiff G, Campbell C, Lopez R, Tamimi TA, Yerian L, Zein NN, Feldstein AE. Neutrophil to lymphocyte ratio: a new marker for predicting steatohepatitis and fibrosis in patients with nonalcoholic fatty liver disease. *Liver Int* 2012; **32**: 297-302 [PMID: 22097893 DOI: 10.1111/j.1478-3231.2011.02639.x]

71 **Ibusuki R**, Uto H, Arima S, Mawatari S, Setoguchi Y, Iwashita Y, Hashimoto S, Maeda T, Tanoue S, Kanmura S, Oketani M, Ido A, Tsubouchi H. Transgenic expression of human neutrophil peptide-1 enhances hepatic fibrosis in mice fed a choline-deficient, L-amino acid-defined diet. *Liver Int* 2013; **33**: 1549-1556 [PMID: 23682724 DOI: 10.1111/liv.12203]

72 **Talukdar S**, Oh DY, Bandyopadhyay G, Li D, Xu J, McNelis J, Lu M, Li P, Yan Q, Zhu Y, Ofrecio J, Lin M, Brenner MB, Olefsky JM. Neutrophils mediate insulin resistance in mice fed a high-fat diet through secreted elastase. *Nat Med* 2012; **18**: 1407-1412 [PMID: 22863787 DOI: 10.1038/nm.2885]

73 **Brunt EM**. Pathology of nonalcoholic fatty liver disease. *Nat Rev Gastroenterol Hepatol* 2010; **7**: 195-203 [PMID: 20195271 DOI: 10.1038/nrgastro.2010.21]

74 **Gadd VL**, Skoien R, Powell EE, Fagan KJ, Winterford C, Horsfall L, Irvine K, Clouston AD. The portal inflammatory infiltrate and ductular reaction in human nonalcoholic fatty liver disease. *Hepatology* 2014; **59**: 1393-1405 [PMID: 24254368 DOI: 10.1002/hep.26937]

75 **Sumarac-Dumanovic M**, Stevanovic D, Ljubic A, Jorga J, Simic M, Stamenkovic-Pejkovic D, Starcevic V, Trajkovic V, Micic D. Increased activity of interleukin-23/interleukin-17 proinflammatory axis in obese women. *Int J Obes (Lond)* 2009; **33**: 151-156 [PMID: 18982006 DOI: 10.1038/ijo.2008.216]

76 **Tang Y**, Bian Z, Zhao L, Liu Y, Liang S, Wang Q, Han X, Peng Y, Chen X, Shen L, Qiu D, Li Z, Ma X. Interleukin-17 exacerbates hepatic steatosis and inflammation in non-alcoholic fatty liver disease. *Clin Exp Immunol* 2011; **166**: 281-290 [PMID: 21985374 DOI: 10.1111/j.1365-2249.2011.04471.x]

77 **Harley IT**, Stankiewicz TE, Giles DA, Softic S, Flick LM, Cappelletti M, Sheridan R, Xanthakos SA, Steinbrecher KA, Sartor RB, Kohli R, Karp CL, Divanovic S. IL-17 signaling accelerates the progression of nonalcoholic fatty liver disease in mice. *Hepatology* 2014; **59**: 1830-1839 [PMID: 24115079 DOI: 10.1002/hep.26746]

78 **Winer DA**, Winer S, Chng MH, Shen L, Engleman EG. B Lymphocytes in obesity-related adipose tissue inflammation and insulin resistance. *Cell Mol Life Sci* 2014; **71**: 1033-1043 [PMID: 24127133 DOI: 10.1007/s00018-013-1486-y]

79 **Sutti S**, Jindal A, Locatelli I, Vacchiano M, Gigliotti L, Bozzola C, Albano E. Adaptive immune responses triggered by oxidative stress contribute to hepatic inflammation in NASH. *Hepatology* 2014; **59**: 886-897 [PMID: 24115128 DOI: 10.1002/hep.26749]

80 **Albano E**, Mottaran E, Vidali M, Reale E, Saksena S, Occhino G, Burt AD, Day CP. Immune response towards lipid peroxidation products as a predictor of progression of non-alcoholic fatty liver disease to advanced fibrosis. *Gut* 2005; **54**: 987-993 [PMID: 15951547 DOI: 10.1136/gut.2004.057968]

81 **Winer DA**, Winer S, Shen L, Wadia PP, Yantha J, Paltser G, Tsui H, Wu P, Davidson MG, Alonso MN, Leong HX, Glassford A, Caimol M, Kenkel JA, Tedder TF, McLaughlin T, Miklos DB, Dosch HM, Engleman EG. B cells promote insulin resistance through modulation of T cells and production of pathogenic IgG antibodies. *Nat Med* 2011; **17**: 610-617 [PMID: 21499269 DOI: 10.1038/nm.2353]

82 **Tarantino G**, Costantini S, Finelli C, Capone F, Guerriero E, La Sala N, Gioia S, Castello G. Is serum Interleukin-17 associated with early atherosclerosis in obese patients? *J Transl Med* 2014; **12**: 214 [PMID: 25092442 DOI: 10.1186/s12967-014-0214-1]

83 **Tarantino G**, Costantini S, Citro V, Conforti P, Capone F, Sorice A, Capone D. Interferon-alpha 2 but not Interferon-gamma serum levels are associated with intramuscular fat in obese patients with nonalcoholic fatty liver disease. *J Transl Med* 2019; **17**: 8 [PMID: 30602382 DOI: 10.1186/s12967-018-1754-6]

84 **Csak T**, Ganz M, Pespisa J, Kodys K, Dolganiuc A, Szabo G. Fatty acid and endotoxin activate inflammasomes in mouse hepatocytes that release danger signals to stimulate immune cells. *Hepatology* 2011; **54**: 133-144 [PMID: 21488066 DOI: 10.1002/hep.24341]

85 **Wree A**, McGeough MD, Peña CA, Schlattjan M, Li H, Inzaugarat ME, Messer K, Canbay A, Hoffman HM, Feldstein AE. NLRP3 inflammasome activation is required for fibrosis development in NAFLD. *J Mol Med (Berl)* 2014; **92**: 1069-1082 [PMID: 24861026 DOI: 10.1007/s00109-014-1170-1]

86 **Kamari Y**, Shaish A, Vax E, Shemesh S, Kandel-Kfir M, Arbel Y, Olteanu S, Barshack I, Dotan S, Voronov E, Dinarello CA, Apte RN, Harats D. Lack of interleukin-1α or interleukin-1β inhibits transformation of steatosis to steatohepatitis and liver fibrosis in hypercholesterolemic mice. *J Hepatol* 2011; **55**: 1086-1094 [PMID: 21354232 DOI: 10.1016/j.jhep.2011.01.048]

87 **Dixon LJ**, Berk M, Thapaliya S, Papouchado BG, Feldstein AE. Caspase-1-mediated regulation of fibrogenesis in diet-induced steatohepatitis. *Lab Invest* 2012; **92**: 713-723 [PMID: 22411067 DOI: 10.1038/labinvest.2012.45]

88 **Wanninger J**, Neumeier M, Hellerbrand C, Schacherer D, Bauer S, Weiss TS, Huber H, Schäffler A, Aslanidis C, Schölmerich J, Buechler C. Lipid accumulation impairs adiponectin-mediated induction of activin A by increasing TGFbeta in primary human hepatocytes. *Biochim Biophys Acta* 2011; **1811**: 626-633 [PMID: 21070865 DOI: 10.1016/j.bbalip.2010.11.001]

89 **Bansal R**, van Baarlen J, Storm G, Prakash J. The interplay of the Notch signaling in hepatic stellate cells and macrophages determines the fate of liver fibrogenesis. *Sci Rep* 2015; **5**: 18272 [PMID: 26658360 DOI: 10.1038/srep18272]

90 **Schnabl B**, Bradham CA, Bennett BL, Manning AM, Stefanovic B, Brenner DA. TAK1/JNK and p38 have opposite effects on rat hepatic stellate cells. *Hepatology* 2001; **34**: 953-963 [PMID: 11679966 DOI: 10.1053/jhep.2001.28790]

91 **Guy CD**, Suzuki A, Zdanowicz M, Abdelmalek MF, Burchette J, Unalp A, Diehl AM, NASH CRN. Hedgehog pathway activation parallels histologic severity of injury and fibrosis in human nonalcoholic fatty liver disease. *Hepatology* 2012; **55**: 1711-1721 [PMID: 22213086 DOI: 10.1002/hep.25559]

92 **Lauer GM**, Walker BD. Hepatitis C virus infection. *N Engl J Med* 2001; **345**: 41-52 [PMID: 11439948 DOI: 10.1056/NEJM200107053450107]

93 **Blight KJ**, Kolykhalov AA, Reed KE, Agapov EV, Rice CM. Molecular virology of hepatitis C virus: an update with respect to potential antiviral targets. *Antivir Ther* 1998; **3**: 71-81 [PMID: 10726057]

94 **Tomei L**, Failla C, Santolini E, De Francesco R, La Monica N. NS3 is a serine protease required for processing of hepatitis C virus polyprotein. *J Virol* 1993; **67**: 4017-4026 [PMID: 7685406]

95 **Thomas DL**, Seeff LB. Natural history of hepatitis C. *Clin Liver Dis* 2005; **9**: 383-398, vi [PMID: 16023972 DOI: 10.1016/j.cld.2005.05.003]

96 **Lohmann V**, Körner F, Koch J, Herian U, Theilmann L, Bartenschlager R. Replication of subgenomic hepatitis C virus RNAs in a hepatoma cell line. *Science* 1999; **285**: 110-113 [PMID: 10390360]

97 **Bartenschlager R**. Hepatitis C virus replicons: potential role for drug development. *Nat Rev Drug Discov* 2002; **1**: 911-916 [PMID: 12415250 DOI: 10.1038/nrd942]

98 **Tomei L**, Altamura S, Paonessa G, De Francesco R, Migliaccio G. HCV antiviral resistance: the impact of in vitro studies on the development of antiviral agents targeting the viral NS5B polymerase. *Antivir Chem Chemother* 2005; **16**: 225-245 [PMID: 16130521]

99 **European Association for the Study of the Liver**. EASL Recommendations on Treatment of Hepatitis C 2016. *J Hepatol* 2017; **66**: 153-194 [PMID: 27667367 DOI: 10.1016/j.jhep.2016.09.001]

100 **Wang N**, Liang Y, Devaraj S, Wang J, Lemon SM, Li K. Toll-like receptor 3 mediates establishment of an antiviral state against hepatitis C virus in hepatoma cells. *J Virol* 2009; **83**: 9824-9834 [PMID: 19625408 DOI: 10.1128/JVI.01125-09]

101 **Ank N**, Iversen MB, Bartholdy C, Staeheli P, Hartmann R, Jensen UB, Dagnaes-Hansen F, Thomsen AR, Chen Z, Haugen H, Klucher K, Paludan SR. An important role for type III interferon (IFN-lambda/IL-28) in TLR-induced antiviral activity. *J Immunol* 2008; **180**: 2474-2485 [PMID: 18250457]

102 **Coenen M**, Nischalke HD, Krämer B, Langhans B, Glässner A, Schulte D, Körner C, Sauerbruch T, Nattermann J, Spengler U. Hepatitis C virus core protein induces fibrogenic actions of hepatic stellate cells *via* toll-like receptor 2. *Lab Invest* 2011; **91**: 1375-1382 [PMID: 21537327 DOI: 10.1038/labinvest.2011.78]

103 **Schulze-Krebs A**, Preimel D, Popov Y, Bartenschlager R, Lohmann V, Pinzani M, Schuppan D. Hepatitis C virus-replicating hepatocytes induce fibrogenic activation of hepatic stellate cells. *Gastroenterology* 2005; **129**: 246-258 [PMID: 16012951]

104 **Aweya JJ**, Tan YJ. Modulation of programmed cell death pathways by the hepatitis C virus. *Front Biosci (Landmark Ed)* 2011; **16**: 608-618 [PMID: 21196192]

105 **Mazzocca A**, Sciammetta SC, Carloni V, Cosmi L, Annunziato F, Harada T, Abrignani S, Pinzani M. Binding of hepatitis C virus envelope protein E2 to CD81 up-regulates matrix metalloproteinase-2 in human hepatic stellate cells. *J Biol Chem* 2005; **280**: 11329-11339 [PMID: 15611113 DOI: 10.1074/jbc.M410161200]

106 **Bataller R**, Paik YH, Lindquist JN, Lemasters JJ, Brenner DA. Hepatitis C virus core and nonstructural proteins induce fibrogenic effects in hepatic stellate cells. *Gastroenterology* 2004; **126**: 529-540 [PMID: 14762790]

107 **Lin W**, Tsai WL, Shao RX, Wu G, Peng LF, Barlow LL, Chung WJ, Zhang L, Zhao H, Jang JY, Chung RT. Hepatitis C virus regulates transforming growth factor beta1 production through the generation of reactive oxygen species in a nuclear factor kappaB-dependent manner. *Gastroenterology* 2010; **138**: 2509-2518, 2518.e1 [PMID: 20230822 DOI: 10.1053/j.gastro.2010.03.008]

108 **Tanwar S**, Trembling PM, Dusheiko GM. Hepatitis C Therapy: Lessons of the Last Two Decades. *Curr Hepat Rep* 2012; **11**: 119-127 [DOI: 10.1007/s11901-012-0141-7]

109 **Liu Z**, Wei X, Chen T, Huang C, Liu H, Wang Y. Characterization of fibrosis changes in chronic hepatitis C patients after virological cure: A systematic review with meta-analysis. *J Gastroenterol Hepatol* 2017; **32**: 548-557 [PMID: 27503423 DOI: 10.1111/jgh.13500]

110 **Akhtar E**, Manne V, Saab S. Cirrhosis regression in hepatitis C patients with sustained virological response after antiviral therapy: a meta-analysis. *Liver Int* 2015; **35**: 30-36 [PMID: 24766091 DOI: 10.1111/liv.12576]

111 **Issa R**, Zhou X, Constandinou CM, Fallowfield J, Millward-Sadler H, Gaca MD, Sands E, Suliman I, Trim N, Knorr A, Arthur MJ, Benyon RC, Iredale JP. Spontaneous recovery from micronodular cirrhosis: evidence for incomplete resolution associated with matrix cross-linking. *Gastroenterology* 2004; **126**: 1795-1808 [PMID: 15188175]

112 **Wanless IR**, Nakashima E, Sherman M. Regression of human cirrhosis. Morphologic features and the genesis of incomplete septal cirrhosis. *Arch Pathol Lab Med* 2000; **124**: 1599-1607 [PMID: 11079009 DOI: 10.1043/0003-9985(2000)124<1599:ROHC>2.0.CO;2]

113 **Fernández M**, Semela D, Bruix J, Colle I, Pinzani M, Bosch J. Angiogenesis in liver disease. *J Hepatol* 2009; **50**: 604-620 [PMID: 19157625 DOI: 10.1016/j.jhep.2008.12.011]

114 **Trautwein C**, Friedman SL, Schuppan D, Pinzani M. Hepatic fibrosis: Concept to treatment. *J Hepatol*

2015; **62**: S15-S24 [PMID: 25920084 DOI: 10.1016/j.jhep.2015.02.039]
115 **Iredale JP**, Benyon RC, Pickering J, McCullen M, Northrop M, Pawley S, Hovell C, Arthur MJ. Mechanisms of spontaneous resolution of rat liver fibrosis. Hepatic stellate cell apoptosis and reduced hepatic expression of metalloproteinase inhibitors. *J Clin Invest* 1998; **102**: 538-549 [PMID: 9691091 DOI: 10.1172/JCI1018]
116 **Fallowfield JA**, Mizuno M, Kendall TJ, Constandinou CM, Benyon RC, Duffield JS, Iredale JP. Scar-associated macrophages are a major source of hepatic matrix metalloproteinase-13 and facilitate the resolution of murine hepatic fibrosis. *J Immunol* 2007; **178**: 5288-5295 [PMID: 17404313]
117 **Ramachandran P**, Pellicoro A, Vernon MA, Boulter L, Aucott RL, Ali A, Hartland SN, Snowdon VK, Cappon A, Gordon-Walker TT, Williams MJ, Dunbar DR, Manning JR, van Rooijen N, Fallowfield JA, Forbes SJ, Iredale JP. Differential Ly-6C expression identifies the recruited macrophage phenotype, which orchestrates the regression of murine liver fibrosis. *Proc Natl Acad Sci USA* 2012; **109**: E3186-E3195 [PMID: 23100531 DOI: 10.1073/pnas.1119964109]
118 **Iredale JP**. Hepatic stellate cell behavior during resolution of liver injury. *Semin Liver Dis* 2001; **21**: 427-436 [PMID: 11586470 DOI: 10.1055/s-2001-17557]
119 **Gressner AM**. The cell biology of liver fibrogenesis - an imbalance of proliferation, growth arrest and apoptosis of myofibroblasts. *Cell Tissue Res* 1998; **292**: 447-452 [PMID: 9582401]
120 **Oakley F**, Trim N, Constandinou CM, Ye W, Gray AM, Frantz G, Hillan K, Kendall T, Benyon RC, Mann DA, Iredale JP. Hepatocytes express nerve growth factor during liver injury: evidence for paracrine regulation of hepatic stellate cell apoptosis. *Am J Pathol* 2003; **163**: 1849-1858 [PMID: 14578185 DOI: 10.1016/S0002-9440(10)63544-4]
121 **Fischer R**, Cariers A, Reinehr R, Häussinger D. Caspase 9-dependent killing of hepatic stellate cells by activated Kupffer cells. *Gastroenterology* 2002; **123**: 845-861 [PMID: 12198711]
122 **Schnabl B**, Purbeck CA, Choi YH, Hagedorn CH, Brenner D. Replicative senescence of activated human hepatic stellate cells is accompanied by a pronounced inflammatory but less fibrogenic phenotype. *Hepatology* 2003; **37**: 653-664 [PMID: 12601363 DOI: 10.1053/jhep.2003.50097]
123 **Troeger JS**, Mederacke I, Gwak GY, Dapito DH, Mu X, Hsu CC, Pradere JP, Friedman RA, Schwabe RF. Deactivation of hepatic stellate cells during liver fibrosis resolution in mice. *Gastroenterology* 2012; **143**: 1073-1083.e22 [PMID: 22750464 DOI: 10.1053/j.gastro.2012.06.036]
124 **Kisseleva T**, Cong M, Paik Y, Scholten D, Jiang C, Benner C, Iwaisako K, Moore-Morris T, Scott B, Tsukamoto H, Evans SM, Dillmann W, Glass CK, Brenner DA. Myofibroblasts revert to an inactive phenotype during regression of liver fibrosis. *Proc Natl Acad Sci USA* 2012; **109**: 9448-9453 [PMID: 22566629 DOI: 10.1073/pnas.1201840109]
125 **Rincon D**, Ripoll C, Lo Iacono O, Salcedo M, Catalina MV, Alvarez E, Nuñez O, Matilla AM, Clemente G, Bañares R. Antiviral therapy decreases hepatic venous pressure gradient in patients with chronic hepatitis C and advanced fibrosis. *Am J Gastroenterol* 2006; **101**: 2269-2274 [PMID: 17032192 DOI: 10.1111/j.1572-0241.2006.00743.x]
126 **Pockros PJ**, Hamzeh FM, Martin P, Lentz E, Zhou X, Govindarajan S, Lok AS. Histologic outcomes in hepatitis C-infected patients with varying degrees of virologic response to interferon-based treatments. *Hepatology* 2010; **52**: 1193-1200 [PMID: 20658462 DOI: 10.1002/hep.23809]
127 **Fort J**, Pilette C, Veal N, Oberti F, Gallois Y, Douay O, Rosenbaum J, Calès P. Effects of long-term administration of interferon alpha in two models of liver fibrosis in rats. *J Hepatol* 1998; **29**: 263-270 [PMID: 9722208]
128 **Inagaki Y**, Nemoto T, Kushida M, Sheng Y, Higashi K, Ikeda K, Kawada N, Shirasaki F, Takehara K, Sugiyama K, Fujii M, Yamauchi H, Nakao A, de Crombrugghe B, Watanabe T, Okazaki I. Interferon alfa down-regulates collagen gene transcription and suppresses experimental hepatic fibrosis in mice. *Hepatology* 2003; **38**: 890-899 [PMID: 14512876 DOI: 10.1053/jhep.2003.50408]
129 **Poynard T**, McHutchison J, Manns M, Trepo C, Lindsay K, Goodman Z, Ling MH, Albrecht J. Impact of pegylated interferon alfa-2b and ribavirin on liver fibrosis in patients with chronic hepatitis C. *Gastroenterology* 2002; **122**: 1303-1313 [PMID: 11984517]
130 **Di Bisceglie AM**, Shiffman ML, Everson GT, Lindsay KL, Everhart JE, Wright EC, Lee WM, Lok AS, Bonkovsky HL, Morgan TR, Ghany MG, Morishima C, Snow KK, Dienstag JL; HALT-C Trial Investigators. Prolonged therapy of advanced chronic hepatitis C with low-dose peginterferon. *N Engl J Med* 2008; **359**: 2429-2441 [PMID: 19052125 DOI: 10.1056/NEJMoa0707615]
131 **Afdhal NH**, Levine R, Brown Jr R, Freilich B, O'Brien M, Brass C. Colchicine versus PEG-interferon alfa 2b long term therapy: results of the 4 year COPILOT trial. *J Hepatol* 2008; **48**: S4 [DOI: 10.1016/s0168-8278(08)60005-7]
132 **Klein S**, Van Beuge MM, Granzow M, Beljaars L, Schierwagen R, Kilic S, Heidari I, Huss S, Sauerbruch T, Poelstra K, Trebicka J. HSC-specific inhibition of Rho-kinase reduces portal pressure in cirrhotic rats without major systemic effects. *J Hepatol* 2012; **57**: 1220-1227 [PMID: 22878469 DOI: 10.1016/j.jhep.2012.07.033]
133 **Kaps L**, Nuhn L, Aslam M, Brose A, Foerster F, Rosigkeit S, Renz P, Heck R, Kim YO, Lieberwirth I, Schuppan D, Zentel R. In Vivo Gene-Silencing in Fibrotic Liver by siRNA-Loaded Cationic Nanohydrogel Particles. *Adv Healthc Mater* 2015; **4**: 2809-2815 [PMID: 26627192 DOI: 10.1002/adhm.201500826]
134 **Canbay A**, Guicciardi ME, Higuchi H, Feldstein A, Bronk SF, Rydzewski R, Taniai M, Gores GJ. Cathepsin B inactivation attenuates hepatic injury and fibrosis during cholestasis. *J Clin Invest* 2003; **112**: 152-159 [PMID: 12865404 DOI: 10.1172/JCI17740]
135 **Canbay A**, Feldstein A, Baskin-Bey E, Bronk SF, Gores GJ. The caspase inhibitor IDN-6556 attenuates hepatic injury and fibrosis in the bile duct ligated mouse. *J Pharmacol Exp Ther* 2004; **308**: 1191-1196 [PMID: 14617689 DOI: 10.1124/jpet.103.060129]
136 **Patsenker E**, Popov Y, Stickel F, Jonczyk A, Goodman SL, Schuppan D. Inhibition of integrin alphavbeta6 on cholangiocytes blocks transforming growth factor-beta activation and retards biliary fibrosis progression. *Gastroenterology* 2008; **135**: 660-670 [PMID: 18538673 DOI: 10.1053/j.gastro.2008.04.009]
137 **Omenetti A**, Porrello A, Jung Y, Yang L, Popov Y, Choi SS, Witek RP, Alpini G, Venter J, Vandongen HM, Syn WK, Baroni GS, Benedetti A, Schuppan D, Diehl AM. Hedgehog signaling regulates epithelial-mesenchymal transition during biliary fibrosis in rodents and humans. *J Clin Invest* 2008; **118**: 3331-3342 [PMID: 18802480 DOI: 10.1172/JCI35875]
138 **Philips GM**, Chan IS, Swiderska M, Schroder VT, Guy C, Karaca GF, Moylan C, Venkatraman T, Feuerlein S, Syn WK, Jung Y, Witek RP, Choi S, Michelotti GA, Rangwala F, Merkle E, Lascola C, Diehl

AM. Hedgehog signaling antagonist promotes regression of both liver fibrosis and hepatocellular carcinoma in a murine model of primary liver cancer. *PLoS One* 2011; **6**: e23943 [PMID: 21912653 DOI: 10.1371/journal.pone.0023943]
139 **Thabut D**, Shah V. Intrahepatic angiogenesis and sinusoidal remodeling in chronic liver disease: new targets for the treatment of portal hypertension? *J Hepatol* 2010; **53**: 976-980 [PMID: 20800926 DOI: 10.1016/j.jhep.2010.07.004]
140 **Tugues S**, Fernandez-Varo G, Muñoz-Luque J, Ros J, Arroyo V, Rodés J, Friedman SL, Carmeliet P, Jiménez W, Morales-Ruiz M. Antiangiogenic treatment with sunitinib ameliorates inflammatory infiltrate, fibrosis, and portal pressure in cirrhotic rats. *Hepatology* 2007; **46**: 1919-1926 [PMID: 17935226 DOI: 10.1002/hep.21921]
141 **Karlmark KR**, Zimmermann HW, Roderburg C, Gassler N, Wasmuth HE, Luedde T, Trautwein C, Tacke F. The fractalkine receptor CXCR1 protects against liver fibrosis by controlling differentiation and survival of infiltrating hepatic monocytes. *Hepatology* 2010; **52**: 1769-1782 [PMID: 21038415 DOI: 10.1002/hep.23894]
142 **Sahin H**, Borkham-Kamphorst E, Kuppe C, Zaldivar MM, Grouls C, Al-samman M, Nellen A, Schmitz P, Heinrichs D, Berres ML, Doleschel D, Scholten D, Weiskirchen R, Moeller MJ, Kiessling F, Trautwein C, Wasmuth HE. Chemokine Cxcl9 attenuates liver fibrosis-associated angiogenesis in mice. *Hepatology* 2012; **55**: 1610-1619 [PMID: 22237831 DOI: 10.1002/hep.25545]
143 **Barry-Hamilton V**, Spangler R, Marshall D, McCauley S, Rodriguez HM, Oyasu M, Mikels A, Vaysberg M, Ghermazien H, Wai C, Garcia CA, Velayo AC, Jorgensen B, Biermann D, Tsai D, Green J, Zaffryar-Eilot S, Holzer A, Ogg S, Thai D, Neufeld G, Van Vlasselaer P, Smith V. Allosteric inhibition of lysyl oxidase-like-2 impedes the development of a pathologic microenvironment. *Nat Med* 2010; **16**: 1009-1017 [PMID: 20818376 DOI: 10.1038/nm.2208]
144 **Harrison SA**, Fecht W, Brunt EM, Neuschwander-Tetri BA. Orlistat for overweight subjects with nonalcoholic steatohepatitis: A randomized, prospective trial. *Hepatology* 2009; **49**: 80-86 [PMID: 19053049 DOI: 10.1002/hep.22575]
145 **Promrat K**, Kleiner DE, Niemeier HM, Jackvony E, Kearns M, Wands JR, Fava JL, Wing RR. Randomized controlled trial testing the effects of weight loss on nonalcoholic steatohepatitis. *Hepatology* 2010; **51**: 121-129 [PMID: 19827166 DOI: 10.1002/hep.23276]
146 **Vilar-Gomez E**, Martinez-Perez Y, Calzadilla-Bertot L, Torres-Gonzalez A, Gra-Oramas B, Gonzalez-Fabian L, Friedman SL, Diago M, Romero-Gomez M. Weight Loss Through Lifestyle Modification Significantly Reduces Features of Nonalcoholic Steatohepatitis. *Gastroenterology* 2015; **149**: 367-378.e5; quiz e14-15 [PMID: 25865049 DOI: 10.1053/j.gastro.2015.04.005]
147 **Cariou B**, Hanf R, Lambert-Porcheron S, Zaïr Y, Sauvinet V, Noël B, Flet L, Vidal H, Staels B, Laville M. Dual peroxisome proliferator-activated receptor α/δ agonist GFT505 improves hepatic and peripheral insulin sensitivity in abdominally obese subjects. *Diabetes Care* 2013; **36**: 2923-2930 [PMID: 23715754 DOI: 10.2337/dc12-2012]
148 **Belfort R**, Harrison SA, Brown K, Darland C, Finch J, Hardies J, Balas B, Gastaldelli A, Tio F, Pulcini J, Berria R, Ma JZ, Dwivedi S, Havranek R, Fincke C, DeFronzo R, Bannayan GA, Schenker S, Cusi K. A placebo-controlled trial of pioglitazone in subjects with nonalcoholic steatohepatitis. *N Engl J Med* 2006; **355**: 2297-2307 [PMID: 17135584 DOI: 10.1056/NEJMoa060326]
149 **Promrat K**, Lutchman G, Uwaifo GI, Freedman RJ, Soza A, Heller T, Doo E, Ghany M, Premkumar A, Park Y, Liang TJ, Yanovski JA, Kleiner DE, Hoofnagle JH. A pilot study of pioglitazone treatment for nonalcoholic steatohepatitis. *Hepatology* 2004; **39**: 188-196 [PMID: 14752837 DOI: 10.1002/hep.20012]
150 **Sanyal AJ**, Chalasani N, Kowdley KV, McCullough A, Diehl AM, Bass NM, Neuschwander-Tetri BA, Lavine JE, Tonascia J, Unalp A, Van Natta M, Clark J, Brunt EM, Kleiner DE, Hoofnagle JH, Robuck PR, NASH CRN. Pioglitazone, vitamin E, or placebo for nonalcoholic steatohepatitis. *N Engl J Med* 2010; **362**: 1675-1685 [PMID: 20427778 DOI: 10.1056/NEJMoa0907929]
151 **Porez G**, Prawitt J, Gross B, Staels B. Bile acid receptors as targets for the treatment of dyslipidemia and cardiovascular disease. *J Lipid Res* 2012; **53**: 1723-1737 [PMID: 22550135 DOI: 10.1194/jlr.R024794]
152 **Neuschwander-Tetri BA**, Loomba R, Sanyal AJ, Lavine JE, Van Natta ML, Abdelmalek MF, Chalasani N, Dasarathy S, Diehl AM, Hameed B, Kowdley KV, McCullough A, Terrault N, Clark JM, Tonascia J, Brunt EM, Kleiner DE, Doo E; NASH Clinical Research Network. Farnesoid X nuclear receptor ligand obeticholic acid for non-cirrhotic, non-alcoholic steatohepatitis (FLINT): a multicentre, randomised, placebo-controlled trial. *Lancet* 2015; **385**: 956-965 [PMID: 25468160 DOI: 10.1016/S0140-6736(14)61933-4]
153 **Safadi R**, Konikoff FM, Mahamid M, Zelber-Sagi S, Halpern M, Gilat T, Oren R; FLORA Group. The fatty acid-bile acid conjugate Aramchol reduces liver fat content in patients with nonalcoholic fatty liver disease. *Clin Gastroenterol Hepatol* 2014; **12**: 2085-2091.e1 [PMID: 24815326 DOI: 10.1016/j.cgh.2014.04.038]
154 **Dongiovanni P**, Petta S, Mannisto V, Mancina RM, Pipitone R, Karja V, Maggioni M, Kakela P, Wiklund O, Mozzi E, Grimaudo S, Kaminska D, Rametta R, Craxi A, Fargion S, Nobili V, Romeo S, Pihlajamaki J, Valenti L. Statin use and non-alcoholic steatohepatitis in at risk individuals. *J Hepatol* 2015; **63**: 705-712 [PMID: 25980762 DOI: 10.1016/j.jhep.2015.05.006]
155 **Carbone LJ**, Angus PW, Yeomans ND. Incretin-based therapies for the treatment of non-alcoholic fatty liver disease: A systematic review and meta-analysis. *J Gastroenterol Hepatol* 2016; **31**: 23-31 [PMID: 26111358 DOI: 10.1111/jgh.13026]
156 **Sanyal AJ**, Mofrad PS, Contos MJ, Sargeant C, Luketic VA, Sterling RK, Stravitz RT, Shiffman ML, Clore J, Mills AS. A pilot study of vitamin E versus vitamin E and pioglitazone for the treatment of nonalcoholic steatohepatitis. *Clin Gastroenterol Hepatol* 2004; **2**: 1107-1115 [PMID: 15625656]
157 **Lavine JE**, Schwimmer JB, Van Natta ML, Molleston JP, Murray KF, Rosenthal P, Abrams SH, Scheimann AO, Sanyal AJ, Chalasani N, Tonascia J, Ünalp A, Clark JM, Brunt EM, Kleiner DE, Hoofnagle JH, Robuck PR; Nonalcoholic Steatohepatitis Clinical Research Network. Effect of vitamin E or metformin for treatment of nonalcoholic fatty liver disease in children and adolescents: the TONIC randomized controlled trial. *JAMA* 2011; **305**: 1659-1668 [PMID: 21521847 DOI: 10.1001/jama.2011.520]
158 **Zein CO**, Lopez R, Fu X, Kirwan JP, Yerian LM, McCullough AJ, Hazen SL, Feldstein AE. Pentoxifylline decreases oxidized lipid products in nonalcoholic steatohepatitis: new evidence on the potential therapeutic mechanism. *Hepatology* 2012; **56**: 1291-1299 [PMID: 22505276 DOI: 10.1002/hep.25778]
159 **Fleming KM**, Aithal GP, Card TR, West J. The rate of decompensation and clinical progression of disease

in people with cirrhosis: a cohort study. *Aliment Pharmacol Ther* 2010; **32**: 1343-1350 [PMID: 21050236 DOI: 10.1111/j.1365-2036.2010.04473.x]

160 **Ratib S**, Fleming KM, Crooks CJ, Aithal GP, West J. 1 and 5 year survival estimates for people with cirrhosis of the liver in England, 1998-2009: a large population study. *J Hepatol* 2014; **60**: 282-289 [PMID: 24128415 DOI: 10.1016/j.jhep.2013.09.027]

161 **Puoti C**, Guarisco R, Spilabotti L, Bellis L, Mitidieri Costanza O, Dell' Unto O, Elmo MG. Should we treat HCV carriers with normal ALT levels? The '5Ws' dilemma. *J Viral Hepat* 2012; **19**: 229-235 [PMID: 22404720 DOI: 10.1111/j.1365-2893.2011.01485.x]

162 **Park JJ**, Park JY, Kim DY, Park YN, Ahn SH, Chon CY, Han KH. Prediction of significant fibrosis in chronic hepatitis C patients with normal ALT. *Hepatogastroenterology* 2011; **58**: 1321-1327 [PMID: 21937403 DOI: 10.5754/hge11041]

163 **Rockey DC**, Caldwell SH, Goodman ZD, Nelson RC, Smith AD; American Association for the Study of Liver Diseases. Liver biopsy. *Hepatology* 2009; **49**: 1017-1044 [PMID: 19243014 DOI: 10.1002/hep.22742]

164 **Ebaid A**. Analytical solutions for the mathematical model describing the formation of liver zones *via* Adomian's method. *Comput Math Methods Med* 2013; **2013**: 547954 [PMID: 24069066 DOI: 10.1155/2013/547954]

165 **Betts JYK**, Wise J, Johnson E, Poe B, Kruse D, Korol O, Johnson J, Womble M, DeSaix P. Anatomy & Physiology. Texas: OpenStax, 2013

166 **Chouhan MD**, Lythgoe MF, Mookerjee RP, Taylor SA. Vascular assessment of liver disease-towards a new frontier in MRI. *Br J Radiol* 2016; **89**: 20150675 [PMID: 27115318 DOI: 10.1259/bjr.20150675]

World Journal of Gastroenterology

Submit a Manuscript: https://www.f6publishing.com

World J Gastroenterol 2020 January 14; 26(2): 134-153

DOI: 10.3748/wjg.v26.i2.134

ISSN 1007-9327 (print) ISSN 2219-2840 (online)

ORIGINAL ARTICLE

Basic Study

Construction of a risk score prognosis model based on hepatocellular carcinoma microenvironment

Fa-Peng Zhang, Yi-Pei Huang, Wei-Xin Luo, Wan-Yu Deng, Chao-Qun Liu, Lei-Bo Xu, Chao Liu

ORCID number: Fa-Peng Zhang (0000-0002-1361-5536); Yi-Pei Huang (0000-0003-3098-9123); Wei-Xin Luo (0000-0001-6804-2520); Wan-Yu Deng (0000-0001-7789-3861); Chao-Qun Liu (0000-0002-0491-573X); Lei-Bo Xu (0000-0002-9236-5343); Chao Liu (0000-0001-6659-4372).

Author contributions: Zhang FP, Xu LB and Liu C designed the research; Zhang FP, Huang YP and Luo WX collected and analyzed data; Deng WY and Liu CQ prepared the figures; Zhang FP, Xu LB and Liu C wrote and revised the manuscript.

Supported by National Natural Science Foundation of China, No. 81972255, No. 81772597 and No. 81672412; Guangdong Natural Science Foundation, No. 2017A030311002; Guangdong Science and Technology Foundation, No. 2017A020215196; Fundamental Research Funds for the Central Universities of Sun Yat-Sen University, No. 17ykpy44; Science Foundation of Jiangxi, No. 20181BAB214002; Education Department Science and Technology Foundation of Jiangxi, No. GJJ170936; and Grant from Guangdong Science and Technology Department, No. 2017B030314026.

Institutional review board statement: This study was reviewed and approved by the Ethics Committee of the Sun Yat-Sen Memorial Hospital, Guangzhou, China.

Conflict-of-interest statement: All authors declare no conflict-of-

Fa-Peng Zhang, Yi-Pei Huang, Wei-Xin Luo, Wan-Yu Deng, Chao-Qun Liu, Lei-Bo Xu, Chao Liu, Department of Biliary Pancreatic Surgery, Sun Yat-Sen Memorial Hospital, Sun Yat-Sen University, Guangzhou 510120, Guangdong Province, China

Fa-Peng Zhang, Yi-Pei Huang, Wei-Xin Luo, Wan-Yu Deng, Chao-Qun Liu, Lei-Bo Xu, Chao Liu, Guangdong Provincial Key Laboratory of Malignant Tumor Epigenetics and Gene Regulation, Sun Yat-Sen Memorial Hospital, Sun Yat-Sen University, Guangzhou 510120, Guangdong Province, China

Wan-Yu Deng, College of Life Science, Shangrao Normal University, Shangrao 334001, Jiangxi Province, China

Corresponding author: Chao Liu, MD, PhD, Chairman, Director, Professor, Department of Hepato-Pancreato-Biliary Surgery, Sun Yat-Sen Memorial Hospital, Sun Yat-Sen University, Guangzhou 510120, Guangdong Province, China. liuchao3@mail.sysu.edu.cn

Abstract

BACKGROUND

Hepatocellular carcinoma (HCC) is a common cancer with a poor prognosis. Previous studies revealed that the tumor microenvironment (TME) plays an important role in HCC progression, recurrence, and metastasis, leading to poor prognosis. However, the effects of genes involved in TME on the prognosis of HCC patients remain unclear. Here, we investigated the HCC microenvironment to identify prognostic genes for HCC.

AIM

To identify a robust gene signature associated with the HCC microenvironment to improve prognosis prediction of HCC.

METHODS

We computed the immune/stromal scores of HCC patients obtained from The Cancer Genome Atlas based on the ESTIMATE algorithm. Additionally, a risk score model was established based on Differentially Expressed Genes (DEGs) between high and lowimmune/stromal score patients.

RESULTS

The risk score model consisting of eight genes was constructed and validated in the HCC patients. The patients were divided into high- or low-risk groups. The genes (Disabled homolog 2, Musculin, C-X-C motif chemokine ligand 8, Galectin 3, B-cell-activating transcription factor, Killer cell lectin like receptor B1, Endoglin and adenomatosis polyposis coli tumor suppressor) involved in our risk score

interest related to this article.

Data sharing statement: The data used in this manuscript are accessible at https://cancergenome.nih.gov/, https://icgc.org/, and https://www.ncbi.nlm.nih.gov/geo/.

ARRIVE guidelines statement: The authors have read the ARRIVE guidelines, and the manuscript was prepared and revised according to the ARRIVE guidelines.

Manuscript source: Invited Manuscript

Received: September 30, 2019
Peer-review started: September 30, 2019
First decision: November 10, 2019
Revised: November 23, 2019
Accepted: December 7, 2019
Article in press: January 7, 2020
Published online: January 14, 2020

P-Reviewer: Elshaarawy O, Sukocheva O
S-Editor: Tang JZ
L-Editor: Ma JY
E-Editor: Qi LL

model were considered to be potential immunotherapy targets, and they may provide better performance in combination. Functional enrichment analysis showed that the immune response and T cell receptor signaling pathway represented the major function and pathway, respectively, related to the immune-related genes in the DEGs between high- and low-risk groups. The receiver operating characteristic (ROC) curve analysis confirmed the good potency of the risk score prognostic model. Moreover, we validated the risk score model using the International Cancer Genome Consortium and the Gene Expression Omnibus database. A nomogram was established to predict the overall survival of HCC patients.

CONCLUSION
The risk score model and the nomogram will benefit HCC patients through personalized immunotherapy.

Key words: Hepatocellular carcinoma; Prognostic model; Immune related gene; Microenvironment; Risk score; Overall survival

Core tip: We constructed a risk score model based on hepatocellular carcinoma (HCC) microenvironment that could predict the overall survival (OS) of HCC. It has a high sensitivity and specificity in predicting the OS, and was validated using the Gene Expression Omnibus and the International Cancer Genome Consortium dataset. In addition, the risk score model is associated with immunosuppressive environment and immune checkpoint expression, which will assist clinicians in selecting personalized immunotherapy for HCC patients.

Citation: Zhang FP, Huang YP, Luo WX, Deng WY, Liu CQ, Xu LB, Liu C. Construction of a risk score prognosis model based on hepatocellular carcinoma microenvironment. *World J Gastroenterol* 2020; 26(2): 134-153
URL: https://www.wjgnet.com/1007-9327/full/v26/i2/134.htm
DOI: https://dx.doi.org/10.3748/wjg.v26.i2.134

INTRODUCTION

Hepatocellular carcinoma (HCC) is the sixth most common cancer worldwide and is the main cause of cancer-related death[1]. Although there are multiple methods to treat HCC, including surgical resection, liver transplantation, radiofrequency ablation and chemotherapy, the efficacy is limited by high recurrence rates and low rates of surgery and transplants because this cancer is usually diagnosed in a late stage[2-4]. Recently, immunotherapy has emerged as a novel and effective therapy and is being applied in various tumors including HCC[5]. In particular, treatment targeting immune checkpoints has achieved success and improved patient survival[6-8]. However, only a small number of patients receiving immunotherapy treatment responded to the treatment due to the immunosuppressive microenvironment. Hence, it is necessary to investigate biomarkers that enable us to predict the benefit of immunotherapy, which may help in clinical decision making for individualized treatment.

The HCC microenvironment includes various cells, such as hepatic stellate cells, cancer-associated fibroblasts, endothelial cells, neuroendocrine cells, immune cells, bone-marrow derived cells, and the extracellular matrix (ECM), which plays a crucial role in tumor initiation, progression, drug resistance and immune escaping[9-15]. Immune cell infiltration is closely related to the survival of patients[16-20], indicating that understanding and reshaping the tumor microenvironment (TME) may improve the efficacy of cancer treatments in the future[21-23]. ESTIMATE was an algorithm designed by Yoshihara *et al*[24] to calculate immune and stromal scores based on the gene expression profile. Subsequent studies have applied the ESTIMATE algorithm in multiple cancers such as prostate cancer[25], breast cancer[26], and colon cancer[27], showing the capability of such big-data based algorithms, although the efficacy on HCC has not been verified.

In our study, we investigated the TME and the gene expression profile of HCC to construct a risk score prognostic model for HCC based on The Cancer Genome Atlas (TCGA) database. Furthermore, we have validated this model using the International Cancer Genome Consortium (ICGC) and Gene Expression Omnibus (GEO) databases.

MATERIALS AND METHODS

Gene expression datasets

The data of this study was mainly obtained from public databases. The transcriptional profiles and clinical materials from HCC patients were downloaded from the TCGA website (https://cancergenome.nih.gov/). HCC patients with R0 surgical resection were chosen, who did not receive other treatment for their disease and had a survival time of more than 1 mo. Among these patients, 361 HCC samples with complete transcriptional data and the corresponding clinical information were selected for consequent analyses. Immune and stromal scores were calculated by applying the ESTIMATE algorithm to the mRNA expression data[24]. For further verification, the code of LIRI-JP (n = 232) obtained from the ICGC database (https://icgc.org/) and the dataset GSE14520 (n = 221) downloaded from the GEO (https://www.ncbi.nlm.nih.gov/geo/) database were selected for validation. The data downloaded from the TCGA, ICGC, and GEO databases were publicly available and accessible. The present study was conducted following pertinent guidelines and regulations approved by the TCGA, ICGC, and GEO.

Differentially expressed genes analysis

To select the intersection genes, 361 HCC patients obtained from the TCGA dataset were divided into high and low immune/stromal score groups according to the ESTIMATE results. The differentially expressed genes (DEGs) were identified using the package limma[28] in R software (Version 3.6.1; https://www.r-project.org/), and the cutoffs were fold change > 1.5 and adjust $P < 0.05$. Volcano plot and heatmaps were generated using the ggplot2 and pheatmap package in R software, respectively.

Overall survival curve

Kaplan-Meier (K-M) plots were generated to illustrate the correlation of immune/stromal scores with patients' overall survival (OS). The relationship was tested by the log-rank test.

Functional enrichment analysis of DEGs

The Gene Ontology (GO) and Kyoto Encyclopedia of Genes and Genomes (KEGG) pathway enrichment analyses of DEGs were performed using the Database for Annotation, Visualization and Integrated Discovery (Version: 6.8; https:// david.ncifcrf.gov/) to investigate the potential function of the DEGs[29]. Significant biological processes and pathways were presented using the ggplot2 R packages.

Construction and validation of the risk score prognostic model

Univariate, the Least Absolute Shrinkage and Selection Operator (LASSO) and multivariate Cox regression analyses were performed to explore the relationship between DEGs and patients' OS. In the univariate Cox regression analysis, $P < 0.05$ was considered significant. To further narrow down correlated genes, the LASSO with L1-penalty was applied[30]. Based on the LASSO analysis, the pivotal genes were extracted from DEGs which were regarded as significant in the univariate Cox regression analysis. Then, a sub-selection of genes associated with patient prognosis was identified[31]. LASSO Cox regression analysis was performed using the glmnet R package (Version: 2.0). To evaluate the contribution of each gene to prognosis, the multivariate Cox regression analysis was performed. A stepwise method was used to further determine the best rprognostic model. Finally, eight genes were selected to construct a risk score prognosis model. HCC patients were divided into low- and high-risk groups based on the median risk score. The K-M survival curves for the cases with low or high risk were performed. The predictive ability of the risk score prognosis model was assessed by the survival receiver operating characteristic (ROC) package in R software. The concordance index (C-index) was calculated to investigate the risk score prognostic model performance[32]. Then, the risk score prognosis model was verified using the ICGC and GEO dataset, respectively.

Estimated immune cell type fractions

CIBERSORT is a gene expression-based deconvolution algorithm to describe the cell constitution of tissues[33]. LM22 is defined as "barcodes" with 547 gene expression signatures that distinguish 22 human hematopoietic cell phenotypes, including

plasma cells, myeloid subsets, seven T cell types, naive and memory B cells and natural killer (NK) cells. We used CIBERSORT in combination with LM22 to sort the portions of 22 human immune cell types in HCC samples. For each sample, the sum of all estimate immune cell type fractions equals to 1[34].

Independence of the risk score prognostic model

Among 361 HCC patients with survival data, 289 patients with full clinical parameters, including gender, age, histologic grade, pathologic stage and vascular invasion, were subjected to consequent analyses. Univariate and multivariate Cox regression analyses were performed to assess the predictive ability of the risk score prognostic model for HCC patients. All statistical tests were two-sided, and *P* values < 0.05 were considered as statistically significant.

Construction and validation of the nomogram

The nomogram is widely utilized to predict the prognosis of cancer patients' prognosis[35]. In the present study, a nomogram was generated based on the independent prognostic factors identified by multivariate analysis to investigate the probability of 1-, 3-, and 5-year OS of HCC patients. The nomogram and calibration plots were generated using the rms R package (Version: 5.1-3). The calibration curve of the nomogram was drawn to evaluate the nomogram prediction possibilities against the observed rates[36].

Statistical analysis

The R software v3.6.1 (R Foundation for Statistical Computing, Vienna, Austria) and GraphPad Prism v8.0 (GraphPad Software Inc., United States) were used for statistical analyses. All statistical tests were two-tailed with a statistical significance level set at 0.05.

RESULTS

Immune scores and stromal scores are significantly related to HCC prognosis

The flow chart of the study procedure is presented in Figure 1. In this study, 361 HCC patients with complete gene expression data and the corresponding clinical information were downloaded from the TCGA database for subsequent analysis. As shown in Supplementary Table 1, patients were 59.65 ± 13.33 years old, including 116 females (32.1%) and 245 females (67.9%). According to the ESTIMATE algorithm, immune scores ranged from -1209.16 and 2934.36, and stromal scores ranged from -1741.56 to 1195.07. Then, we investigated the relationship between immune/stromal scores and clinical characteristics. The result showed that the immune score was significantly negatively correlated with the pathologic stage ($P = 0.032$) (Figure 2B), but not with histologic grade ($P = 0.968$) (Figure 2A). In contrast, the stromal score was significantly negatively related to histologic stage ($P = 0.008$) (Figure 2C), but not with pathologic grade ($P = 0.329$) (Figure 2D).

To investigate the influence of immune/stromal scores on prognosis, we divided 316 HCC patients into high- and low-score groups and constructed K-M curves. We found that the immune scores and stromal scores were significantly positively correlated with OS (Figure 2E and F). Overall, we found that the immune and stromal scores were significantly correlated with poor prognosis.

Comparison of gene expression profiles with immune scores and stromal scores in HCC

To explore the difference of gene expression profiles between high- and low-immune/stromal score groups, we compared 361 HCC cases obtained from the TCGA database. Volcano maps in Supplementary Figure 1 showed the differential gene results of the low *vs* high score group differential gene results. Heatmaps showed the most different 100 gene expression profiles of cases belonging to low and high immune scores/stromal scores groups. In comparison to the high immune scores group, 689 genes were downregulated and 106 genes were upregulated in the low-immune score group (Supplementary Table 2). Similarly, there were 906 downregulated genes and 91 upregulated genes in the low stromal - score group (Supplementary Table 3). In addition, Venn diagrams (Figure 3A) showed that 13 genes (Supplementary Table 4) were commonly upregulated in the low score groups, and 473 genes were commonly downregulated (Supplementary Table 5).

Furthermore, the potential functions of the DEGs were evaluated by GO analysis and KEGG pathway. The top 5 GO terms identified included immune response, inflammatory response, cell adhesion, chemotaxis and extracellular matrix

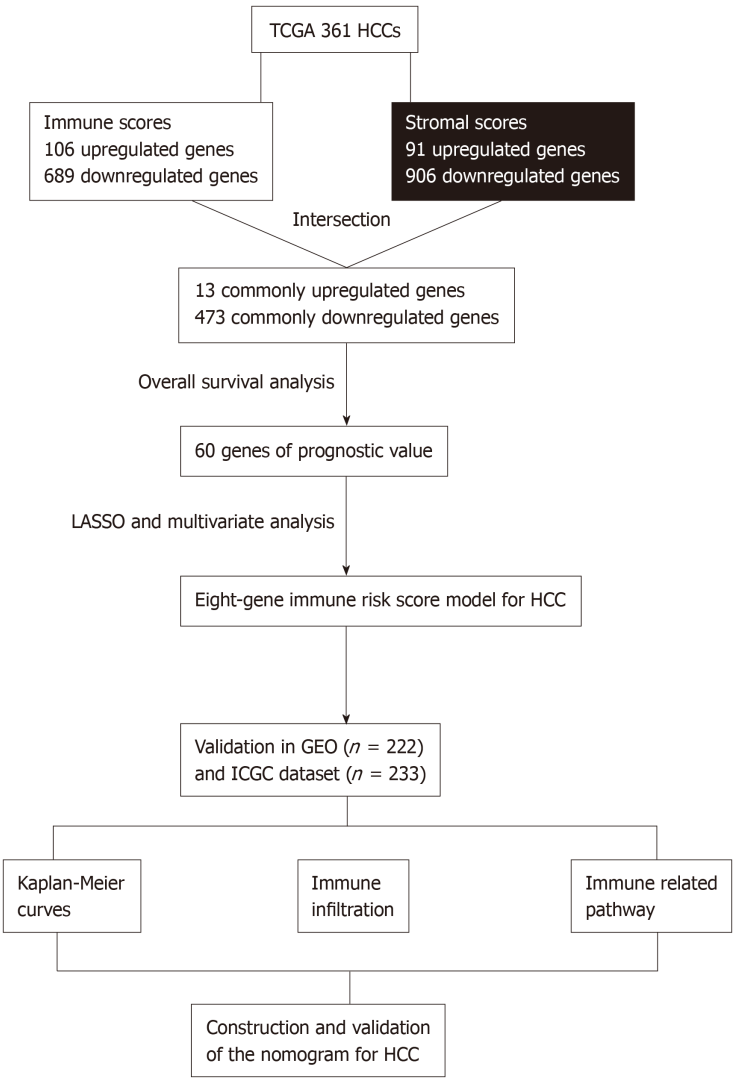

Figure 1 Overall design of the present study. TCGA: The Cancer Genome Atlas database; HCC: Hepatocellular carcinoma; LASSO: Least absolute shrinkage and selection operator; GEO: Gene Expression Omnibus databases; ICGC: International Cancer Genome Consortium database.

organization (Supplementary Figure 2). The KEGG pathway analysis revealed that the DEGs were enriched in the tumor necrosis factor signaling pathway, cytokine-cytokine receptor interaction, complement and coagulation cascades, chemokine signaling pathway, and cell adhesion molecules (Figure 3B).

Construction of a risk score model and evaluation of its predictive ability in the TCGA HCC cohort

To explore the potential roles of DEGs in OS, a univariate analysis was performed. The results showed that 60 of the 486 intersection DEGs were significantly correlated with OS in HCC patients (Supplementary Table 6). To screen the most prognostic genes, LASSO analysis was performed. The contributions of 60 intersection DEGS were weighted by their relative coefficients (Supplementary Figure 3A and B). As a result, 13 genes were selected (Supplementary Table 7). Lastly, a multivariate analysis was performed, and 8 genes were chosen to establish a risk score model (Supplementary Figure 3C and Supplementary Table 8), and the final risk score formula was as follows: Risk score = [0.184 × expression level of Disabled homolog 2 (DAB2)] + [0.102 × expression level of Musculin (MSC)] + [0.118 × expression level of C-X-C motif chemokine ligand 8 (CXCL8)] + [0.147 × expression level of Galectin 3 (LGALS3)] + [0.147 × expression level of B-cell-activating transcription factor (BATF)] + [0.48 × expression level of killer cell lectin like receptor B1 (KLRB1)] + [0.393 × expression level of Endoglin (ENG)] + [0.113 × expression level of Adenomatosis polyposis coli tumor suppressor (APCS)]. We then calculated the risk score according to the formula and divided the patients into high- or low-risk groups based on the median risk score. According to the K-M analysis (Figure 4A), there was a significant difference in

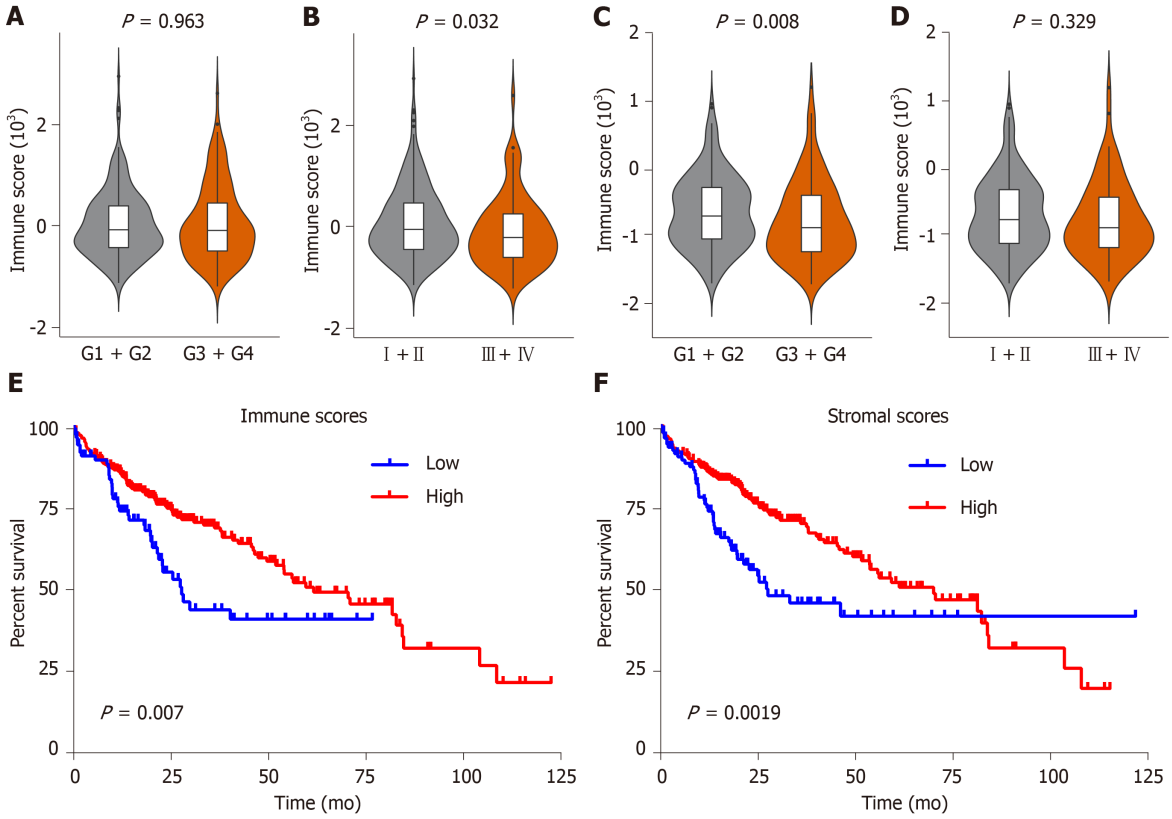

Figure 2 Immune and stromal scores are associated with clinical characteristics and overall survival of hepatocellular carcinoma patients in the Cancer Genome Atlas database dataset. A-D: Correlation of the immune/stromal score with histologic grade and pathologic stage; E: Hepatocellular carcinoma (HCC) cases were divided into two groups based on their immune scores, as indicated by the log-rank test; F: Similarly, HCC cases were divided into two groups based on their stromal scores, as indicated by the log-rank test. TCGA: The Cancer Genome Atlas database; HCC: Hepatocellular carcinoma.

patients' OS between high- and low-risk groups, and patients in the high-risk group had significantly shorter OS than those in the low-risk group. Figure 4B shows the distribution of the risk score and gene expression data. The prediction capability of the risk score model was evaluated by calculating the area under the ROC curve (AUC) (Figure 4C). The AUC of the prognostic model for OS was 0.778, 0.754 and 0.75 for the first, third, and fifth years, respectively, suggesting that the risk score model had good performance.

Validating the risk score model in GEO and ICGC dataset

To verify the robustness of our findings, this risk score model was further evaluated using the GEO and ICGC dataset, which included 222 and 233 HCC patients. The patients from the GEO and ICGC dataset were divided into high- and low-risk groups based on the previous formula. In agreement with the previous results, patients in the high-risk group had significantly worse OS than the low-risk group (Figure 4E and I). Figure 4F and J show the distribution of the risk score and gene expression data from the GEO and ICGC HCC cohort. Furthermore, the risk score model yielded an AUC of 0.661 at 1 year, 0.663 at 3 years and 0.676 at 5 years based on the GEO HCC cohort data (Figure 4G), and an AUC of 0.753 at 1 years, 0.65 at 3 years, and 0.715 at 5 years based on the ICGC HCC cohort data (Figure 4K). Recently, Long *et al*[36] constructed an immune prognostic model (IPM) including two genes (Triggering Receptor Expressed On Monocytes 1 and Exonuclease 1) to assess the prognosis of HCC patients. We calculated the C-indexes to compare the prognostic values of their model and our risk score model. As shown in Figure 4D, 4H and 4L, the concordance index of the risk score model for the first-, third-, and fifth-year OS was higher than the IPM in the TCGA, GEO and ICGC HCC cohorts, indicating that our risk score model had a better performance in evaluating prognosis. Above all, the risk score prognosis model is robust and efficient.

The difference of immune infiltration between the low- and high-risk HCC patients in the TCGA database

We estimated the difference of immune infiltration between low- and high-risk HCC patients in 22 subpopulations of immune cells using the CIBERSORT algorithm. The

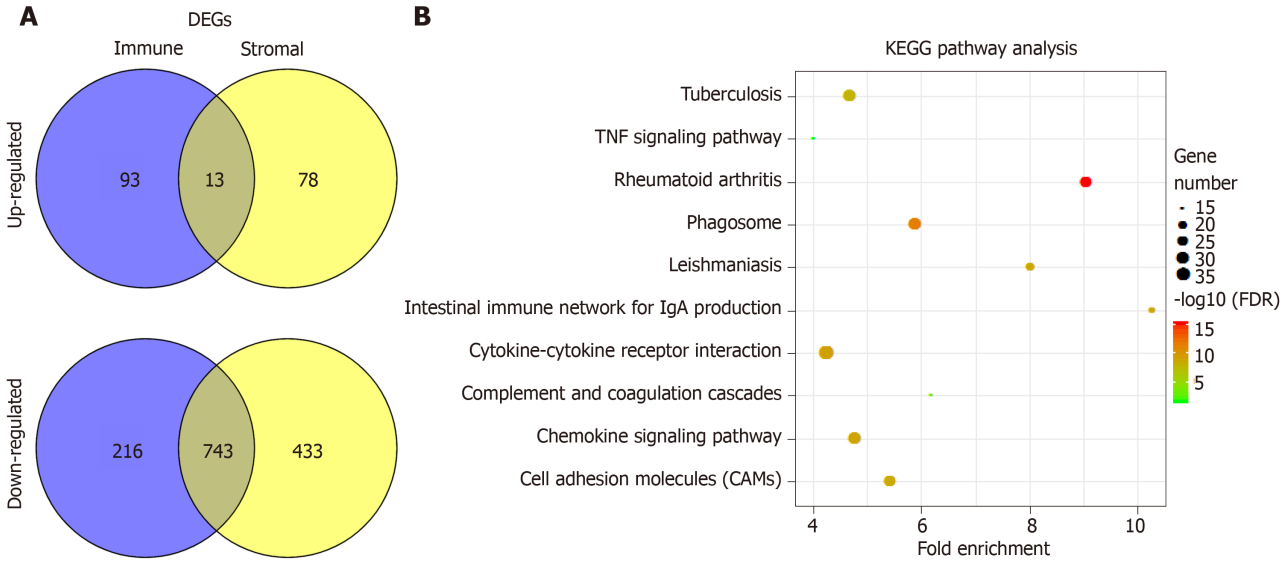

Figure 3 Comparison of gene expression profile with immune scores and stromal scores of hepatocellular carcinoma in the Cancer Genome Atlas database dataset. A: Venn diagrams showing the number of commonly upregulated or downregulated differentially expressed genes (DEGs) in stromal and immune score groups; B: Kyoto encyclopedia of genes and genomes (KEGG) analysis of DEGs, top 10 GO terms were displayed. False discovery rate of KEGG analysis was acquired from the database for annotation, visualization and integrated discovery functional annotation tool. DEGs: Differentially expressed genes; TNF: Tumor necrosis factor; KEGG: Kyoto encyclopedia of genes and genomes; DAVID: Database for annotation, visualization and integrated discovery.

proportion of immune cells in HCC varied significantly between the high- and low-risk groups (Figure 5A and B). Figure 5C shows that a high fraction of M0 macrophages, T regulatory cells (Tregs) and T follicular helper cells (Tfh) mainly infiltrated in high-risk group patients. In contrast, a high fraction of CD8 T cells, resting CD4 memory T cells and monocytes mainly infiltrated in low-risk HCC patients. In addition, the proportions of different tumor-infiltrating immune cells (TIICs) showed a weak to moderate correlation (Figure 5D). Therefore, these results indicated that the different immune infiltration in patients with HCC could be used as a prognostic indicator and targets for immunotherapy.

Immunotherapy is increasingly applied to the clinical management of multiple tumors. However, only a part of patients with cancer showed a response to immunotherapy, and the efficacy of immunotherapy can be improved by identifying the type of immune infiltration. Hence, we investigated the relationship between patient risk scores and the expression of commonly immune checkpoints, and the results showed that the risk score was significantly associated with the expression of cytotoxic T-Lymphocyte associated protein 4 (CTLA-4), programmed cell death 1 (PD-1), and T-cell immunoglobulin mucin receptor 3 (TIM-3) ($P < 0.05$) (Figure 6A, Supplementary Table 9). Furthermore, we explored the expression of the immune checkpoints in the high- and low-risk HCC patients. High-risk HCC patients had significantly higher expression of CTLA-4, PD-1 and TIM-3 than the low-risk HCC patients ($P < 0.05$) (Figure 6B-D). Additionally, there was no significant difference in the expression of T Cell Immunoreceptor With Ig And ITIM Domains and Lymphocyte-activation gene 3 between the high- and low-risk HCC group (Supplementary Figure 4A and B). This suggests that the immunosuppressive microenvironment in high-risk patients may be responsible for their poor prognosis.

Alteration in immune-related pathways between high- and low-risk group patients

To investigate the difference of immune genes between high- and low-risk patients, we compared the gene expression profiles between the two groups. A total of 332 immune-related genes were extracted from the Molecular Signatures Database v6.2[20] [(Immune system process M13664, Immune response M19817); http://www.broadinstitute.org/gsea/msigdb/index.jsp]. The results showed that there were 193 immune-related genes in the DEGs between high- and low-risk groups (Supplementary Figure 4C). Furthermore, the GO and KEGG pathway analysis was performed to identify the potential functions of the 193 immune-related genes that were differentially expressed (Figure 6E and F, Supplementary Figure 4D and E) (Supplementary Table 10). The top 5 GO terms identified included immune response, inflammatory response, innate immune response, and cell-cell signaling (Figure 6E). The KEGG pathway analysis showed that these genes were enriched in the T cell receptor signaling pathway, cytokine-cytokine receptor interaction, rheumatoid

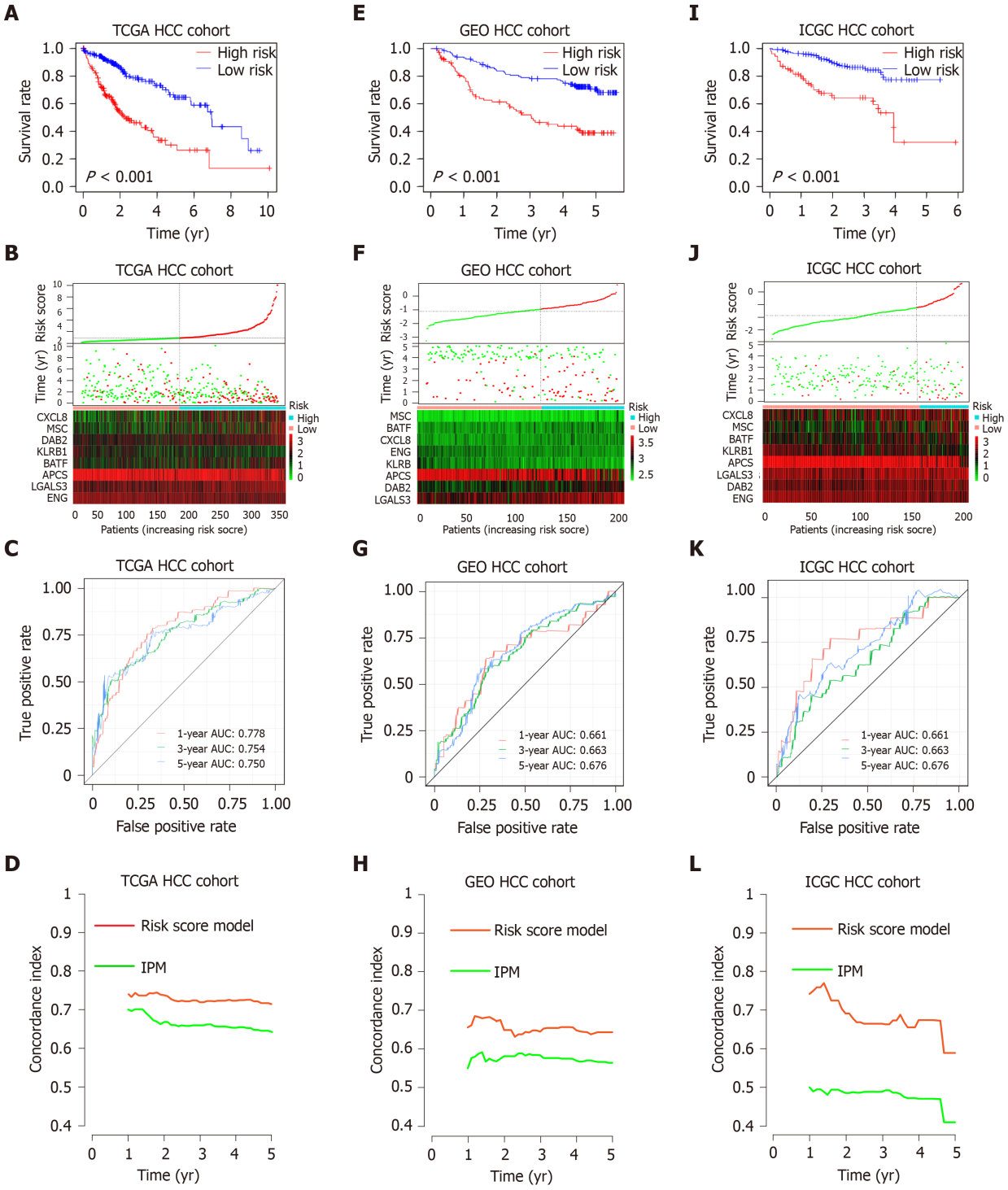

Figure 4 Prognostic analysis of the risk score model. A-C: Kaplan-Meier survival, risk score and time-dependent receiver operating characteristic (ROC) curves of the risk score model for the Cancer Genome Atlas database (TCGA) hepatocellular carcinoma (HCC) cohort; E-G: Kaplan-Meier survival, risk score and time-dependent ROC curves of the risk score model for the Gene Expression Omnibus databases (GEO) HCC cohort; I-K: Kaplan-Meier survival, risk score and time-dependent ROC curves of the risk score model for the International Cancer Genome Consortium database (ICGC) HCC cohort. A, E and I: OS was significantly higher in the low-risk score group than in the high-risk score group; B, F and J: Relationship between the risk score (upper) and the expression of eight prognostic immune genes (lower) is shown; C, G and K: Time-dependent ROC curve analysis of the risk score model; D, H and L: The concordance index (C-index) was used to evaluate prognostic performance for survival prediction. Performance was compared between the risk score model and immune prognostic model by calculating the C-index in the TCGA, GEO and ICGC HCC cohorts. TCGA: The Cancer Genome Atlas database; GEO: Gene Expression Omnibus databases; ICGC: International Cancer Genome Consortium database; IPM: Immune prognostic model; HCC: Hepatocellular carcinoma.

arthritis, chemokine signaling pathway and tuberculosis (Figure 6F).

The risk score model is independent of conventional clinical characteristics

As shown in Figure 7, the risk score was significantly correlated with patient age, histologic grade, pathologic stage and vascular invasion (Figure 7A-Figure D, $P <$

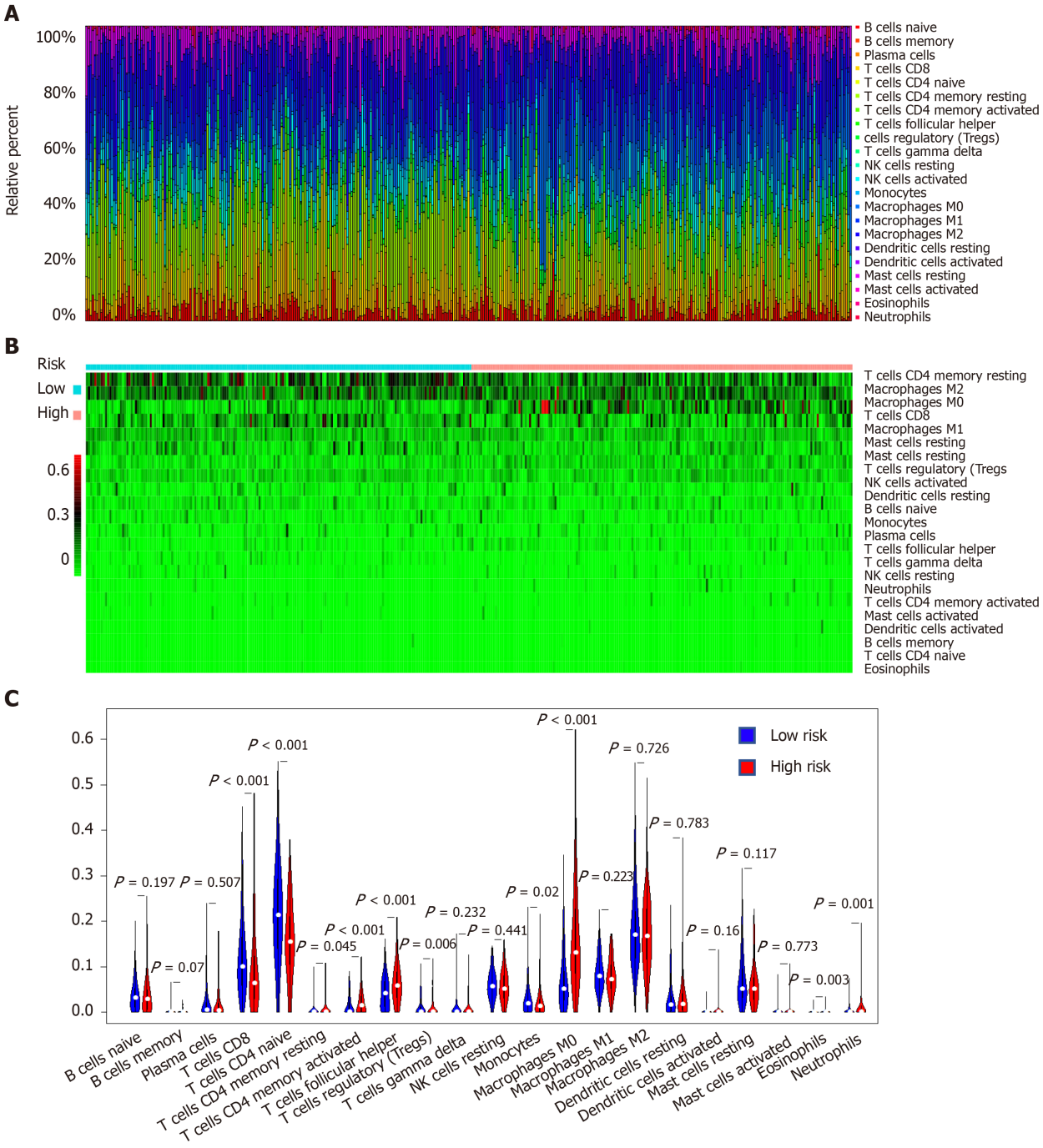
A
Relative percent
100%
80%
60%
40%
20%
0%
B cells naive
B cells memory
Plasma cells
T cells CD8
T cells CD4 naive
T cells CD4 memory resting
T cells CD4 memory activated
T cells follicular helper
cells regulatory (Tregs)
T cells gamma delta
NK cells resting
NK cells activated
Monocytes
Macrophages M0
Macrophages M1
Macrophages M2
Dendritic cells resting
Dendritic cells activated
Mast cells resting
Mast cells activated
Eosinophils
Neutrophils
B
Risk
Low
High
0.6
0.3
0
T cells CD4 memory resting
Macrophages M2
Macrophages M0
T cells CD8
Macrophages M1
Mast cells resting
Mast cells resting
T cells regulatory (Tregs
NK cells activated
Dendritic cells resting
B cells naive
Monocytes
Plasma cells
T cells follicular helper
T cells gamma delta
NK cells resting
Neutrophils
T cells CD4 memory activated
Mast cells activated
Dendritic cells activated
B cells memory
T cells CD4 naive
Eosinophils
C
Low risk
High risk
0.6
0.5
0.4
0.3
0.2
0.1
0.0
P = 0.197
P = 0.07
P = 0.507
P < 0.001
P < 0.001
P < 0.001
P = 0.045
P < 0.001
P = 0.006
P < 0.001
P = 0.232
P = 0.441
P = 0.02
P < 0.001
P = 0.223
P = 0.726
P = 0.783
P = 0.16
P = 0.117
P = 0.773
P = 0.003
P = 0.001
B cells naive
B cells memory
Plasma cells
T cells CD8
T cells CD4 naive
T cells CD4 memory resting
T cells CD4 memory activated
T cells follicular helper
T cells regulatory (Tregs)
T cells gamma delta
NK cells resting
Monocytes
Macrophages M0
Macrophages M1
Macrophages M2
Dendritic cells resting
Dendritic cells activated
Mast cells resting
Mast cells activated
Eosinophils
Neutrophils

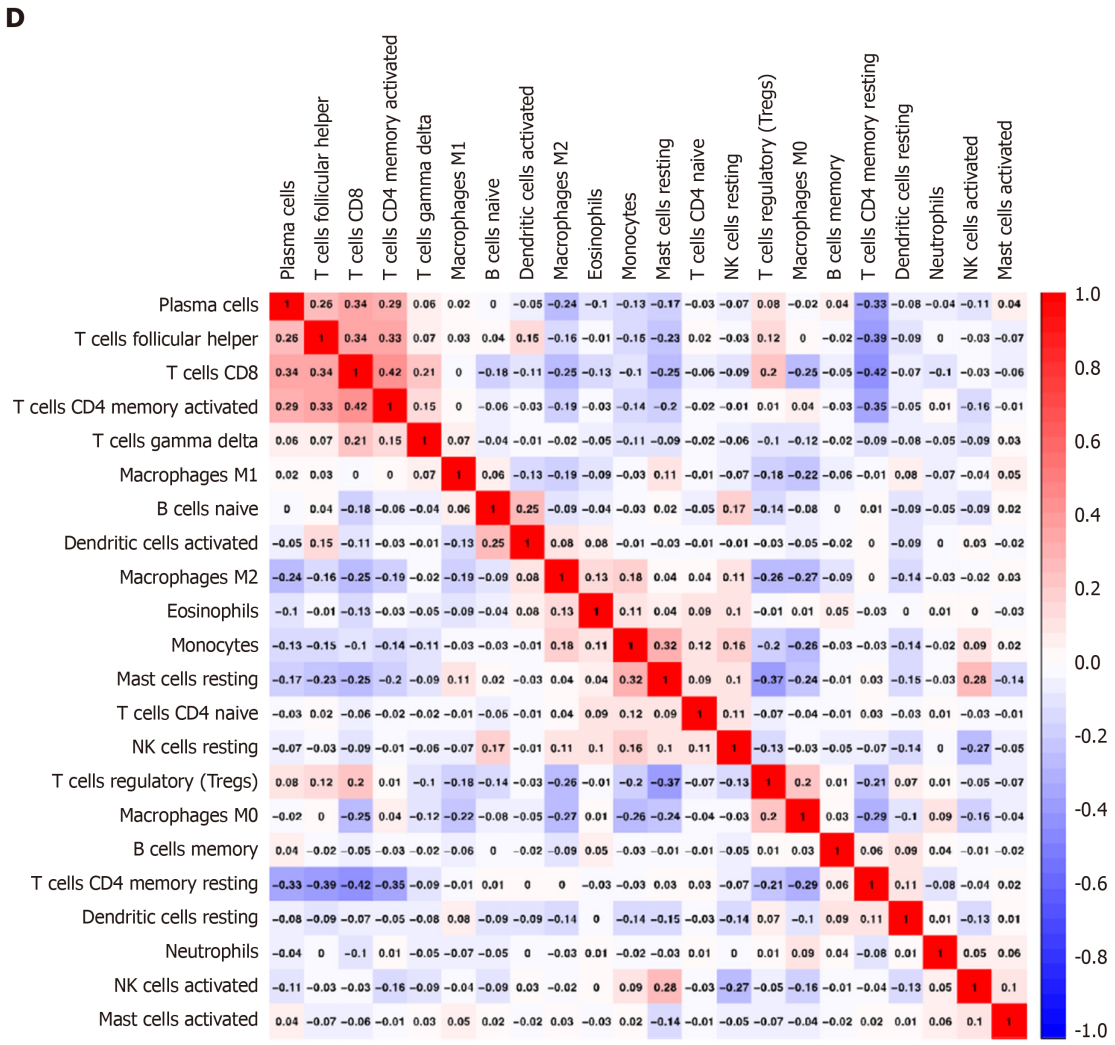

Figure 5 Landscape of immune infiltration in high- and low-risk hepatocellular carcinoma patients in the Cancer Genome Atlas database dataset. A: Relative proportion of immune infiltration in high- and low-risk patients; B: Heat map of the 22 immune cell proportions in high- and low-risk patients; C: Violin plots visualizing significantly different immune cells between high-risk and low-risk patients; D: Correlation matrix of all 22 immune cell proportions.

0.05). To explore the independent prediction of the risk score model, univariate and multivariate analyses were performed, the results showed that risk score and pathologic stage were independent prognostic indicators (Figure 7E). Taken together, these results indicated that the risk score model was an independent prognostic factor for OS.

Developing and validating a nomogram based on the risk score model

To establish a clinically applicable method to assess the prognosis of HCC patients, we developed a nomogram that included risk score and pathologic stage (Figure 7F). The concordance index of the nomogram was 0.71. The calibration plot for the possibility of 1-, 3- and 5-year survival showed good agreement between the prediction by risk score and actual observations (Figure 7G-I). The AUC was 0.77, 0.799 and 0.773 for the 1, 3 and 5-year survival times, respectively. These results demonstrate that the nomogram might be a better model for predicting OS, and aid clinical management. Schematic diagram of the main altered pathway in the high- and low-risk patients is shown in Figure 8.

DISCUSSION

HCC remains a major challenge for public health worldwide[1,37]. Despite multiple therapeutic methods, such as surgical resection, liver transplantation, radiofrequency ablation and chemotherapy, the efficacy is limited. Moreover, effective prognostic indicators that can be utilized to guide cancer therapy is still lacking. Previous studies have shown that the TME is associated with tumor progression and patient

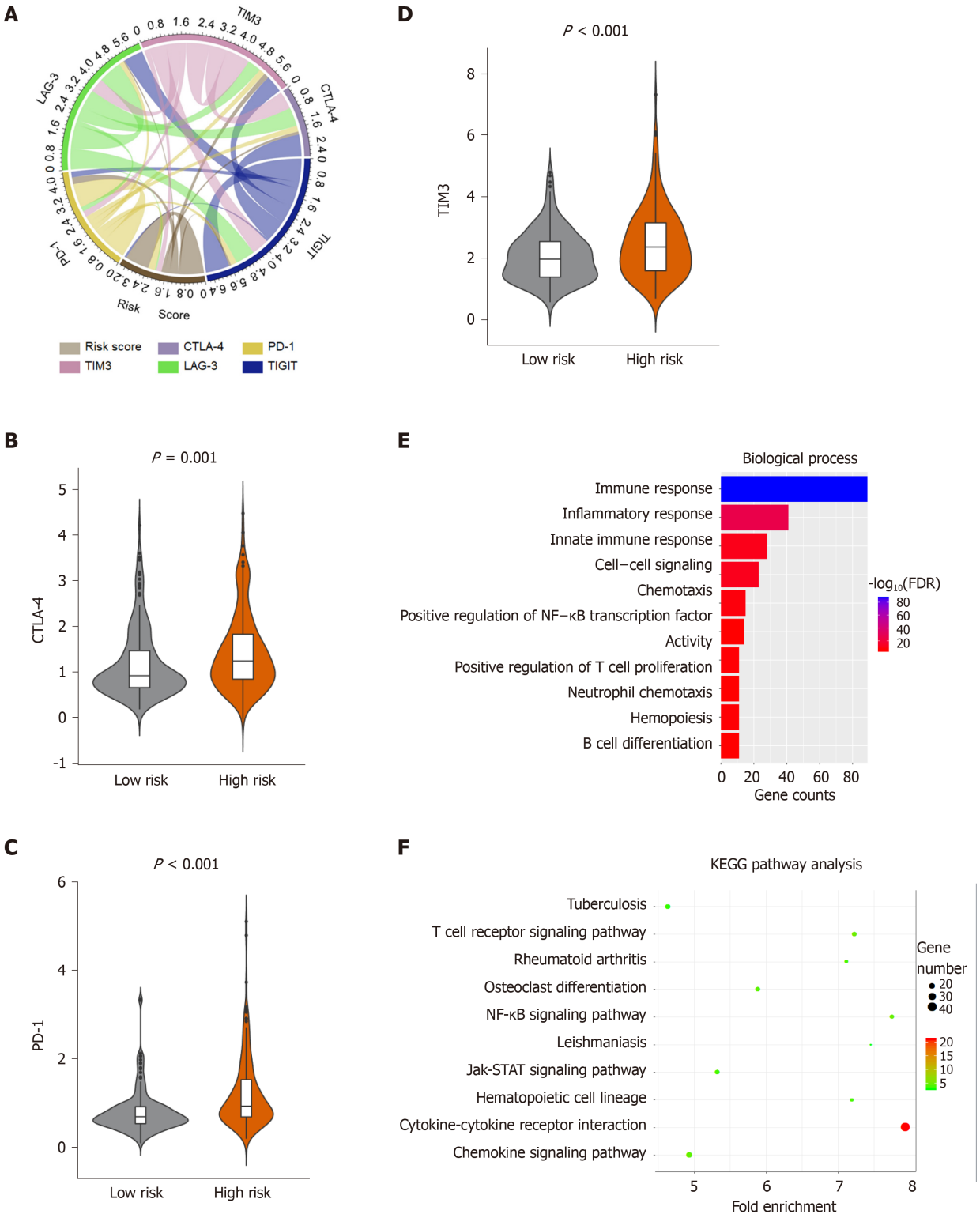

Figure 6 Enrichment analysis of the immune prognostic model. A: Correlation of the risk score with the expression of several prominent immune checkpoints; B-D: Violin plots visualizing significantly different immune checkpoints between high-risk and low-risk patients; E-F: The Gene Ontology (GO) and Kyoto encyclopedia of genes and genomes (KEGG) analysis of immune related genes, top 10 GO terms were displayed. False Discovery Rate of GO and KEGG analysis was acquired from the DAVID functional annotation tool. CTLA-4: Cytotoxic T-Lymphocyte associated protein 4; PD-1: Programmed cell death 1; TIM-3: T-cell immunoglobulin mucin receptor 3; KEGG: Kyoto encyclopedia of genes and genomes; FDR: False discovery rate.

prognosis[38-40]. Therefore, it is important to investigate the TME to identify biomarkers that can predict HCC patients' OS.

The ESTIMATE algorithm has been applied to multiple cancers, showing the effectiveness of the algorithms for big data analysis[41-44]. To investigate the TME of HCC, the ESTIMATE algorithm was applied to attain immune and stromal scores, where the results showed that high immune scores and stromal scores were

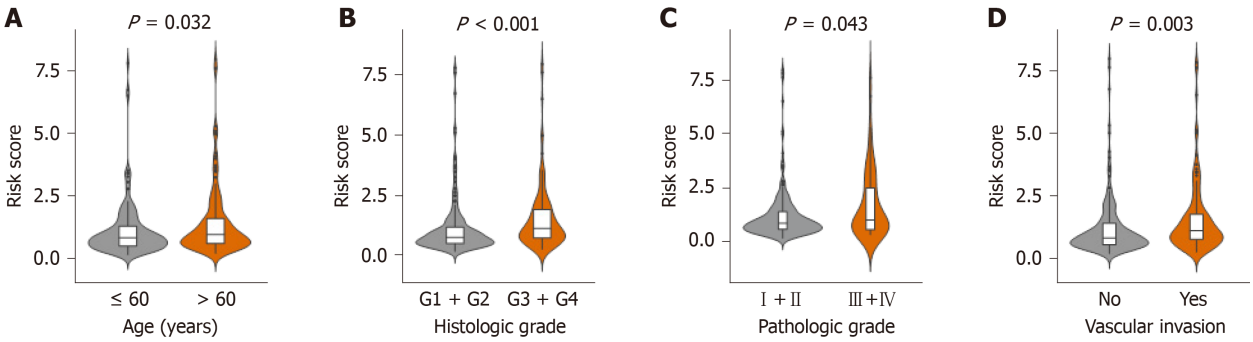

E

Univariate and multivariate regression analysis

Characteristics	Hazard ratio (95%CI)	*P*
Univariate analysis		
Age	1.02 (1.00, 1.04)	0.038
Gender (male/female)	0.69 (0.45, 1.07)	0.098
Histologic grade (G4+G3/G2+G1)	1.24 (0.80, 1.90)	0.334
Pathologic stage (IV/III/II/I)	1.55 (1.22, 1.97)	< 0.001
Vascular Invasion (macro/micro/none)	1.35 (0.87, 2.10)	0.181
Risk Score (high/low)	1.53 (1.37, 1.72)	< 0.001
Multivariate analysis		
Age	1.01 (0.99, 1.03)	0.181
Pathologic stage (IV/III/II/I)	1.35 (1.06, 1.72)	0.017
Risk Score (high/low)	1.48 (1.31, 1.67)	< 0.001

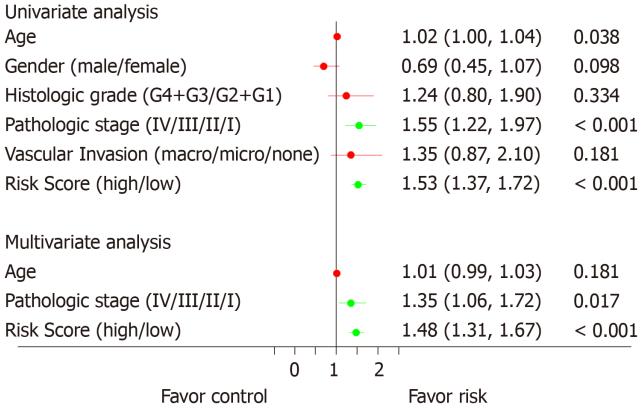

F

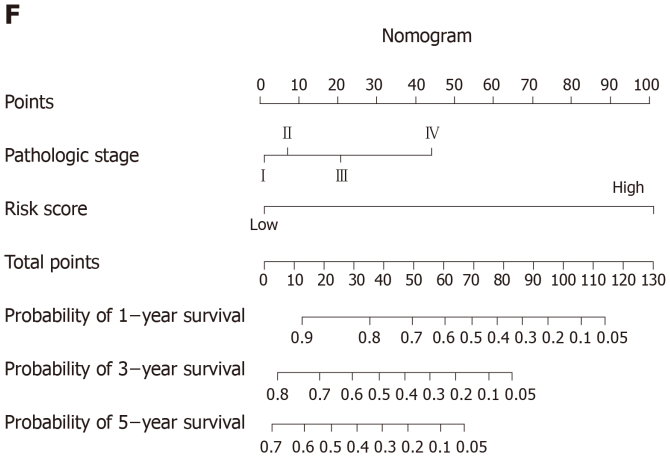

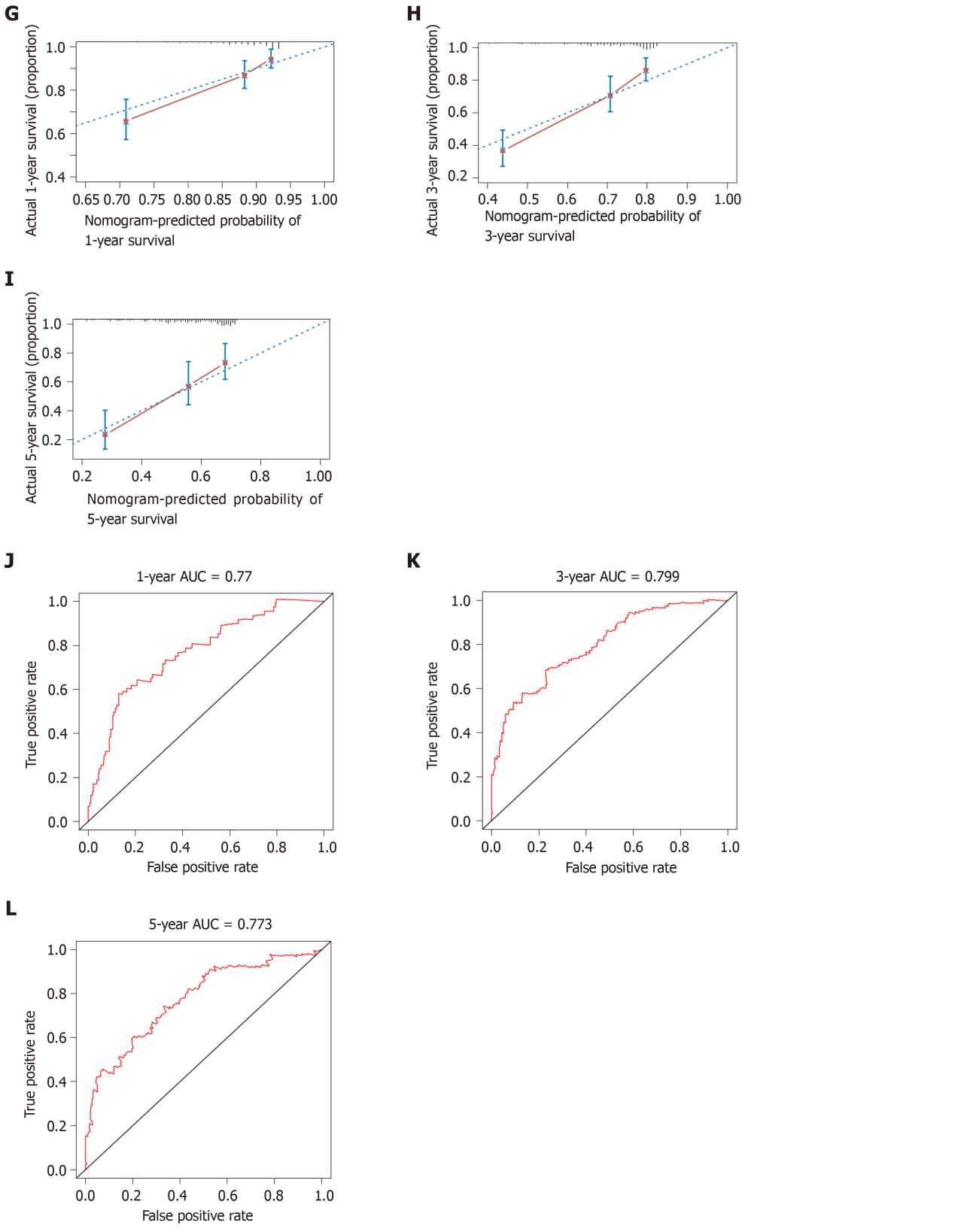

Figure 7 Relationship between the risk score model and other clinical information. A: Correlation of the risk score with the age; B: Correlation of the risk score with the histologic grade; C: Correlation of the risk score with the pathologic stage; D: Correlation of the risk score with the vascular invasion; E: Univariate and multivariate regression analysis of the relation between the risk score prognostic model and clinicopathological features regarding prognostic value; F: Nomogram for predicting the probability of 1-, 3-, and 5-year overall survival (OS) for hepatocellular carcinoma patients; G-I: Calibration plot of the nomogram for predicting the probability of OS at 1, 3, and 5 years; J-L: Time-dependent receiver operating characteristic curve analyses of the nomogram. ROC: Receiver operating characteristic curve; CI: Confidence interval.

significantly associated with worse OS, indicating that the TME was related to the prognosis of HCC patients. Subsequently, we divided HCC patients into high- and

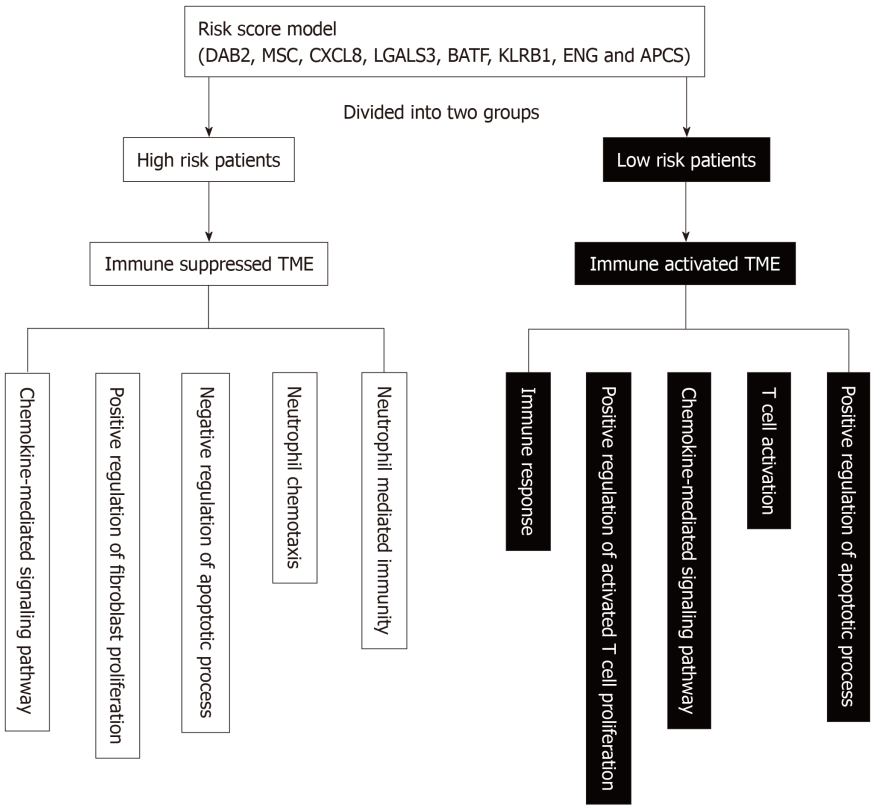

Figure 8 Schematic diagram of the main altered pathway in the high- and low-risk patients. TME: tumor microenvironment; DAB2: Disabled homolog 2; MSC: Musculin; CXCL8: C-X-C Motif chemokine ligand 8; LGALS3: Galectin 3; BATF: B-Cell-activating transcription factor; KLRB1: Killer cell lectin like receptor B1; ENG: Endoglin; APCS: Adenomatosis polyposis coli tumor suppressor.

low-immune/stromal score groups to screen prognostic genes. We then analyzed the intersection DEGs yielded from the comparison of high *vs* low immune/stromal scores groups. GO analysis suggested that the DEGs were mainly involved in the TME, such as immune response, inflammatory response, cell adhesion, chemotaxis and extracellular matrix organization. The results were constitent with previous reports that immune cells and ECM molecules in the TME were interrelated[45-48], hence reshaping the immune microenvironment may improve the effect of cancer treatment[49-51]. The DEGs were identified, and univariate, LASSO and multivariate analyses were performed to construct a risk score model that could identify HCC patients with unfavorable outcomes. The AUC for the risk score model for predicting the 1-, 3-, and 5-year survival were 0.778, 0.754 and 0.75, respectively. Also, the risk score model was validated in the GEO and ICGC dataset. The results suggested that eight immune-related genes had a good performance for survival prediction, indicating that shaping the TME may inhibit or eliminate tumors, resulting in a favorable prognosis. The genes (DAB2, MSC, CXCL8, LGALS3, BATF, KLRB1, ENG and APCS) that compose our risk score model could be considered to be potential targets, and they may provide better performance in combination.

DAB2 is an adapter protein with signaling roles in the domain of endocytosis, cell differentiation, cell adhesion, angiogenesis, and homeostasis[52,53]. Previous studies have reported that DAB2 is a negative regulator of immune function[54]. DAB2 is expressed by macrophages, and it functions as a negative immune regulator of TLR4 endocytosis and signaling, controlling the inflammatory response to endotoxins[55]. In addition, a recent study revealed that low expression of DAB2 by dendritic cell (DC) enhanced IL-12 and IL-6 expression, besides improving the ability of DCs for antigen uptake, migration and T cell stimulation. DAB2-silenced DCs inhibited tumor growth[53]. MSC, a member of the basic helix-loop-helix transcription factors, enforced Foxp3 expression and promoted the unidirectional development of induced Treg cells (iTreg cells) by repressing the Th2 developmental program[56,57]. However, the role of MSC in HCC remains unclear. CXCL8 is a chemotactic factor secreted by malignant cells and various immune cells of multiple cancer types, which promotes tumor progression, recurrence and metastasis through shaping pro-tumoral vascularization, inflammation and immunity[58,59]. Accumulating studies demonstrate that CXCL8 is a

prognostic marker and is a potential therapeutic target for HCC[60-62]. LGALS3, a glycan-binding protein secreted by cancer cells, has been regarded as an important regulator of multiple functions critical to cancer biology[63]. LGALS3, which is an important biomarker in prostate cancer[64,65], plays important roles in the progression and metastasis of colon cancer, acute myeloid leukemia, melanoma and pituitary tumors[66-69], and correlates with the infiltration of M2 macrophages[70]; BATF contains basic leucine zipper domains, is a member of the AP-1/ATF superfamily of transcription factors, plays a role in the growth and expansion of interleukin 17 (IL-17)-producing helper T cell (Th17) and iNKT cells expressing IL-17[71-73], the differentiation of Th17, Tfh and $CD8^+$ T cells[74], and controls the tumor formation and the progression of colorectal cancer[75]. KLRB1 (CD161) is a C-type lectin receptor expressed by most NK cells and subsets of T cells[76]. Previous studies indicated that KLRB1expressed by $CD4^+$ or $CD8^+$ T cells was associated with favorable outcomes in certain cancers such as lung cancer[77,78]. Recent studies demonstrated that the expression of LLT1 (ligand of KLRB1) by tumor cells may facilitate their escape from the immune system. Hence, the KLRB1/LLT1 receptor/ligand system appears to be a novel therapeutic target in the treatment of cancer[79,80]. ENG is a transforming growth factor beta 1 (TGFβ1) binding receptor. Teama *et al*[81] found that high expression of ENG/ TGFβ1 may contribute to carcinogenesis and the progression of HCC in cirrhotic patients. APCS (Amyloid P Component, Serum), a glycoprotein belonging to the pentraxin family of proteins, has a characteristic pentameric organization. Further functions of ENG and APCS remain unknown. In our study, increased expression of ENG and APCS correlated with a favorable outcome in HCC. To our knowledge, the eight gene signature related risk score prognostic model has not been previously reported and could be a novel prognostic factor of HCC.

In addition, multivariate Cox analyses demonstrated that the risk score and pathologic stage were independent prognostic indicators. Subsequently, a nomogram that included risk score and the pathologic stage was constructed. The calibration plot for the possibility of 1-, 3- and 5-year survival showed good agreement between the prediction by risk score and actual observation. The main feature of the nomogram is that it affords a personalized scoring system for patients and is feasible to predict prognosis. During the progression of tumor, the immune system plays a dual role in the complicated interactions between tumor and host; it conveys protective immunity by recognizing tumor-specific antigens to eliminate tumor cells, but also benefits tumor progression, either by altering tumor immunogenicity or by creating a microenvironment that can promote tumor outgrowth or aid in a subsequent metastatic cascade[82-85]. Therefore, tumor cell escape can occur through various immunosuppressive mechanisms, such as recruiting immunosuppressive cells (*e.g.*, Treg cells), increasing the expression of inhibitory ligands such as Programmed death ligand 1 (PD-L1), and decreasing the expression of major histocompatibility complex class I molecules, which results in immune tolerance[86-88]. Moreover, a potential antitumor immune response can be unleashed by blocking the function of immunosuppressive cells and immunosuppressive mechanisms[89]. We explored the immune mechanisms and the component of TIICs subpopulation between patients in the low- and high-risk groups. The results have shown that a high fraction of M0 macrophages, Tregs and Tfh were found in patients in the high-risk group. In contrast, a high fraction of CD8 T cell, resting memory CD4 T cells and monocytes was mainly found in low-risk group patients. We also explored the expression of the immune checkpoints between the high- and low-risk HCC patients. The high-risk HCC patients had significantly higher expression of CTLA-4, PD-1 and TIM-3 than the low-risk HCC patients ($P < 0.05$). Previous studies revealed that resting memory CD4 T cells can be further differentiated and endowed with multiple functions, including restoration of immune tolerance to self-antigen or alloantigen and the promotion of CD8+ T cells to anti-tumor[90,91]. Tregs, which expressed CTLA-4, plays a vital role in the inhibition of anti-tumor immune responses. Treatment with an anti-CTLA-4 antibody has emerged as an effective therapy for the treatment of cancer[92-96]. In our model, high-risk HCC patients had higher fraction of Tregs and a higher expression of CTLA-4, and a worse prognosis, indicating that the immunosuppressive environment and high expression of immune checkpoints may be responsible for the poor prognosis. Furthermore, these results suggest that treatment with antibodies against immune checkpoints will benefit the high-risk HCC patients more than the low-risk patients, hence resulting in a better prognosis.

In this study, we constructed a novel risk score model for prognostic prediction of HCC. One of the advantages of our risk score model is that it has high sensitivity and specificity in predicting the OS, being further validated using external databases. In addition, the risk score model is associated with the immunosuppressive environment and immune checkpoint expression, thus assisting clinicians in selecting personalized immunotherapy for HCC patients.

However, there are several limitations in our study. Firstly, the risk score model needs to be further validated in multicenter clinical trials and prospective studies. Secondly, the functional and mechanistic studies of the eight immune-related genes should be further carried out.

In summary, our research established and validated a risk score model that is based on eight immune-related genes to predict the OS of HCC, which may help in clinical decision making for individualized treatment. Notably, the risk score model provides an immunological viewpoint to clarify the mechanisms that determine the clinical outcome of HCC.

ARTICLE HIGHLIGHTS

Research background

Hepatocellular carcinoma (HCC) is a common malignant tumor with a poor prognosis. In recent years, immunotherapy has emerged as a novel and effective therapy and is being applied in various tumors including HCC. However, the influence of genes involved in the tumor microenvironment on the prognosis of HCC patients remains unclear. And the high-throughput studies that investigated the potential prognostic role of immune prognostic models in HCC are still lacking.

Research motivation

So far, only a small number of HCC patients receiving immunotherapy treatment exhibited responses due to the immunosuppressive microenvironment. Hence, it is necessary to investigate the HCC microenvironment to identify prognostic genes that enable us to predict the benefit of immunotherapy, which may help in clinical decision making for individualized treatment.

Research objectives

To identify a robust gene signature associated with the HCC microenvironment to improve prognosis prediction and effectiveness of immunotherapy of HCC, we analyzed the data from The Cancer Genome Atlas (TCGA), Gene Expression Omnibus (GEO) and International Cancer Genome Consortium (ICGC) databases.

Research methods

We computed the immune/stromal scores of HCC patients obtained from TCGA based on the ESTIMATE algorithm. Univariate analysis, multivariate analysis and the least absolute shrinkage and selection operator, were utilized to construct our predictive model. This model was performed based on the significant differentially expressed genes screened established based on mRNA expression profiles from the TCGA database. The robustness of this model was validated using GEO and ICGC datasets.

Research results

The risk score model consisting of eight genes (Disabled homolog 2, Musculin, C-X-C motif chemokine ligand 8, Galectin 3, B-cell-activating transcription factor, Killer cell lectin like receptor B1, Endoglin, and Adenomatosis polyposis coli tumor suppressor) was constructed and validated based on HCC patients who were divided into high- or low-risk group. The receiver operating characteristic curve analysis confirmd the good potency of the risk score prognostic model. Moreover, we investigated the relationship between patient risk scores and the expression of common immune checkpoints, and the results showed that the risk score was significantly associated with the expression of Cytotoxic T-Lymphocyte associated protein 4, Programmed cell death 1, and T-cell immunoglobulin mucin receptor 3. To establish a clinically applicable method to assess the prognosis of HCC patients, a nomogram involving risk score and the pathologic stage was formulated.

Research conclusions

Our research established and validated a risk score model that is based on eight immune-related genes to predict the overall survival of HCC, which may help in clinical decision making for individualized treatment. The risk score model and the nomogram will benefit HCC patients through personalized immunotherapy.

Research perspectives

The risk score model provides an immunological viewpoint to clarify the mechanisms that determine the clinical outcome of HCC. Identifying effective molecular biomarkers and predictive markers of immunotherapy is a future direction for improving the effectiveness of immunotherapy.

REFERENCES

1 **Ferlay J**, Soerjomataram I, Dikshit R, Eser S, Mathers C, Rebelo M, Parkin DM, Forman D, Bray F. Cancer incidence and mortality worldwide: sources, methods and major patterns in GLOBOCAN 2012. *Int*

J Cancer 2015; **136**: E359-E386 [PMID: 25220842 DOI: 10.1002/ijc.29210]
2 **Heimbach JK**, Kulik LM, Finn RS, Sirlin CB, Abecassis MM, Roberts LR, Zhu AX, Murad MH, Marrero JA. AASLD guidelines for the treatment of hepatocellular carcinoma. *Hepatology* 2018; **67**: 358-380 [PMID: 28130846 DOI: 10.1002/hep.29086]
3 **Kuhlmann JB**, Blum HE. Locoregional therapy for cholangiocarcinoma. *Curr Opin Gastroenterol* 2013; **29**: 324-328 [PMID: 23337933 DOI: 10.1097/MOG.0b013e32835d9dea]
4 **Bruix J**, Sherman M; American Association for the Study of Liver Diseases. Management of hepatocellular carcinoma: an update. *Hepatology* 2011; **53**: 1020-1022 [PMID: 21374666 DOI: 10.1002/hep.24199]
5 **Sprinzl MF**, Galle PR. Current progress in immunotherapy of hepatocellular carcinoma. *J Hepatol* 2017; **66**: 482-484 [PMID: 28011330 DOI: 10.1016/j.jhep.2016.12.009]
6 **Topalian SL**, Drake CG, Pardoll DM. Immune checkpoint blockade: a common denominator approach to cancer therapy. *Cancer Cell* 2015; **27**: 450-461 [PMID: 25858804 DOI: 10.1016/j.ccell.2015.03.001]
7 **Rotte A**, Jin JY, Lemaire V. Mechanistic overview of immune checkpoints to support the rational design of their combinations in cancer immunotherapy. *Ann Oncol* 2018; **29**: 71-83 [PMID: 29069302 DOI: 10.1093/annonc/mdx686]
8 **Zhou G**, Sprengers D, Boor PPC, Doukas M, Schutz H, Mancham S, Pedroza-Gonzalez A, Polak WG, de Jonge J, Gaspersz M, Dong H, Thielemans K, Pan Q, IJzermans JNM, Bruno MJ, Kwekkeboom J. Antibodies Against Immune Checkpoint Molecules Restore Functions of Tumor-Infiltrating T Cells in Hepatocellular Carcinomas. *Gastroenterology* 2017; **153**: 1107-1119.e10 [PMID: 28648905 DOI: 10.1053/j.gastro.2017.06.017]
9 **Belli C**, Trapani D, Viale G, D'Amico P, Duso BA, Della Vigna P, Orsi F, Curigliano G. Targeting the microenvironment in solid tumors. *Cancer Treat Rev* 2018; **65**: 22-32 [PMID: 29502037 DOI: 10.1016/j.ctrv.2018.02.004]
10 **Chen F**, Zhuang X, Lin L, Yu P, Wang Y, Shi Y, Hu G, Sun Y. New horizons in tumor microenvironment biology: challenges and opportunities. *BMC Med* 2015; **13**: 45 [PMID: 25857315 DOI: 10.1186/s12916-015-0278-7]
11 **Yin Z**, Jiang K, Li R, Dong C, Wang L. Multipotent mesenchymal stromal cells play critical roles in hepatocellular carcinoma initiation, progression and therapy. *Mol Cancer* 2018; **17**: 178 [PMID: 30593276 DOI: 10.1186/s12943-018-0926-6]
12 **Catalano V**, Turdo A, Di Franco S, Dieli F, Todaro M, Stassi G. Tumor and its microenvironment: a synergistic interplay. *Semin Cancer Biol* 2013; **23**: 522-532 [PMID: 24012661 DOI: 10.1016/j.semcancer.2013.08.007]
13 **Affo S**, Yu LX, Schwabe RF. The Role of Cancer-Associated Fibroblasts and Fibrosis in Liver Cancer. *Annu Rev Pathol* 2017; **12**: 153-186 [PMID: 27959632 DOI: 10.1146/annurev-pathol-052016-100322]
14 **Liu LZ**, Zhang Z, Zheng BH, Shi Y, Duan M, Ma LJ, Wang ZC, Dong LQ, Dong PP, Shi JY, Zhang S, Ding ZB, Ke AW, Cao Y, Zhang XM, Xi R, Zhou J, Fan J, Wang XY, Gao Q. CCL15 Recruits Suppressive Monocytes to Facilitate Immune Escape and Disease Progression in Hepatocellular Carcinoma. *Hepatology* 2019; **69**: 143-159 [PMID: 30070719 DOI: 10.1002/hep.30134]
15 **Zhou SL**, Zhou ZJ, Hu ZQ, Huang XW, Wang Z, Chen EB, Fan J, Cao Y, Dai Z, Zhou J. Tumor-Associated Neutrophils Recruit Macrophages and T-Regulatory Cells to Promote Progression of Hepatocellular Carcinoma and Resistance to Sorafenib. *Gastroenterology* 2016; **150**: 1646-1658.e17 [PMID: 26924089 DOI: 10.1053/j.gastro.2016.02.040]
16 **Garnelo M**, Tan A, Her Z, Yeong J, Lim CJ, Chen J, Lim KH, Weber A, Chow P, Chung A, Ooi LL, Toh HC, Heikenwalder M, Ng IO, Nardin A, Chen Q, Abastado JP, Chew V. Interaction between tumour-infiltrating B cells and T cells controls the progression of hepatocellular carcinoma. *Gut* 2017; **66**: 342-351 [PMID: 26669617 DOI: 10.1136/gutjnl-2015-310814]
17 **Zhang M**, Pang HJ, Zhao W, Li YF, Yan LX, Dong ZY, He XF. VISTA expression associated with CD8 confers a favorable immune microenvironment and better overall survival in hepatocellular carcinoma. *BMC Cancer* 2018; **18**: 511 [PMID: 29720116 DOI: 10.1186/s12885-018-4435-1]
18 **Kurebayashi Y**, Ojima H, Tsujikawa H, Kubota N, Maehara J, Abe Y, Kitago M, Shinoda M, Kitagawa Y, Sakamoto M. Landscape of immune microenvironment in hepatocellular carcinoma and its additional impact on histological and molecular classification. *Hepatology* 2018; **68**: 1025-1041 [PMID: 29603348 DOI: 10.1002/hep.29904]
19 **Zheng C**, Zheng L, Yoo JK, Guo H, Zhang Y, Guo X, Kang B, Hu R, Huang JY, Zhang Q, Liu Z, Dong M, Hu X, Ouyang W, Peng J, Zhang Z. Landscape of Infiltrating T Cells in Liver Cancer Revealed by Single-Cell Sequencing. *Cell* 2017; **169**: 1342-1356.e16 [PMID: 28622514 DOI: 10.1016/j.cell.2017.05.035]
20 **Brunner SM**, Rubner C, Kesselring R, Martin M, Griesshammer E, Ruemmele P, Stempfl T, Teufel A, Schlitt HJ, Fichtner-Feigl S. Tumor-infiltrating, interleukin-33-producing effector-memory CD8(+) T cells in resected hepatocellular carcinoma prolong patient survival. *Hepatology* 2015; **61**: 1957-1967 [PMID: 25645298 DOI: 10.1002/hep.27728]
21 **Barnes TA**, Amir E. HYPE or HOPE: the prognostic value of infiltrating immune cells in cancer. *Br J Cancer* 2017; **117**: 451-460 [PMID: 28704840 DOI: 10.1038/bjc.2017.220]
22 **Yarchoan M**, Xing D, Luan L, Xu H, Sharma RB, Popovic A, Pawlik TM, Kim AK, Zhu Q, Jaffee EM, Taube JM, Anders RA. Characterization of the Immune Microenvironment in Hepatocellular Carcinoma. *Clin Cancer Res* 2017; **23**: 7333-7339 [PMID: 28928158 DOI: 10.1158/1078-0432.CCR-17-0950]
23 **Sia D**, Jiao Y, Martinez-Quetglas I, Kuchuk O, Villacorta-Martin C, Castro de Moura M, Putra J, Camprecios G, Bassaganyas L, Akers N, Losic B, Waxman S, Thung SN, Mazzaferro V, Esteller M, Friedman SL, Schwartz M, Villanueva A, Llovet JM. Identification of an Immune-specific Class of Hepatocellular Carcinoma, Based on Molecular Features. *Gastroenterology* 2017; **153**: 812-826 [PMID: 28624577 DOI: 10.1053/j.gastro.2017.06.007]
24 **Yoshihara K**, Shahmoradgoli M, Martínez E, Vegesna R, Kim H, Torres-Garcia W, Treviño V, Shen H, Laird PW, Levine DA, Carter SL, Getz G, Stemke-Hale K, Mills GB, Verhaak RG. Inferring tumour purity and stromal and immune cell admixture from expression data. *Nat Commun* 2013; **4**: 2612 [PMID: 24113773 DOI: 10.1038/ncomms3612]
25 **Shah N**, Wang P, Wongvipat J, Karthaus WR, Abida W, Armenia J, Rockowitz S, Drier Y, Bernstein BE, Long HW, Freedman ML, Arora VK, Zheng D, Sawyers CL. Regulation of the glucocorticoid receptor via a BET-dependent enhancer drives antiandrogen resistance in prostate cancer. *Elife* 2017; **6** [PMID: 28891793 DOI: 10.7554/eLife.27861]
26 **Priedigkeit N**, Watters RJ, Lucas PC, Basudan A, Bhargava R, Horne W, Kolls JK, Fang Z, Rosenzweig

MQ, Brufsky AM, Weiss KR, Oesterreich S, Lee AV. Exome-capture RNA sequencing of decade-old breast cancers and matched decalcified bone metastases. *JCI Insight* 2017; **2** [PMID: 28878133 DOI: 10.1172/jci.insight.95703]
27 **Alonso MH**, Aussó S, Lopez-Doriga A, Cordero D, Guinó E, Solé X, Barenys M, de Oca J, Capella G, Salazar R, Sanz-Pamplona R, Moreno V. Comprehensive analysis of copy number aberrations in microsatellite stable colon cancer in view of stromal component. *Br J Cancer* 2017; **117**: 421-431 [PMID: 28683472 DOI: 10.1038/bjc.2017.208]
28 **Ritchie ME**, Phipson B, Wu D, Hu Y, Law CW, Shi W, Smyth GK. limma powers differential expression analyses for RNA-sequencing and microarray studies. *Nucleic Acids Res* 2015; **43**: e47 [PMID: 25605792 DOI: 10.1093/nar/gkv007]
29 **Dennis G**, Sherman BT, Hosack DA, Yang J, Gao W, Lane HC, Lempicki RA. DAVID: Database for Annotation, Visualization, and Integrated Discovery. *Genome Biol* 2003; **4**: P3 [PMID: 12734009]
30 **Gui J**, Li H. Penalized Cox regression analysis in the high-dimensional and low-sample size settings, with applications to microarray gene expression data. *Bioinformatics* 2005; **21**: 3001-3008 [PMID: 15814556 DOI: 10.1093/bioinformatics/bti422]
31 **Wu TT**, Chen YF, Hastie T, Sobel E, Lange K. Genome-wide association analysis by lasso penalized logistic regression. *Bioinformatics* 2009; **25**: 714-721 [PMID: 19176549 DOI: 10.1093/bioinformatics/btp041]
32 **Long J**, Zhang L, Wan X, Lin J, Bai Y, Xu W, Xiong J, Zhao H. A four-gene-based prognostic model predicts overall survival in patients with hepatocellular carcinoma. *J Cell Mol Med* 2018; **22**: 5928-5938 [PMID: 30247807 DOI: 10.1111/jcmm.13863]
33 **Newman AM**, Liu CL, Green MR, Gentles AJ, Feng W, Xu Y, Hoang CD, Diehn M, Alizadeh AA. Robust enumeration of cell subsets from tissue expression profiles. *Nat Methods* 2015; **12**: 453-457 [PMID: 25822800 DOI: 10.1038/nmeth.3337]
34 **Bense RD**, Sotiriou C, Piccart-Gebhart MJ, Haanen JBAG, van Vugt MATM, de Vries EGE, Schröder CP, Fehrmann RSN. Relevance of Tumor-Infiltrating Immune Cell Composition and Functionality for Disease Outcome in Breast Cancer. *J Natl Cancer Inst* 2017; **109** [PMID: 27737921 DOI: 10.1093/jnci/djw192]
35 **Iasonos A**, Schrag D, Raj GV, Panageas KS. How to build and interpret a nomogram for cancer prognosis. *J Clin Oncol* 2008; **26**: 1364-1370 [PMID: 18323559 DOI: 10.1200/JCO.2007.12.9791]
36 **Long J**, Wang A, Bai Y, Lin J, Yang X, Wang D, Yang X, Jiang Y, Zhao H. Development and validation of a TP53-associated immune prognostic model for hepatocellular carcinoma. *EBioMedicine* 2019; **42**: 363-374 [PMID: 30885723 DOI: 10.1016/j.ebiom.2019.03.022]
37 **Bruix J**, Gores GJ, Mazzaferro V. Hepatocellular carcinoma: clinical frontiers and perspectives. *Gut* 2014; **63**: 844-855 [PMID: 24531850 DOI: 10.1136/gutjnl-2013-306627]
38 **Conway EM**, Pikor LA, Kung SH, Hamilton MJ, Lam S, Lam WL, Bennewith KL. Macrophages, Inflammation, and Lung Cancer. *Am J Respir Crit Care Med* 2016; **193**: 116-130 [PMID: 26583808 DOI: 10.1164/rccm.201508-1545CI]
39 **Jiang Y**, Zhang Q, Hu Y, Li T, Yu J, Zhao L, Ye G, Deng H, Mou T, Cai S, Zhou Z, Liu H, Chen G, Li G, Qi X. ImmunoScore Signature: A Prognostic and Predictive Tool in Gastric Cancer. *Ann Surg* 2018; **267**: 504-513 [PMID: 28002059 DOI: 10.1097/SLA.0000000000002116]
40 **Li Y**, Lu Z, Che Y, Wang J, Sun S, Huang J, Mao S, Lei Y, Chen Z, He J. Immune signature profiling identified predictive and prognostic factors for esophageal squamous cell carcinoma. *Oncoimmunology* 2017; **6**: e1356147 [PMID: 29147607 DOI: 10.1080/2162402X.2017.1356147]
41 **Liu W**, Ye H, Liu YF, Xu CQ, Zhong YX, Tian T, Ma SW, Tao H, Li L, Xue LC, He HQ. Transcriptome-derived stromal and immune scores infer clinical outcomes of patients with cancer. *Oncol Lett* 2018; **15**: 4351-4357 [PMID: 29541203 DOI: 10.3892/ol.2018.7855]
42 **Jia D**, Li S, Li D, Xue H, Yang D, Liu Y. Mining TCGA database for genes of prognostic value in glioblastoma microenvironment. *Aging (Albany NY)* 2018; **10**: 592-605 [PMID: 29676997 DOI: 10.18632/aging.101415]
43 **Vincent KM**, Findlay SD, Postovit LM. Assessing breast cancer cell lines as tumour models by comparison of mRNA expression profiles. *Breast Cancer Res* 2015; **17**: 114 [PMID: 26289960 DOI: 10.1186/s13058-015-0613-0]
44 **Luebker SA**, Zhang W, Koepsell SA. Comparing the genomes of cutaneous melanoma tumors to commercially available cell lines. *Oncotarget* 2017; **8**: 114877-114893 [PMID: 29383127 DOI: 10.18632/oncotarget.22928]
45 **Lu P**, Takai K, Weaver VM, Werb Z. Extracellular matrix degradation and remodeling in development and disease. *Cold Spring Harb Perspect Biol* 2011; **3** [PMID: 21917992 DOI: 10.1101/cshperspect.a005058]
46 **Bonnans C**, Chou J, Werb Z. Remodelling the extracellular matrix in development and disease. *Nat Rev Mol Cell Biol* 2014; **15**: 786-801 [PMID: 25415508 DOI: 10.1038/nrm3904]
47 **Pickup MW**, Mouw JK, Weaver VM. The extracellular matrix modulates the hallmarks of cancer. *EMBO Rep* 2014; **15**: 1243-1253 [PMID: 25381661 DOI: 10.15252/embr.201439246]
48 **Peranzoni E**, Rivas-Caicedo A, Bougherara H, Salmon H, Donnadieu E. Positive and negative influence of the matrix architecture on antitumor immune surveillance. *Cell Mol Life Sci* 2013; **70**: 4431-4448 [PMID: 23649148 DOI: 10.1007/s00018-013-1339-8]
49 **Yu SJ**, Ma C, Heinrich B, Brown ZJ, Sandhu M, Zhang Q, Fu Q, Agdashian D, Rosato U, Korangy F, Greten TF. Targeting the crosstalk between cytokine-induced killer cells and myeloid-derived suppressor cells in hepatocellular carcinoma. *J Hepatol* 2019; **70**: 449-457 [PMID: 30414862 DOI: 10.1016/j.jhep.2018.10.040]
50 **Wong CC**, Tse AP, Huang YP, Zhu YT, Chiu DK, Lai RK, Au SL, Kai AK, Lee JM, Wei LL, Tsang FH, Lo RC, Shi J, Zheng YP, Wong CM, Ng IO. Lysyl oxidase-like 2 is critical to tumor microenvironment and metastatic niche formation in hepatocellular carcinoma. *Hepatology* 2014; **60**: 1645-1658 [PMID: 25048396 DOI: 10.1002/hep.27320]
51 **Cariani E**, Missale G. Immune landscape of hepatocellular carcinoma microenvironment: Implications for prognosis and therapeutic applications. *Liver Int* 2019; **39**: 1608-1621 [PMID: 31314948 DOI: 10.1111/liv.14192]
52 **Finkielstein CV**, Capelluto DG. Disabled-2: A modular scaffold protein with multifaceted functions in signaling. *Bioessays* 2016; **38** Suppl 1: S45-S55 [PMID: 27417122 DOI: 10.1002/bies.201670907]
53 **Ahmed MS**, Byeon SE, Jeong Y, Miah MA, Salahuddin M, Lee Y, Park SS, Bae YS. *Dab2*, a negative regulator of DC immunogenicity, is an attractive molecular target for DC-based immunotherapy. *Oncoimmunology* 2015; **4**: e984550 [PMID: 25949867 DOI: 10.4161/2162402x.2014.984550]

54 **Yi S**, Chang R, Hu J, Qiu Y, Wang Q, Cao Q, Yuan G, Su G, Zhou C, Wang Y, Kijlstra A, Yang P. Disabled-2 (DAB2) Overexpression Inhibits Monocyte-Derived Dendritic Cells' Function in Vogt-Koyanagi-Harada Disease. *Invest Ophthalmol Vis Sci* 2018; **59**: 4662-4669 [PMID: 30267088 DOI: 10.1167/iovs.18-24630]

55 **Hung WS**, Ling P, Cheng JC, Chang SS, Tseng CP. Disabled-2 is a negative immune regulator of lipopolysaccharide-stimulated Toll-like receptor 4 internalization and signaling. *Sci Rep* 2016; **6**: 35343 [PMID: 27748405 DOI: 10.1038/srep35343]

56 **Santarlasci V**, Mazzoni A, Capone M, Rossi MC, Maggi L, Montaini G, Rossettini B, Cimaz R, Ramazzotti M, Barra G, De Palma R, Maggi E, Liotta F, Cosmi L, Romagnani S, Annunziato F. Musculin inhibits human T-helper 17 cell response to interleukin 2 by controlling STAT5B activity. *Eur J Immunol* 2017; **47**: 1427-1442 [PMID: 28612433 DOI: 10.1002/eji.201746996]

57 **Wu C**, Chen Z, Dardalhon V, Xiao S, Thalhamer T, Liao M, Madi A, Franca RF, Han T, Oukka M, Kuchroo V. The transcription factor musculin promotes the unidirectional development of peripheral T_{reg} cells by suppressing the T_H2 transcriptional program. *Nat Immunol* 2017; **18**: 344-353 [PMID: 28114290 DOI: 10.1038/ni.3667]

58 **Sanmamed MF**, Carranza-Rua O, Alfaro C, Oñate C, Martín-Algarra S, Perez G, Landazuri SF, Gonzalez A, Gross S, Rodriguez I, Muñoz-Calleja C, Rodríguez-Ruiz M, Sangro B, López-Picazo JM, Rizzo M, Mazzolini G, Pascual JI, Andueza MP, Perez-Gracia JL, Melero I. Serum interleukin-8 reflects tumor burden and treatment response across malignancies of multiple tissue origins. *Clin Cancer Res* 2014; **20**: 5697-5707 [PMID: 25224278 DOI: 10.1158/1078-0432.CCR-13-3203]

59 **Huang W**, Chen Z, Zhang L, Tian D, Wang D, Fan D, Wu K, Xia L. Interleukin-8 Induces Expression of FOXC1 to Promote Transactivation of CXCR1 and CCL2 in Hepatocellular Carcinoma Cell Lines and Formation of Metastases in Mice. *Gastroenterology* 2015; **149**: 1053-67.e14 [PMID: 26065367 DOI: 10.1053/j.gastro.2015.05.058]

60 **Schinke C**, Giricz O, Li W, Shastri A, Gordon S, Barreyro L, Bhagat T, Bhattacharyya S, Ramachandra N, Bartenstein M, Pellagatti A, Boultwood J, Wickrema A, Yu Y, Will B, Wei S, Steidl U, Verma A. IL8-CXCR2 pathway inhibition as a therapeutic strategy against MDS and AML stem cells. *Blood* 2015; **125**: 3144-3152 [PMID: 25810490 DOI: 10.1182/blood-2015-01-621631]

61 **Lin C**, He H, Liu H, Li R, Chen Y, Qi Y, Jiang Q, Chen L, Zhang P, Zhang H, Li H, Zhang W, Sun Y, Xu J. Tumour-associated macrophages-derived CXCL8 determines immune evasion through autonomous PD-L1 expression in gastric cancer. *Gut* 2019; **68**: 1764-1773 [PMID: 30661053 DOI: 10.1136/gutjnl-2018-316324]

62 **Li XP**, Yang XY, Biskup E, Zhou J, Li HL, Wu YF, Chen ML, Xu F. Co-expression of CXCL8 and HIF-1α is associated with metastasis and poor prognosis in hepatocellular carcinoma. *Oncotarget* 2015; **6**: 22880-22889 [PMID: 26078356 DOI: 10.18632/oncotarget.4412]

63 **Ruvolo PP**. Galectin 3 as a guardian of the tumor microenvironment. *Biochim Biophys Acta* 2016; **1863**: 427-437 [PMID: 26264495 DOI: 10.1016/j.bbamcr.2015.08.008]

64 **Wang Y**, Balan V, Gao X, Reddy PG, Kho D, Tait L, Raz A. The significance of galectin-3 as a new basal cell marker in prostate cancer. *Cell Death Dis* 2013; **4**: e753 [PMID: 23907467 DOI: 10.1038/cddis.2013.277]

65 **Balan V**, Wang Y, Nangia-Makker P, Kho D, Bajaj M, Smith D, Heilbrun L, Raz A, Heath E. Galectin-3: a possible complementary marker to the PSA blood test. *Oncotarget* 2013; **4**: 542-549 [PMID: 23625538 DOI: 10.18632/oncotarget.923]

66 **Han L**, Wu Z, Zhao Q. Revealing the molecular mechanism of colorectal cancer by establishing LGALS3-related protein-protein interaction network and identifying signaling pathways. *Int J Mol Med* 2014; **33**: 581-588 [PMID: 24398765 DOI: 10.3892/ijmm.2014.1620]

67 **Cheng CL**, Hou HA, Lee MC, Liu CY, Jhuang JY, Lai YJ, Lin CW, Chen HY, Liu FT, Chou WC, Chen CY, Tang JL, Yao M, Huang SY, Ko BS, Wu SJ, Tsay W, Tien HF. Higher bone marrow LGALS3 expression is an independent unfavorable prognostic factor for overall survival in patients with acute myeloid leukemia. *Blood* 2013; **121**: 3172-3180 [PMID: 23449638 DOI: 10.1182/blood-2012-07-443762]

68 **Braeuer RR**, Zigler M, Kamiya T, Dobroff AS, Huang L, Choi W, McConkey DJ, Shoshan E, Mobley AK, Song R, Raz A, Bar-Eli M. Galectin-3 contributes to melanoma growth and metastasis via regulation of NFAT1 and autotaxin. *Cancer Res* 2012; **72**: 5757-5766 [PMID: 22986745 DOI: 10.1158/0008-5472.CAN-12-2424]

69 **Ruebel KH**, Jin L, Qian X, Scheithauer BW, Kovacs K, Nakamura N, Zhang H, Raz A, Lloyd RV. Effects of DNA methylation on galectin-3 expression in pituitary tumors. *Cancer Res* 2005; **65**: 1136-1140 [PMID: 15734994 DOI: 10.1158/0008-5472.Can-04-3578]

70 **Jia W**, Kidoya H, Yamakawa D, Naito H, Takakura N. Galectin-3 accelerates M2 macrophage infiltration and angiogenesis in tumors. *Am J Pathol* 2013; **182**: 1821-1831 [PMID: 23499465 DOI: 10.1016/j.ajpath.2013.01.017]

71 **Ciofani M**, Madar A, Galan C, Sellars M, Mace K, Pauli F, Agarwal A, Huang W, Parkhurst CN, Muratet M, Newberry KM, Meadows S, Greenfield A, Yang Y, Jain P, Kirigin FK, Birchmeier C, Wagner EF, Murphy KM, Myers RM, Bonneau R, Littman DR. A validated regulatory network for Th17 cell specification. *Cell* 2012; **151**: 289-303 [PMID: 23021777 DOI: 10.1016/j.cell.2012.09.016]

72 **Jordan-Williams KL**, Poston S, Taparowsky EJ. BATF regulates the development and function of IL-17 producing iNKT cells. *BMC Immunol* 2013; **14**: 16 [PMID: 23537103 DOI: 10.1186/1471-2172-14-16]

73 **Guler R**, Roy S, Suzuki H, Brombacher F. Targeting Batf2 for infectious diseases and cancer. *Oncotarget* 2015; **6**: 26575-26582 [PMID: 26376615 DOI: 10.18632/oncotarget.5576]

74 **Kurachi M**, Barnitz RA, Yosef N, Odorizzi PM, DiIorio MA, Lemieux ME, Yates K, Godec J, Klatt MG, Regev A, Wherry EJ, Haining WN. The transcription factor BATF operates as an essential differentiation checkpoint in early effector CD8+ T cells. *Nat Immunol* 2014; **15**: 373-383 [PMID: 24584090 DOI: 10.1038/ni.2834]

75 **Punkenburg E**, Vogler T, Büttner M, Amann K, Waldner M, Atreya R, Abendroth B, Mudter J, Merkel S, Gallmeier E, Rose-John S, Neurath MF, Hildner K. Batf-dependent Th17 cells critically regulate IL-23 driven colitis-associated colon cancer. *Gut* 2016; **65**: 1139-1150 [PMID: 25838550 DOI: 10.1136/gutjnl-2014-308227]

76 **Lebbink RJ**, Meyaard L. Non-MHC ligands for inhibitory immune receptors: novel insights and implications for immune regulation. *Mol Immunol* 2007; **44**: 2153-2164 [PMID: 17188357 DOI: 10.1016/j.molimm.2006.11.014]

77 **Braud VM**, Biton J, Becht E, Knockaert S, Mansuet-Lupo A, Cosson E, Damotte D, Alifano M, Validire P, Anjuère F, Cremer I, Girard N, Gossot D, Seguin-Givelet A, Dieu-Nosjean MC, Germain C. Expression

of LLT1 and its receptor CD161 in lung cancer is associated with better clinical outcome. *Oncoimmunology* 2018; **7**: e1423184 [PMID: 29721382 DOI: 10.1080/2162402X.2017.1423184]
78 **Gentles AJ**, Newman AM, Liu CL, Bratman SV, Feng W, Kim D, Nair VS, Xu Y, Khuong A, Hoang CD, Diehn M, West RB, Plevritis SK, Alizadeh AA. The prognostic landscape of genes and infiltrating immune cells across human cancers. *Nat Med* 2015; **21**: 938-945 [PMID: 26193342 DOI: 10.1038/nm.3909]
79 **Fergusson JR**, Hühn MH, Swadling L, Walker LJ, Kurioka A, Llibre A, Bertoletti A, Holländer G, Newell EW, Davis MM, Sverremark-Ekström E, Powrie F, Capone S, Folgori A, Barnes E, Willberg CB, Ussher JE, Klenerman P. CD161(int)CD8+ T cells: a novel population of highly functional, memory CD8+ T cells enriched within the gut. *Mucosal Immunol* 2016; **9**: 401-413 [PMID: 26220166 DOI: 10.1038/mi.2015.69]
80 **Bialoszewska A**, Malejczyk J. Biological and Clinical Significance of Human NKRP1A/LLT1 Receptor/Ligand Interactions. *Crit Rev Immunol* 2018; **38**: 479-489 [PMID: 31002602 DOI: 10.1615/CritRevImmunol.2019029559]
81 **Teama S**, Fawzy A, Teama S, Helal A, Drwish AD, Elbaz T, Desouky E. Increased Serum Endoglin and Transforming Growth Factor β1 mRNA Expression and Risk of Hepatocellular Carcinoma in Cirrhotic Egyptian Patients. *Asian Pac J Cancer Prev* 2016; **17**: 2429-2434 [PMID: 27268609]
82 **Dunn GP**, Bruce AT, Ikeda H, Old LJ, Schreiber RD. Cancer immunoediting: from immunosurveillance to tumor escape. *Nat Immunol* 2002; **3**: 991-998 [PMID: 12407406 DOI: 10.1038/ni1102-991]
83 **Schreiber RD**, Old LJ, Smyth MJ. Cancer immunoediting: integrating immunity's roles in cancer suppression and promotion. *Science* 2011; **331**: 1565-1570 [PMID: 21436444 DOI: 10.1126/science.1203486]
84 **O'Donnell JS**, Teng MWL, Smyth MJ. Cancer immunoediting and resistance to T cell-based immunotherapy. *Nat Rev Clin Oncol* 2019; **16**: 151-167 [PMID: 30523282 DOI: 10.1038/s41571-018-0142-8]
85 **Efremova M**, Rieder D, Klepsch V, Charoentong P, Finotello F, Hackl H, Hermann-Kleiter N, Löwer M, Baier G, Krogsdam A, Trajanoski Z. Targeting immune checkpoints potentiates immunoediting and changes the dynamics of tumor evolution. *Nat Commun* 2018; **9**: 32 [PMID: 29296022 DOI: 10.1038/s41467-017-02424-0]
86 **Zou W**, Chen L. Inhibitory B7-family molecules in the tumour microenvironment. *Nat Rev Immunol* 2008; **8**: 467-477 [PMID: 18500231 DOI: 10.1038/nri2326]
87 **Pardoll DM**. The blockade of immune checkpoints in cancer immunotherapy. *Nat Rev Cancer* 2012; **12**: 252-264 [PMID: 22437870 DOI: 10.1038/nrc3239]
88 **DuPage M**, Mazumdar C, Schmidt LM, Cheung AF, Jacks T. Expression of tumour-specific antigens underlies cancer immunoediting. *Nature* 2012; **482**: 405-409 [PMID: 22318517 DOI: 10.1038/nature10803]
89 **Ribas A**, Wolchok JD. Cancer immunotherapy using checkpoint blockade. *Science* 2018; **359**: 1350-1355 [PMID: 29567705 DOI: 10.1126/science.aar4060]
90 **Rosenberg J**, Huang J. $CD8^+$ T Cells and NK Cells: Parallel and Complementary Soldiers of Immunotherapy. *Curr Opin Chem Eng* 2018; **19**: 9-20 [PMID: 29623254 DOI: 10.1016/j.coche.2017.11.006]
91 **Crouse J**, Xu HC, Lang PA, Oxenius A. NK cells regulating T cell responses: mechanisms and outcome. *Trends Immunol* 2015; **36**: 49-58 [PMID: 25432489 DOI: 10.1016/j.it.2014.11.001]
92 **Selby MJ**, Engelhardt JJ, Quigley M, Henning KA, Chen T, Srinivasan M, Korman AJ. Anti-CTLA-4 antibodies of IgG2a isotype enhance antitumor activity through reduction of intratumoral regulatory T cells. *Cancer Immunol Res* 2013; **1**: 32-42 [PMID: 24777248 DOI: 10.1158/2326-6066.CIR-13-0013]
93 **Bulliard Y**, Jolicoeur R, Windman M, Rue SM, Ettenberg S, Knee DA, Wilson NS, Dranoff G, Brogdon JL. Activating Fc γ receptors contribute to the antitumor activities of immunoregulatory receptor-targeting antibodies. *J Exp Med* 2013; **210**: 1685-1693 [PMID: 23897982 DOI: 10.1084/jem.20130573]
94 **Peggs KS**, Quezada SA, Chambers CA, Korman AJ, Allison JP. Blockade of CTLA-4 on both effector and regulatory T cell compartments contributes to the antitumor activity of anti-CTLA-4 antibodies. *J Exp Med* 2009; **206**: 1717-1725 [PMID: 19581407 DOI: 10.1084/jem.20082492]
95 **Simpson TR**, Li F, Montalvo-Ortiz W, Sepulveda MA, Bergerhoff K, Arce F, Roddie C, Henry JY, Yagita H, Wolchok JD, Peggs KS, Ravetch JV, Allison JP, Quezada SA. Fc-dependent depletion of tumor-infiltrating regulatory T cells co-defines the efficacy of anti-CTLA-4 therapy against melanoma. *J Exp Med* 2013; **210**: 1695-1710 [PMID: 23897981 DOI: 10.1084/jem.20130579]
96 **Romano E**, Kusio-Kobialka M, Foukas PG, Baumgaertner P, Meyer C, Ballabeni P, Michielin O, Weide B, Romero P, Speiser DE. Ipilimumab-dependent cell-mediated cytotoxicity of regulatory T cells ex vivo by nonclassical monocytes in melanoma patients. *Proc Natl Acad Sci USA* 2015; **112**: 6140-6145 [PMID: 25918390 DOI: 10.1073/pnas.1417320112]

World Journal of Gastroenterology

Submit a Manuscript: https://www.f6publishing.com

World J Gastroenterol 2020 January 14; 26(2): 154-167

DOI: 10.3748/wjg.v26.i2.154

ISSN 1007-9327 (print) ISSN 2219-2840 (online)

ORIGINAL ARTICLE

Retrospective Cohort Study

Novel methylation gene panel in adjacent normal tissues predicts poor prognosis of colorectal cancer in Taiwan

Chih-Hsiung Hsu, Cheng-Wen Hsiao, Chien-An Sun, Wen-Chih Wu, Tsan Yang, Je-Ming Hu, Chi-Hua Huang, Yu-Chan Liao, Chao-Yang Chen, Fu-Huang Lin, Yu-Ching Chou

ORCID number: Chih-Hsiung Hsu (0000-0003-4423-4231); Cheng-Wen Hsiao (0000-0002-1141-0211); Chien-An Sun (0000-0001-9041-0537); Wen-Chih Wu (0000-0002-8787-8056); Tsan Yang (0000-0002-8265-6438); Je-Ming Hu (0000-0002-7377-0984); Chi-Hua Huang (0000-0002-2766-1939); Yu-Chan Liao (0000-0002-7405-0145); Chao-Yang Chen (0000-0002-2246-7635); Fu-Huang Lin (0000-0001-9878-9625); Yu-Ching Chou (0000-0003-4823-6541).

Author contributions: Hsu CH and Chou YC designed the research; Hsiao CW, Sun CA, Wu WC, and Yang T performed the research; Hsiao CW, Hu JM, and Chen CY collected the data; Hsu CH, Huang CH, Liao YC, Lin FH, and Chou YC analyzed the data; Hsu CH and Chou YC wrote the paper.

Supported by the Ministry of Science and Technology, Taiwan, No. MOST 104-2314-B-016-010-MY2 and No. MOST 106-2320-B-016-018; and the Ministry of National Defense, Taiwan, No. MAB-107-075, No. MAB-108-057 and No. MAB-109-061.

Institutional review board statement: This study was approved by the TSGH Institutional Review Board (TSGHIRB approval number: 098-05-292 and 2-105-05-129).

Informed consent statement: Written informed consent was obtained from all patients before enrollment into the study to evaluate their prognosis.

Chih-Hsiung Hsu, Je-Ming Hu, Yu-Ching Chou, Graduate Institute of Medical Sciences, National Defense Medical Center, Taipei 114, Taiwan

Chih-Hsiung Hsu, Teaching Office, Tri-Service General Hospital, National Defense Medical Center, Taipei 114, Taiwan

Cheng-Wen Hsiao, Je-Ming Hu, Chao-Yang Chen, Division of Colorectal Surgery, Department of Surgery, Tri-Service General Hospital, National Defense Medical Center, Taipei 114, Taiwan

Chien-An Sun, Department of Public Health, College of Medicine, Fu-Jen Catholic University, New Taipei City 242, Taiwan

Chien-An Sun, Big Data Research Center, College of Medicine, Fu-Jen Catholic University, New Taipei City 242, Taiwan

Wen-Chih Wu, Chi-Hua Huang, Yu-Chan Liao, Fu-Huang Lin, Yu-Ching Chou, School of Public Health, National Defense Medical Center, Taipei 114, Taiwan

Wen-Chih Wu, Department of Surgery, Suao and Yuanshan Branches of Taipei Veterans General Hospital, Yilan County 264, Taiwan

Tsan Yang, Department of Health Business Administration, Meiho University, Pingtung County 912, Taiwan

Je-Ming Hu, Chao-Yang Chen, Adjunct Instructor, School of Medicine, National Defense Medical Center, Taipei 114, Taiwan

Corresponding author: Yu-Ching Chou, PhD, Associate Professor, School of Public Health, National Defense Medical Center, No. 161 Sec. 6, Minquan E. Road, Neihu District, Taipei 114, Taiwan. trishow@mail.ndmctsgh.edu.tw

Abstract

BACKGROUND

It is evident that current clinical criteria are suboptimal to accurately estimate patient prognosis. Studies have identified epigenetic aberrant changes as novel prognostic factors for colorectal cancer (CRC).

AIM

To estimate whether a methylation gene panel in different clinical stages can reflect a different prognosis.

Conflict-of-interest statement: We have no financial relationships to disclose.

Data sharing statement: No additional data are available.

STROBE statement: The authors have read the STROBE Statement-checklist of items, and the manuscript was prepared and revised according to the STROBE Statement-checklist of items.

Manuscript source: Invited Manuscript

Received: October 24, 2019
Peer-review started: October 24, 2019
First decision: December 5, 2019
Revised: December 14, 2019
Accepted: December 21, 2019
Article in press: December 21, 2019
Published online: January 14, 2020

P-Reviewer: Brisinda G, Mohamed SY, Wang K
S-Editor: Gong ZM
L-Editor: Wang TQ
E-Editor: Liu JH

METHODS
We enrolled 120 CRC patients from Tri-Service General Hospital in Taiwan and used the candidate gene approach to select six genes involved in carcinogenesis pathways. Patients were divided into two groups based on the methylation status of the six evaluated genes, namely, the < 3 aberrancy group and ≥ 3 aberrancy group. Various tumor stages were divided into two subgroups (local and advanced stages) on the basis of the pathological type of the following tissues: Tumor and adjacent normal tissues (matched normal). We assessed DNA methylation in tumors and adjacent normal tissues from CRC patients and analyzed the association between DNA methylation with different cancer stages and the prognostic outcome including time to progression (TTP) and overall survival.

RESULTS
We observed a significantly increasing trend of hazard ratio as the number of hypermethylated genes increased both in normal tissue and tumor tissue. The 5-year TTP survival curves showed a significant difference between the ≥ 3 aberrancy group and the < 3 aberrancy group. Compared with the < 3 aberrancy group, a significantly shorter TTP was observed in the ≥ 3 aberrancy group. We further analyzed the interaction between CRC prognosis and different cancer stages (local and advanced) according to the methylation status of the selected genes in both types of tissues. There was a significantly shorter 5-year TTP for tumors at advanced stages with the promoter methylation status of selected genes than for those with local stages. We found an interaction between cancer stages and the promoter methylation status of selected genes in both types of tissues.

CONCLUSION
Our data provide a significant association between the methylation markers in normal tissues with advanced stage and prognosis of CRC. We recommend using these novel markers to assist in clinical decision-making.

Key words: DNA methylation; Panel genes; Clinical stage; Prognosis outcome; Adjacent normal tissues; Colorectal cancer

Core tip: Our data show that a novel methylation gene panel in adjacent normal tissues predicts a poor prognosis of colorectal cancer. We recommend that the matched normal tissues of patients with colorectal cancer could be an alternative source of prognostic markers to assist clinical decision-making.

Citation: Hsu CH, Hsiao CW, Sun CA, Wu WC, Yang T, Hu JM, Huang CH, Liao YC, Chen CY, Lin FH, Chou YC. Novel methylation gene panel in adjacent normal tissues predicts poor prognosis of colorectal cancer in Taiwan. *World J Gastroenterol* 2020; 26(2): 154-167
URL: https://www.wjgnet.com/1007-9327/full/v26/i2/154.htm
DOI: https://dx.doi.org/10.3748/wjg.v26.i2.154

INTRODUCTION

Colorectal cancer (CRC) is a leading cause of cancer-related morbidity and mortality worldwide. In 2017, in the United States, approximately 135430 patients were newly diagnosed with CRC, and 50260 deaths from CRC were reported[1]. Survival of patients with CRC is closely linked to the tumor stage at diagnosis, and the 5-year relative survival rates are 64.9% for all stages and 89.9% for local, 71.3% for regional, and 13.9% for distant disease[2]. Cancer staging systems enable reasonable adjuvant treatment, help stratify tumors according to the risk of recurrence, and help establish precise prognoses. Using resection specimens, the pathologic staging of CRC is conducted according to the tumor-node-metastasis (TNM) classification from the Seventh Edition of the American Joint Committee on Cancer (AJCC) Staging Manual.

According to the TNM staging system, the survival of patients with CRC is related to the size of the primary tumor (T), nearby affected lymph nodes (N), and distant metastasis (M)[3]. According to this classification, patients with stage II CRC have a low or high risk based on clinical risk factors including tumor size, number of lymph nodes investigated, tumor differentiation, perforation, obstruction, and lymphovascular invasion. Routine adjuvant therapy after surgical resection is recommended for patients with high-risk stage II CRC as well as for those with stage III and IV tumors[4]. However, 10%-20% of patients with stage II CRC and 30%-40% of patients with stage III CRC ultimately develop recurrence after therapeutic intervention. Low-risk patients with stage II CRC show a good prognosis, as only a small proportion of these patients experience relapse[5]. The prognostic factors that define these relapse-prone patients should be identified to optimize treatment selection.

Several studies have been conducted to identify novel prognostic and predictive biomarkers for CRC, including both genetic and epigenetic aberrant changes. Genetic abnormalities include microsatellite instability; chromosomal instability; mutations of cancer driver genes such as *KRAS, BRAF, TP53*, and *PIK3CA*; certain proteins; microRNAs; and gene expression signatures[6,7]. Research has demonstrated that the epigenetic mechanism of DNA methylation plays an important role in several essential biological processes, such as development, cell differentiation, and gene silencing[8]. Epigenetic silencing of multiple genes involved in DNA repair, cell cycle, and apoptosis through promoter hypermethylation is a common event in various cancers including CRC[9]. These molecular biomarkers could be used to stratify patients with the same tumor stage according to different molecular factors for optimal adjuvant chemotherapy[10,11].

Previous studies have demonstrated that *CDKN2A*, *hMLH1*, and *MGMT* hypermethylation, which is related to carcinogenesis pathways *via* gene silencing, could serve as a diagnostic prognostic marker for CRC[12,13]. In the present study, in addition to the aforementioned genes, we selected three other candidate genes, namely, *CSF2*, *DIS3L2*, and *OAF*; *CSF2* and *DIS3L2*, which are involved in inhibitory effects on tumor growth[14,15], were selected from a previous study[16]. *OAF* (the out at first homolog gene), selected from PRECOG (PREdiction of Clinical Outcomes from Genomic Profiles, https://precog.stanford.edu/) and MethHC (a database of DNA Methylation and gene expression in Human Cancer, http://methhc.mbc.nctu.edu.tw/php/index.php), is located at chromosome 11q23.2 and is ubiquitously expressed in the liver (RPKM 56.8) and colon (RPKM 31.5) (NCBI Gene, https://www.ncbi.nlm.nih.gov/gene). To the best of our knowledge, little is known about this gene. According to browser data from genome-wide association studies (FANTOM CAT, http://fantom.gsc.riken.jp/cat/v1/#/), the *OAF* locus is related to small-cell lung carcinoma[17].

To determine the effect of the methylation status of candidate genes on the relationship between the histological stage and prognosis of CRC, we examined DNA methylation in tumor tissues and adjacent normal tissues (matched normal). In this study, we propose the understanding that the methylation status of a multiple-gene panel, even in matched normal tissues, combined with different clinical stages may predict the prognosis and provide clinical recommendations for optimal treatment for CRC.

MATERIALS AND METHODS

Patients and specimen collection

The methods applied in this study are described in detail elsewhere[13]. In this hospital-based retrospective cohort study, we analyzed the data of patients diagnosed with CRC between 2006 and 2010 who underwent surgical resection at Tri-Service General Hospital (TSGH), Taiwan, to evaluate their prognosis in 5 years. Written informed consent was obtained from all patients before enrollment into the study to evaluate their prognosis. This study was approved by the TSGH Institutional Review Board (TSGHIRB approval number: 098-05-292 and 2-105-05-129). According to the clinical practice guideline of the Division of Colon and Rectum of TSGH, the enrollees should return for a check-up once every 3 mo in the first year after undergoing surgical resection and once every 3-6 mo thereafter. From the cancer registration database of TSGH, information on registered patients, including their sex, age at surgery (continuous variable), adjuvant chemotherapy, histological grade, and tumor location and their follow-up data on recurrence, metastasis, and survival, was obtained.

Time to progression (TTP) and overall survival (OS) were calculated from the date

of surgery to the presentation of disease progression (including cancer recurrence or metastasis), death from any cause, or till the last follow-up date before December 31, 2010. On the basis of the inclusion criteria, 120 tumor tissues and matched normal tissues (240 samples) were obtained from the enrollees.

DNA extraction and methylation-specific PCR

Cellulose-coated magnetic beads were employed to extract genomic DNA from the samples by using the MagCore Compact Automated Nucleic Acid Extractor (Catalogue No. MCA0801; RBC Bioscience, Taipei, Taiwan) and the Genomic DNA Tissue Kit (Catalogue No. 69504; Qiagen, Taipei, Taiwan), according to the manufacturer's protocol. Isolated DNA was treated with sodium bisulfite using the EZ DNA Methylation Kit (Zymo Research Corporation, Orange, CA, United States).

The promoter methylation status of *CDKN2A*, *hMLH1*, *MGMT*, *CSF2*, *DIS3L2*, and *OAF* genes was assessed using methylation-specific PCR (MS-PCR), as described in our previous research[13]. The reaction solution (25 μL) contained HotStart Taq Premix (12.5 μL, RBC Bioscience, Taipei, Taiwan), 1.2-μL aliquots of forward and reverse primers, and bisulfite-converted DNA.

For MS-PCR, we used the following oligonucleotide primers: *CDKN2A*: 5′-TTATTAGAGGGTGGGGCGGATCGC-3′ (forward primer) and 5′-GACCCCGAACCGCGACCGTAA-3′ (reverse primer) to amplify the methylated sequence (PCR annealing at 62 °C, product size: 150 bp) and 5′-TTATTAGAGGGTGGGGTGGATTGT-3′ (forward primer) and 5′-CAACCCCAAACCACAACCATAA-3′ (reverse primer) to amplify the unmethylated sequence (PCR annealing at 62 °C, product size: 151 bp); *hMLH1*: 5′-ACGTAGACGTTTTATTAGGGTCGC-3′ (forward primer) and 5′-CCTCATCGTAACTACCCGCG-3′ (reverse primer) to amplify the methylated sequence (PCR annealing at 60 °C, product size: 118 bp) and 5′-TTTTGATGTAGATGTTTTATTAGGGTTGT-3′ (forward primer) and 5′-ACCACCTCATCATAACTACCCACA-3′ (reverse primer) to amplify the unmethylated sequence (PCR annealing at 60 °C, product size: 124 bp); *MGMT*: 5′-TTTCGACGTTCGTAGGTTTTCGC-3′ (forward primer) and 5′-GCACTCTTCCGAAAACGAAACG-3′ (reverse primer) to amplify the methylated sequence (PCR annealing at 53 °C, product size: 81 bp) and 5′-TTTGTGTTTTGATGTTTGTAGGTTTTTGT-3′ (forward primer) and 5′-AACTCCACACTCTTCCAAAAACAAAACA-3′ (reverse primer) to amplify the unmethylated sequence (PCR annealing at 53 °C, product size: 93 bp); *CSF2*: 5′-TGATTATTTAGGGAAAAGGTTTATC-3′ (forward primer) and 5′-ATAACCACAAAATACCAAAAAAACG-3′ (reverse primer) to amplify the methylated sequence (PCR annealing at 56 °C, product size: 105 bp) and 5′-ATTATTTAGGGAAAAGGTTTATTGT-3′ (forward primer) and 5′-AATAACCACAAAATACCAAAAAAACA-3′ (reverse primer) to amplify the unmethylated sequence (PCR annealing at 60 °C, product size: 104 bp); *DIS3L2*: 5′-GTCGTAGTTGAATCGTCGATTAC-3′ (forward primer) and 5′-TTACTAAAAAAAATACTCTTCCGAA-3′ (reverse primer) to amplify the methylated sequence (PCR annealing at 54 °C, product size: 134 bp) and 5′-GTTGTAGTTGAATTGTTGATTATGA-3′ (forward primer) and 5′-TTACTAAAAAAAATACTCTTCCAAA-3′ (reverse primer) to amplify the unmethylated sequence (PCR annealing at 55 °C, product size: 134 bp); and *OAF*: 5′-GTTATTGTCGTGGAGCGTTAGC-3′ (forward primer) and 5′-CCTACCTCCCGTACTTCCCG-3′ (reverse primer) to amplify the methylated sequence (PCR annealing at 59.4 °C, product size: 170 bp) and 5′-TTATTGTTGTGGAGTGTTAGTGTTT-3′ (forward primer) and 5′-CCTACCTCCCATACTTCCCACAT-3′ (reverse primer) to amplify the unmethylated sequence (PCR annealing at 59.4 °C, product size: 169 bp). The PCR cycling conditions were as follows: 10 min at 95 °C; 35 cycles of denaturation for 30 s at 95 °C; 30-s annealing at gene-appropriate temperature; 30-s extension at 72 °C; and final extension for 4 min at 72 °C. After the amplification, PCR products were mixed with a loading buffer, electrophoresed (for 25 min) on a 2% agarose gel by using 0.2 μL of gel-stained dye, and visualized using an ultraviolet transilluminator.

Statistical analysis

Patients were divided into two groups based on the methylation status of the six evaluated genes, namely, < 3 aberrancy group and ≥ 3 aberrancy group. In addition, various tumor stages were divided into two subgroups (local and advanced stages) on the basis of the pathological type of the following tissues: Tumor and adjacent normal tissues (matched normal). Associations of the number of hypermethylated genes under study and different clinical stages with TTP or OS were assessed using the univariate Cox proportional hazards regression model. The multivariate Cox

regression model was then employed to estimate the independent prognostic effect of the number of methylated genes, with adjustment for sex, age at surgery (continuous variable), adjuvant chemotherapy, histological grade, and tumor location, based on a previous study[13]. The positive predictive value (PPV) and negative predictive value (NPV) of the ≥ 3 aberrancy group in predicting the prognosis of CRC were calculated. The area under the receiver operating characteristic (ROC) curve is reported along with its 95% confidence interval (CI). The 5-year TTP and OS curves for the < 3 aberrancy and ≥ 3 aberrancy groups were plotted using the Kaplan–Meier method and were compared using the log-rank test. Statistical analyses were performed using IBM Statistical Package for the Social Sciences (SPSS) V.22 (IBM SPSS Statistics 22). All statistical tests were two-sided, and *P* values less than 0.05 were considered statistically significant.

RESULTS

Patient characteristics

In the study, 120 CRC tumor samples and adjacent normal samples from the TSGH tumor bank were analyzed. The relationship between the methylation status of the selected genes and the demographic and clinicopathological features of patients with CRC was evaluated. As shown in Table 1, the progression of CRC in 5 years indicated that 37.5% of the enrollees had cancer recurrence or metastasis, and 19.2% of the enrollees died during the period. Although the six genes were methylated in both tumor and matched normal tissue samples, the percentage of methylation was higher in tumor tissues than in normal tissues (*CDKN2A*, 67.3% *vs* 32.7%; *MGMT*, 76.3% *vs* 23.7%; *MLH1*, 51.6% *vs* 48.4%; *CSF2*, 51.6% *vs* 48.4%; *DIS3L2*, 55.1% *vs* 44.9%; *OAF*, 68.1% *vs* 31.9%). In addition, progression was detected in significantly higher percentages in the normal tissue with OAF hypermethylation and in the ≥ 3 aberrancy group. The PPV and NPV of ≥ 3 aberrancies in predicting the progression of CRC were 51.4% and 68.2% in normal tissues and 43.9% and 76.3% in tumor tissues, respectively. The PPV and NPV of the ≥ 3 aberrancy group in predicting the survival of CRC were 20.0% and 81.2% in normal tissues and 18.3% and 78.9% in tumor tissues, respectively. No other associations were found between the methylation statuses of the six genes and the demographic and clinicopathological characteristics of the study patients.

Prognostic outcome

The association between the number of hypermethylated genes and the 5-year TTP and OS of patients with CRC was separately assessed. We observed a significantly increasing trend of hazard ratio (HR) as the number of hypermethylated genes increased both in normal tissue ($P = 0.02$) and tumor tissue ($P = 0.02$) (Table 2).

The 5-year TTP survival curves showed a significant difference between the ≥ 3 aberrancy group and the < 3 aberrancy group ($P = 0.02$ for normal tissue; $P < 0.01$ for tumor tissue) (Figure 1). Compared with the < 3 aberrancy group, a significantly shorter TTP was observed in the ≥ 3 aberrancy group [HR (95%CI) = 1.99 (1.03-3.85) for normal tissue, 3.26 (1.27-8.39) for tumor tissue], even after adjustment for confounders in multivariable analysis [HR (95%CI) = 2.01 (1.00-4.01) for normal tissue, 3.18 (1.21-8.39) for tumor tissue].

Although there was an increasing trend of HR of the 5-year OS of patients with CRC with the increasing number of hypermethylated genes in normal tissue, this difference did not reach statistical significance ($P = 0.33$) (Table 3). The Kaplan–Meier curves of 5-year OS of patients with CRC between the ≥ 3 aberrancy group and the < 3 aberrancy group are shown in Figure 2. The log-rank test revealed no significant differences between the groups in both types of tissues over the entire Kaplan–Meier curve. The area under the ROC curve of CRC progression and survival was 0.59 (95%CI: 0.49-0.70, $P = 0.09$) and 0.48 (95%CI: 0.35-0.61, $P = 0.77$) in tumor tissue, respectively. The area under the ROC curve of CRC progression and survival was 0.59 (95%CI: 0.48-0.69, $P = 0.11$) and 0.51 (95%CI: 0.38-0.64, $P = 0.91$) in normal tissue, respectively.

Cancer stages and methylation status

We further analyzed the interaction between CRC prognosis and different cancer stages (local and advanced) according to the methylation status of the selected genes in both types of tissues. Table 4 reveals a significantly shorter 5-year TTP for tumors at advanced stages with the promoter methylation status of selected genes than for those with local stages. The adjusted HR of *OAF* methylation in normal tissue in patients with advanced stages was 20.3 (100%CI: 4.12-100). In addition, we found an

Table 1 Characteristics and distribution of methylation status in patients with colorectal cancer (*n* = 120), *n* (%)

Variables	Total	Methylation status			
		OAF		≥ 3 of genes[1]	
		Normal	Tumors	Normal	Tumors
Sex					
Male	60 (50.0)	13 (28.9)	28 (62.2)	16 (26.7)	41 (68.3)
Female	60 (50.0)	16 (34.8)	34 (73.9)	19 (31.7)	41 (68.3)
Age in yr at surgery					
Mean (SD)	63.8 (14.8)	62.6 (12.6)	63.2 (15.0)	62.5 (13.5)	62.5 (15.3)
< 65	61 (50.8)	15 (30.0)	33 (66.0)	19 (31.1)	45 (73.8)
≥ 65	59 (49.2)	14 (34.1)	29 (70.7)	16 (27.1)	37 (62.7)
Stage					
	19 (15.8)	2 (16.7)	6 (50.0)	6 (31.6)	10 (52.6)
	39 (32.5)	6 (20.7)	22 (75.9)	11 (28.2)	26 (66.7)
	40 (33.3)	14 (45.2)	22 (71.0)	11 (27.5)	29 (72.5)
	22 (18.3)	7 (36.8)	12 (63.2)	7 (31.8)	17 (77.3)
Adjuvant chemotherapy					
No	32 (28.3)	5 (22.7)	13 (59.1)	13 (40.6)	23 (71.9)
Yes	81 (71.7)	24 (36.9)	46 (70.8)	22 (27.2)	55 (67.9)
Lymph/vascular invasion					
No	44 (97.8)	12 (35.3)	21 (61.8)	18 (40.9)	28 (63.6)
Yes	1 (2.2)	0 (0)	1 (100.0)	0 (0)	1 (100.0)
Histological grade[2]					
Well or Moderately	96 (88.9)	23 (31.9)	45 (62.5)	31 (32.3)	62 (64.6)
Poor or undifferentiated	12 (11.1)	5 (45.5)	10 (90.9)	2 (16.7)	11 (91.7)
Tumor location[2]					
Colon	89 (78.8)	19 (28.4)	46 (68.7)	27 (30.3)	59 (66.3)
Rectum	24 (21.2)	10 (50.0)	13 (65.0)	8 (33.3)	19 (79.2)
Progression in 5 yr					
No	75 (62.5)	11 (22.0)[a]	33 (66.0)	17 (22.7)[a]	46 (61.3)
Yes	45 (37.5)	18 (43.9)	29 (70.7)	18 (40.0)	36 (80.0)
All-cause death in 5 yr					
No	97 (80.8)	22 (31.0)	50 (70.4)	28 (28.9)	67 (69.1)
Yes	23 (19.2)	7 (35.0)	12 (60.0)	7 (30.4)	15 (65.2)

[1]Including *CDKN2A*, *hMLH1*, *MGMT*, *CSF2*, *DIS3L2*, and *OAF*.
[2]The total number of patients with colorectal cancer does not correspond because of missing data.
[a]$P < 0.05$. *OAF*: The out at first homolog gene; SD: Standard deviation.

interaction between cancer stages and the promoter methylation status of selected genes in both types of tissues. In normal tissue, there was a significant joint effect that increased the association of CRC progression with advanced cancer stages in the ≥3 aberrancy group (Me/advanced), with an HR of 33.4 (95%CI: 7.49-149; $P < 0.01$); after adjusting for confounders, the HR was 28.8 (95%CI: 6.24-133; $P < 0.01$). A similar result was observed in the tumor tissue, in which the crude and adjusted HRs were 23.1 (95%CI: 3.14-170; $P < 0.01$) and 20.8 (95%CI: 2.75-157; $P < 0.01$), respectively. With regard to the effect of the interaction between methylation of the gene promoter region and different cancer stages on the 5-year OS of patients with CRC, no significant joint effect was observed in both types of tissues (Table 5).

DISCUSSION

The TNM staging system, which is based on anatomical information including the size and extent of the primary tumor, is widely used to guide clinical treatment strategy and predict the prognosis of cancer. However, CRC is an etiologically

Table 2 Relationship between the number of hypermethylated genes and 5-year time to progression of colorectal cancer patients, *n* (%)

	Normal tissues						Tumor tissues					
	No. of subjects	No. of cases	Crude		Adjusted		No. of subjects	No. of cases	Crude		Adjusted	
			HR	95%CI	HR	95%CI			HR	95%CI	HR	95%CI
NO. of hypermethylated genes												
0	9	3 (33.3)	1.00	Referent	1.00	Referent	3	1 (33.3)	1.00	Referent	1.00	Referent
1	34	8 (23.5)	0.76	0.15-3.74	0.64	0.13-3.23	7	0 (0)	N/A	N/A	N/A	N/A
2	42	16 (38.1)	1.58	0.36-6.94	1.62	0.34-7.62	28	8 (28.6)	0.47	0.05-4.20	0.65	0.07-5.88
3	21	12 (57.1)	2.66	0.58-12.19	2.18	0.46-10.4	39	15 (38.5)	1.02	0.13-7.86	1.36	0.17-10.7
4	11	3 (27.3)	1.28	0.21-7.65	1.48	0.18-12.2	23	14 (60.9)	2.12	0.28-16.3	2.56	0.33-20.2
5	3	3 (100)	7.26[a]	1.00-52.84	4.70	0.57-39.0	17	6 (35.3)	1.17	0.14-9.71	1.52	0.17-13.5
6	0	0	N/A	N/A	N/A	N/A	3	1 (33.3)	1.13	0.07-18.0	2.10	0.12-38.3
P value[1]				0.02		0.02				0.02		0.02
≥ 3 of genes[2]	35	18 (51.4)	1.99[a]	1.03-3.85	2.01[a]	1.00-4.01	82	36(43.9)	3.26[a]	1.27-8.39	3.18[a]	1.21-8.39

[1]*P* for trend.
[2]Including *CDKN2A*, *hMLH1*, *MGMT*, *CSF2*, *DIS3L2*, and *OAF*.
[a]*P* < 0.05. Adjusted for gender, age at surgery (continuous), adjuvant chemotherapy, histological grade, and tumor location. CI: Confidence interval; HR: Hazard ratio; N/A: Not applicable.

heterogeneous disease involving several distinct biologic pathways, and the survival status of different patients at the same TNM stage varies[3,18].

Aberrant DNA methylation of certain loci is characteristic of certain human cancers, which leads to silencing of tumor-suppressor genes through methylation of the CpG islands in promoters[19,20]. Gene hypermethylation has been reported to be a robust and reliable diagnostic method and, thus, a promising source of biomarkers for cancer[21,22]. Moreover, the gene methylation status can be used as a biomarker for the prognosis of cancer; it can predict the cancer outcome, malignant potential of the tumor, and risk of tumor recurrence regardless of therapy[23]. In the present paper, we provide the results of an analysis of 120 tumor tissues and matched normal tissues from patients with CRC. The promoter methylation status of the selected genes confirmed the presence of DNA methylation: Methylation in *CDKN2A*, *hMLH1*, *MGMT*, *CSF2*, *DIS3L2*, and *OAF* was significantly associated with an increased risk of CRC progression, as revealed by Cox proportional hazards regression analysis and Kaplan–Meier analysis. In addition, the ≥ 3 aberrancy group, defined by the presence of three or more methylated genes, showed an increased risk of 5-year TTP of CRC, with a significant joint effect between DNA methylation and clinical stage, especially in matched normal tissues.

Hence, our findings can be used together with clinical staging to guide the re-evaluation of clinical management of cancer, and they can serve as suitable indicators to identify patients at a higher risk of recurrence and requiring intensive follow-up. Our results revealed that the presence of three or more methylated genes we selected, which was used for marking subgroups of patients with CRC, could be a useful biomarker for cancer prognosis and provide an indication of the need for aggressive surveillance. Our findings showed that predicting prognosis with high accuracy is important, which can be best achieved with a panel of individually well-performing biomarkers rather than any single marker alone[24].

Several studies have shown that the use of gene promoter panels, usually comprising more than four genes, improves the prediction of prognosis, which is consistent with our finding[25-27]. De Sousa e Melo *et al*[28] showed that the hypermethylation of a panel of WNT target genes, specifically *ASCL2*, *LGR5*, *APCDD1*, *DKK1*, and *AXIN2*, was a strong predictor of CRC recurrence. Exner *et al*[25] found that the CpG island methylator phenotype (CIMP) panel, including *CDKN2A*, *MINT1*, *MINT2*, *MINT31*, and *MLH1*, was an independent poor prognostic factor for disease-free survival (DFS) and OS in rectal cancers. Kim *et al*[27] assessed the methylation status of a panel of genes including *p16*, *p14*, *MINT1*, *MINT2*, *MINT31*, *hMLH1*, *DKK3*, *WNT5A*, *AXIN2*, and *TFAP2E* in patients with CRC and found that higher number of methylations among the panel genes was related to worse clinical outcomes.

However, some studies have reported no relationship between the methylation

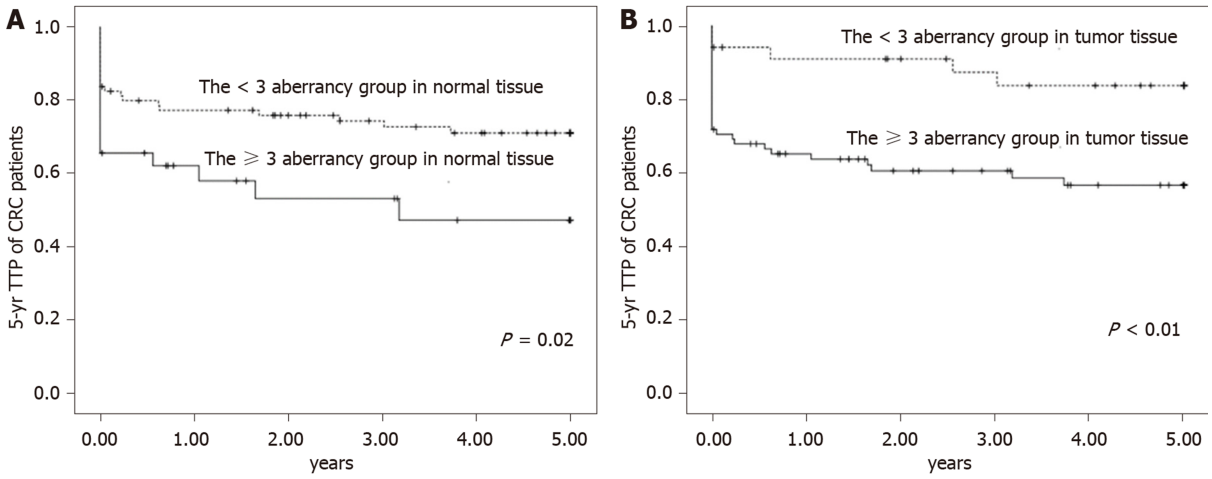

Figure 1 Kaplan–Meier survival curves depicting the effect of ≥ 3 aberrancies in (A) normal tissue and (B) tumor tissue on 5-year time to progression of colorectal cancer patients. Vertical tick marks indicate censored events. TTP: Time to progression; CRC: Colorectal cancer.

status of gene panels and the prognosis of CRC. Recent meta-analyses have also shown no significant effect of the CIMP status on prognosis in 8 of 11 and 13 of 19 previously published studies[29,30]. This inconsistency in results may be attributed to several reasons, including the high heterogeneity of CIMP definitions, the different ethnicities of the study population, and the study method used to detect CpG island methylation.

In addition, genome-wide DNA hypomethylation plays a pivotal role in the development of CRC, as this feature induces genomic instability and global loss of imprinting (LOI); moreover, it facilitates the aberrant expression of proto-oncogenes/oncogenes[31,32]. Rodriguez *et al*[33] suggested that DNA hypomethylation may induce a cascade effect with direct impact on the progression pathway and hence on patient outcomes. Global hypomethylation usually occurs in repetitive transposable elements, such as long interspersed nucleotide element-1 (LINE-1), which comprises approximately 18% of the human genome. Several studies have demonstrated that LINE-1 hypomethylation is significantly correlated with shorter OS, DFS, and cancer-specific survival[34].

In this study, we found that the methylation status of the gene panel in adjacent normal tissues was significantly associated with a poor prognosis. Recently, an increasing number of studies on carcinogenesis have demonstrated that molecular and microscopic changes in normal tissues surrounding tumors lead to cancer progression. Such changes are generally considered a result of the "field effect". Field effect theory postulates that repeated exposure to environmental carcinogens could lead to multiple epigenetic and genetic alterations in normal-appearing tissues; the organ site is at an increased risk of developing premalignant lesions and is prone to cancer recurrence. Several studies have shown that the aberrant methylation status of specific genes could be a potential marker of the CRC field effect[35,36], which is in line with our finding that compared with tumor tissues, aberrant DNA methylation in adjacent normal tissues is associated with a poor prognosis after surgical resection.

CDKN2A (*p16*), which has critical roles in cell cycle progression, cellular senescence, and the development of human cancers, is the most frequently studied methylation biomarker[37]. Many studies, including subgroup evaluations, have demonstrated statistically significant relationships between *CDKN2A* hypermethylation and poor prognosis[38,39]. The DNA mismatch repair (MMR) defects that result from aberrant *hMLH1* methylation are linked to hereditary nonpolyposis CRC[40]. Kuan *et al*[41] and Iida *et al*[42] have found a significant association between *hMLH1* methylation and a worse prognosis in TNM stages I–IV. Somatic epigenetic inactivation of *MGMT* has been reported as an early event in CRC, in which it is known to be associated with *KRAS* and TP53 mutations. The methylation status of *MGMT* is a key prognostic factor for treatment with alkylating drugs such as temozolomide and carmustine, especially in metastatic CRC[43]. Lee *et al*[44] showed that CSF2 was the most upregulated gene of significance for tumor development and invasiveness among those associated with positive regulation of tyrosine phosphorylation of *STAT5*, and it could serve as an important prognosticator of urothelial carcinoma.

DIS3L2 inactivation was associated with mitotic abnormalities and altered the expression of mitotic checkpoint proteins. Overexpression of *DIS3L2* inhibited the growth of human cancer cell lines[45]. In this study, we evaluated the methylation

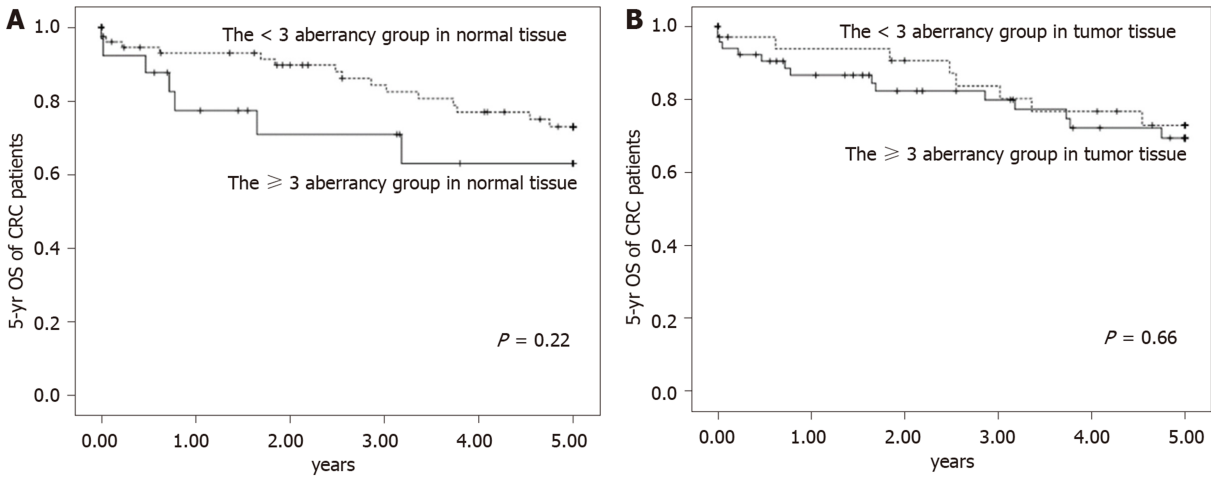

Figure 2 Kaplan–Meier survival curves depicting the effect of ≥ 3 aberrancies in (A) normal tissue and (B) tumor tissue on 5-year overall survival of colorectal cancer patients. Vertical tick marks indicate censored events. OS: Overall survival; CRC: Colorectal cancer.

status of *OAF* selected from PRECOG[46] and MethHC[47]. In PRECOG and MethHC, low *OAF* expression was associated with a worse survival outcome, and the methylation frequency of *OAF* in tumor tissues was significantly higher than that in normal tissues. Little is known about this gene, and few studies have shown decreased expression of *OAF* in patients with metastatic breast cancer[48] or ulcerative colitis[49]. Few studies have assessed the association between the methylation status of *CSF2*, *DIS3L2*, and *OAF* and CRC prognosis.

This study has several limitations. The results of this study should be carefully interpreted because of the small sample size. A larger prospective cohort study is warranted to validate these results. Moreover, the enrollees of the present study were from a single population of Taiwan. The utility of the gene panel as a prognostic biomarker for CRC must be validated in other ethnic populations. Finally, data from healthy individuals were unavailable, and the results may not be representative of those in asymptomatic individuals. The development of an acceptable protocol may help study the methylation status of tumor suppressor genes; their distribution in promoter regions; their distribution in the proximal colon, distal colon, and rectum; and their time sequence dependence in healthy individuals, particularly in those who are developing CRC.

It is evident that the current clinical criteria are suboptimal to accurately estimate patient prognosis and outcomes. A new set of methylation markers was identified from our data, particularly in the adjacent normal tissues in patients with advanced stage, providing a basis to apply and investigate the potential of these markers to predict the prognosis of CRC. Future research in large and independent cohorts could define the utility of the new set of markers and address whether the modification of treatment/management decisions based on additional prognostic information from this marker would improve the TTP and OS of patients with CRC. We recommend using these novel markers in adjacent normal tissues of patients with CRC to assist in clinical decision-making.

Table 3 Relationship between the number of hypermethylated genes and 5-year overall survival of colorectal cancer patients, *n* (%)

	Normal tissues						Tumor tissues					
	No. of subjects	No. of cases	Crude		Adjusted		No. of subjects	No. of cases	Crude		Adjusted	
			HR	95%CI	HR	95%CI			HR	95%CI	HR	95%CI
NO. of methylated genes												
0	9	1 (11.11)	1.00	Referent	1.00	Referent	3	1 (33.33)	1.00	Referent	1.00	Referent
1	34	7 (20.59)	1.52	0.19-12.4	1.19	0.14-10.1	7	0 (0)	N/A	N/A	N/A	N/A
2	42	8 (19.05)	1.76	0.22-14.1	0.89	0.10-8.40	28	7 (25)	0.95	0.12-7.72	0.73	0.08-6.55
3	21	4 (19.05)	1.79	0.20-16.0	1.41	0.15-13.2	39	6 (15.38)	0.66	0.08-5.47	0.59	0.07-5.2
4	11	2 (18.18)	2.11	0.19-23.3	1.40	0.10-18.8	23	6 (26.09)	1.24	0.15-10.3	1.16	0.13-10.2
5	3	1 (33.33)	4.89	0.30-78.8	4.91	0.29-83.4	17	3 (17.65)	0.84	0.09-8.06	0.60	0.05-7.13
6	0	0 (0)	N/A	N/A	N/A	N/A	3	0 (0)	N/A	N/A	N/A	N/A
P value[1]				0.33		0.40				0.59		0.64
≥ 3 of genes[2]	35	7 (20.0)	1.31	0.54-3.18	1.50	0.59-3.81	82	15 (18.3)	1.13	0.48-2.66	1.21	0.47-3.10

Adjusted for gender, age at surgery (continuous), adjuvant chemotherapy, histological grade and tumor location.
[1]*P* for trend.
[2]Including *CDKN2A*, *hMLH1*, *MGMT*, *CSF2*, *DIS3L2*, and *OAF*. CI: Confidence interval; HR: Hazard ratio; N/A: Not applicable.

Table 4 Interaction between gene promoter region methylation and different cancer stages for 5-year time to progression of colorectal cancer patients, *n* (%)

	Normal tissues						Tumor tissues					
	No. of subjects	No. of cases	Crude		Adjusted		No. of subjects	No. of cases	Crude		Adjusted	
			HR	95%CI	HR	95%CI			HR	95%CI	HR	95%CI
OAF												
UnMe/local (1 and 2)[1]	33	3 (9.1)	1.00	Referent	1.00	Referent	13	0 (0.0)	1.00	Referent	1.00	Referent
UnMe/advanced (3 and 4)[2]	29	20 (69.0)	14.7[a]	3.38-63.6	16.6[a]	3.69-74.6	16	12 (75.0)	N/A	N/A	N/A	N/A
Me/local (1 and 2)[3]	8	0 (0.0)	N/A	N/A	N/A	N/A	28	3 (10.7)	N/A	N/A	N/A	N/A
Me/advanced (3 and 4)[4]	21	18 (85.7)	19.0[a]	4.30-84.6	20.3[a]	4.12-100	34	26 (76.5)	N/A	N/A	N/A	N/A
P value[1]				< 0.01		< 0.01						
≥ 3 of genes[6]												
UnMe/local (1 and 2)[1]	41	2 (4.88)	1.00	Referent	1.00	Referent	22	2 (9.09)	1.00	Referent	1.00	Referent
UnMe/advanced (3 and 4)[2]	44	25 (56.8)	13.3[a]	3.10-57.0	11.9[a]	2.72-51.8	16	7 (43.8)	7.17	0.80-64.2	6.56	0.72-59.4
Me/local (1 and 2)[3]	17	1 (5.88)	N/A	N/A	N/A	N/A	36	1 (2.78)	0.63	0.04-9.99	0.59	0.04-9.62
Me/advanced (3 and 4)[4]	18	17 (94.4)	33.4[a]	7.49-149	28.8[a]	6.24-133	46	35 (76.1)	23.1[a]	3.14-170	20.8[a]	2.75-157
P value[5]				< 0.01		< 0.01				< 0.01		< 0.01

[1]DNA promoter region unmethylation with cancer stage 1 or 2;
[2]DNA promoter region unmethylation with cancer stage 3 or 4;
[3]DNA promoter region methylation with cancer stage 1 or 2;
[4]Me/advanced (3 and 4): DNA promoter region methylation with cancer stage 3 or 4;
[5]*P* for the joint effect interaction;
[6]Including *CDKN2A*, *hMLH1*, *MGMT*, *CSF2*, *DIS3L2*, and *OAF*.
[a]*P* < 0.05. Adjusted for gender, age at surgery (continuous), adjuvant chemotherapy, histological grade, and tumor location. CI: Confidence interval; HR: Hazard ratio; *OAF*: The out at first homolog gene; N/A: Not applicable.

Table 5 Interaction between gene promoter region methylation and different cancer stages for 5-year overall survival of colorectal cancer patients, *n* (%)

	Normal tissues						Tumor tissues					
	No. of subjects	No. of cases	Crude		Adjusted		No. of subjects	No. of cases	Crude		Adjusted	
			HR	95%CI	HR	95%CI			HR	95%CI	HR	95%CI
OAF												
UnMe/local (1 and 2)[1]	33	5 (15.2)	1.00	Referent	1.00	Referent	13	2 (15.4)	1.00	Referent	1.00	Referent
UnMe/advanced (3 and 4)[2]	29	8 (27.6)	2.24	0.73-6.86	4.84[a]	1.22-19.2	16	6 (37.5)	3.12	0.63-15.5	15.7[a]	1.98-124
Me/local (1 and 2)[3]	8	2 (25.0)	2.32	0.45-12.0	7.04	0.82-60.4	28	5 (17.9)	1.44	0.28-7.44	3.74	0.54-26.0
Me/advanced (3 and 4)[4]	21	5 (23.8)	1.85	0.53-6.41	5.96[a]	1.16-30.6	34	7 (20.6)	1.78	0.37-8.60	6.86	0.93-50.5
P value[5]				0.33		0.03				0.47		0.06
≥ 3 of genes[6]												
UnMe/local (1 and 2)[1]	41	5 (12.2)	1.00	Referent	1.00	Referent	22	3 (13.6)	1.00	Referent	1.00	Referent
UnMe/advanced (3 and 4)[2]	44	11 (25.0)	2.57	0.89-7.40	5.28[a]	1.35-20.6	16	5 (31.3)	2.68	0.64-11.2	5.53	1.00-30.6
Me/local (1 and 2)[3]	17	4 (23.5)	2.69	0.72-10.0	4.46	0.93-21.5	36	6 (16.7)	1.59	0.40-6.35	2.04	0.38-11.1
Me/advanced (3 and 4)[4]	18	3 (16.7)	1.86	0.44-7.82	4.27	0.76-23.8	46	9 (19.6)	2.09	0.56-7.76	3.93	0.78-19.8
P value[5]				0.40		0.10				0.27		0.10

[1]DNA promoter region unmethylation with cancer stage 1 or 2;
[2]DNA promoter region unmethylation with cancer stage 3 or 4;
[3]DNA promoter region methylation with cancer stage 1 or 2;
[4]Me/advanced (3 and 4): DNA promoter region methylation with cancer stage 3 or 4;
[5]*P* for the joint effect interaction;
[6]Including *CDKN2A*, *hMLH1*, *MGMT*, *CSF2*, *DIS3L2*, and *OAF*.
[a]$P < 0.05$. Adjusted for gender, age at surgery (continuous), adjuvant chemotherapy, histological grade, and tumor location. CI: Confidence interval; HR: Hazard ratio; *OAF*: The out at first homolog gene; N/A: Not applicable.

ARTICLE HIGHLIGHTS

Research background

Cancer staging systems, including tumor-node-metastasis classification, facilitate reasonable adjuvant treatment and help predict the prognoses of tumors. However, part of low-risk colorectal cancer (CRC) patients experience relapse after therapeutic intervention. The prognostic factors that define these relapse-prone patients should be identified to optimize treatment selection. Recently, there were several novel prognostic biomarkers for CRC which involve epigenetic aberrant changes have been reported.

Research motivation

To determine the effect of the methylation status of a novel methylation gene panel on the relationship between the cancer stage and prognosis of CRC.

Research objectives

This study aimed to explore the relationship between the methylation status of candidate genes and prognosis of CRC.

Research methods

One hundred and twenty CRC patients from Taiwan were enrolled to evaluate the association between hypermethylation of candidate genes and prognosis. The promoter methylation status of *CDKN2A*, *hMLH1*, *MGMT*, *CSF2*, *DIS3L2*, and *OAF* genes in tumor and adjacent normal tissues was assessed using methylation-specific PCR. Associations of the number of hypermethylated genes under study and different clinical stages with time to progression (TTP) or overall survival (OS) were assessed using the Cox proportional hazards regression model. Kaplan-Meier univariate assay was performed to analyze potential prognostic factors including TTP and OS.

Research results

The ≥ 3 aberrancy methylation group showed a significantly shorter 5-year TTP than the < 3 aberrancy methylation group. There was a significant interaction between CRC prognosis and different cancer stages (local and advanced) according to the methylation status of the selected genes in both types of tissues. However, the 5-year OS of patients with CRC in the ≥ 3 aberrancy group and the < 3 aberrancy group revealed no significant differences in both types of tissues.

Research conclusions

Our data identified these novel methylation markers, particularly in the adjacent normal tissues in patients with advanced stage, and provided a basis to apply and investigate the potential of these markers to predict the prognosis of CRC.

Research perspectives

Based on our findings, these novel markers in adjacent normal tissues of patients with CRC are recommended to help in clinical decision-making. Future cohort researches are needed to validate the utility of the new set of markers and address whether the modification of treatment/management decisions based on additional prognostic information from these markers would improve the TTP and OS of patients with CRC.

REFERENCES

1 **Siegel RL**, Miller KD, Fedewa SA, Ahnen DJ, Meester RGS, Barzi A, Jemal A. Colorectal cancer statistics, 2017. *CA Cancer J Clin* 2017; **67**: 177-193 [PMID: 28248415 DOI: 10.3322/caac.21395]
2 **Howlader N**, Noone A, Krapcho M, Miller D, Bishop K, Kosary C, Yu M, Ruhl J, Tatalovich Z, Mariotto A. SEER cancer statistics review, 1975–2014. Bethesda, MD: National Cancer Institute 2017; 2018. Available from: https://seer.cancer.gov/archive/csr/1975_2014/
3 **Edge SB**. AJCC cancer staging manual. *Springer* 2010; **7**: 97-100
4 **DeSantis CE**, Lin CC, Mariotto AB, Siegel RL, Stein KD, Kramer JL, Alteri R, Robbins AS, Jemal A. Cancer treatment and survivorship statistics, 2014. *CA Cancer J Clin* 2014; **64**: 252-271 [PMID: 24890451 DOI: 10.3322/caac.21235]
5 **Broadbridge VT**, Karapetis CS, Beeke C, Woodman RJ, Padbury R, Maddern G, Kim SW, Roder D, Hakendorf P, Price TJ. Do metastatic colorectal cancer patients who present with late relapse after curative surgery have a better survival? *Br J Cancer* 2013; **109**: 1338-1343 [PMID: 23860523 DOI: 10.1038/bjc.2013.388]
6 **Lech G**, Słotwiński R, Słodkowski M, Krasnodębski IW. Colorectal cancer tumour markers and biomarkers: Recent therapeutic advances. *World J Gastroenterol* 2016; **22**: 1745-1755 [PMID: 26855534 DOI: 10.3748/wjg.v22.i5.1745]
7 **Hur K**, Toiyama Y, Okugawa Y, Ide S, Imaoka H, Boland CR, Goel A. Circulating microRNA-203 predicts prognosis and metastasis in human colorectal cancer. *Gut* 2017; **66**: 654-665 [PMID: 26701878 DOI: 10.1136/gutjnl-2014-308737]
8 **Gevensleben H**, Holmes EE, Goltz D, Dietrich J, Sailer V, Ellinger J, Dietrich D, Kristiansen G. PD-L1 promoter methylation is a prognostic biomarker for biochemical recurrence-free survival in prostate cancer patients following radical prostatectomy. *Oncotarget* 2016; **7**: 79943-79955 [PMID: 27835597 DOI: 10.18632/oncotarget.13161]
9 **Hashimoto Y**, Zumwalt TJ, Goel A. DNA methylation patterns as noninvasive biomarkers and targets of epigenetic therapies in colorectal cancer. *Epigenomics* 2016; **8**: 685-703 [PMID: 27102979 DOI: 10.2217/epi-2015-0013]
10 **Yi JM**, Dhir M, Van Neste L, Downing SR, Jeschke J, Glöckner SC, de Freitas Calmon M, Hooker CM, Funes JM, Boshoff C, Smits KM, van Engeland M, Weijenberg MP, Iacobuzio-Donahue CA, Herman JG, Schuebel KE, Baylin SB, Ahuja N. Genomic and epigenomic integration identifies a prognostic signature in colon cancer. *Clin Cancer Res* 2011; **17**: 1535-1545 [PMID: 21278247 DOI: 10.1158/1078-0432.CCR-10-2509]
11 **Walther A**, Johnstone E, Swanton C, Midgley R, Tomlinson I, Kerr D. Genetic prognostic and predictive markers in colorectal cancer. *Nat Rev Cancer* 2009; **9**: 489-499 [PMID: 19536109 DOI: 10.1038/nrc2645]
12 **Imperiale TF**, Ransohoff DF, Itzkowitz SH, Levin TR, Lavin P, Lidgard GP, Ahlquist DA, Berger BM. Multitarget stool DNA testing for colorectal-cancer screening. *N Engl J Med* 2014; **370**: 1287-1297 [PMID: 24645800 DOI: 10.1056/NEJMoa1311194]
13 **Chang HF**, Wu CC, Sun CA, Chu CM, Lin FG, Hsieh JF, Hsu CH, Huang CH, Yang T, Tsai YM, Kuan JC, Chou YC. Clinical stage and risk of recurrence and mortality: interaction of DNA methylation factors in patients with colorectal cancer. *J Investig Med* 2016; **64**: 1200-1207 [PMID: 27296458 DOI: 10.1136/jim-2016-000086]
14 **Butterfield LH**, Zhao F, Lee S, Tarhini AA, Margolin KA, White RL, Atkins MB, Cohen GI, Whiteside TL, Kirkwood JM, Lawson DH. Immune Correlates of GM-CSF and Melanoma Peptide Vaccination in a Randomized Trial for the Adjuvant Therapy of Resected High-Risk Melanoma (E4697). *Clin Cancer Res* 2017; **23**: 5034-5043 [PMID: 28536308 DOI: 10.1158/1078-0432.CCR-16-3016]
15 **Costa P**, Romão L, Gama-Carvalho M. Transcriptomic screen for DIS3 and DIS3L1 exosome subunits associated functional networks in colorectal cancer. BioSys PhD Day, Faculdade de Ciências da Universidade de Lisboa, 11 dezembro. 2015; Available from: http://repositorio.insa.pt/bitstream/10400.18/3657/1/Poster_Biosys%20Paulo%20Costa%202015.pdf
16 **Wu WC**, Hsu CH, Kuan JC, Hsieh JF, Sun CA, Yang T, Wu CC, Chou YC. Predicting the progress of colon cancer by DNA methylation markers of the p16 gene in feces - Evidence from an animal model. *Genet Mol Biol* 2013; **36**: 323-328 [PMID: 24130437 DOI: 10.1590/S1415-47572013000300004]
17 **David D**, Anand D, Araújo C, Gloss B, Fino J, Dinger M, Lindahl P, Pöyhönen M, Hannele L, Lavinha J. Identification of OAF and PVRL1 as candidate genes for an ocular anomaly characterized by Peters anomaly type 2 and ectopia lentis. *Exp Eye Res* 2018; **168**: 161-170 [PMID: 29305299 DOI: 10.1016/j.exer.2017.12.012]
18 **Gunderson LL**, Jessup JM, Sargent DJ, Greene FL, Stewart AK. Revised TN categorization for colon cancer based on national survival outcomes data. *J Clin Oncol* 2010; **28**: 264-271 [PMID: 19949014 DOI:

10.1200/JCO.2009.24.0952]
19 **Berger SL**. The complex language of chromatin regulation during transcription. *Nature* 2007; **447**: 407-412 [PMID: 17522673 DOI: 10.1038/nature05915]
20 **Jones PA**. Functions of DNA methylation: islands, start sites, gene bodies and beyond. *Nat Rev Genet* 2012; **13**: 484-492 [PMID: 22641018 DOI: 10.1038/nrg3230]
21 **Jung M**, Pützer S, Gevensleben H, Meller S, Kristiansen G, Dietrich D. Diagnostic and prognostic value of SHOX2 and SEPT9 DNA methylation and cytology in benign, paramalignant, and malignant ascites. *Clin Epigenetics* 2016; **8**: 24 [PMID: 26937257 DOI: 10.1186/s13148-016-0192-7]
22 **Wick W**, Weller M, van den Bent M, Sanson M, Weiler M, von Deimling A, Plass C, Hegi M, Platten M, Reifenberger G. MGMT testing--the challenges for biomarker-based glioma treatment. *Nat Rev Neurol* 2014; **10**: 372-385 [PMID: 24912512 DOI: 10.1038/nrneurol.2014.100]
23 **Ng JM**, Yu J. Promoter hypermethylation of tumour suppressor genes as potential biomarkers in colorectal cancer. *Int J Mol Sci* 2015; **16**: 2472-2496 [PMID: 25622259 DOI: 10.3390/ijms16022472]
24 **Ahmed D**, Danielsen SA, Aagesen TH, Bretthauer M, Thiis-Evensen E, Hoff G, Rognum TO, Nesbakken A, Lothe RA, Lind GE. A tissue-based comparative effectiveness analysis of biomarkers for early detection of colorectal tumors. *Clin Transl Gastroenterol* 2012; **3**: e27 [PMID: 23324654 DOI: 10.1038/ctg.2012.21]
25 **Exner R**, Pulverer W, Diem M, Spaller L, Woltering L, Schreiber M, Wolf B, Sonntagbauer M, Schröder F, Stift J, Wrba F, Bergmann M, Weinhäusel A, Egger G. Potential of DNA methylation in rectal cancer as diagnostic and prognostic biomarkers. *Br J Cancer* 2015; **113**: 1035-1045 [PMID: 26335606 DOI: 10.1038/bjc.2015.303]
26 **Luo X**, Huang R, Sun H, Liu Y, Bi H, Li J, Yu H, Sun J, Lin S, Cui B, Zhao Y. Methylation of a panel of genes in peripheral blood leukocytes is associated with colorectal cancer. *Sci Rep* 2016; **6**: 29922 [PMID: 27453436 DOI: 10.1038/srep29922]
27 **Kim SH**, Park KH, Shin SJ, Lee KY, Kim TI, Kim NK, Rha SY, Ahn JB. CpG Island Methylator Phenotype and Methylation of Wnt Pathway Genes Together Predict Survival in Patients with Colorectal Cancer. *Yonsei Med J* 2018; **59**: 588-594 [PMID: 29869456 DOI: 10.3349/ymj.2018.59.5.588]
28 **de Sousa E Melo F**, Colak S, Buikhuisen J, Koster J, Cameron K, de Jong JH, Tuynman JB, Prasetyanti PR, Fessler E, van den Bergh SP, Rodermond H, Dekker E, van der Loos CM, Pals ST, van de Vijver MJ, Versteeg R, Richel DJ, Vermeulen L, Medema JP. Methylation of cancer-stem-cell-associated Wnt target genes predicts poor prognosis in colorectal cancer patients. *Cell Stem Cell* 2011; **9**: 476-485 [PMID: 22056143 DOI: 10.1016/j.stem.2011.10.008]
29 **Juo YY**, Johnston FM, Zhang DY, Juo HH, Wang H, Pappou EP, Yu T, Easwaran H, Baylin S, van Engeland M, Ahuja N. Prognostic value of CpG island methylator phenotype among colorectal cancer patients: a systematic review and meta-analysis. *Ann Oncol* 2014; **25**: 2314-2327 [PMID: 24718889 DOI: 10.1093/annonc/mdu149]
30 **Freitas M**, Ferreira F, Carvalho S, Silva F, Lopes P, Antunes L, Salta S, Diniz F, Santos LL, Videira JF, Henrique R, Jerónimo C. A novel DNA methylation panel accurately detects colorectal cancer independently of molecular pathway. *J Transl Med* 2018; **16**: 45 [PMID: 29486770 DOI: 10.1186/s12967-018-1415-9]
31 **Kushwaha G**, Dozmorov M, Wren JD, Qiu J, Shi H, Xu D. Hypomethylation coordinates antagonistically with hypermethylation in cancer development: a case study of leukemia. *Hum Genomics* 2016; **10** Suppl 2: 18 [PMID: 27461342 DOI: 10.1186/s40246-016-0071-5]
32 **Porcellini E**, Laprovitera N, Riefolo M, Ravaioli M, Garajova I, Ferracin M. Epigenetic and epitranscriptomic changes in colorectal cancer: Diagnostic, prognostic, and treatment implications. *Cancer Lett* 2018; **419**: 84-95 [PMID: 29360561 DOI: 10.1016/j.canlet.2018.01.049]
33 **Rodriguez J**, Frigola J, Vendrell E, Risques RA, Fraga MF, Morales C, Moreno V, Esteller M, Capellà G, Ribas M, Peinado MA. Chromosomal instability correlates with genome-wide DNA demethylation in human primary colorectal cancers. *Cancer Res* 2006; **66**: 8462-9468 [PMID: 16951157 DOI: 10.1158/0008-5472.CAN-06-0293]
34 **Ye D**, Jiang D, Li Y, Jin M, Chen K. The role of LINE-1 methylation in predicting survival among colorectal cancer patients: a meta-analysis. *Int J Clin Oncol* 2017; **22**: 749-757 [PMID: 28343299 DOI: 10.1007/s10147-017-1106-1]
35 **Luo Y**, Yu M, Grady WM. Field cancerization in the colon: a role for aberrant DNA methylation? *Gastroenterol Rep (Oxf)* 2014; **2**: 16-20 [PMID: 24760232 DOI: 10.1093/gastro/got039]
36 **Azuara D**, Aussó S, Rodriguez-Moranta F, Guardiola J, Sanjuan X, Lobaton T, Boadas J, Piqueras M, Monfort D, Guinó E, Moreno V, Capellá G, de Oca J. New Methylation Biomarker Panel for Early Diagnosis of Dysplasia or Cancer in High-Risk Inflammatory Bowel Disease Patients. *Inflamm Bowel Dis* 2018; **24**: 2555-2564 [PMID: 30099509 DOI: 10.1093/ibd/izy255]
37 **Li J**, Poi MJ, Tsai MD. Regulatory mechanisms of tumor suppressor P16(INK4A) and their relevance to cancer. *Biochemistry* 2011; **50**: 5566-5582 [PMID: 21619050 DOI: 10.1021/bi200642e]
38 **Bihl MP**, Foerster A, Lugli A, Zlobec I. Characterization of CDKN2A(p16) methylation and impact in colorectal cancer: systematic analysis using pyrosequencing. *J Transl Med* 2012; **10**: 173 [PMID: 22925370 DOI: 10.1186/1479-5876-10-173]
39 **Kohonen-Corish MR**, Tseung J, Chan C, Currey N, Dent OF, Clarke S, Bokey L, Chapuis PH. KRAS mutations and CDKN2A promoter methylation show an interactive adverse effect on survival and predict recurrence of rectal cancer. *Int J Cancer* 2014; **134**: 2820-2828 [PMID: 24259266 DOI: 10.1002/ijc.28619]
40 **Lu Y**, Wajapeyee N, Turker MS, Glazer PM. Silencing of the DNA mismatch repair gene MLH1 induced by hypoxic stress in a pathway dependent on the histone demethylase LSD1. *Cell Rep* 2014; **8**: 501-513 [PMID: 25043185 DOI: 10.1016/j.celrep.2014.06.035]
41 **Kuan JC**, Wu CC, Sun CA, Chu CM, Lin FG, Hsu CH, Kan PC, Lin SC, Yang T, Chou YC. DNA methylation combinations in adjacent normal colon tissue predict cancer recurrence: evidence from a clinical cohort study. *PLoS One* 2015; **10**: e0123396 [PMID: 25815725 DOI: 10.1371/journal.pone.0123396]
42 **Iida S**, Kato S, Ishiguro M, Matsuyama T, Ishikawa T, Kobayashi H, Higuchi T, Uetake H, Enomoto M, Sugihara K. PIK3CA mutation and methylation influences the outcome of colorectal cancer. *Oncol Lett* 2012; **3**: 565-570 [PMID: 22740953 DOI: 10.3892/ol.2011.544]
43 **Belhadj S**, Moutinho C, Mur P, Setien F, Llinàs-Arias P, Pérez-Salvia M, Pons T, Pineda M, Brunet J, Navarro M, Capellá G, Esteller M, Valle L. Germline variation in O^6-methylguanine-DNA methyltransferase (MGMT) as cause of hereditary colorectal cancer. *Cancer Lett* 2019; **447**: 86-92 [PMID:

30677446 DOI: 10.1016/j.canlet.2019.01.019]
44 **Lee YY**, Wu WJ, Huang CN, Li CC, Li WM, Yeh BW, Liang PI, Wu TF, Li CF. CSF2 Overexpression Is Associated with STAT5 Phosphorylation and Poor Prognosis in Patients with Urothelial Carcinoma. *J Cancer* 2016; **7**: 711-721 [PMID: 27076853 DOI: 10.7150/jca.14281]
45 **Astuti D**, Morris MR, Cooper WN, Staals RH, Wake NC, Fews GA, Gill H, Gentle D, Shuib S, Ricketts CJ, Cole T, van Essen AJ, van Lingen RA, Neri G, Opitz JM, Rump P, Stolte-Dijkstra I, Müller F, Pruijn GJ, Latif F, Maher ER. Germline mutations in DIS3L2 cause the Perlman syndrome of overgrowth and Wilms tumor susceptibility. *Nat Genet* 2012; **44**: 277-284 [PMID: 22306653 DOI: 10.1038/ng.1071]
46 **Gentles AJ**, Newman AM, Liu CL, Bratman SV, Feng W, Kim D, Nair VS, Xu Y, Khuong A, Hoang CD, Diehn M, West RB, Plevritis SK, Alizadeh AA. The prognostic landscape of genes and infiltrating immune cells across human cancers. *Nat Med* 2015; **21**: 938-945 [PMID: 26193342 DOI: 10.1038/nm.3909]
47 **Huang WY**, Hsu SD, Huang HY, Sun YM, Chou CH, Weng SL, Huang HD. MethHC: a database of DNA methylation and gene expression in human cancer. *Nucleic Acids Res* 2015; **43**: D856-D861 [PMID: 25398901 DOI: 10.1093/nar/gku1151]
48 **Saito T**, Mikami Y, Kinugasa M, Mori K, Sugimoto M, Uchida K. Genes for prognosis of cancer. U.S. Patent Application No 12/183,610, 2009. Available from: https://patentimages.storage.googleapis.com/08/9e/de/9cb348d7d14ec5/US20090011423A1.pdf
49 **Kwon JH**, Wu F. Microrna-based diagnostic testing and therapies for inflammatory bowel disease and related diseases. U.S. Patent Application No 12/934,820, 2011. Available from: https://patents.google.com/patent/US20110117111A1/en

World Journal of Gastroenterology

Submit a Manuscript: https://www.f6publishing.com

World J Gastroenterol 2020 January 14; 26(2): 168-183

DOI: 10.3748/wjg.v26.i2.168

ISSN 1007-9327 (print) ISSN 2219-2840 (online)

ORIGINAL ARTICLE

Observational Study

Assessment of lncRNA GAS5, lncRNA HEIH, lncRNA BISPR and its mRNA BST2 as serum innovative non-invasive biomarkers: Recent insights into Egyptian patients with hepatitis C virus type 4

Nourhan M El Samaloty, Marwa I Shabayek, Ramy S Ghait, Shohda A El-Maraghy, Sherine M Rizk, Maha M El-Sawalhi

ORCID number: Nourhan M El Samaloty (0002-0000-5329-1994); Marwa I Shabayek (0000-0002-5329-1994); Ramy S Ghait (0000-0002-5329-1995); Shohda A El-Maraghy (0002-0000-5329-1995); Sherine M Rizk (0000-0002-5329-1998); Maha M El-Sawalhi (0000-0002-6598-4392).

Author contributions: El-Sawalhi MM, Shabayek MI, El-Maraghy SA and Rizk SM conceived and designed the study; El Samaloty NM and Ghait RS performed the experiments; El Samaloty NM, Shabayek MI, El-Maraghy SA, Rizk SM and El-Sawalhi MM analyzed the data and wrote the paper; all authors have read and approve the final manuscript.

Institutional review board statement: This study was approved by the Research Ethics Committee for Experimental and Clinical studies at the Faculty of Pharmacy, Cairo University (approval number: BC 1955).

Informed consent statement: Written informed consents were obtained from all participants before being included in the study.

Conflict-of-interest statement: The authors declare that they have no conflict of interest.

STROBE statement: The authors have read the STROBE guidelines, and the manuscript was prepared and revised according to the

Nourhan M El Samaloty, Marwa I Shabayek, Biochemistry Section, Pharmacology, Toxicology and Biochemistry Department, Faculty of Pharmaceutical Sciences and Pharmaceutical Industries, Future University, Cairo 11795, Egypt

Ramy S Ghait, Internal Medicine, Gastroenterology and Hepatology Department, Faculty of Medicine, Ain Shams University, Cairo 11566, Egypt

Shohda A El-Maraghy, Sherine M Rizk, Maha M El-Sawalhi, Biochemistry Department, Faculty of Pharmacy, Cairo University, Cairo 11562, Egypt

Corresponding author: Marwa I Shabayek, PhD, Assistant Professor, Associate Professor, Faculty of Pharmaceutical Sciences and Pharmaceutical Industries, Future University, 90th New Cairo Street, Cairo 11795, Egypt. marwa.ismail@fue.edu.eg

Abstract

BACKGROUND

Hepatitis C virus (HCV) infection and its consequent complications are undeniably a public health burden worldwide, particularly in Egypt. Emerging evidence suggests that many lncRNAs have relevant roles in viral infections and antiviral responses.

AIM

To investigate the expression profiles of circulating lncRNAGAS5, lncRNAHEIH, lncRNABISPR and mRNABST2 in naïve, treated and relapsed HCV Egyptian patients, to elucidate relation to HCV infection and their efficacy as innovative biomarkers for the diagnosis and prognosis of HCV GT4.

METHODS

One hundred and thirty HCV-infected Egyptian patients and 20 healthy controls were included in this study. Serum lncRNAs and mRNABST2 were measured using quantitative real-time polymerase chain reaction (qRT-PCR).

RESULTS

Our results indicated that serum lncRNAGAS5 and LncRNABISPR were upregulated, whereas mRNA BST2 and LncRNA HEIH were downregulated in naïve patients. In contrast, HCV patients treated with sofosbuvir and simeprevir; with sofosbuvir and daclatasvir; or with sofosbuvir, daclatasvir and ribavirin

exhibited lower levels of lncRNAGAS5 and lncRNABISPR with higher mRNABST2 compared to naïve patients. Notably, patients relapsed from sofosbuvir and simeprevir showed higher levels of these lncRNAs with lower mRNABST2 compared to treated patients. LncRNAGAS5 and lncRNABISPR were positively correlated with viral load and ALT at $P < 0.001$, whereas mRNABST2 was negatively correlated with viral load at $P < 0.001$ and ALT at $P < 0.05$. Interestingly, a significant positive correlation between lncRNA HEIH and AFP was observed at $P < 0.001$.

CONCLUSION

Differential expression of these RNAs suggests their involvement in HCV pathogenesis or antiviral response and highlights their promising roles in diagnosis and prognosis of HCV.

Key words: lncRNA GAS5; lncRNA BISPR; mRNA BST2; lncRNA HEIH; Hepatitis C; Biomarkers

Core tip: The expression profiles of the studied RNAs in naïve, treated and relapsed hepatitis C virus (HCV) Egyptian patients suggest their involvement in HCV-pathogenesis or antiviral response. Additionally, lncRNA GAS5, lncRNA HEIH, lncRNA BISPR and mRNA BST2 could serve as potential diagnostic biomarkers in HCV GT4 Egyptian patients while, lncRNA GAS5, lncRNA BISPR and mRNA BST2 could also be considered novel prognostic biomarkers for treatment in HCV patients. Importantly, lncRNA HEIH might represent a powerful prognostic marker for differentiating relapsed patients from SOF + SIM treatment. Finally, these biomarkers can be used in combination to complete the whole picture of diagnosis, prognosis and follow-up of HCV.

Citation: El Samaloty NM, Shabayek MI, Ghait RS, El-Maraghy SA, Rizk SM, El-Sawalhi MM. Assessment of lncRNA GAS5, lncRNA HEIH, lncRNA BISPR and its mRNA BST2 as serum innovative non-invasive biomarkers: Recent insights into Egyptian patients with hepatitis C virus type 4. *World J Gastroenterol* 2020; 26(2): 168-183
URL: https://www.wjgnet.com/1007-9327/full/v26/i2/168.htm
DOI: https://dx.doi.org/10.3748/wjg.v26.i2.168

Manuscript source: Unsolicited Manuscript

Received: October 8, 2019
Peer-review started: October 8, 2019
First decision: December 5, 2019
Revised: December 11, 2019
Accepted: December 22, 2019
Article in press: December 22, 2019
Published online: January 14, 2020

P-Reviewer: Cui J
S-Editor: Ma YJ
L-Editor: A
E-Editor: Zhang YL

INTRODUCTION

Viral hepatitis is the seventh leading cause of mortality worldwide. Hepatitis C virus (HCV) comprises almost half of this mortality, ultimately leading to cirrhosis and hepatocellular carcinoma (HCC)[1]. In 2008, the predominance of HCV infection in Egypt was the most noteworthy in the world, near 15% of the populace were seropositive, and approximately 90% of patients were infected with genotype 4 (GT4). In 2015, the National Demographic Health Survey proved a noticeable drop in HCV burden to 6.3% among the population[2]. Actually, Egypt launched one of the largest treatment programmes for controlling viral hepatitis with direct-acting antiviral (DAAs)-based regimens that aim to treat above 250000 chronically infected individuals per year[3].

The era of DAAs was successful for HCV elimination, the sustained viral response (SVR) outcomes improved significantly, and many studies reported decreased risk of liver-related morality with antiviral treatment of HCV[4,5]. Sofosbuvir combination-based regimens were designed as a promising regimen for the treatment of HCV GT4 patients[6].

A substantial effort has been directed to elucidate the molecular mechanisms of HCV, identifying new diagnostic and prognostic markers and therapeutic targets to improve the clinical outcome of HCV patients. LncRNAs are transcripts greater than 200 nucleotides (nt) with poor coding potential[7], that play important roles in regulating gene expression[8]. Emerging evidence suggests that lncRNAs play relevant roles in viral infection and in antiviral responses[9]. A recent study described deregulation of the lncRNA transcriptome in HCV-infected cells[10].

Growth arrest-specific 5 (GAS5) is a 650 nt tumour suppressor lncRNA that has been reported to suppress migration and invasion of some HCC cell lines[11]. It also inhibited the pathogenesis of liver fibrosis via RNAs crosstalk[12]. In HCV-infected Huh7 cells, lncRNA GAS5 has been shown to be upregulated and exhibit a potential antiviral activity. It did not affect virus entry but suppressed HCV replication[13].

Another potential lncRNA is bone marrow stromal cell antigen 2 lncBST2, which has been renamed lncRNA BISPR from BST2 IFN-stimulated positive regulator. LncRNA BISPR was found to be upregulated after treatment with different doses of interferon (IFN), type I IFNα2, in different cells. Moreover, lncRNA BISPR was reported to be upregulated in HCV-infected livers and cultured cells, probably, because of the induction of the IFN signaling pathway in these cells[10,14].

A third interesting lncRNA, called high expression in hepatocellular carcinoma (HEIH), is an oncogenic lncRNA that promotes tumor progression and has been proposed as key regulatory hubs in HCC progression. The expression level of lncRNA-HEIH in HBV-related HCC was significantly associated with recurrence and was identified as an independent prognostic factor for survival[15]. In addition, lncRNA-HEIH in serum and exosomes was identified as a potential biomarker in the HCV-related HCC[16].

mRNA bone marrow stromal cell antigen 2 (BST-2 or Tetherin), which is expressed in most human tissues, has been revealed to inhibit the release of several enveloped viruses[17]. In HCV Huh 7.5 cells, it was demonstrated that BST2 moderately restricted HCV release and production, while the virus lacks mechanisms to respond to this restriction[18].

To date, the expression profiles of the above-mentioned RNAs in HCV GT4 patients and their clinical relevance as biomarkers for HCV have not been studied yet. Therefore, we aimed to assess the serum levels of lncRNA GAS5, lncRNA HEIH, lncRNA BISPR and mRNA BST2 in naïve, treated and relapsed Egyptian HCV patients to examine their relation to HCV infection and their potential usefulness as new diagnostic and prognostic biomarkers for HCV GT4. Additionally, the possible correlations between these RNAs and the clinical data were also analysed.

MATERIALS AND METHODS

Patients and treatment regimen

One hundred and thirty HCV-infected Egyptian patients and 20 healthy controls were recruited in this study. The HCV patient samples were collected from the Department of Internal Medicine, Gastroenterology and Hepatology Clinic- Ain Shams Hospital from March 2017- March 2018. The study included six groups; group I healthy controls (n = 20). Group II naïve HCV patients without treatment (n = 30). Groups from III to V comprised HCV patients treated daily with three different 12-week oral treatment regimens as follows: Group III (SOF + SIM) (n = 30) received combination of sofosbuvir (SOF 400 mg) and simeprevir (SIM 150 mg). Group IV (SOF + DAC) (n = 20) received combination of SOF (400 mg) and daclatasvir (DAC 60 mg). Group V (SOF + DAC + RBV) (n = 20) received fixed dose combination of SOF (400 mg) and DAC (60 mg) with ribavirin (RBV) at weight-based doses of 600, 800 and 1000 mg for patients with body weight less than 60 kg, between 60-80 kg, and more than 80 kg respectively[19]. Group VI included HCV patients who relapsed after 12-wk treatment with SOF + SIM (n = 30). Patients on therapy showed SVR (undetectable HCV RNA at the end of 12-wk treatment and remained free from HCV RNA for further 12 wk). In contrast, relapsed patients showed undetectable HCV RNA after completion of 12-week treatment however, after further 12 wk the HCV RNA was detected and was nearly high as those of naïve patients. All enrolled HCV patients presented positive outcomes when tested for serum anti-HCV antibodies with detectable serum HCV RNA GT4, and they had abnormal serum aminotransferases for 6 months. Naïve patients had not previously received any HCV treatment or antiviral therapy. Patients with cirrhotic liver, HCC, alcohol-induced liver injury, HBV antigen or antibody, thyroid dysfunction, hypertension, renal insufficiency, and other major diseases were excluded. All participants were age and gender matched. The study protocol was approved by the Research Ethics Committee for Experimental and Clinical studies at the Faculty of Pharmacy, Cairo University, Cairo, Egypt (approval number: BC 1955) and was conducted in accordance with the ethical guidelines of the Declaration of Helsinki. All participants received the required information regarding the study, and their written informed consents were obtained.

Blood sampling and laboratory assays

Venous blood samples were collected from all participants using serum collection

tubes. The separated sera were aliquoted and stored at -80 °C for the analysis of lncRNAs and mRNA expressions. An aliquot of the serum was used to assess the routine workup; serum alanine aminotransferase (ALT), aspartate aminotransferase (AST), alkaline phosphatase (ALP), prothrombin time (PT), international normalized ratio (INR), albumin, total bilirubin; which were analysed spectrophotometrically (Spectrum Diagnostic, Cairo, Egypt). Alpha-fetoprotein (AFP), hepatitis B surface antigen, anti-HCV titres, anti-schistosomal antibodies, and hepatitis B core antibodies were assessed by enzyme-linked immunosorbent assay (Aviva System Biology, CA, United States).

HCV RNA quantification (viral load) and genotyping

Serum HCV RNA was extracted by a viral RNA extraction kit (Qiagen, CA, United States) according to the manufacturer's protocol, and it was quantified by quantitative Real Time-PCR (qRT-PCR) (TaqMan assay reagents and Ambion, the RNA Company-one step, CA, United States). Genotyping was done based on the core region sequence using the Ohno method. This method used genotype-specific primers and depends on the PCR amplification of the HCV core gene[20].

Serum LncRNAs and mRNA assay

RNA extraction: Total RNA was extracted from 200 µL serum by the miRNeasy Mini Kit (Qiagen, Hilden, German) using QIAZOL lysis reagent according to the manufacturer's instructions. The extracted RNA was dissolved in 50 µL RNase-free water and stored at −80 °C until analysis. The quality of RNA was determined using nanodrop (Thermo Scientific, United States).

Reverse transcription: Reverse transcription was done using RT² first strand Kit (Qiagen, Hilden, Germany), 8 µL total RNA template were reverse transcribed in a final reaction mix volume of 20 µL. For synthesis of cDNA, the RT reaction was incubated for 60 min at 37 °C, and for 5 min at 95 °C. The cDNA produced were stored at −20 °C till analysis.

qRT-PCR: Relative expression levels of the LncRNAs and mRNA were evaluated using the RT² SYBR Green Master Mix kit (Qiagen, Hilden, Germany) according to the manufacturer's instructions. The housekeeping gene, Hs_GAPDH_1_SG was selected as the internal control. Briefly, for analysis of the LncRNAs, 2 µL cDNA product was used as a template in a 25 µL total reaction volume containing 12.5 µL RT² SYBR Green PCR Master Mix, 9.5 µL nuclease-free water, and 1 µL RT² LncRNA PCR primer assay. Readily made primers by Qiagen were used for amplification. The primer sequences used are as follows: lncRNA GAS5 (sense: CACACA GGCATTAGACAGA, antisense: GCTCCACACAGTGTAGTCA), lncRNA BISPR (sense: GCCAACAAACAATGTCGGTCT, antisense: CAGAGACACAGATG CTGCCTAA) and lncRNA HEIH (sense: CCTCTTGTGCCCCTTTCTT, antisense: ATGGCTTCTCGCATCCTAT). qRT-PCR was performed with a Qiagen Rotor Gene Q6 Plex Real-Time PCR system (Qiagen, Hilden, Germany), with a PCR initial activation at 95 °C for 10 min, followed by 40 cycles of 95 °C for 15 s and 60 °C for 60 s. Data were analysed with Rotor Gene Q software with the automatic threshold cycle (Ct) setting. The relative expression for each LncRNA after normalization to Hs_GAPDH_1_SG was calculated using the $2^{-\Delta\Delta ct}$ method.

For the assessment of mRNA BST2 relative expression, qRT-PCR was performed in 25 µL reaction mixture prepared by mixing 12.5 µL master mix, 2.5 µL primer assay, 5 µL cDNA, and 5 µL RNAase-free water. The primer sequence for the mRNA BST2 analysis is (sense: TCAGGAGTCCCTGGAGAAGA, antisense: ATGGAG CTGCCAGAGTTCAC). The reaction was performed with a PCR initial activation at 95 °C for 15 min followed by 40 cycles at 95 °C for 15 s, 55 °C for 30 s and 72 °C for 30 s. The data were examined with Rotor Gene Q software with the automatic threshold cycle (Ct) setting. The relative expression of mRNA BST2 after normalization to Hs_GAPDH_1_SG was calculated using the $2^{-\Delta\Delta ct}$ method.

Statistical analysis

The results were reported as the mean ± SD. Ordinary one-way analysis of variance (ANOVA) was used for normally distributed variables followed by the Tukey HSD multiple comparisons test. Viral load levels were log transformed to enable parametric statistical tests. The normality of the variable's distribution was assessed using the Shapiro Wilks test. To test the association between lncRNA Gas 5, lncRNA BISPR, lncRNA HEIH and mRNA BST2 and different biochemical parameters, Pearson's linear correlation and multiple regression analysis were performed. *P* values < 0.05 were considered significant, with a 95%CI. The diagnostic precision of lncRNAs and mRNAs was assessed by receiver-operating-characteristic (ROC)

analysis. Univariate and multiple binary logistic regression analyses were completed to detect predictors associated with the risk of HCV and of treatment or relapsed outcome. The significant data in the univariate analysis were further analysed by multiple analysis to determine the independent variables that affected the response. All statistical analyses were performed using SPSS Statistics v. 20 for Windows (SPSS, Chicago, IL). The graphs were plotted using GraphPad Prism 7.

RESULTS

Demographic and clinical data of the study participants

Naïve HCV patients had significantly higher levels of viral load, AST, ALT, ALP, AFP, PT, bilirubin and INR along with lower albumin levels compared to healthy controls. Meanwhile, HCV-infected patients treated with various treatment regimen showed undetected viral load together with significantly lower serum levels of hepatic enzyme markers compared to naïve HCV patients. On the other hand, relapsed patients exhibited marked increase in viral load levels together with significantly higher serum ALP and AFP compared to SOF + SIM treated group as illustrated in Table 1.

Serum lncRNAs and mRNA expression levels in healthy controls, naïve HCV patients and in HCV patients treated with different treatment regimens

Compared to healthy controls, serum expression levels of LncRNA GAS5 and LncRNA BISPR were upregulated, while, LncRNA HEIH and mRNA BST2 were downregulated in the naïve HCV group (Figure 1).

The levels of lncRNA GAS5 and lncRNA BISPR were significantly lower in the three treated groups, whereas, the serum levels of mRNA BST2 were significantly higher compared with that of the naïve group.

However, no significant difference was observed between the relative expression of lncRNA HEIH in the three treated groups versus that in the naïve HCV patients (Figure 1).

Correlation analyses of different serum molecular markers and clinical data in all studied groups

Pearson's correlation analyses of lncRNA GAS5, lncRNA BISPR, lncRNA HEIH and mRNA BST2 expression with all the studied parameters are presented in Table 2. Expression of lncRNA GAS5 revealed significant positive correlations with ALT, AST, ALP, AFP, PT, viral load, lncRNA BISPR and lncRNA HEIH. LncRNA GAS5 levels were negatively correlated with albumin and mRNA BST2. Meanwhile, lncRNA BISPR was positively correlated with ALT, ALP, INR, AFP, PT and viral load, whereas lncRNA BISPR was negatively correlated with albumin and mRNA BST2. Additionally, serum lncRNA HEIH levels were significantly positively correlated with AFP and negatively correlated with AST and mRNA BST2. On the other hand, serum expression of mRNA BST2 was significantly negatively correlated with ALT, ALP, AFP, PT and viral load and was positively correlated with albumin.

On performing multiple linear regression calculations, using lncRNA GAS5 as the dependent variable and AST, ALT, bilirubin, albumin, INR, AFP, viral load, PT, ALP, lncRNA BISPR, lncRNA HEIH and mRNA BST2 as independent variables, only AFP, ALP, lncRNA BISPR, lncRNA HEIH and mRNA BST2 remained significant ($\beta = 0.16$, $P < 0.05$; $\beta = 0.28$, $P < 0.001$; $\beta = 0.37$, $P < 0.001$, $\beta = 0.15$, $P < 0.05$; $\beta = -0.13$, $P < 0.05$, respectively). However, in using lncRNA BISPR as the dependent variable and AST, ALT, bilirubin, albumin, INR, AFP, viral load, PT, ALP, lncRNA GAS5, lncRNA HEIH and mRNA BST2 as independent variables, only viral load and lncRNA GAS5 were significant ($\beta = 0.14$, $P < 0.05$; $\beta = 0.57$, $P < 0.001$, respectively).

Via multiple regression analysis using lncRNA HEIH as the dependent variable and AST, ALT, bilirubin, albumin, INR, AFP, viral load, PT, ALP, lncRNA GAS5, lncRNA BISPR and mRNA BST2 as independent variables, only AFP and lncRNA GAS5, were significant ($\beta = 0.66$, $P < 0.001$, $\beta = 0.19$, $P < 0.05$, respectively). However, in multiple regression analysis using mRNA BST2 as the dependent variable and AST, ALT, bilirubin, albumin, INR, AFP, viral load, PT, ALP, lncRNA GAS5, lncRNA BISPR and lncRNA HEIH as independent variables, only albumin and lncRNA GAS5 were still significant ($\beta = 0.24$, $P < 0.01$; $\beta = -0.22$, $P < 0.05$, respectively).

Diagnostic performances of serum lncRNAs and mRNA

ROC analysis demonstrated that the studied lncRNAs and mRNA could differentiate between the naïve group and the healthy controls (Figure 2) with an AUC = 0.88 for LncRNA GAS5, sensitivity = 86%, specificity = 90% at a cut-off = 1.2-fold. For

Table 1 Demographic and clinical data of the study participants

Parameters	Healthy control	Naïve	SOF + SIM	SOF + DAC	SOF + DAC + RBV	Relapsed
	(*n* = 20)	(*n* = 30)	(*n* = 30)	(*n* = 20)	(*n* = 20)	(*n* = 30)
Age (yr)	40.2 ± 5	44.3 ± 6.9	42.2 ± 6.7	42.8 ± 7.2	39.7 ± 5.1	44.1 ± 6.5
Gender (M/F)	16/4	26/4	27/3	19/1	19/1	25/5
ALT (IU/L)	9.2 ± 6.2	37.2 ± 25[b]	18.7 ± 8.2[ad]	17.6 ± 5.6[ad]	26.7 ± 2.4[adeg]	23.7 ± 6.9[d]
AST (IU/L)	10.3 ± 4.2	34.4 ± 16.4[b]	27.4 ± 13.7[bc]	26.9 ± 6.9[bc]	32.7 ± 5.2[b]	23.3 ± 6.3[d]
Albumin (g/dL)	3.8 ± 0.27	2.7 ± 0.43[b]	3.2 ± 0.5[bd]	3.9 ± 0.3[dh]	4 ± 0.4[adh]	3 ± 0.4[d]
ALP (IU/L)	53.7 ± 6.8	130.6 ± 21[b]	86.1 ± 16[bd]	78.4 ± 16[bd]	81.2 ± 12.4[bd]	99.4 ± 11.2[bf]
Bilirubin (mg/dL)	0.9 ± 0.1	1.1 ± 0.4[a]	1.2 ± 0.5[b]	1.1 ± 0.4	0.9 ± 0.3[ce]	1.2 ± 0.4
INR	1.06 ± 0.07	1.4 ± 0.25[b]	1.5 ± 0.25[b]	1.3 ± 0.19[b]	1.2 ± 0.22[adfh]	1.4 ± 0.27
AFP (ng/mL)	7.6 ± 1.3	15 ± 8.6[b]	7.3 ± 0.8[d]	7 ± 1[d]	6.9 ± 1[d]	32 ± 9.6[bf]
PT	11.7 ± 0.5	14.8 ± 2[b]	13.7 ± 1.4[bd]	13.1 ± 1.2[bd]	12.6 ± 1.5[de]	14.1 ± 1.1
Viral load (log copies/mL)	0	6.47 ± 0.7[c]	0[d]	0[d]	0[d]	6.38 ± 0.39[f]

[a]$P < 0.05$,
[b]$P < 0.01$, *vs* control group;
[c]$P < 0.05$,
[d]$P < 0.01$, *vs* naïve group;
[e]$P < 0.05$,
[f]$P < 0.01$, *vs* SOF + SIM group;
[g]$P < 0.05$,
[h]$P < 0.01$, *vs* SOF + DAC group. The data are expressed as the mean ± SD. The data were analysed by one-way ANOVA followed by Tukey HSD multiple comparison test. Naïve: Hepatitis C virus naïve patients without any treatment; SOF + SIM: Hepatitis C virus-infected patients treated with sovaldi and simeprevir; SOF + DAC: Hepatitis C virus-infected patients treated with combined therapy sovaldi and daclatasvir; SOF + DAC + RBV: Hepatitis C virus-infected patients treated with triplet therapy sovaldi, daclatasvir and ribavirin; Relapsed: Relapsed HCV patients from SOF + SIM treatment; ALT: Alanine aminotransferases; AST: Aspartate aminotransferases; ALP: Alkaline phosphatase; INR: International normalized ratio AFP: Alfa fetoprotein; PT: Prothrombin time.

LncRNA BISPR, the AUC = 0.82, the sensitivity = 80%, and the specificity = 70% at a cut-off = 1.1-fold. For lncRNA HEIH and mRNA BST2, the AUC = 0.88, the sensitivity = 90%, and the specificity = 80% at a cut-off = 0.76-fold, and AUC = 0.85 sensitivity = 95%, specificity = 84% at a cut-off = 0.65-fold, respectively.

ROC analysis revealed that all the studied lncRNAs and mRNA could also discriminate between the naïve group and the HCV patients treated with different treatment regimens (Figure 3). The prognostic accuracy of lncRNA GAS5 in SOF + SIM treatment had an AUC = 0.94, sensitivity = 93%, specificity = 84% at a cut-off = 0.95 fold, while in SOF + DAC with an AUC = 0.90, sensitivity = 83%, specificity = 85% at a cut-off = 0.94-fold, and SOF + DAC + RBV with an AUC = 0.90, sensitivity = 90%, specificity = 90% at a cut-off = 1.1-fold. The prognostic relevance of lncRNA BISPR in SOF + SIM treatment showed AUC = 0.95, sensitivity = 93%, specificity = 87% at a cut-off = 0.7-fold, in SOF + DAC with an AUC = 0.93, sensitivity = 93%, specificity = 80% at a cut-off = 0.77-fold and in SOF+DAC+RBV with an AUC = 0.90, sensitivity = 93%, specificity = 80% at a cut-off = 0.77-fold. In addition, the significance of lncRNA HEIH in the SOF + SIM, SOF + DAC and SOF + DAC + RBV treatment groups had AUC = 0.74, 0.61, and 0.53, respectively, with sensitivity and specificity values of 73% and 70%, 60% and 60%, and 66% and 40% at cut-off values of 0.2-fold, 0.36-fold, 0.28-fold, respectively. Additionally, the prognostic significance of mRNA BST2 in the SOF + SIM, SOF + DAC and SOF + DAC + RBV treatment groups demonstrated AUC = 0.86, 0.94, and 0.88, respectively, with sensitivity and specificity values of 90% and 80%, 85% and 87%, and 90% and 80% at cut-off values of at 0.83-fold, at 1.1-fold, at 0.76-fold, respectively.

Univariate and multiple logistic regression results

Analysis of univariate and multiple logistic regression were employed to discriminate between naïve patients and healthy controls (Table 3). In the univariate analysis, ALT, AST, ALP, AFP, albumin, and expression levels of lncRNA GAS5, lncRNA BISPR, lncRNA HEIH and mRNA BST2 were designated as significant predictors associated with the diagnosis of naïve HCV patients. On conducting multiple analysis, LncRNA GAS5 and mRNA BST2 were designated as significant independent variables that could be used in the diagnosis of HCV.

Concerning the result variables in response to SOF + SIM, SOF + DAC or SOF + DAC + RBV therapies, univariate and multiple logistic regression analyses were

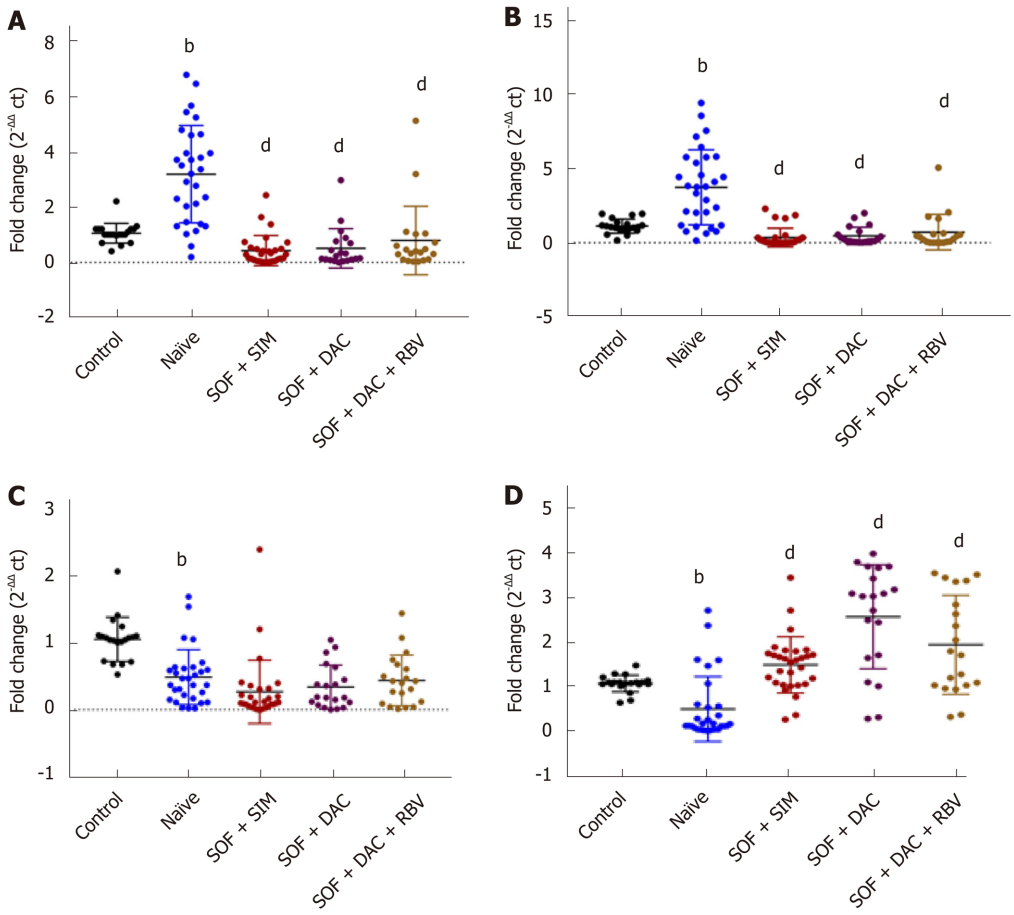

Figure 1 Serum expression levels of lncRNAs and mRNA in healthy controls, hepatitis C virus naïve patients and hepatitis C virus treated patients with different treatment regimens. A: LncRNA GAS5; B: LncRNA BISPR; C: LncRNA HEIH; D: mRNA BST2. $^{b}P < 0.01$, *vs* control group; $^{d}P < 0.01$, *vs* naïve group; Data were analyzed by On e-way ANOVA test followed by Tukey HSD multiple comparison test.

performed (Table 4). Expression levels of lncRNA GAS5, lncRNA BISPR and mRNA BST2 and serum levels of ALT, AFP, ALP and albumin were nominated as significant predictor variables in the univariate analysis of SOF + SIM treatment. In multiple analysis, lncRNA GAS5, lncRNA BISPR and mRNA BST2 were chosen as significant independent variables that might predict the response to SOF + SIM therapy. Serum levels of ALT, AFP, and ALP and expression levels of lncRNA GAS5, lncRNA BISPR and mRNA BST2 were selected as significant predictor variables in the univariate analysis of SOF + DAC treatment (Table 4). When multiple analysis was employed, lncRNA GAS5 and lncRNA BISPR showed the highest odds ratios upon holding all variables constant. Expression levels of lncRNA GAS5, lncRNA BISPR, mRNA BST2 and AFP were selected as significant predictors in the univariate analysis of SOF + DAC + RBV treatment (Table 4). Upon multiple analysis, lncRNA GAS5 and lncRNA BISPR were designated as significant independent variables that might predict the response to SOF + DAC + RBV therapy.

Remarkably, lncRNA GAS5 and lncRNA BISPR levels were positive predictors, whereas the level of mRNA BST2 was an independent negative predictor of treatment responses in all treatment groups.

Differential expression of serum lncRNAs and mRNA in relapsed, naïve and SOF + SIM-treated HCV patients

In relapsed patients, expression of lncRNA GAS5, lncRNA BISPR and lncRNA HEIH revealed significantly higher levels than those of the SOF + SIM treated group. In contrast, mRNA expression levels were significantly lower than in the SOF + SIM-treated group (Figure 4). Moreover, relapsed patients showed significantly lower lncRNA GAS5and lncRNA BISPR values compared to those of the naïve group, whereas lncRNA HEIH demonstrated a significantly higher value than that of naïve group (Figure 4).

ROC curve analysis of serum lncRNAs and mRNA in relapsed, naïve and SOF +

Table 2 Pearson's correlation between studied LncRNA GAS5, LncRNA BISPR, LncRNA HEIH, mRNA BST2 and clinical parameters in the different studied groups

Variables	LncRNA Gas5		LncRNA BISPR		LncRNA HEIH		MRNA BST2	
	r	*P* value	*r*	*P* value	*r*	*P* value	*r*	*P* value
Age (yr)	0.051	0.53	0.138	0.09	0.095	0.24	-0.043	0.60
Sex (M/F)	0.070	0.39	-0.043	0.60	0.037	0.65	-0.062	0.44
ALT (IU/L)	0.332	0.001[c]	0.287	0.001[c]	-0.072	0.37	-0.194	0.01[a]
AST (IU/L)	0.016	0.04[a]	0.141	0.08	-0.222	0.006[b]	0.008	0.92
Albumin (g/dL)	-0.454	0.001[c]	-0.419	0.001[c]	-0.0157	0.05	0.434	0.001[c]
Bilirubin (mg/dL)	0.088	0.28	0.049	0.54	0.034	0.67	-0.083	0.31
ALP (IU/L)	0.589	0.001[c]	0.517	0.001[c]	0.044	0.59	-0.346	0.001[c]
INR	0.136	0.09	0.172	0.03[a]	-0.062	0.45	0.021	0.79
AFP	0.476	0.001[c]	0.176	0.03[a]	0.640	0.001[c]	-0.347	0.001[c]
PT	0.405	0.001[c]	0.300	0.001[c]	0.081	0.32	-0.206	0.01[a]
Viral load (log copies/mL)	0.276	0.001[c]	0.374	0.001[c]	0.056	0.49	-0.284	0.001[c]
LncRNA Gas5			0.607	0.001[c]	0.318	0.001[c]	-0.465	0.001[c]
LncRNA BST2	0.607	0.001[c]			0.040	0.62	-0.371	0.001[c]
LncRNA HEIH	0.318	0.001[c]	0.040	0.62			-0.235	0.004[b]
mRNA BST2	-0.465	0.001[c]	-0.371	0.001[c]	-0.235	0.004[b]		

[a]$P < 0.05$,
[b]$P < 0.01$,
[c]$P < 0.001$, indicates statistical significance. ALT: Alanine aminotransferases; AST: Aspartate aminotransferases; ALP: Alkaline phosphatase; INR: International normalized ratio AFP: Alfa fetoprotein; PT: Prothrombin time.

SIM-treated HCV patients

ROC curve analysis showed that serum lncRNA GAS5, lncRNA BISPR, lncRNA HEIH and mRNA BST2 could discriminate the relapsed group from the SOF + SIM-treated group with AUC = 0.91, 0.84, 0.95, and 0.86 respectively, with sensitivities and specificities at cut-off values of 90% and 84% at 0.96-fold, 90% and 87% at 0.77-fold, 90% and 80% at 0.32-fold, and 86% and 84% at 0.98-fold, respectively (Figure 5).

Logistic regression results

Univariate and multiple logistic regression analyses were presented to choose the predictor variables related with relapsed HCV patients from SOF + SIM therapy (Table 5). Based on univariate analysis, serum ALT, ALP, lncRNA GAS5, lncRNA BISPR and lncRNA HEIH were designated as positive significant predictor variables, while mRNA BST2 was designated as a significant negative predictor variable. In multiple analysis, only serum lncRNA GAS5 and lncRNA HEIH could be significant independent predictors of relapsed HCV patients from SOF + SIM therapy.

DISCUSSION

HCV infection is a complex multifactorial process that involves multiple viral and host interactions. Besides, the high mutation rate of HCV that enables the virus to generate escape mutants resistant to treatment[21], emphasizing the need for a proper understanding of the pathogenesis of HCV infection, and various research efforts should be oriented to develop novel diagnostic and prognostic molecular tools.

The present study demonstrated for the first-time differential expression of lncRNA GAS5, lncRNA HEIH, lncRNA BISPR and mRNA BST2 in the sera of naïve, treated and relapsed HCV GT4 Egyptian patients.

We found that naïve patients exhibited elevated serum levels of lncRNA GAS5 and lncRNA BISPR compared to healthy controls. A recent study in Huh 7 cells reported upregulation of lncRNA GAS5 expression during the progression of HCV infection[13]. The authors showed that GAS5 overexpression inhibited HCV infection, while GAS5 knockdown promoted HCV infection. Furthermore, GAS5 was found to directly bound HCV NS3 protein with its 5′ end 200 sequences and acted as a decoy to inhibit the function of this key viral protein that is essential for viral replication. Here, the

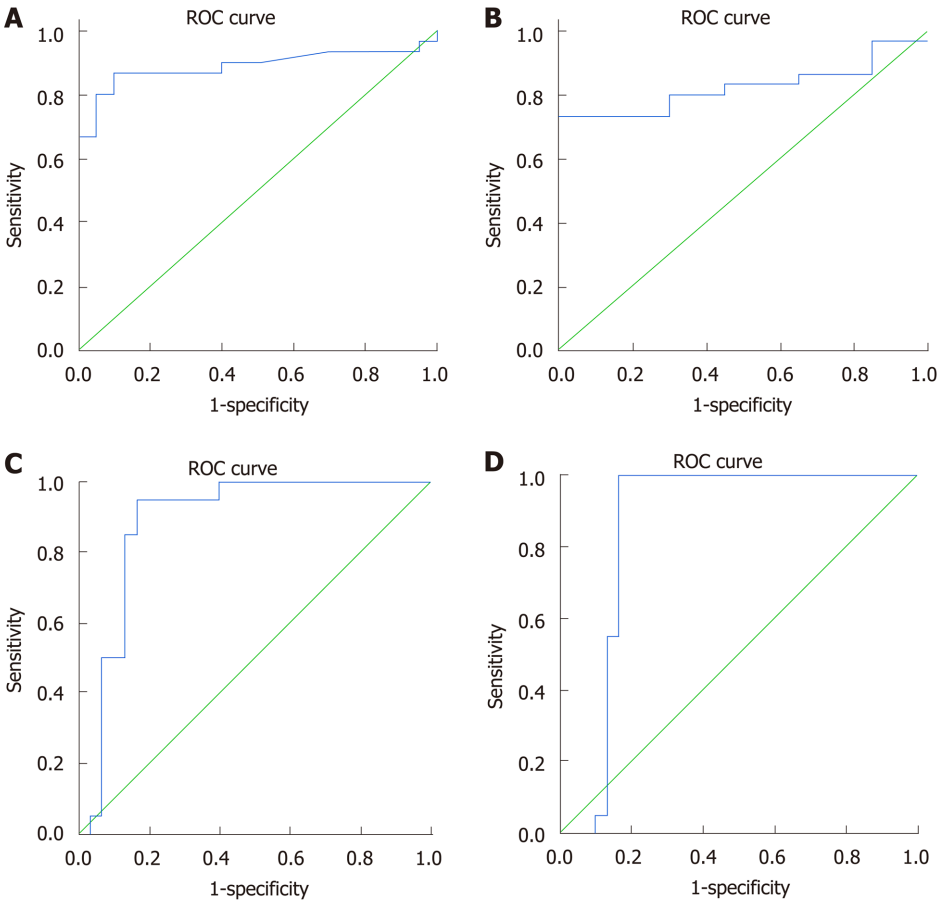

Figure 2 Serum LncRNAs and mRNA as diagnostic biomarker for naïve patients. ROC curve analysis for lncRNA Gas 5 (AUC = 0.88) (A), BISPR (AUC = 0.82) (B), HEIH (AUC = 0.88) (C) and mRNA BST2 (AUC = 0.85) (D) as diagnostic biomarkers discriminating naïve patients from healthy controls.

observed increase in serum lncRNA GAS5 in naïve patients supports these *in vitro* findings and implicates GAS5 in the antiviral response that occurs along with HCV infection.

Meanwhile, the observed upregulation of lncRNA BISPR in the sera of our naïve HCV patients confirms the findings of Barriocanal *et al*[14], in which significant increases in lncRNA BISPR levels were demonstrated in HCV-infected Huh 7 cells and in liver samples from HCV-infected donors compared to HCV-negative controls. These findings also showed that lncRNA BISPR expression was highly upregulated in HuH7 cells in response to IFN, suggesting that lncRNA BISPR could be induced by IFN to control the potency of the antiviral IFN response.

Unlike lncRNA GAS5 and lncRNA BISPR, the current study revealed significant downregulation of lncRNA HEIH and mRNA BST2 levels in the sera of naïve HCV patients versus healthy controls. To our knowledge, no previous studies had assessed the expression levels of lncRNA HEIH in the serum of naïve HCV patients in relation to healthy controls. Nevertheless, a recent study stated that serum exosomal lncRNA-HEIH levels in HCV-related HCC patients were remarkably higher than its levels in patients with HCV-induced cirrhosis and both were higher than lncRNA-HEIH levels in HCV patients[16]. Additionally, Zhefeng *et al*[22] found an association between the expression of LncRNA-HEIH in plasma and HCC risk. Accordingly, in the current study, it can be suggested that naïve HCV patients with low levels of lncRNA HEIH might be less susceptible to HCC risk at this stage of the disease; however, additional prospective studies are needed to confirm this assumption.

According to the present findings, mRNA BST2 was significantly downregulated in naïve HCV patients versus healthy controls. Additionally, there was a significant negative correlation between lncRNA BISPR and its mRNA, indicating that upregulation of lncRNA BISPR expression might lead to downregulation of its mRNA. In contrast, a previous study using isolated HuH7 cells showed that inhibition of lncBISPR by RNA interference led to decreased levels of mRNA BST2[14]. However, our study is the first to assess the expression of both lncRNA BISPR and its mRNA in HCV G4 Egyptian patients; further studies are required to explore the exact

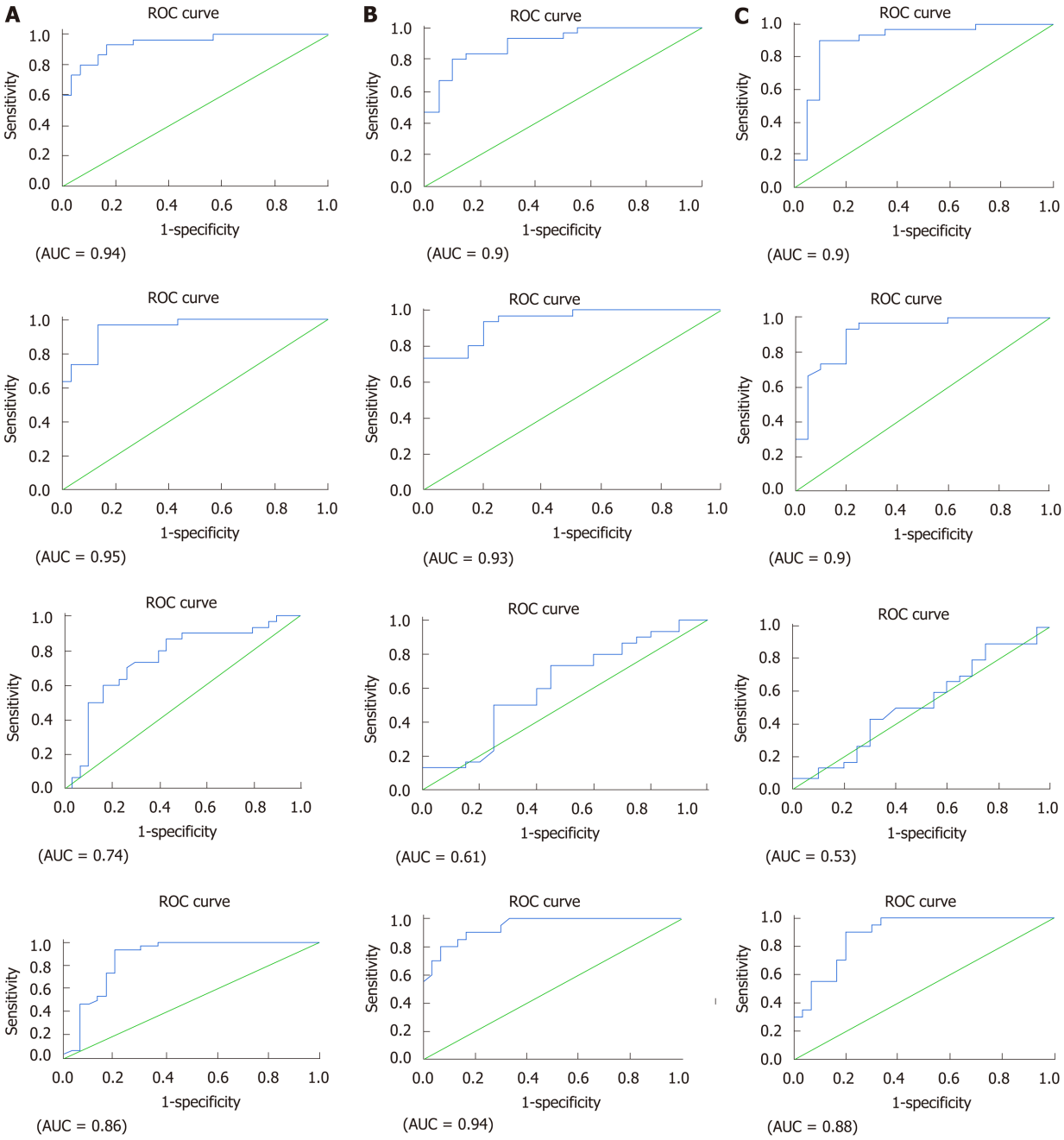

Figure 3 Serum LncRNAs and mRNA as prognostic biomarker for hepatitis C virus treated patients with different treatment reginens. ROC curve analysis for SOF + SIM (A), SOF + DAC (B), and SOF + DAC + RBV (C) as prognostic biomarkers discriminate treated from naïve patients. 1st LncRNA gas 5; 2nd LncRNA BISPR; 3rd LncRNA HEIH; 4th mRNA BST2.

mechanistic relevance of lncRNA BISPR and mRNA BST2 in those patients.

Of note, the study's results indicated that lncRNA Gas5, lncRNA BISPR and lncRNA HEIH and mRNA BST2 could discriminate naïve HCV patients from controls by ROC curve analysis; thus, they could be promising diagnostic biomarkers in HCV infection.

One of the main novelties in present study was the significant decline in circulating lncRNA GAS5 and lncRNA BISPR in HCV patients treated with SOF + SIM, SOF + DAC and SOF + DAC + RBV compared to naïve HCV patients. Recently, it has been reported that treatment of the cells with IFN and ruxolitinib, an inhibitor of the JAK/STAT pathway, or transfection of siRNAs that target STAT2 in IFN-treated cells, significantly reduced BISPR levels compared to those of control cells[10]. It should be noted that in this study, the expression levels of lncRNA GAS5and lncRNA BISPR were positively correlated with viral load, ALT, ALP and AFP, implicating both lncRNA GAS5 and lncRNA BISPR as key players in HCV disease progression and/or host viral response against HCV. Herein, both lncRNA GAS5 and lncRNA BISPR

Table 3 Factors that discriminate between naïve patients (*n* = 30) and healthy controls (*n* = 20) using logistic regression analysis

Parameter	B	SE	*P* value	Odds ratio	Odds ratio (95%CI)
Univariate analysis					
LncRNA-Gas5	1.95	0.675	0.004[b]	7.08	1.88-26.59
LncRNA-BISPR	1.2	0.421	0.004[b]	3.32	1.45-7.57
LncRNA-HEIH	-3.8	1.079	0.005[b]	0.02	0.003-0.184
mRNA BST2	-1.71	0.606	0.003[b]	0.17	0.05-0.587
ALT (IU/L)	0.2	0.06	0.001[b]	1.22	1.09-1.38
AST (IU/L)	0.42	0.135	0.002[b]	1.52	1.16-1.98
AFP (ng/ml)	0.358	0.165	0.03[a]	1.43	1.03-1.97
ALP (IU/L)	0.209	0.067	0.002[b]	1.23	1.080-1.4
Albumin (mg/dl)	-20.26	9.95	0.04[a]	0.01	0.00-0.471
Multiple analysis					
LncRNA-Gas5	2.4	0.766	0.002[b]	11.12	2.47-49.88
mRNA-BST2	-2.71	1.013	0.007[b]	0.066	0.009-0.484

[a]$P < 0.05$,
[b]$P < 0.01$, indicates statistical significance.

were excellent in discriminating the HCV groups treated with SOF + SIM, SOF + DAC or SOF + DAC + RBV from naïve HCV patients. Interestingly, lncRNA GAS5 and lncRNA BISPR had the highest prognostic accuracy in the SOF + SIM treatment group.

In the current investigations the serum levels of mRNA BST2 were significantly higher in all treated HCV patients compared to the levels in naïve HCV patients. In fact, it has been reported that BISPR protein may regulate host response to viral infection either by inhibiting the release of nascent viral particles or by restricting HCV production[23]. Furthermore, mRNA BST2 was negatively correlated with viral load, ALT, ALP, and AFP, supporting the pivotal role of BST2 protein in eradicating HCV in those treated patients. As far as we are aware, there are no reports on lncRNA GAS5, lncRNA BISPR and mRNA BST2 expression in treated HCV patients, and no data were available to oppose or correspond with our results.

To the best of the author's knowledge, this study is the first to address the expression level of lncRNAs and mRNA in the sera of Egyptian HCV G4 patients who experienced a viral relapse or disease reactivation after 12-wk treatment with SOF + SIM. It is well known that HCV attains alternative strategies to efficiently replicate in hepatocytes, thus HCV can become less susceptible to anti-viral drugs, and patients who have been treated can relapse[24]. Indeed, the most interesting finding was the remarkable upregulation of lncRNA HEIH in relapsed HCV patients when compared to SOF + SIM-treated patients. Moreover, significantly higher expression of lncRNA GAS5 and lncRNA BISPR along with a significant reduction in mRNA BST2 expression were observed in relapsed HCV patients when compared to SOF + SIM-treated patients. lncRNA HEIH was the best prognostic marker to distinguish relapsed HCV patients from SOF + SIM-treated HCV patients. In fact, lncRNA HEIH has been suggested to be a potential biomarker in HCV-related HCC[16]. Our results elaborated a significant positive correlation between lncRNA HEIH and AFP and confirms that lncRNA HEIH could be a potential biomarker for the prognosis of/and the monitoring of the progression of relapsed HCV patients.

Study limitations

This study is limited by the relatively small number of patients and the fact that all the patients were enrolled from a single centre (Gastroenterology and Hepatology Clinic-Ain Shams Hospital in Egypt). Further multicenter studies with large number of participants infected with either HCV or other infectious agents unlike HCV should be conducted to justify the specificity of these markers. Moreover, a prospective longitudinal study is needed to follow the same group of patients before and after treatment to confirm the potential of these biomarkers as prognostic tools for HCV and occurrence of relapse after therapy.

In conclusion, differential expression of lncRNA GAS5, lncRNA HEIH, lncRNA BISPR and mRNA BST2 in naïve, treated and relapsed HCV Egyptian patients suggests their involvement in HCV-pathogenesis or antiviral response. In addition,

Table 4 Factors that predict response to SOF + SIM (*n* = 30), SOF + DAC (*n* = 20) or SOF + DAC + RBV (*n* = 20) treatment regimens using logistic regression analysis

Paramete	B	SE	*P* value	Odds ratio	Odds ratio (95%CI)
Univariate analysis (SOF + SIM)					
LncRNA-Gas5	2.135	0.583	< 0.001[c]	8.45	2.69-26.50
LncRNA-BISPR	1.733	0.482	< 0.001[c]	5.65	2.19-14.56
mRNA BST2	-2.029	0.501	< 0.001[c]	0.13	0.04-0.351
ALT (IU/L)	0.084	0.03	0.005[b]	1.08	1.025-1.153
AFP (ng/mL)	0.715	0.299	0.01[a]	2.044	1.137-3.675
ALP (IU/L)	0.209	0.067	0.002[b]	1.232	1.080-1.405
Albumin (mg/dL)	-1.947	0.635	0.002[b]	0.143	0.041-0.495
Multivariate analysis					
LncRNA-Gas5	1.397	0.704	0.04[a]	4.04	1.01-16.073
LncRNA-BISPR	1.613	820	0.04[a]	5.01	1.007-25.02
mRNA BST2	-3.149	1.307	0.01[a]	0.043	0.003-0.556
Univariate analysis (SOF + DAC)					
LncRNA-Gas5	1.54	0.48	0.002[b]	4.69	1.80-12.26
LncRNA-BISPR	1.86	0.61	0.003[b]	6.43	1.91-21.59
mRNA BST2	-1.677	0.415	< 0.001[c]	0.187	0.083-0.422
ALT (IU/L)	0.125	0.048	0.01[a]	1.13	1.031-1.245
AFP (ng/mL)	0.715	0.299	0.01[a]	2.044	1.137-3.675
ALP (IU/L)	0.729	0.296	0.01[a]	2.073	1.161-3.699
Multivariate analysis					
LncRNA-Gas5	1.17	0.54	0.03[a]	3.05	1.06-8.79
LncRNA-BISPR	1.42	0.69	0.03[a]	4.17	1.07-16.1
Univariate analysis (SOF + DAC + RBV)					
LncRNA-Gas5	1.12	0.33	0.001[b]	3.07	1.6-5.88

[a]$P < 0.05$,
[b]$P < 0.01$, indicates statistical significance. ALT: Alanine aminotransferases; AFP: Alfa fetoprotein; ALP: Alkaline phosphatase.

lncRNA GAS5, lncRNA HEIH, lncRNA BISPR and mRNA BST2 could serve as potential diagnostic biomarkers in HCV GT4 Egyptian patients while, lncRNA GAS5, lncRNA BISPR and mRNA BST2 could also be considered novel prognostic biomarkers for treatment in HCV patients. Importantly, lncRNA HEIH might represent a powerful prognostic marker for differentiating relapsed patients from SOF + SIM treatment. Finally, these biomarkers can be used in combination to complete the whole picture of diagnosis, prognosis and follow-up of HCV.

Table 5 Factors that predict relapsed hepatitis C virus patients (*n* = 30) from SOF + SIM therapy (*n* = 30) using logistic regression analysis

Parameter	B	SE	*P* value	Odds ratio	Odds ratio (95%CI)
Univariate analysis					
LncRNA-Gas5	2.35	0.564	< 0.001[b]	10.48	3.47-31.67
LncRNA-BISPR	2.27	0.555	< 0.001[b]	9.69	3.26-28.73
LncRNA-HEIH	1.99	0.599	0.001[b]	7.31	2.26-23.63
mRNA BST2	-3.15	0.858	< 0.001[b]	0.042	0.08-0.228
ALT (IU/L)	0.87	0.037	0.01[a]	1.09	1.01-1.17
ALP (IU/L)	0.069	0.022	0.002[b]	1.07	1.02-1.11
Multivariate analysis					
LncRNA-Gas5	1.46	0.69	0.03[a]	4.322	1.12-16.70
LncRNA-HEIH	1.4	0.714	0.04[a]	8.885	1.00-16.51

[a]*P* < 0.05,
[b]*P* < 0.01, indicates statistical significance. ALT: Alanine aminotransferases; ALP: Alkaline phosphatase.

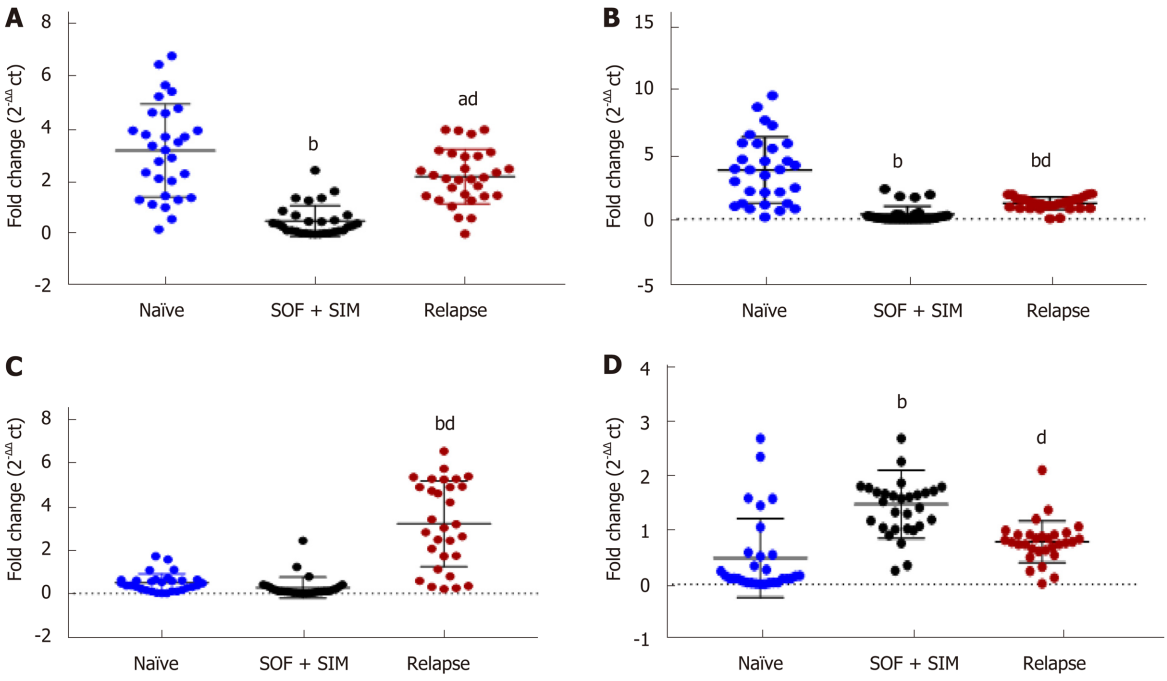

Figure 4 Differential expression of serum lncRNAs and mRNA levels in hepatitis C virus relapsed, naïve and SOF + SIM treated hepatitis C virus patients.[a]*P* < 0.05, [b]*P* < 0.01, *vs* naïve group; [d]*P* < 0.01, *vs* SOF + SIM group.

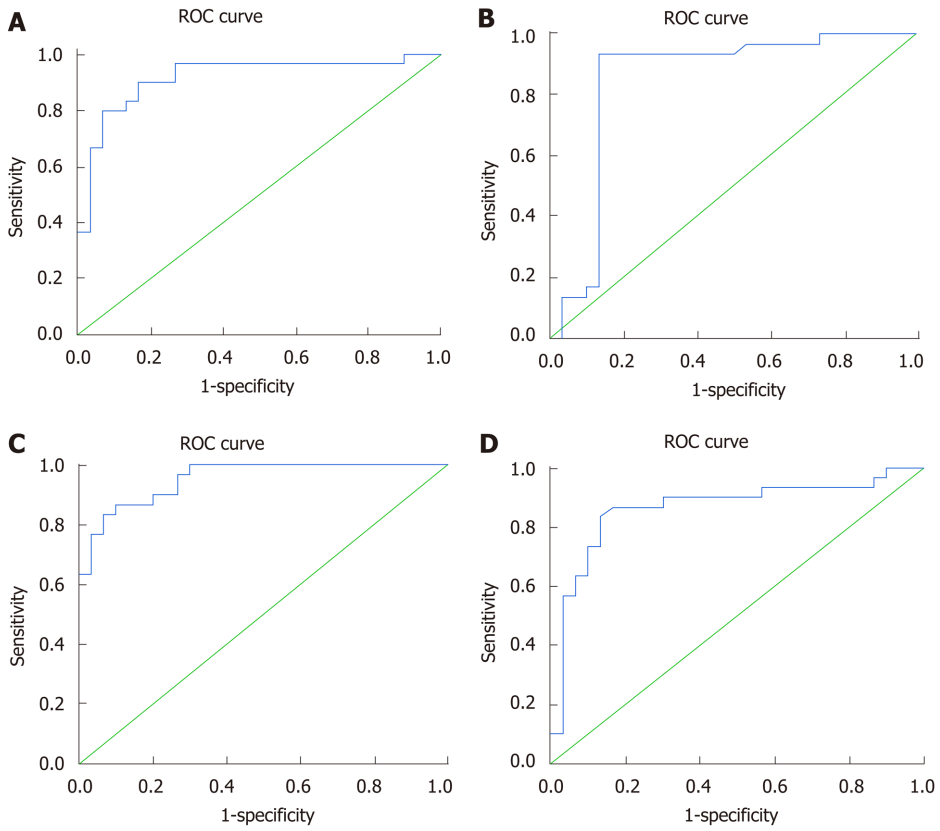

Figure 5 Serum LncRNAs and mRNA as prognostic biomarker for relapsed patients. ROC curve analysis for lncRNA Gas 5 (AUC = 0.91) (A), BISPR (AUC = 0.84) (B), HEIH (AUC = 0.95) (C) and mRNA BST2 (AUC = 0.86) (D) as prognostic biomarkers discriminating relapsed from treated from SOF + SIM patients.

ARTICLE HIGHLIGHTS

Research Background

Hepatitis C virus (HCV) infection is a complex multifactorial process that involves multiple viral and host interactions. Besides, the high mutation rate of HCV that enables the virus to generate escape mutants resistant to treatment, emphasizing the need for a proper understanding of the pathogenesis of HCV infection, and various research efforts should be oriented to develop novel diagnostic and prognostic molecular tools.

Research motivation

lncRNAs are transcripts greater than 200 nucleotides with poor coding potential, that play important roles in regulating gene expression. Emerging evidence suggests that lncRNAs play relevant roles in viral infection and in antiviral responses. To date, the expression profiles of lncRNA GAS5, lncRNA HEIH, lncRNA BISPR and its mRNA BST2 in HCV GT4 patients and their clinical relevance as biomarkers for HCV infection have not been studied yet.

Research objectives

To assess the serum levels of lncRNA GAS5, lncRNA HEIH, lncRNA BISPR and mRNA BST2 in naïve, treated and relapsed Egyptian HCV patients to examine their relation to HCV infection and their potential usefulness as new diagnostic and prognostic biomarkers for HCV GT4.

Research methods

Serum lncRNAs and mRNABST2 were measured using quantitative real-time polymerase chain reaction. The study included six groups; group I healthy controls and group II naïve HCV patients without treatment. Groups from III to V comprised HCV patients treated daily with three different 12-wk oral treatment regimens as follows: Group III received combination of sofosbuvir and simeprevir. Group IV received combination of sofosbuvir and daclatasvir. Group V received sofosbuvir and daclatasvir with ribavirin. Group VI included HCV patients who relapsed after 12-week treatment with sofosbuvir and simeprevir.

Research results

We found that serum levels of lncRNAGAS5 and LncRNABISPR were upregulated, whereas mRNA BST2 and LncRNA HEIH levels were downregulated in naïve patients compared to healthy controls. In contrast, HCV patients treated with sofosbuvir and simeprevir; with sofosbuvir and daclatasvir; or with sofosbuvir, daclatasvir and ribavirin exhibited lower levels of

lncRNAGAS5 and lncRNABISPR with higher mRNABST2 compared to naïve patients. Notably, patients relapsed from sofosbuvir and simeprevir showed higher levels of these lncRNAs with lower mRNABST2 compared to treated patients. Moreover, lncRNA GAS5, lncRNA BISPR and mRNA BST2 could differentiate naïve patients from controls and treated patients, whereas lncRNA HEIH best differentiated relapsed from treated patients.

Research conclusions

Differential expression of lncRNA GAS5, lncRNA HEIH, lncRNA BISPR and mRNA BST2 in naïve, treated and relapsed HCV Egyptian patients suggests their involvement in HCV-pathogenesis or antiviral response. In addition, lncRNA GAS5, lncRNA HEIH, lncRNA BISPR and mRNA BST2 could serve as potential diagnostic biomarkers in HCV GT4 Egyptian patients while, lncRNA GAS5, lncRNA BISPR and mRNA BST2 could also be considered novel prognostic biomarkers for treatment in HCV patients. Importantly, lncRNA HEIH might represent a powerful prognostic marker for differentiating relapsed patients from sofosbuvir and simeprevir treatment.

Research perspectives

Further multicentre studies with large number of participants infected with either HCV or other infectious agents unlike HCV should be conducted to justify the specificity of these markers. Moreover, a prospective longitudinal study is needed to follow the same group of patients before and after treatment to confirm the potential of these biomarkers as prognostic tools for HCV and occurrence of relapse after therapy.

REFERENCES

1 **Jefferies M**, Rauff B, Rashid H, Lam T, Rafiq S. Update on global epidemiology of viral hepatitis and preventive strategies. *World J Clin Cases* 2018; **6**: 589-599 [PMID: 30430114 DOI: 10.12998/wjcc.v6.i13.589]

2 **Kouyoumjian SP**, Chemaitelly H, Abu-Raddad LJ. Characterizing hepatitis C virus epidemiology in Egypt: systematic reviews, meta-analyses, and meta-regressions. *Sci Rep* 2018; **8**: 1661 [PMID: 29374178 DOI: 10.1038/s41598-017-17936-4]

3 **Ayoub HH**, Abu-Raddad LJ. Impact of treatment on hepatitis C virus transmission and incidence in Egypt: A case for treatment as prevention. *J Viral Hepat* 2017; **24**: 486-495 [PMID: 28039923 DOI: 10.1111/jvh.12671]

4 **van der Meer AJ**, Veldt BJ, Feld JJ, Wedemeyer H, Dufour JF, Lammert F, Duarte-Rojo A, Heathcote EJ, Manns MP, Kuske L, Zeuzem S, Hofmann WP, de Knegt RJ, Hansen BE, Janssen HL. Association between sustained virological response and all-cause mortality among patients with chronic hepatitis C and advanced hepatic fibrosis. *JAMA* 2012; **308**: 2584-2593 [PMID: 23268517 DOI: 10.1001/jama.2012.144878]

5 **Lee MH**, Yang HI, Lu SN, Jen CL, You SL, Wang LY, Wang CH, Chen WJ, Chen CJ; R. E.V.E.A.L.-HCV Study Group. Chronic hepatitis C virus infection increases mortality from hepatic and extrahepatic diseases: a community-based long-term prospective study. *J Infect Dis* 2012; **206**: 469-477 [PMID: 22811301 DOI: 10.1093/infdis/jis385]

6 **Abdel-Moneim A**, Abood A, Abdel-Gabaar M, Zanaty MI, Ramadan M. Effectiveness of sofosbuvir/pegylated-interferon plus ribavirin in treatment of hepatitis C virus genotype 4 patients. *Clin Exp Hepatol* 2018; **4**: 191-196 [PMID: 30324144 DOI: 10.5114/ceh.2018.78123]

7 **Iyer MK**, Niknafs YS, Malik R, Singhal U, Sahu A, Hosono Y, Barrette TR, Prensner JR, Evans JR, Zhao S, Poliakov A, Cao X, Dhanasekaran SM, Wu YM, Robinson DR, Beer DG, Feng FY, Iyer HK, Chinnaiyan AM. The landscape of long noncoding RNAs in the human transcriptome. *Nat Genet* 2015; **47**: 199-208 [PMID: 25599403 DOI: 10.1038/ng.3192]

8 **Wu R**, Su Y, Wu H, Dai Y, Zhao M, Lu Q. Characters, functions and clinical perspectives of long non-coding RNAs. *Mol Genet Genomics* 2016; **291**: 1013-1033 [PMID: 26885843 DOI: 10.1007/s00438-016-1179-y]

9 **Fortes P**, Morris KV. Long noncoding RNAs in viral infections. *Virus Res* 2016; **212**: 1-11 [PMID: 26454188 DOI: 10.1016/j.virusres.2015]

10 **Barriocanal M**, Fortes P. Long Non-coding RNAs in Hepatitis C Virus-Infected Cells. *Front Microbiol* 2017; **8**: 1833 [PMID: 29033906 DOI: 10.3389/fmicb.2017.01833]

11 **Hu L**, Ye H, Huang G, Luo F, Liu Y, Liu Y, Yang X, Shen J, Liu Q, Zhang J. Long noncoding RNA GAS5 suppresses the migration and invasion of hepatocellular carcinoma cells via miR-21. *Tumour Biol* 2016; **37**: 2691-2702 [PMID: 26404135 DOI: 10.1007/s13277-015-4111-x]

12 **Littlejohn GO**. Fibrositis/fibromyalgia syndrome in the workplace. *Rheum Dis Clin North Am* 1989; **15**: 45-60 [PMID: 2644678 DOI: 10.1074/jbc.M115.683813]

13 **Qian X**, Xu C, Zhao P, Qi Z. Long non-coding RNA GAS5 inhibited hepatitis C virus replication by binding viral NS3 protein. *Virology* 2016; **492**: 155-165 [PMID: 26945984 DOI: 10.1016/j.virol.2016.02.020]

14 **Barriocanal M**, Carnero E, Segura V, Fortes P. Long Non-Coding RNA BST2/BISPR is Induced by IFN and Regulates the Expression of the Antiviral Factor Tetherin. *Front Immunol* 2014; **5**: 655 [PMID: 25620967 DOI: 10.3389/fimmu.2014.00655]

15 **Yang F**, Zhang L, Huo XS, Yuan JH, Xu D, Yuan SX, Zhu N, Zhou WP, Yang GS, Wang YZ, Shang JL, Gao CF, Zhang FR, Wang F, Sun SH. Long noncoding RNA high expression in hepatocellular carcinoma facilitates tumor growth through enhancer of zeste homolog 2 in humans. *Hepatology* 2011; **54**: 1679-1689 [PMID: 21769904 DOI: 10.1002/hep.24563]

16 **Zhang C**, Yang X, Qi Q, Gao Y, Wei Q, Han S. lncRNA-HEIH in serum and exosomes as a potential biomarker in the HCV-related hepatocellular carcinoma. *Cancer Biomark* 2018; **21**: 651-659 [PMID: 29286922 DOI: 10.3233/CBM-170727]

17 **Erikson E**, Adam T, Schmidt S, Lehmann-Koch J, Over B, Goffinet C, Harter C, Bekeredjian-Ding I, Sertel S, Lasitschka F, Keppler OT. In vivo expression profile of the antiviral restriction factor and tumor-

targeting antigen CD317/BST-2/HM1.24/tetherin in humans. *Proc Natl Acad Sci USA* 2011; **108**: 13688-13693 [PMID: 21808013 DOI: 10.1073/pnas.1101684108]

18 **Dafa-Berger A**, Kuzmina A, Fassler M, Yitzhak-Asraf H, Shemer-Avni Y, Taube R. Modulation of hepatitis C virus release by the interferon-induced protein BST-2/tetherin. *Virology* 2012; **428**: 98-111 [PMID: 22520941 DOI: 10.1016/j.virol.2012.03.011]

19 **Dahari H**, Canini L, Graw F, Uprichard SL, Araújo ES, Penaranda G, Coquet E, Chiche L, Riso A, Renou C, Bourliere M, Cotler SJ, Halfon P. HCV kinetic and modeling analyses indicate similar time to cure among sofosbuvir combination regimens with daclatasvir, simeprevir or ledipasvir. *J Hepatol* 2016; **64**: 1232-1239 [PMID: 26907973 DOI: 10.1016/j.jhep.2016.02.022]

20 **Ohno O**, Mizokami M, Wu RR, Saleh MG, Ohba K, Orito E, Mukaide M, Williams R, Lau JY. New hepatitis C virus (HCV) genotyping system that allows for identification of HCV genotypes 1a, 1b, 2a, 2b, 3a, 3b, 4, 5a, and 6a. *J Clin Microbiol* 1997; **35**: 201-207 [PMID: 8968908]

21 **Wyles D**, Mangia A, Cheng W, Shafran S, Schwabe C, Ouyang W, Hedskog C, McNally J, Brainard DM, Doehle BP, Svarovskaia E, Miller MD, Mo H, Dvory-Sobol H. Long-term persistence of HCV NS5A resistance-associated substitutions after treatment with the HCV NS5A inhibitor, ledipasvir, without sofosbuvir. *Antivir Ther* 2018; **23**: 229-238 [PMID: 28650844 DOI: 10.3851/IMP3181]

22 **Yang ZF**, Li J, Ma ZY, Yang XS, Dai B, An JZ, Li HM. Association between expression of LncRNA-HEIH in plasma and hepatocellular carcinoma risk: A case-control study. *Xiandai Zhongliu Yixue* 2015; **23**: 80–84

23 **Mahauad-Fernandez WD**, Okeoma CM. The role of BST-2/Tetherin in host protection and disease manifestation. *Immun Inflamm Dis* 2016; **4**: 4-23 [PMID: 27042298 DOI: 10.1002/iid3.92]

24 **Medrano J**, Barreiro P, Resino S, Tuma P, Rodríguez V, Vispo E, Labarga P, Madejón A, García-Samaniego J, Jiménez-Nácher I, Martín-Carbonero L, Soriano V. Rate and timing of hepatitis C virus relapse after a successful course of pegylated interferon plus ribavirin in HIV-infected and HIV-uninfected patients. *Clin Infect Dis* 2009; **49**: 1397-1401 [PMID: 19814621 DOI: 10.1086/630205]

World Journal of Gastroenterology

Submit a Manuscript: https://www.f6publishing.com

World J Gastroenterol 2020 January 14; 26(2): 184-198

DOI: 10.3748/wjg.v26.i2.184

ISSN 1007-9327 (print) ISSN 2219-2840 (online)

ORIGINAL ARTICLE

Observational Study

Impact of *GFRA1* gene reactivation by DNA demethylation on prognosis of patients with metastatic colon cancer

Wan-Ru Ma, Peng Xu, Zhao-Jun Liu, Jing Zhou, Lian-Kun Gu, Jun Zhang, Da-Jun Deng

ORCID number: Wan-Ru Ma (0000-0002-9697-7355); Peng Xu (0000-0002-7559-8559); Zhao-Jun Liu (0000-0003-0924-7862); Jing Zhou (0000-0001-9814-6574); Lian-Kun Gu (0000-0003-0791-1280); Jun Zhang (0000-0001-9796-994X); Da-Jun Deng (0000-0001-5161-5943).

Author contributions: Deng DJ and Zhang J designed the research; Ma WR, Xu P, Zhou J, and Gu LK performed the research; Ma WR and Liu ZJ analyzed the data; Ma WR, Xu P, Zhang J, and Deng DJ wrote the paper. Ma WR and Xu P contributed equally to this work. Zhang J is an equal corresponding author.

Supported by the National Natural Science Foundation of China A3 Foresight Program, No. 31261140372; Beijing Science and Technology Commission, No. Z151100001615022; and the Science Foundation of Peking University Cancer Hospital, No. 2017-25.

Institutional review board statement: This study was reviewed and approved by The Institutional Review Board of the Peking University Cancer Hospital and Institute.

Informed consent statement: The patients were not required to give informed consent to the study because the analysis used anonymous data that were obtained after each patient agreed to treatment by written consent.

Conflict-of-interest statement: The authors declare that they have no competing interests.

Wan-Ru Ma, Zhao-Jun Liu, Jing Zhou, Lian-Kun Gu, Da-Jun Deng, Key Laboratory of Carcinogenesis and Translational Research (MOE/Beijing), Division of Etiology, Peking University Cancer Hospital and Institute, Beijing 100143, China

Peng Xu, Jun Zhang, Shihezi University School of Medicine, Shihezi 832000, Xinjiang Uygur Autonomous Region, China

Peng Xu, Morphological Center of Basic Medical School of Xinjiang Medical University, Urumqi 830011, Xinjiang Uygur Autonomous Region, China

Corresponding author: Da-Jun Deng, MD, Professor, Laboratory of Carcinogenesis and Translational Research (MOE/Beijing), Division of Etiology, Peking University Cancer Hospital and Institute, No. 52, Fucheng Road, Haidian District, Beijing 100142, China. dengdajun@bjmu.edu.cn

Abstract

BACKGROUND

The expression of the membrane receptor protein GFRA1 is frequently upregulated in many cancers, which can promote cancer development by activating the classic RET-RAS-ERK and RET-RAS-PI3K-AKT pathways. Several therapeutic anti-GFRA1 antibody-drug conjugates are under development. Demethylation (or hypomethylation) of *GFRA1* CpG islands (dmGFRA1) is associated with increased gene expression and metastasis risk of gastric cancer. However, it is unknown whether dmGFRA1 affects the metastasis of other cancers, including colon cancer (CC).

AIM

To study whether dmGFRA1 is a driver for CC metastasis and GFRA1 is a potential therapeutic target.

METHODS

CC and paired surgical margin tissue samples from 144 inpatients and normal colon mucosal biopsies from 21 noncancer patients were included in this study. The methylation status of *GFRA1* islands was determined by MethyLight and denaturing high-performance liquid chromatography and bisulfite-sequencing. Kaplan-Meier analysis was used to explore the effect of dmGFRA1 on the survival of CC patients. Impacts of *GFRA1* on CC cell proliferation and migration were evaluated by a battery of biological assays *in vitro* and *in vivo*. The phosphorylation of AKT and ERK proteins was examined by Western blot analysis.

Data sharing statement: The data and materials of the study are available from the corresponding author upon reasonable request.

STROBE statement: The authors have read the STROBE Statement-checklist of items, and the manuscript was prepared according to the STROBE Statement-checklist of items.

Manuscript source: Unsolicited manuscript

Received: October 8, 2019
Peer-review started: October 8, 2019
First decision: November 11, 2019
Revised: December 14, 2019
Accepted: December 21, 2019
Article in press: December 21, 2019
Published online: January 14, 2020

P-Reviewer: Kim SY, Lucarelli M
S-Editor: Wang J
L-Editor: Wang TQ
E-Editor: Ma YJ

RESULTS

The proportion of dmGFRA1 in CC, surgical margin, and normal colon tissues by MethyLight was 68.4%, 73.4%, and 35.9% (median; nonparametric test, $P = 0.001$ and < 0.001), respectively. Using the median value of dmGFRA1 peak area proportion as the cutoff, the proportion of dmGFRA1-high samples was much higher in poorly differentiated CC samples than in moderately or well-differentiated samples (92.3%% *vs* 55.8%, Chi-square test, $P = 0.002$) and significantly higher in CC samples with distant metastasis than in samples without (77.8% *vs* 46.0%, $P = 0.021$). The overall survival of patients with dmGFRA1-low CC was significantly longer than that of patients with dmGFRA1-high CC (adjusted hazard ratio = 0.49, 95% confidence interval: 0.24-0.98), especially for 89 CC patients with metastatic CC (adjusted hazard ratio = 0.41, 95% confidence interval: 0.18-0.91). These data were confirmed by the mining results from TCGA datasets. Furthermore, *GFRA1* overexpression significantly promoted the proliferation/invasion of RKO and HCT116 cells and the growth of RKO cells in nude mice but did not affect their migration. *GFRA1* overexpression markedly increased the phosphorylation levels of AKT and ERK proteins, two key molecules in two classic GFRA1 downstream pathways.

CONCLUSION

GFRA1 expression is frequently reactivated by DNA demethylation in CC tissues and is significantly associated with a poor prognosis in patients with CC, especially those with metastatic CC. GFRA1 can promote the proliferation/growth of CC cells, probably by the activation of AKT and ERK pathways. GFRA1 might be a therapeutic target for CC patients, especially those with metastatic potential.

Key words: *GFRA1*; Demethylation; CpG island; Colon cancer; Metastasis; Membrane receptor

Core tip: *GFRA1* reactivation by DNA demethylation is a frequent event in colon cancer (CC) development and that the high level of GFRA1 demethylation in CC tissues is correlated with high metastasis risk of CC and shorter overall survival of patients, especially patients with metastatic CC. We find that GFRA1 overexpression enhances the proliferation and growth of CC cells *in vitro* and *in vivo*, probably by activation of the GFRA1-GDNF downstream pathway. These data indicate that reactivation of *GFRA1* by DNA demethylation is an important prognosis factor for CC and the cancer-related cell membrane protein GFRA1 may be a therapeutic target for CC patients.

Citation: Ma WR, Xu P, Liu ZJ, Zhou J, Gu LK, Zhang J, Deng DJ. Impact of *GFRA1* gene reactivation by DNA demethylation on prognosis of patients with metastatic colon cancer. *World J Gastroenterol* 2020; 26(2): 184-198
URL: https://www.wjgnet.com/1007-9327/full/v26/i2/184.htm
DOI: https://dx.doi.org/10.3748/wjg.v26.i2.184

INTRODUCTION

Although advances have been made in the treatment of colorectal carcinoma (CRC), it remains the most common gastrointestinal cancer worldwide[1]. CRC is annually diagnosed in 1.4 million individuals and leads to 700000 deaths worldwide[2]. Metastasis is the leading cause of CRC-related death[3]. Although the biological mechanisms associated with CRC metastasis have been extensively studied[4], the sensitivity and specificity of existing clinical biomarkers for predicting the prognosis of CRC patients are not satisfactory. Recognition of specific biomarkers is important for predicting prognosis, including metastasis, of colorectal cancer. Molecular therapy targets for patients with metastatic CRC are also urgently needed.

GFRA1 is a cell surface membrane receptor for glial cell-derived neurotrophic factor (GDNF)[5,6]. The GDNF-GFRA1 complex binds to and activates the tran-

smembrane RET proto-oncogene receptor, induces the phosphorylation of RET tyrosine residues, and activates the RAS-ERK and PI3K-AKT signaling pathways, thus mediating the development of the nervous system and kidneys, as well as cancer growth[6-9]. The *GFRA1* gene is not only normally expressed in neural cells, especially in enteric neurons, but is also abnormally overexpressed in many cancers[9-17]. *GFRA1* overexpression can affect multiple biological behaviors of cancer cells, including proliferation, metastasis, and perineural invasion. *GFRA1* overexpression is associated with a poor overall survival (OS) of patients with pancreatic or breast cancer[12,16]. Anti-GFRA1 autoantibodies can be detected in patients with luminal A (hormone receptor-positive) breast cancer[18,19]. Apparently, the cancer-associated GFRA1 protein is a potential therapeutic target. Several preclinical anti-GFRA1 antibody-drug conjugates for breast cancer treatment have been developed[20,21].

It is well known that the methylation of CpG islands around the transcription start site (TSS-CGIs) epigenetically inactivates gene transcription, and TSS-CGI demethylation is essential for methylated gene reactivation. Our recent studies have shown that *GFRA1* alleles are epigenetically silenced by the methylation of *GFRA1* TSS-CGI (mGFRA1) in many normal non-nervous cells in adult tissues and are abnormally reactivated in cancer cells by the demethylation (or hypomethylation) of the *GFRA1* TSS-CGI (dmGFRA1)[22]. The presence of dmGFRA1 was consistently found to be associated with an increased metastasis risk of gastric carcinoma and short OS in multiple cohorts in China, Japan, and Korea[22]. The results of our prospective study further showed that dmGFRA1 could be a potential biomarker for prediction of metastasis of gastric carcinoma in Chinese patients[23]. However, no studies have reported the impacts of the reactivation of *GFRA1* expression by dmGFRA1 on CRC progression.

In this study, we examined the demethylation status of TSS-CGIs in *GFRA1* alleles in colon carcinoma (CC) and paired surgical margin (SM) tissue samples and normal colon mucosal biopsy samples from noncancer patients. We observed that *GFRA1* was significantly demethylated in both CC and SM tissues compared with that in normal colon biopsies and that the high dmGFRA1 level was significantly correlated with poor differentiation, metastasis, and short OS for CC patients, especially those with metastatic CC. GFRA1 overexpression could promote the proliferation/growth of CC cells *in vitro* and *in vivo*, probably by increasing the phosphorylation levels of two key proteins ERK and AKT in two classical GDNF-GFRA1 downstream pathways in CC cells.

MATERIALS AND METHODS

Human colon samples

CC and paired SM (> 5 cm from the cancerous mass) tissue samples and related clinicopathological information were obtained from 144 patients at Peking University Cancer Hospital. Normal colon mucosal biopsies from 21 noncancer patients from the same hospital were also included in this study. The Institutional Review Board of the Peking University Cancer Hospital and Institute approved the study, and all of the patients provided written informed consent.

Cell lines and culture

The human CC cell line HCT116 was kindly provided by Professor Yuanjia Chen at Peking Union Medical College Hospital, and RKO was purchased from American Type Culture Collection. The HEK293FT cell line was provided by Dr. Zhang ZQ at Peking University Cancer Hospital and Institute. These cell lines were cultured in RPMI 1640 medium (Gibco, GrandIsland, NY, United States) containing 10% fetal bovine serum (FBS; Gibco) and 1% penicillin-streptomycin (Gibco), and maintained at 37 °C in a 5% CO_2-containing atmosphere. These cell lines were tested and authenticated by Beijing JianLian Genes Technology Co., LTD before they were used in this study. STR patterns were analyzed using the Goldeneye 20A STR Identifiler PCR Amplification Kit as we previously reported[22].

More human cell lines were used in the pilot study, including the gastric cell lines BGC823, GES1, MGC803, and SGC7901, cervical cancer cell lines HeLa and Siha, and breast cancer cell line MCF7, kindly provided by Dr. Yang K; the gastric cancer cell line AGS and lung cancer cell line H1299 provided by Dr. Shou CC; the lung cancer cell line A549 provided by Dr. Zhang ZQ at Peking University Cancer Hospital; the gastric cell line MKN74 provided by Dr. Yashuhito Y at Tokyo Medical and Dental University; the prostate cancer cell line PC-3 purchased from Cell Line Bank, Chinese Acad Med Sci; the liver cancer cell line HepG2 provided by Dr. Zhang ZQ; the gastric cancer cell line MKN45 purchased from National Laboratory Cell Resource Sharing

Platform; and the colon cancer (CC) cell lines Colo205 and SW480 provided by Professor Chen YJ at Peking Union Medical College Hospital. A549, BGC823 GES1, H1299, HepG2, MGC803, MKN45, MKN74, and SGC7901 cells were cultured in RPMI1640 medium with 10% FBS. Colo205, HeLa, MCF7, Siha, and SW480 cells were cultured in DMEM with 10% FBS. AGS and PC3 cells were cultured in F12 medium with 10% FBS. AGS and PC3 cells were cultured in F12 medium with 10% FBS.

The Cancer Genome Atlas methylation and transcriptome dataset mining

The methylation information on 31 CpG sites within the *GFRA1* TSS-CGI (by the 450K methylation array) in CC and SM samples from 268 of 454 patients and related clinical information were downloaded from the Cancer Genome Atlas (TCGA) database. OS information was available for 190 patients. The methylation level for each CpG site was expressed using the β value, calculated as M/(M+U), where M is the signal from methylated beads, and U is the signal from unmethylated beads at the targeted CpG site. When the β value for a CpG site was < 0.2, it was classified as demethylation-positive CpG (dmCpG). The total number of dmCpG sites was used to represent the *GFRA1* demethylation level for each sample. The median dmCpG number of 2 for the 268 samples was used as the cutoff value to define dmGFRA1. A sample containing ≥ 2 dmCpG sites was classified as dmGFRA1-high; otherwise, dmGFRA1-low (Table S1). The information on the *GFRA1* mRNA level in CC samples from 453 patients was also downloaded from the TCGA database. The OS information for 350 patients was used in the online OS analysis at the website (bioinformatica. Mty.itesm.mx: 8080/Biomatec/SurvivaX.Jsp)[24].

GFRA1 viral expression vector supernatant and transfection

GFRA1 transcript isoform b (*GFRA1b*, 1380 nt) is the main mature mRNA for this gene in cancer[7,25]. Therefore, the full-length human *GFRA1b* viral expression vector supernatant (pLenti-GFRA1b) was purchased from Obio Technology Corp (Cat. no.CK1116, Shanghai, China). The *GFRA1b* expression viral supernatant or mock viral supernatant control was used to transfect HCT116 and RKO cells following the manufacturer's instructions. To obtain stably-transfected cells, we selected the transfected cells by culturing them in medium containing 0.5 μg/mL puromycin (Sigma, St Louis, MO, United States) for at least two weeks after transfection.

Quantitative RT-PCR

Total RNA was extracted using the Ultrapure RNA Kit (Beijing ComWin Biotech Co., Ltd, China) and the quality and concentration of RNA samples were monitored using the Nanodrop 2000 system (Thermo Fisher Scientific, Waltham, MA, United States). Qualified RNA samples were used to synthesize cDNA using the Trans-Script First-Strand cDNA Synthesis SuperMix (TransGen Biotech, Beijing, China). *GFRA1* mRNA 150-bp amplicon was detected by quantitative RT-PCR (qRT-PCR) using a primer set (forward, 5′-GATATATTCC GGGTGGTCCC ATTC-3′, and reverse 5′-GGTGCACGGG GTGATGTACGC-3′) and SYBR Green PCR master mix reagents (Roche, Mannheim, Germany) at an annealing temperature of 58.5 °C on an ABI-7500 platform[22]. *GFRA1* mRNA levels were normalized to *Alu* reference RNA as previously reported[25,26]. The relative mRNA level was calculated using the classic ΔΔCt method. Each sample was analyzed in triplicate.

DNA extraction and bisulfite conversion of genomic DNA

Genomic DNA was extracted using the QIAamp DNA Mini Kit (Qiagen, Cat# 51306, Hiden, Germany). Bisulfite conversion was performed by adding 5 M sodium bisulfite to 1.8 μg DNA samples[27].

Hot-start PCR, bisulfite-sequencing, and denaturing high-performance liquid chromatography analysis

A CpG-free universal primer set (forward, 5′-GGTGTTGGAA ATTTTTTAAAGG-3′ and reverse, 5′-AAAACACTTC TTCCTTCCACAT-3′) and bisulfite-modified DNA were used to amplify both methylated and demethylated *GFRA1* TSS-CGIs at an annealing temperature of 55.0 °C[22]. The PCR products were clone-sequenced and then analyzed quantitatively by denaturing high-performance liquid chromatography (DHPLC) using the WAVE DNA Fragment Analysis System[22,28]. Briefly, 522-bp PCR products of methylated and demethylated *GFRA1* were separated using a DNASep analytical column (Transgenomic) at a partial denaturing temperature of 55.5 °C. Genomic DNA obtained from blood samples with and without *M.sssI* methylation was used as the mGFRA1- and dmGFRA1-positive controls, respectively. The peak areas corresponding to the mGFRA1 and dmGFRA1 products were used to calculate the proportion of dmGFRA1 (the proportion of dmGFRA1-peak area = dmGFRA1-peak area/the sum of the dmGFRA1-peak and mGFRA1-peak areas). When a

dmGFRA1-peak was detected in a sample, it was defined as dmGFRA1-positive sample; otherwise, dmGFRA1-negative (Table S1).

MethyLight assay

The dmGFRA1 levels in all of tissue samples were detected with the MethyLight assay, a previously established and optimized quantitative assay at our lab[22,27]. The median value of dmGFRA1 proportion for CC tissue samples was used as the cutoff to define dmGFRA1-high and dmGFRA1-low CC (Table S1).

Western blot analysis

Cells were collected and lysed to obtain protein lysates. The resulting proteins were then electrophoresed using a 10% SDS-PAGE gel and transferred onto a PVDF membrane. After blocking with 5% nonfat milk overnight at 4 °C, the membrane was incubated with the corresponding primary antibodies [anti-GFRA1 (AF714), R&D systems, Minneapolis, United States; anti-GAPDH (60004-1), Protein Tech, China; anti-ERK (4695S), anti-p-ERK (4370S), anti-AKT (4691T), and anti-p-AKT (4060T), Cell Signaling Technology, United States] for 1 h at room temperature. The membrane was then washed three times with PBST (PBS with 0.1% Tween-20). After washing, the membrane was incubated with the corresponding horseradish peroxidase-conjugated rabbit anti-goat or mouse IgG at room temperature for 1 h. Signals were visualized using the Immobilon Western Chemiluminescent HRP Substrate Kit (Millipore, United States).

Cell proliferation and migration assays using the IncuCyte platform

HCT116 and RKO cells were seeded in 96-well plates (2000 cells/well, 5 wells/group) and cultured for at least 96 h to obtain the proliferation curves. Cells were photographed every 6 h in a long-term dynamic observation platform (IncuCyte, Essen, MI, United States). Cell confluence was analyzed using IncuCyte ZOOM software (Essen, Ann Arbor, MI, United States). For continuous observation of cell migration, the cells were seeded in 96-well plates at a density of 10000 cells/well and cultured for 24 h. After a scratch wound was created, the cells were washed three times with PBS. The cells were regularly cultured and photographed every 6 h for at least 96 h. The relative wound width was calculated using the same software[29].

Animal experiments

RKO cells stably transfected with the control or *GFRA1b* expression vector were trypsinized, washed twice with PBS, and then subcutaneously injected into the bilateral inguinal regions of female BALB/c mice (body weight 18-20 g; age 6 weeks, Beijing Huafukang Bioscience Co. Inc.; 2×10^6 cells per injection). There were eight mice in each experimental group. On the 29th day post-transplantation, the mice were sacrificed. The tumors were then removed from the mice and weighed.

Statistical analysis

All statistical analyses were performed using SPSS 18.0 software. The Mann–Whitney *U*-test was conducted for non-normally distributed data. Student's *t*-test was used for normally distributed data. The log-rank test was used to compare survival durations between groups. All statistical tests were two-sided, and $P < 0.05$ was considered statistically significant.

RESULTS

Reactivation of GFRA1 expression by DNA demethylation in cancer cells and CC tissues

To study the relationship between dmGFRA1 and *GFRA1* mRNA levels, we first analyzed the demethylation status of *GFRA1* CpG islands in a set of cancer cell lines ($n = 20$). The peak for dmGFRA1 products was detected in seven cell lines (GES1, HEK293T, PC3, MCF7, A549, and HepG2) using the DHPLC analysis (Figure 1A). Bisulfite sequencing confirmed the DHPLC results (Figure 1B). High levels of *GFRA1* mRNA were detected in five dmGFRA-positive cell lines but not in 15 dmGFRA1-negative cell lines (including the four CC cell lines Colo205, HCT116, RKO, and SW480) ($P < 0.001$, Figure 1C). Correlation analysis showed that the dmGFRA1 proportion was positively and significantly correlated with the *GFRA1* mRNA levels in these cell lines (Spearman's test, $R = + 0.33$, $P = 0.041$, Figure 1D). This was confirmed by bioinformatics analysis using TCGA demethylation and expression datasets for 267 CC patients: Higher levels of *GFRA1* mRNA were detected in dmGFRA1-high CC samples than in dmGFRA1-low CC samples ($P = 0.005$, Figure S1).

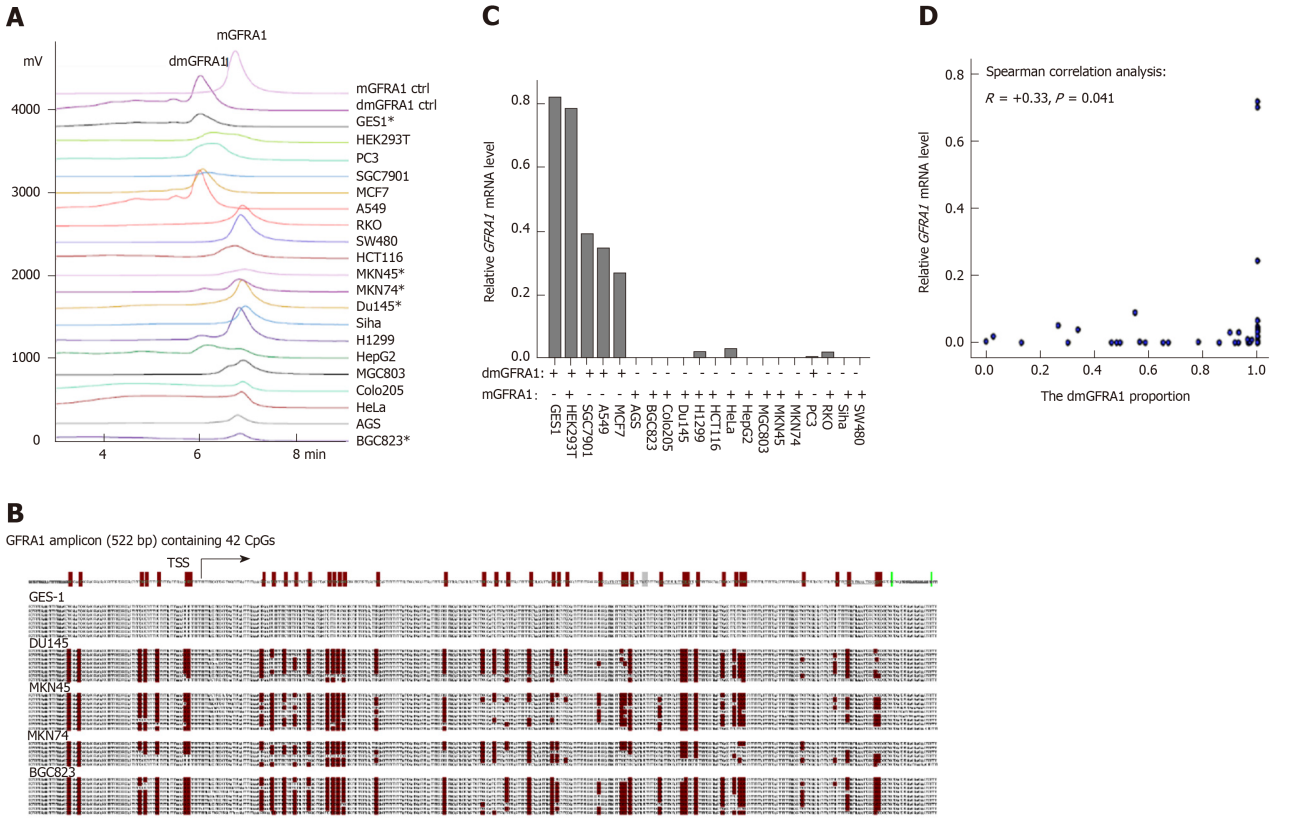

Figure 1 Demethylation and expression status of the *GFRA1* gene in human cancer cell lines. A: Chromatograms of methylated and demethylated *GFRA1* (mGFRA1 and dmGFRA1) PCR products for 20 cell lines using denaturing high performance liquid chromatography. Blood DNA with and without *M.sssI* methylation was used as mGFRA1 and dmGFRA1 controls, respectively; B: The results of bisulfate sequencing for four representative cell lines containing only dmGFRA1 alleles or mGFRA1 alleles. Each line represents one clone; each red dot represents one methylated CpG site. The *GFRA1* amplicon containing 42 CpG sites is also displayed at the top; C: Comparison of relative *GFRA1* mRNA levels in 20 cell lines with different demethylation statuses; D: Dot chart for correlation between the levels of dmGFRA1 and *GFRA1* mRNA in these cell lines.

Then, a MethyLight assay established by us was used to determine the dmGFRA1 proportion in tissue samples. Compared with that in the normal colon biopsies from noncancer patients (n = 21), the dmGFRA1 peak area proportion in CC and SM samples from inpatients (n = 97) was significantly increased (median: 35.9% *vs* 68.4% *vs* 73.4%; Mann-Whitney U-test, P = 0.001 and < 0.001, Figure 2A). The DHPLC results were confirmed by MethyLight analysis (Pearson correlation: R = + 0.676, P < 0.001, Figure 2B). Bisulfite-sequencing confirmed these results of five representative CC samples (Figure S2). The mRNA and protein levels of the *GFRA1* gene were significantly higher in the representative SM samples than in the normal biopsies (Figure 2C and 2D). Interestingly, the dmGFRA1, mRNA, and protein levels for the *GFRA1* gene in the SM samples were slightly higher than those in the CC samples. According to the publicly available human protein atlas database[30], relative to the normal colon mucosa, GFRA1 protein was mainly increased in the cytoplasm of stromal cells in immunohistochemical staining analysis (Figure S3). These results indicate that dmGFRA1 is a prevalent event in CC development and is associated with increased gene expression.

GFRA1 demethylation correlates with increased metastasis risk of CC and decreased OS

To study the impact of dmGFRA1 on metastasis of CC, CC and paired SM tissue samples from total 144 inpatients were included in this study. Higher dmGFRA1 levels (by MethyLight) were detected in poorly differentiated CC tissues than in moderately or well-differentiated CC tissues (Mann-Whitney U-test, P < 0.001, Table S2). To better demonstrate the demethylation difference for the *GFRA1* gene between CC patients with different clinicopathological characteristics and to characterize survival factors, we further subclassified these patients into dmGFRA1-high and dmGFRA1-low groups using the median dmGFRA1 proportion as the cutoff value. The proportion of dmGFRA1-high samples remained significantly higher in the poorly differentiated CC samples than in the moderately or well-differentiated CC samples (92.3% *vs* 45.8%, Chi-square test, P = 0.002, Table 1). Most importantly, the

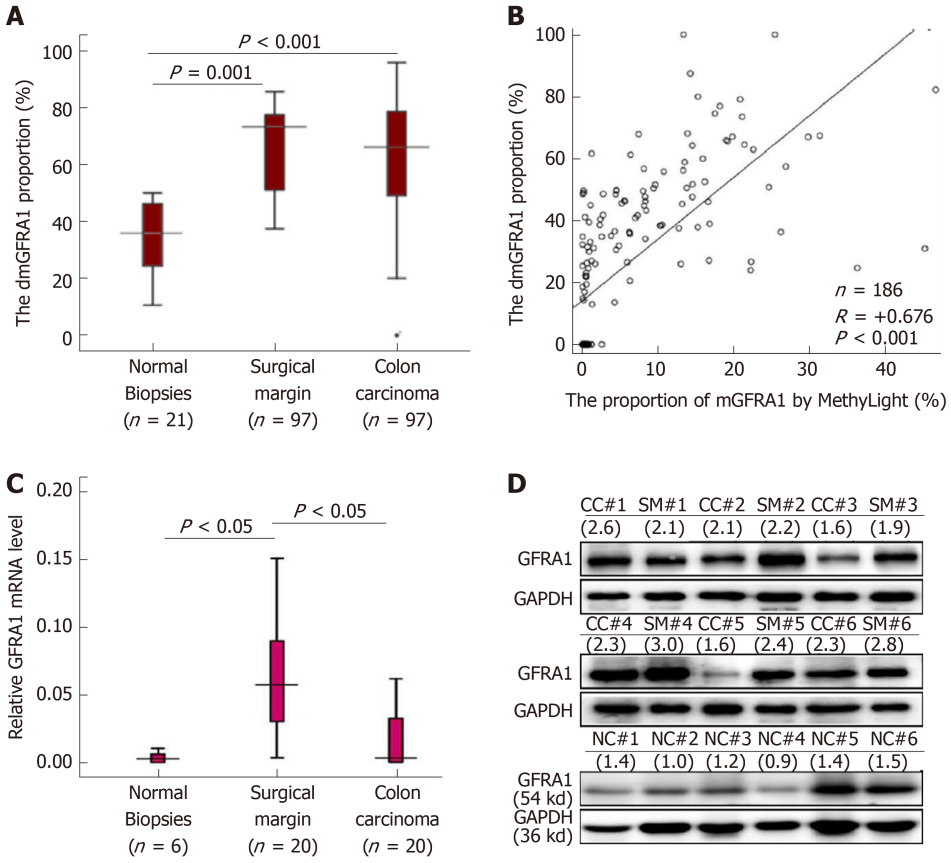

Figure 2 Demethylation and expression status of the *GFRA1* gene in colon carcinoma. A: The demethylated *GFRA1* (dmGFRA1) peak area proportions in normal colon mucosal biopsies from noncancer patients (n = 21) as well as CC and SM samples from inpatients (n = 97) based on MethyLight analysis; B: Correlation analysis of the methylated *GFRA1* (mGFRA1) levels in colon cancer and paired surgical margin tissue samples from 93 patients by denaturing high performance liquid chromatography and MethyLight; C: *GFRA1* mRNA levels in representative colon tissue samples with different pathological lesions by qRT-PCR analysis; D: GFRA1 protein levels in the representative colon tissue samples with different pathological lesions based on Western blot analysis. The density ratio of GFRA1 to GAPDH is listed below each sample id. Note: The mGFRA1 peak area proportion (%) = 100%-the dmGFRA1 peak area proportion (%). dmGFRA1: Demethylated *GFRA1*; mGFRA1: Methylated *GFRA1*.

proportion of dmGFRA1-high samples was significantly higher in CC tissues with distant metastasis than in those without (P = 0.021, Table 1). A similar difference was also found between CC tissues with and without lymphatic metastasis (P = 0.134). This suggests that *GFRA1* reactivation by DNA demethylation may favor CC metastasis.

Kaplan-Meier survival analysis showed that patients with dmGFRA1-high CC had a shorter OS than patients with dmGFRA1-low CC (log-rank test, P = 0.038, Figure 3A). Multivariate analysis showed that dmGFRA1-low CC was an independent favor survival factor after adjustment for age, sex, CC location, differentiation, presence of vascular embolus, local invasion, and metastasis [adjusted hazard ratio (HR) = 0.49, 95% confidence interval (CI): 0.24-0.98, P = 0.044, Table 2]. Notably, sub-stratification analysis revealed that dmGFRA1-low CC was also a significant factor for good OS in 89 CC patients with distant or lymphatic metastasis (log-rank test, P = 0.035, Figure 3B; adjusted HR = 0.41, 95%CI: 0.18-0.91, P = 0.029, Table 2).

These data were confirmed by the analysis results using TCGA datasets. Higher levels of *GFRA1* mRNA were detected in CC samples with vascular embolus than in those without (Mann-Whitney U-test P = 0.039, Table S3). The proportion of samples with high *GFRA1* expression was also slightly higher in CC tissues with distant metastasis than in those without (59.4% *vs* 47.5%, Chi-square test, P = 0.080). Kaplan-Meier survival analysis indicated that patients with dmGFRA1-high and *GFRA1* expression-high CC had a shorter OS than patients with dmGFRA1-low and *GFRA1* expression-low CC, but this difference was not statistically significant (Figure S4). Moreover, patients with *GFRA1* expression-high CC had a shorter OS than patients with *GFRA1* expression-low CC among the 350 CC patients in TCGA (P < 0.005; HR = 2.95, 95%CI: 1.26-4.17, Figure S5).

GFRA1 overexpression promotes the proliferation of CC cells in vitro

GFRA1b is the main *GFRA1* mRNA isoform in gastrointestinal cancers[25]. To study the

Table 1 Comparison of *GFRA1* demethylation-high proportion by MethyLight for colon carcinoma tissues from 144 patients with various clinicopathological characteristics

		dmGFRA1[1]-high cases	dmGFRA1-low cases	dmGFRA1-high proportion (%)	*P* value[1]
Age (yr)	< 60	35	25	58.3	0.091
	≥ 60	37	47	44.0	
Sex	Male	42	46	47.7	0.494
	Female	30	26	53.6	
Location	Sigmoid	33	40	45.2	0.243
	Others	39	32	54.9	
Differentiation	Poor	12	1	92.3	0.002[2]
	Moderate/well	62	69	45.8	
Vascular embolus	Negative	58	65	47.2	0.098
	Positive	14	7	66.7	
pTNM stage	I/II	33	39	45.8	0.314
	III/IV	38	32	54.3	
Local invasion	T1-2	5	6	45.5	
	T3	44	27	62.0	0.004[3]
	T4	22	38	36.7	
Lymphatic metastasis	N0	32	41	43.8	0.134
	N1-3	40	31	56.3	
Distant metastasis	M0	58	68	46.0	0.021[2]
	M1	14	4	77.8	

[1]Chi-square test;
[2]Fisher's exact test;
[3]T3 *vs* T4; dmGFRA1: Demethylation *GFRA1*.

effect of *GFRA1b* on the proliferation and migration of CC cells, we stably transfected RKO and HCT116 cells with human *GFRA1b*-encoding lentiviral vectors (Figure 4A). The effects of *GFRA1b* on biological behaviors of cells were examined using a long-term dynamic observation platform (IncuCyte). The results showed that the proliferation of RKO and HCT116 cells was significantly increased by *GFRA1b* overexpression (Figure 4B). Although *GFRA1b* overexpression did not affect the migration of these cells based on wound-healing analysis (Figure 4C), however, it promoted the invasion of both cell lines (Figure 4D). Because the *GFRA1* gene is silenced by DNA methylation in any of the tested CC cell lines (SW480, Colo205, HCT116, and RKO; Figure 1A and 1B), we did not study the effect of downregulation of *GFRA1* expression on the biological behavior of CC cells.

GFRA1 overexpression promotes the growth of human CC cells in nude mice

To further investigate whether *GFRA1b* overexpression could promote the growth of CC cells *in vivo*, we subcutaneously injected RKO cells stably transfected with the *GFRA1b* or empty control vector into the bilateral inguinal regions of female BALB/c mice (eight mice per group). Tumor establishment was observed in all eight mice injected with *GFRA1b*-expressing RKO cells but in only four of eight mice injected with RKO cells without *GFRA1b* expression on the 29th day post-transplantation (Figure 5A). The average tumor weight in the *GFRA1b*-expressing group was significantly higher than that in the control group (median, 0.518 g *vs* 0.161 g, P = 0.036) (Figure 5B). The GFRA1 protein was detected at a high level in a representative tumor from the *GFRA1b*-expressing group using the Western blot analysis (Figure 5C).

GFRA1 overexpression increases the phosphorylation of ERK and AKT proteins

To explore the effect of *GFRA1b* overexpression on GDNF-GFRA1 downstream signaling pathways in CC cells, we analyzed the phosphorylation status of ERK and AKT proteins, two important molecules in the classic GDNF-GFRA1 downstream pathways (Figure 6A) in RKO and HCT116 cells with and without *GFRA1b* overexpression. The results of Western blot analysis showed that the phosphorylation levels of ERK and AKT proteins (p-AKT and p-ERK) in the GFRA1b-expressing cells were higher than those in the control cells, although the total amounts of AKT and ERK proteins were not changed in either cell line (Figure 6B). This suggests that

Table 2 Results of multivariate analysis for survival factors in colon cancer patients

	All patients (*n* = 144)		Patients with metastatic CC (*n* = 89)	
	Adjusted HR (95%CI)	*P* value	Adjusted HR (95%CI)	*P* value
Low dmGFRA1	0.49 (0.24-0.98)	0.044	0.41 (0.18-0.91)	0.029
Age	1.68 (0.83-3.40)	0.147	1.69 (0.77-3.73)	0.191
Sex	1.45 (0.76-2.76)	0.256	1.44 (0.71-2.91)	0.317
Location	2.60 (1.32-5.14)	0.006	3.22 (1.48-7.01)	0.003
Differentiation	1.95 (0.65-5.89)	0.235	2.02 (0.62-6.61)	0.246
Vascular embolus	0.32 (0.15-0.68)	0.003	0.33 (0.15-0.74)	0.007
Local invasion	1.27 (0.71-2.28)	0.421	1.16 (0.60-2.24)	0.668
Metastasis	4.92 (2.04-11.84)	0.000		

CC: Colon cancer; HR: Hazard ratio; CI: Confidence interval.

overexpression of *GFRA1b* could increase the phosphorylation levels of ERK and AKT proteins, indicating activation of the GDNF-GFRA1 downstream pathways in CC cells.

DISCUSSION

Key results

GDNF-GFRA1 binding can induce phosphorylation of the RET protein and subsequently activate SRC, MAPK, AKT, Rho, and other downstream signaling pathways to regulate cell survival, differentiation, proliferation, and migration[5-8]. GFRA1 is overexpressed in a variety of cancers and promotes cancer cell proliferation and migration[9-17]. In our recent studies, we consistently found that the *GFRA1* gene was abnormally reactivated by TSS-CGI demethylation in gastric carcinomas and this alteration could be used as a biomarker for the prediction of metastasis of gastric carcinoma and OS in Chinese, Japan, and Korean patients in both cross section and prospective cohorts[22,23]. In the present study, we further report that demethylation of *GFRA1* TSS-CGIs was a frequent event during CC development and that high dmGFRA1 level could significantly increase the metastasis risk of CC and decrease the OS of patients with metastatic CC, probably by activating the GDNF-GFRA1-RET-RAS pathways.

GDNF-GFRA1 determines enteric neuron number by controlling precursor proliferation[31,32]. Dysfunction and downregulation of the *GFRA1* gene can trigger neuronal death in the colon and cause Hirschsprung's disease[33,34]. As a growth factor, the GFRA1 protein also promotes the proliferation and perineural invasion of pancreatic, breast, and bile duct cancer cells[12,16,35]. We found that *GFRA1* reactivation by TSS-CGI demethylation was associated with increased CC metastasis risk and decreased OS in patients with metastatic CC, and that *GFRA1b* overexpression promoted the growth of CC cells and enhanced the phosphorylation levels of the AKT and ERK1/2 proteins. These results suggest that *GFRA1* reactivation by DNA demethylation may enhance CC metastasis. Anti-GFRA1 antibody-drug conjugates are under development[20,21]. It is worth studying whether the CC membrane protein GFRA1 may serve as a molecular target for the intervention of CC metastasis using these anti-GFRA1 antibody agents in the future.

Generally, both TSS-CGI methylation and mRNA and protein levels are used to represent the expression states of target genes. It is well recognized that the methylation status of TSS-CGIs is epigenetically maintained in adult human cells and that changes in DNA methylation are more stable than mRNA and protein alterations. TSS-CGI methylation or demethylation changes in a small proportion of the cell population can be very sensitively detected. Thus, DNA methylation alterations may be optimal cancer biomarkers[36]. We previously reported that analysis of the GFRA1 protein in gastric carcinomas from 40 patients in a tissue microarray by immunohistochemical staining failed to demonstrate a statistically significant association of the GFRA1 protein level with clinicopathological parameters and patient OS[22]. By mining the TCGA dataset, we observed that the *GFRA1* mRNA level (by cDNA array) was significantly higher in the dmGFRA1-high CC samples (by 450K array) than in the dmGFRA1-low samples (Figure S1) and that high *GFRA1* expression was also a significant factor for poor survival in CC patients (*n* = 350, Fig-

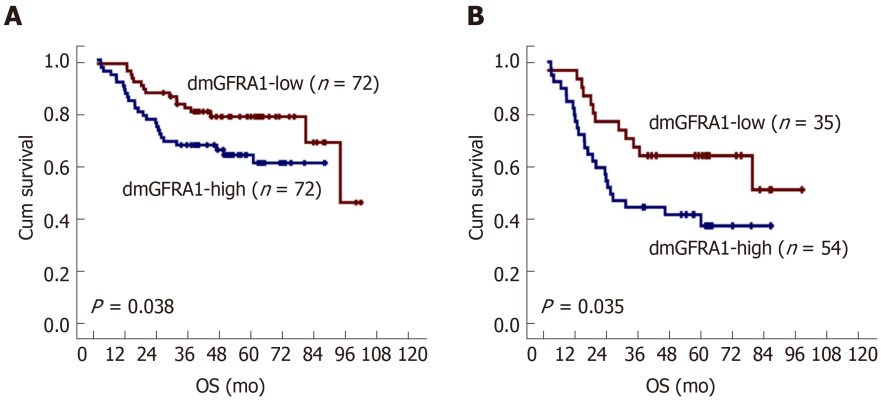

Figure 3 Kaplan-Meier overall survival curves for patient groups with demethylated *GFRA1*-high and demethylated *GFRA1*-low colon cancer. A: For 144 patients; B: For 89 patients with local or distant metastasis. The median *GFRA1* demethylation value by MethyLight was used as the cutoff to define demethylated *GFRA1* (dmGFRA1)-high and dmGFRA1-low samples. The *P* value in the log-rank test is also labeled. dmGFRA1: Demethylated *GFRA1*.

ure S5). While fresh/frozen tissue samples should be used to detect the mRNA level of genes, both fresh and paraffin-fixed tissue samples are suitable for methylation analysis of target CpG islands. Interestingly, significant associations of dmGFRA1 (by MethyLight) with CC differentiation, distant metastasis, and OS were successfully demonstrated among 144 patients, implying that dmGFRA1 is a good biomarker.

In the present study, we also found that the upregulation of *GFRA1b*, the main GFRA1 mRNA isoform in CC tissues, could promote the proliferation or growth of HCT116 and RKO cells *in vitro* and *in vivo*. The increased levels of GDNF-GFRA1 downstream phosphoproteins, p-AKT and p-ERK1/2, in *GFRA1b*-expressing HCT116 and RKO cells indicate that activation of the MAPK signaling pathways by the GFRA1 protein may contribute to the enhancement of proliferation in CC cells.

Strengths and weaknesses of the study

Compared to other studies, our study is the only one that focused on correlation between the dmGFRA1 level and CC metastasis. One of the limitations of our study is that we did not interfere with the expression of *GFRA1* to observe changes of biological behavior by downregulation of *GFRA1* expression, because none of tested colon cell lines highly express GFRA1. Effect of *GFRA1* reactivation by dmGFRA1 on CC metastasis should be confirmed in animal models.

In addition, it was reported that, in addition to CpG methylation, non-CpG methylation was also correlated with gene expression and prognosis of diseases[37-39]. Non-CpG demethylation (or hypomethylation) changes in the *GFRA1* gene was not analyzed in the present study.

Future developments

In this study, we found that DNA demethylation of *GFRA1* TSS-CGIs was associated with the reactivation of gene expression, CC metastasis, and OS of patients. High dmGFRA1 level is a potential biomarker for predicting the prognosis of patients with metastatic CC. A prospective study is expected to confirm our present findings. In addition, it is worth further studying whether dysfunctions of the GFRA1 protein by antibody could prevent metastasis in CC patients.

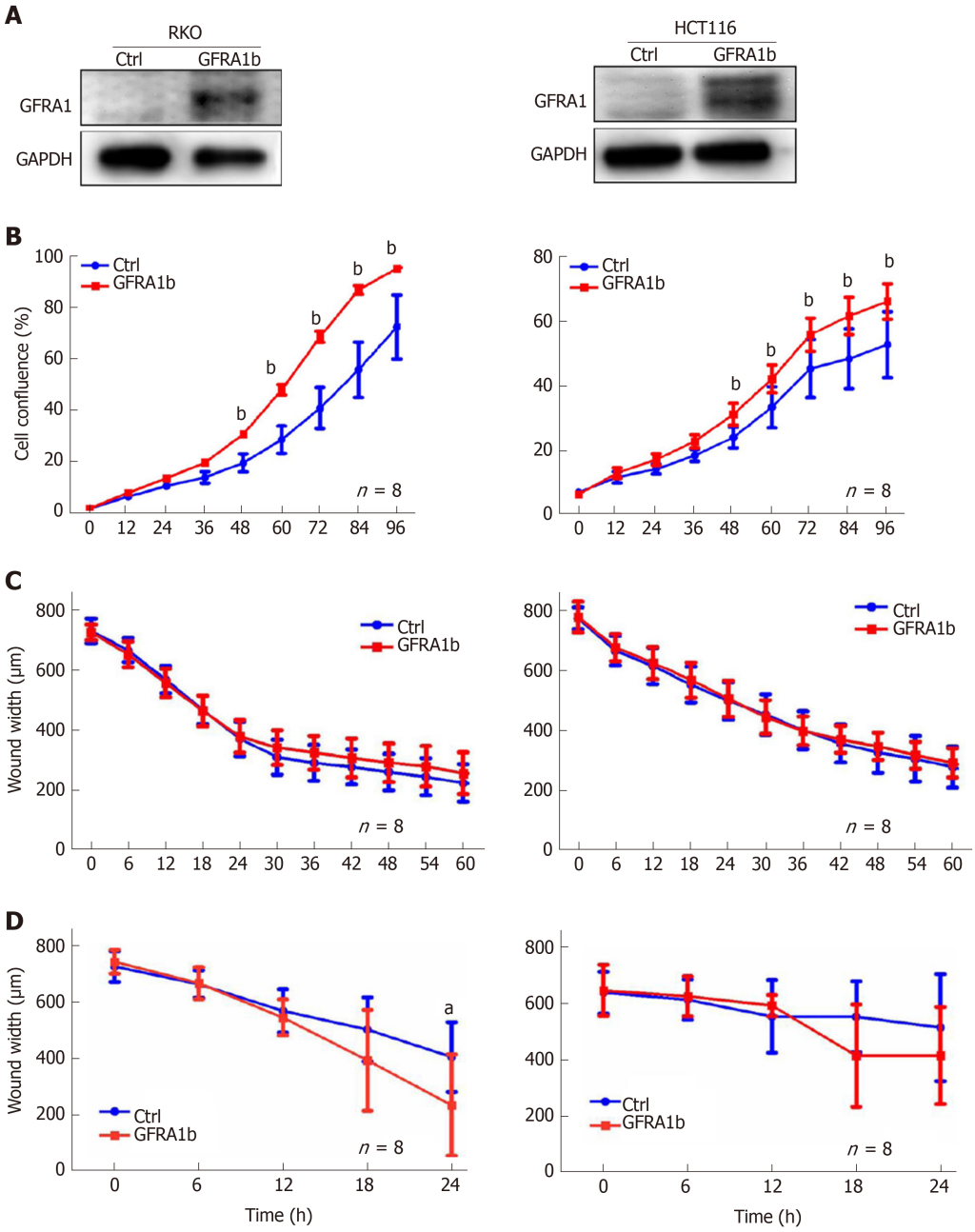

Figure 4 ***GFRA1b*** **overexpression promotes the proliferation of colon cancer cells** ***in vitro.*** A: *GFRA1* expression status in RKO and HCT116 cells transfected with the pLenti-empty control vector or pLenti-*GFRA1b* vector, determined by Western blot; B: Proliferation curves for RKO and HCT116 cells, determined using the IncuCyte systems; C: Migration curves for RKO and HCT116, determined using the IncuCyte systems. Error bars represent S.D.; $^{b}P < 0.01$; D: Invasion curves for RKO and HCT116, determined using the IncuCyte systems. Error bars represent S.D.; $^{a}P < 0.05$. Ctrl: Control.

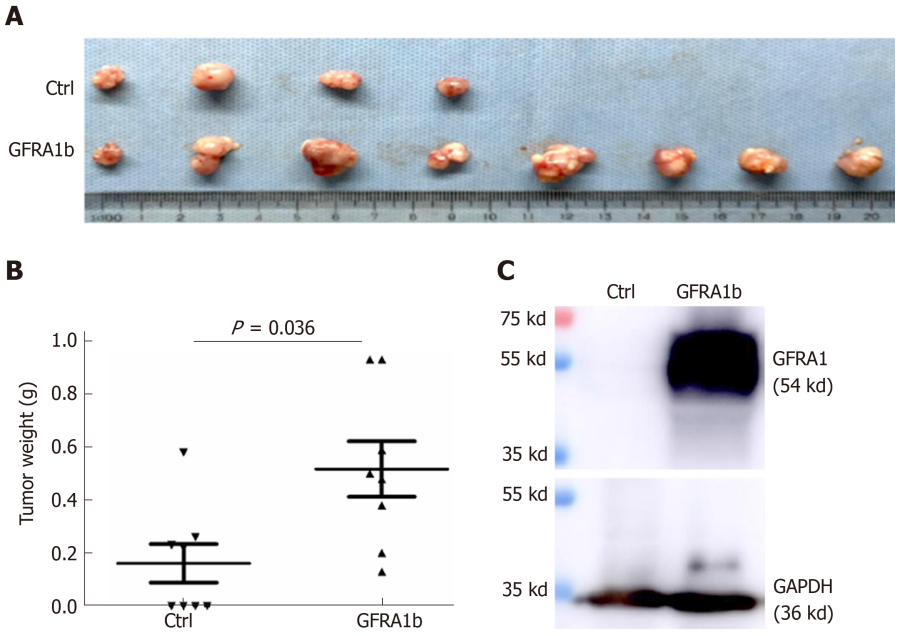

Figure 5 Overexpression of *GFRA1b* promotes the growth of RKO colon cancer cells in nude mice. A: Xenograft tumors in the *GFRA1b*-expressing and negative control (Ctrl) groups on the 29th day post-transplantation. Four mice in the control group did not develop tumors; B: Comparison of the tumor weight in the *GFRA1b*-expressing and negative control groups (0.518 g *vs* 0.161 g; Mann-Whitney *U*-test, *P* = 0.036); C: Expression status of the GFRA1 protein in one representative tumor from the *GFRA1b*-expressing and negative control groups by Western blot. Ctrl: Control.

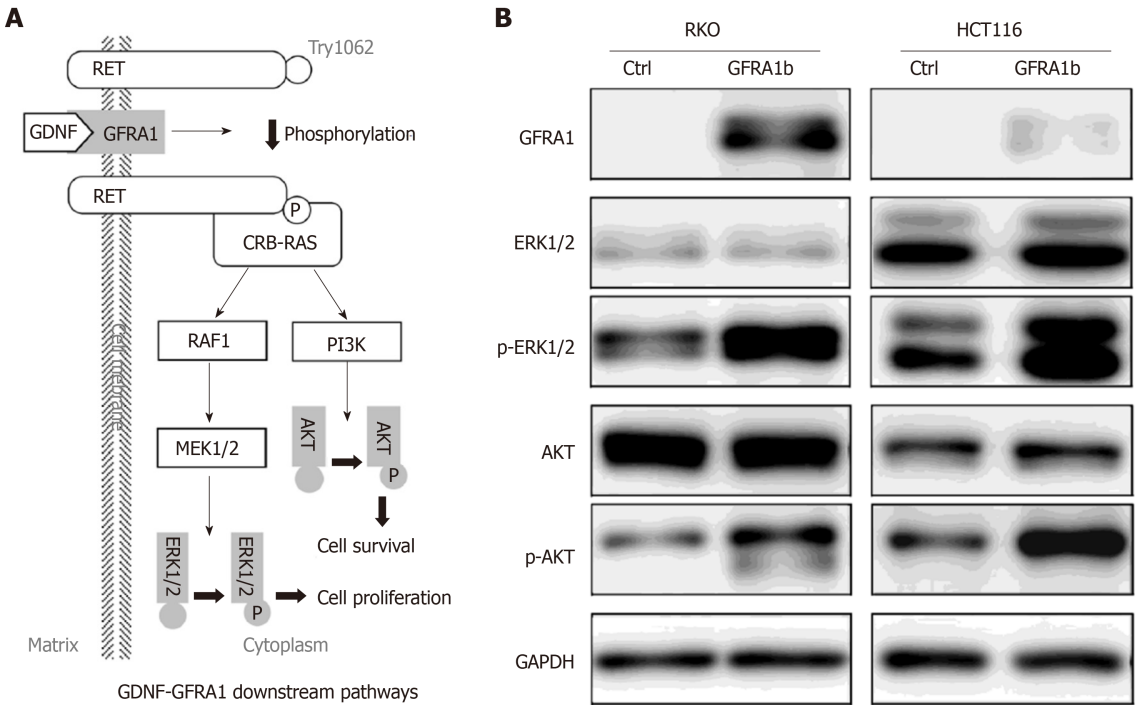

Figure 6 Effect of *GFRA1b* overexpression on the phosphorylation and expression levels of AKT and ERK proteins in colon cancer cells. A: GDNF-GFRA1-related downstream RET-RAS-PI3K-AKT and RET-RAS-RAF1-MEK1/2-ERK1/2 signaling pathways[6-8]; B: Phosphorylation and expression levels of AKT and ERK proteins in RKO and HCT116 cells with and without *GFRA1* overexpression by Western blot. p-AKT and p-ERK represent phosphorylated AKT and ERK proteins, respectively.

ARTICLE HIGHLIGHTS

Research background

The membrane receptor protein GFRA1 is normally expressed in neural cells in many organs, including the colon. The *GFRA1* gene is abnormally and frequently expressed in cancer cells. Anti-GFRA1 autoantibodies can be detected in patients with breast cancer. Several preclinical

anti-GFRA1 antibody-drug conjugates for breast cancer treatment have been developed.

Research motivation
Recently, we reported that the *GFRA1* gene is reactivated by DNA demethylation in gastric cancer, which could be used to predict cancer metastasis. Because *GFRA1* is normally expressed in neural cells in the colon, it is interesting to study whether *GFRA1* reactivation by DNA demethylation is associated with colon cancer (CC) progression and can be used as a therapy target.

Research objectives
To study whether abnormal *GFRA1* demethylation is a driver for CC metastasis and the membrane protein GFRA1 is a potential therapeutic target.

Research methods
CC tissues from 144 patients were included in this study. The level of *GFRA1* demethylation was analyzed by quantitative methylation-specific PCR and bisulfite-sequencing. A set of *in vitro* and *in vivo* experimental assays were used to evaluate the effect of abnormal *GFRA1* expression on CC development.

Research results
The level of *GFRA1* demethylated alleles was significantly increased during CC development and positively associated with poor CC differentiation, distant CC metastasis, and short OS of CC patients. *GFRA1* overexpression significantly promoted CC cell proliferation and invasion *in vitro* and CC growth in nude mice.

Research conclusions
GFRA1 is frequently reactivated by DNA demethylation in CC tissues. *GFRA1* demethylation may be a driver for CC development. GFRA1 protein might be a therapeutic target for CC patients, especially those with metastatic potential.

Research perspectives
A prospective study is expected to confirm our present findings. It is worth further studying whether dysfunctions of the GFRA1 protein by antibody could prevent CC metastasis.

REFERENCES

1 **Mercier J**, Voutsadakis IA. A Systematic Review and Meta-analysis of Retrospective Series of Regorafenib for Treatment of Metastatic Colorectal Cancer. *Anticancer Res* 2017; **37**: 5925-5934 [PMID: 29061771 DOI: 10.21873/anticanres.12039]
2 **Ferlay J**, Colombet M, Soerjomataram I, Mathers C, Parkin DM, Piñeros M, Znaor A, Bray F. Estimating the global cancer incidence and mortality in 2018: GLOBOCAN sources and methods. *Int J Cancer* 2019; **144**: 1941-1953 [PMID: 30350310 DOI: 10.1002/ijc.31937]
3 **Liu X**, Ji Q, Fan Z, Li Q. Cellular signaling pathways implicated in metastasis of colorectal cancer and the associated targeted agents. *Future Oncol* 2015; **11**: 2911-2922 [PMID: 26414153 DOI: 10.2217/fon.15.235]
4 **Liu E**, Kinnebrew G, Li J, Zhang P, Zhang Y, Cheng L, Li L. A Fast and Furious Bayesian Network and Its Application of Identifying Colon Cancer to Liver Metastasis Gene Regulatory Networks. *IEEE/ACM Trans Comput Biol Bioinform* 2019 [PMID: 31581091 DOI: 10.1109/TCBB.2019.2944826]
5 **Cacalano G**, Fariñas I, Wang LC, Hagler K, Forgie A, Moore M, Armanini M, Phillips H, Ryan AM, Reichardt LF, Hynes M, Davies A, Rosenthal A. GFRalpha1 is an essential receptor component for GDNF in the developing nervous system and kidney. *Neuron* 1998; **21**: 53-62 [PMID: 9697851 DOI: 10.1016/s0896-6273(00)80514-0]
6 **Airaksinen MS**, Saarma M. The GDNF family: signalling, biological functions and therapeutic value. *Nat Rev Neurosci* 2002; **3**: 383-394 [PMID: 11988777 DOI: 10.1038/nrn812]
7 **Charlet-Berguerand N**, Le Hir H, Incoronato M, di Porzio U, Yu Y, Jing S, de Franciscis V, Thermes C. Expression of GFRalpha1 receptor splicing variants with different biochemical properties is modulated during kidney development. *Cell Signal* 2004; **16**: 1425-1434 [PMID: 15381258 DOI: 10.1016/j.cellsig.2004.05.006]
8 **Parkash V**, Leppänen VM, Virtanen H, Jurvansuu JM, Bespalov MM, Sidorova YA, Runeberg-Roos P, Saarma M, Goldman A. The structure of the glial cell line-derived neurotrophic factor-coreceptor complex: insights into RET signaling and heparin binding. *J Biol Chem* 2008; **283**: 35164-35172 [PMID: 18845535 DOI: 10.1074/jbc.M802543200]
9 **He R**, Liu P, Xie X, Zhou Y, Liao Q, Xiong W, Li X, Li G, Zeng Z, Tang H. circGFRA1 and GFRA1 act as ceRNAs in triple negative breast cancer by regulating miR-34a. *J Exp Clin Cancer Res* 2017; **36**: 145 [PMID: 29037220 DOI: 10.1186/s13046-017-0614-1]
10 **Fan TC**, Yeo HL, Hsu HM, Yu JC, Ho MY, Lin WD, Chang NC, Yu J, Yu AL. Reciprocal feedback regulation of ST3GAL1 and GFRA1 signaling in breast cancer cells. *Cancer Lett* 2018; **434**: 184-195 [PMID: 30040982 DOI: 10.1016/j.canlet.2018.07.026]
11 **Cavel O**, Shomron O, Shabtay A, Vital J, Trejo-Leider L, Weizman N, Krelin Y, Fong Y, Wong RJ, Amit M, Gil Z. Endoneurial macrophages induce perineural invasion of pancreatic cancer cells by secretion of GDNF and activation of RET tyrosine kinase receptor. *Cancer Res* 2012; **72**: 5733-5743 [PMID: 22971345 DOI: 10.1158/0008-5472.CAN-12-0764]
12 **Gil Z**, Cavel O, Kelly K, Brader P, Rein A, Gao SP, Carlson DL, Shah JP, Fong Y, Wong RJ. Paracrine regulation of pancreatic cancer cell invasion by peripheral nerves. *J Natl Cancer Inst* 2010; **102**: 107-118 [PMID: 20068194 DOI: 10.1093/jnci/djp456]
13 **Borrego S**, Fernández RM, Dziema H, Japón MA, Marcos I, Eng C, Antiñolo G. Evaluation of germline

sequence variants of GFRA1, GFRA2, and GFRA3 genes in a cohort of Spanish patients with sporadic medullary thyroid cancer. *Thyroid* 2002; **12**: 1017-1022 [PMID: 12490080 DOI: 10.1089/105072502320908367]
14 **Frisk T**, Farnebo F, Zedenius J, Grimelius L, Höög A, Wallin G, Larsson C. Expression of RET and its ligand complexes, GDNF/GFRalpha-1 and NTN/GFRalpha-2, in medullary thyroid carcinomas. *Eur J Endocrinol* 2000; **142**: 643-649 [PMID: 10822229 DOI: 10.1530/eje.0.1420643]
15 **Wiesenhofer B**, Stockhammer G, Kostron H, Maier H, Hinterhuber H, Humpel C. Glial cell line-derived neurotrophic factor (GDNF) and its receptor (GFR-alpha 1) are strongly expressed in human gliomas. *Acta Neuropathol* 2000; **99**: 131-137 [PMID: 10672319 DOI: 10.1007/pl00007416]
16 **Wu ZS**, Pandey V, Wu WY, Ye S, Zhu T, Lobie PE. Prognostic significance of the expression of GFRα1, GFRα3 and syndecan-3, proteins binding ARTEMIN, in mammary carcinoma. *BMC Cancer* 2013; **13**: 34 [PMID: 23351331 DOI: 10.1186/1471-2407-13-34]
17 **He S**, Chen CH, Chernichenko N, He S, Bakst RL, Barajas F, Deborde S, Allen PJ, Vakiani E, Yu Z, Wong RJ. GFRα1 released by nerves enhances cancer cell perineural invasion through GDNF-RET signaling. *Proc Natl Acad Sci USA* 2014; **111**: E2008-E2017 [PMID: 24778213 DOI: 10.1073/pnas.1402944111]
18 **Evans RL**, Pottala JV, Egland KA. Classifying patients for breast cancer by detection of autoantibodies against a panel of conformation-carrying antigens. *Cancer Prev Res (Phila)* 2014; **7**: 545-555 [PMID: 24641868 DOI: 10.1158/1940-6207.CAPR-13-0416]
19 **Evans RL**, Pottala JV, Nagata S, Egland KA. Longitudinal autoantibody responses against tumor-associated antigens decrease in breast cancer patients according to treatment modality. *BMC Cancer* 2018; **18**: 119 [PMID: 29386014 DOI: 10.1186/s12885-018-4022-5]
20 **Bhakta S**, Crocker LM, Chen Y, Hazen M, Schutten MM, Li D, Kuijl C, Ohri R, Zhong F, Poon KA, Go MAT, Cheng E, Piskol R, Firestein R, Fourie-O'Donohue A, Kozak KR, Raab H, Hongo JA, Sampath D, Dennis MS, Scheller RH, Polakis P, Junutula JR. An Anti-GDNF Family Receptor Alpha 1 (GFRA1) Antibody-Drug Conjugate for the Treatment of Hormone Receptor-Positive Breast Cancer. *Mol Cancer Ther* 2018; **17**: 638-649 [PMID: 29282299 DOI: 10.1158/1535-7163.MCT-17-0813]
21 **Bosco EE**, Christie RJ, Carrasco R, Sabol D, Zha J, DaCosta K, Brown L, Kennedy M, Meekin J, Phipps S, Ayriss J, Du Q, Bezabeh B, Chowdhury P, Breen S, Chen C, Reed M, Hinrichs M, Zhong H, Xiao Z, Dixit R, Herbst R, Tice DA. Preclinical evaluation of a GFRA1 targeted antibody-drug conjugate in breast cancer. *Oncotarget* 2018; **9**: 22960-22975 [PMID: 29796165 DOI: 10.18632/oncotarget.25160]
22 **Liu Z**, Zhang J, Gao Y, Pei L, Zhou J, Gu L, Zhang L, Zhu B, Hattori N, Ji J, Yuasa Y, Kim W, Ushijima T, Shi H, Deng D. Large-scale characterization of DNA methylation changes in human gastric carcinomas with and without metastasis. *Clin Cancer Res* 2014; **20**: 4598-4612 [PMID: 25009298 DOI: 10.1158/1078-0432.CCR-13-3380]
23 **Liu Z**, Cheng X, Zhang L, Zhou J, Deng D, Ji J. A panel of DNA methylated markers predicts metastasis of pN_0M_0 gastric carcinoma: a prospective cohort study. *Br J Cancer* 2019; **121**: 529-536 [PMID: 31431673 DOI: 10.1038/s41416-019-0552-0]
24 **Aguirre-Gamboa R**, Gomez-Rueda H, Martínez-Ledesma E, Martínez-Torteya A, Chacolla-Huaringa R, Rodriguez-Barrientos A, Tamez-Peña JG, Treviño V. SurvExpress: an online biomarker validation tool and database for cancer gene expression data using survival analysis. *PLoS One* 2013; **8**: e74250 [PMID: 24066126 DOI: 10.1371/journal.pone.0074250]
25 **Peng XU**, Liu Z, Wei LI, Wang C, Xiaodan HA, Xie J, Zhang J. The mRNA Expression of Different Splice Variants of GFRa1 in Gastric Cancer and Colon Cancer Development Process. Journal of Shihezi University. 2015; 727-731 [DOI: 10.13880/j.cnki.65-1174/n.2015.06.012]
26 **Zheng X**, Zhou J, Zhang B, Zhang J, Wilson J, Gu L, Zhu B, Gu J, Ji J, Deng D. Critical evaluation of Cbx7 downregulation in primary colon carcinomas and its clinical significance in Chinese patients. *BMC Cancer* 2015; **15**: 145 [PMID: 25881303 DOI: 10.1186/s12885-015-1172-6]
27 **Liu Z**, Zhou J, Gu L, Deng D. Significant impact of amount of PCR input templates on various PCR-based DNA methylation analysis and countermeasure. *Oncotarget* 2016; **7**: 56447-56455 [PMID: 27487147 DOI: 10.18632/oncotarget.10906]
28 **Deng D**, Deng G, Smith MF, Zhou J, Xin H, Powell SM, Lu Y. Simultaneous detection of CpG methylation and single nucleotide polymorphism by denaturing high performance liquid chromatography. *Nucleic Acids Res* 2002; **30**: E13 [PMID: 11809901 DOI: 10.1093/nar/30.3.e13]
29 **Tian W**, Du Y, Ma Y, Gu L, Zhou J, Deng D. MALAT1-miR663a negative feedback loop in colon cancer cell functions through direct miRNA-lncRNA binding. *Cell Death Dis* 2018; **9**: 857 [PMID: 30154407 DOI: 10.1038/s41419-018-0925-y]
30 **Uhlén M**, Fagerberg L, Hallström BM, Lindskog C, Oksvold P, Mardinoglu A, Sivertsson Å, Kampf C, Sjöstedt E, Asplund A, Olsson I, Edlund K, Lundberg E, Navani S, Szigyarto CA, Odeberg J, Djureinovic D, Takanen JO, Hober S, Alm T, Edqvist PH, Berling H, Tegel H, Mulder J, Rockberg J, Nilsson P, Schwenk JM, Hamsten M, von Feilitzen K, Forsberg M, Persson L, Johansson F, Zwahlen M, von Heijne G, Nielsen J, Pontén F. Proteomics. Tissue-based map of the human proteome. *Science* 2015; **347**: 1260419 [PMID: 25613900 DOI: 10.1126/science.1260419]
31 **Gianino S**, Grider JR, Cresswell J, Enomoto H, Heuckeroth RO. GDNF availability determines enteric neuron number by controlling precursor proliferation. *Development* 2003; **130**: 2187-2198 [PMID: 12668632 DOI: 10.1242/dev.00433]
32 **Nishiyama C**, Uesaka T, Manabe T, Yonekura Y, Nagasawa T, Newgreen DF, Young HM, Enomoto H. Trans-mesenteric neural crest cells are the principal source of the colonic enteric nervous system. *Nat Neurosci* 2012; **15**: 1211-1218 [PMID: 22902718 DOI: 10.1038/nn.3184]
33 **Uesaka T**, Jain S, Yonemura S, Uchiyama Y, Milbrandt J, Enomoto H. Conditional ablation of GFRalpha1 in postmigratory enteric neurons triggers unconventional neuronal death in the colon and causes a Hirschsprung's disease phenotype. *Development* 2007; **134**: 2171-2181 [PMID: 17507417 DOI: 10.1242/dev.001388]
34 **Camilleri M**, Wieben E, Eckert D, Carlson P, Hurley O'Dwyer R, Gibbons D, Acosta A, Klee EW. Familial chronic megacolon presenting in childhood or adulthood: Seeking the presumed gene association. *Neurogastroenterol Motil* 2019; **31**: e13550 [PMID: 30663199 DOI: 10.1111/nmo.13550]
35 **Iwahashi N**, Nagasaka T, Tezel G, Iwashita T, Asai N, Murakumo Y, Kiuchi K, Sakata K, Nimura Y, Takahashi M. Expression of glial cell line-derived neurotrophic factor correlates with perineural invasion of bile duct carcinoma. *Cancer* 2002; **94**: 167-174 [PMID: 11815973 DOI: 10.1002/cncr.10169]
36 **Deng D**, Liu Z, Du Y. Epigenetic alterations as cancer diagnostic, prognostic, and predictive biomarkers. *Adv Genet* 2010; **71**: 125-176 [PMID: 20933128 DOI: 10.1016/B978-0-12-380864-6.00005-5]

37 **Nicolia V**, Cavallaro RA, López-González I, Maccarrone M, Scarpa S, Ferrer I, Fuso A. DNA Methylation Profiles of Selected Pro-Inflammatory Cytokines in Alzheimer Disease. *J Neuropathol Exp Neurol* 2017; **76**: 27-31 [PMID: 28053004 DOI: 10.1093/jnen/nlw099]

38 **Fuso A**, Ferraguti G, Scarpa S, Ferrer I, Lucarelli M. Disclosing bias in bisulfite assay: MethPrimers underestimate high DNA methylation. *PLoS One* 2015; **10**: e0118318 [PMID: 25692551 DOI: 10.1371/journal.pone.0118318]

39 **Fuso A**, Scarpa S, Grandoni F, Strom R, Lucarelli M. A reassessment of semiquantitative analytical procedures for DNA methylation: comparison of bisulfite- and HpaII polymerase-chain-reaction-based methods. *Anal Biochem* 2006; **350**: 24-31 [PMID: 16445884 DOI: 10.1016/j.ab.2005.12.008]

World Journal of Gastroenterology

Submit a Manuscript: https://www.f6publishing.com

World J Gastroenterol 2020 January 14; 26(2): 199-218

DOI: 10.3748/wjg.v26.i2.199

ISSN 1007-9327 (print) ISSN 2219-2840 (online)

ORIGINAL ARTICLE

Observational Study

Rifaximin improves survival in cirrhotic patients with refractory ascites: A real-world study

Xin-Yue Lv, Hui-Guo Ding, Jun-Fu Zheng, Chun-Lei Fan, Lei Li

ORCID number: Xin-Yue Lv (0000-0003-3553-9412); Hui-Guo Ding (0000-0002-8716-4926); Jun-Fu Zheng (0000-0003-3881-4088); Chun-Lei Fan (0000-0001-7573-6045); Lei Li (0000-0002-0295-9480).

Author contributions: Li L designed the study and performed scientific edits to the manuscript; Lv XY and Ding HG analysed and interpreted the data, and wrote the manuscript; Zheng JF was responsible for the patient follow-up; Lv XY and Fan CL were responsible for data collection.

Supported by the State Key Projects Specialized on Infectious Diseases, No. 2017ZX10203202-004 and No. 2017ZX10203202003008; the Digestive Medical Coordinated Development Centre of the Beijing Municipal Administration of Hospitals, No. XXZ0303; Beijing High-level Health Technicians, No. 2013-03-073; Beijing Municipal Administration of Hospitals' Ascent Plan, No. DFL20151602.

Institutional review board statement: The study protocol conformed to the Declaration of Helsinki and was approved by the Biomedical Research Ethics Committee of Peking University First Hospital.

Informed consent statement: All participants provided written informed consent for using samples and materials prior to study enrollment.

Conflict-of-interest statement: All authors declare no conflict of interest. Additionally, they have substantially contributed to this

Xin-Yue Lv, Hui-Guo Ding, Jun-Fu Zheng, Chun-Lei Fan, Lei Li, Department of Gastroenterology and Hepatology, Beijing You An Hospital, Capital Medical University, Beijing 100069, China

Corresponding author: Lei Li, MD, PhD, Associate Professor, Chief Physician, Department of Gastroenterology and Hepatology, Beijing You An Hospital, Capital Medical University, 8 Xitoutiao, Youanmenwai, Beijing 100069, China. m13699119545@163.com

Abstract

BACKGROUND

Rifaximin has been shown to reduce the incidence of hepatic encephalopathy and other complications in patients with cirrhosis. However, few studies have investigated the effect of rifaximin in cirrhotic patients with refractory ascites.

AIM

To evaluate the effects of rifaximin in the treatment of refractory ascites and to preliminarily explore its possible mechanism.

METHODS

A total of 75 cirrhotic patients with refractory ascites were enrolled in the study (50 in a rifaximin and 25 in a control group). Patients in the rifaximin group were divided into two subgroups according to the presence of spontaneous bacterial peritonitis and treatment with or without other antibiotics (19 patients treated with rifaximin and 31 patients treated with rifaximin plus intravenous antibiotics). All patients received conventional treatment for refractory ascites, while patients in the rifaximin group received oral rifaximin-α 200 mg four times daily for at least 2 wk. The ascites grade, fasting weight, liver and kidney function, and inflammatory factors in the plasma were evaluated before and after treatment. In addition, the gut microbiota was determined by metagenomics sequencing to analyse the changes in the characteristics of the gut microbiota before and after rifaximin treatment. The patients were followed for 6 mo.

RESULTS

Compared with the control group, the fasting weight of patients significantly decreased and the ascites significantly subsided after treatment with rifaximin (P = 0.011 and 0.009, respectively). The 6-mo survival rate of patients in the rifaximin group was significantly higher than that in the control group (P = 0.048). The concentration of interferon-inducible protein 10 decreased significantly in the rifaximin group compared with that in the control group (P = 0.024). The abundance of *Roseburia*, *Haemophilus*, and *Prevotella* was significantly reduced after rifaximin treatment, while the abundance of

current study and approved the content of the manuscript.

Data sharing statement: No additional data are available.

STROBE statement: The authors have read the STROBE Statement-checklist of items, and the manuscript was prepared and revised according to the STROBE Statement-checklist of item.

Manuscript source: Unsolicited manuscript

Received: October 18, 2019
Peer-review started: October 18, 2019
First decision: November 22, 2019
Revised: December 6, 2019
Accepted: December 21, 2019
Article in press: December 21, 2019
Published online: January 14, 2020

P-Reviewer: Kamimura K, Ridola L
S-Editor: Tang JZ
L-Editor: Wang TQ
E-Editor: Ma YJ

Lachnospiraceae_noname, *Subdoligranulum*, and *Dorea* decreased and the abundance of *Coprobacillus* increased after treatment with rifaximin plus intravenous antibiotics. The gene expression of virulence factors was significantly reduced after treatment in both subgroups treated with rifaximin or rifaximin plus intravenous antibiotics.

CONCLUSION
Rifaximin mitigates ascites and improves survival of cirrhotic patients with refractory ascites. A possible mechanism is that rifaximin regulates the structure and function of intestinal bacteria, thus improving the systemic inflammatory state.

Key words: Rifaximin; Cirrhosis; Refractory ascites; Inflammatory factors; Gut microbiota; Metagenomics sequencing

Core tip: This study showed that the unabsorbed antibiotics, rifaximin, mitigates ascites and improves the survival of cirrhotic patients with refractory ascites and the possible mechanism is that rifaximin regulates the structure and function of intestinal bacteria, thus improving the systemic inflammatory state.

Citation: Lv XY, Ding HG, Zheng JF, Fan CL, Li L. Rifaximin improves survival in cirrhotic patients with refractory ascites: A real-world study. *World J Gastroenterol* 2020; 26(2): 199-218
URL: https://www.wjgnet.com/1007-9327/full/v26/i2/199.htm
DOI: https://dx.doi.org/10.3748/wjg.v26.i2.199

INTRODUCTION

Patients with refractory ascites have a poor prognosis, with a 6-mo survival rate of 50%[1]. Current management methods include limited intake of sodium, adequate diuretics plus albumin, large-volume paracentesis, and transjugular intrahepatic portosystemic shunt. Liver transplantation (LT) is the only effective strategy to cure cirrhosis and its complications. However, most patients cannot receive LT because of its high cost, the shortage of the donated liver, and many other factors. The role of the gut-liver axis in the occurrence and development of complications of cirrhosis has aroused great attention. Microbiota, dysbiosis, and bacterial translocation (BT) have been shown to be involved in the pathogenesis of cirrhosis. Bacteria and their products are introduced into blood *via* the intestines and then increase the blood levels of endotoxin and inflammatory factors, which, in turn, accelerate liver fibrosis and stimulate the production of vasodilator substances. These events cause reduced systemic vascular resistance and an activated sympathetic nervous system and renin-angiotensin-aldosterone system (RAAS), eventually leading to hyperdynamic circulation, which plays an important role in the pathogenesis of refractory ascites[2-6].

Rifaximin, a non-absorbable rifamycin derivate, exhibits a high antibiotic activity against both aerobic and anaerobic Gram-positive and -negative micro-organisms[7,8]. Furthermore, rifaximin is hardly absorbed by the intestines because of its pyridine ring added to rifamycin; thus, high concentrations are present in the intestines, making it difficult to induce drug-resistant strains[8,9]. Previous studies have shown that rifaximin treatment can reduce the concentrations of interleukin (IL)-6, tumour necrosis factor alpha (TNF-α), and endotoxin in blood, thus improving systemic haemodynamics and decreasing the hepatic venous pressure gradient in patients with cirrhosis[10-12]. Rifaximin has been demonstrated to exert positive effects in the prevention and treatment of hepatic encephalopathy (HE), and to prevent the development of esophagogastric and gastric variceal bleeding, spontaneous bacterial peritonitis (SBP), and hepatorenal syndrome (HRS)[10,13]. Hence, our study evaluated the clinical efficacy of rifaximin and its effects on intestinal flora characteristics and the systemic inflammatory state in cirrhotic patients with refractory ascites.

MATERIALS AND METHODS

Ethical considerations

The study protocol conformed to the Declaration of Helsinki and was approved by the Biomedical Research Ethics Committee of Peking University First Hospital (No. 2017[1367]). All participants provided written informed consent.

Patients and study design

A total of 143 cirrhotic patients with refractory ascites admitted to the Beijing You An Hospital Affiliated to Capital Medical University were screened between November 2016 and May 2018 and, eventually, 75 patients were enrolled in this real-world study. All the patients received routine treatment for refractory ascites according to *Chinese guidelines on the management of ascites and complications in cirrhosis in 2017*[14]: (1) Bed rest, limited sodium intake (salt intake < 6 g/d), maintenance of the balance of water, electrolytes, and acid-base; (2) Alcohol quitting or antiviral treatment; (3) Intravenous infusion with reduced glutathione 1.2 g/d dissolved in 100 mL of 0.9% sodium chloride injection; (4) Oral furosemide 80 mg/d + spironolactone 160 mg/d; (5) Intravenous infusion with human albumin (Switzerland, CSL Behring) 10-20 g, once per day; and (6) Corresponding antibiotics for patients who met the diagnostic criteria for SBP. Additionally, patients in the rifaximin group received oral rifaximin α (Italy, Alpha Wassermann) 200 mg, four times/d for 3 wk to 4 wk. A 6-mo follow-up was performed after treatment to evaluate the survival once per month.

The primary endpoints were clinical efficacies, including changes in the fasting weight, ascites regression, and survival rate, while the secondary endpoints were changes in liver and kidney function. Ascites regression was evaluated according to the change in the grade of ascites according to the *Chinese guidelines on the management of ascites and complications in cirrhosis in 2017*[14,15]: Markedly effective: Change from grade 3 to grade 1 or from grade 3/2 to none; effective: Change from grade 3 to grade 2 or from grade 2 to grade 1; invalid: Increase or no change after the treatment.

Inclusion and exclusion criteria

The inclusion criteria were as follows: (1) Age ranging 18-80 years; (2) Gender was not limited; (3) Diagnosed with cirrhosis based on cirrhosis imaging findings or endoscopic findings of oesophageal varices; and (4) In line with a cirrhotic refractory ascites diagnosis according to *Chinese guidelines on the management of ascites and complications in cirrhosis in 2017*[14]: (1) Lack of a response (defined as a mean fasting weight loss < 0.8 kg over 4 d) to 1-wk treatment with a diuretic (furosemide 80 mg/d or spironolactone 160 mg/d) and a diuretic plus antibiotic (SBP), or the reappearance of grade 2/3 ascites within 4 wk of therapy with large-volume paracentesis combined with a human serum albumin level of 10-20 g/d; or (2) The appearance of diuretic-related complications such as HE, serum creatinine > 2.0 mg/dL, serum sodium < 125 mmol/L, or serum potassium > 6.0 mmol/L. The exclusion criteria were as follows: (1) HE grades 2-4 according to the West Haven diagnostic criteria[16]; (2) Upper gastrointestinal bleeding within 1 wk before enrolment; (3) Combined with other gut diseases; (4) Continued abuse of alcohol and/or symptoms of withdrawal; (5) Combined with invasive tumours; and (6) Combined with other serious diseases.

Clinical and laboratory data

The data concerning demographics, clinical history, aetiology and complications of cirrhosis, and comorbidities were collected. The fasting weight (kg) was recorded. The grades of ascites were defined as follows according to the patient's symptoms, signs, and colour Doppler ultrasound: Grade 1: No abdominal distension, shifting dullness (-), ascites (detected by ultrasound) located in multiple gaps with a depth < 3 cm; grade 2: Moderate symmetric abdominal distension, shifting dullness (±), and a depth of 3-10 cm; and grade 3: Significant abdominal distension, or even abdominal distension leading to umbilical hernia, shifting dullness (+), and a depth of > 10 cm[14,15].

Laboratory indicators were collected on day 0 (d0) and day 15 (d15) and included the WBC, HGB, PLT, ALT, AST, TBil, Alb, BUN, Scr, serum K+, Na+, prothrombin activity, and INR. The MDRD formula was used to calculate the estimate glomerular filtration rate (eGFR).

The diagnostic criteria for SBP and acute kidney injury (AKI) were as follows[14,15]: Patients with one or more of the following symptoms, signs, or laboratory abnormalities could be diagnosed with SBP: (1) Abdominal pain, abdominal tenderness or rebound tenderness, and an increase in abdominal muscular tension; (2) Systemic inflammatory response syndrome: Fever or normothermia, chills, tachycardia, and tachypnoea; (3) Deterioration of liver function without an underlying cause; (4) Sudden absence of a response to diuretics or renal failure; (5)

Polymorphonuclear cell count in ascites ≥ 0.25 × 10^9/L; (6) Positive ascites bacterial culture; (7) Serum procalcitonin concentration > 0.5 ng/mL; and (8) Exclusion of infection in other sites. AKI was diagnosed in case of patients with acute renal failure, manifesting as an acute and significant decrease in GFR and Scr > 133 μmol/L.

Measurement of inflammation and endotoxin markers

The concentrations of IL-6, IL-8, TNF-α, monocyte chemoattractant protein-1, interferon-inducible protein 10 (IP-10), and lipopolysaccharide-binding protein (LBP) were determined with Luminex (Magnetic Luminex Assay; R&D Systems Europe, Ltd., Abingdon OX14 3NB, United Kingdom) in fasting venous plasma samples, which were collected into 10-mL EDTA tubes on d0 and d15 and were quickly separated and then stored in a freezer at -80 °C after centrifugation at 3000 r/min for 15 min.

Analysis of composition of gut microbiota

Fresh faeces were collected in the rifaximin group at d0 and d15 and were stored in a freezer at -80 °C within 2 h. The DNA of the faecal flora was analysed by metagenomics sequencing (Illumina HiSeq), and the gene structure was predicted with Meta Gene Mark, followed by bioinformatics analysis.

Statistical analysis

The statistical review of this study was performed by biomedical statisticians. The Student's *t*-test (including independent sample and paired sample), χ^2 test, Fisher's exact test, Mann-Whitney U test, and PERMANOVA test were selected according to different types of variables. The cumulative incidence was used to describe the rate of death and competing risk model (Gray's test) was used to test the difference of survival rates between the two groups. Data processing was performed using BMI SPSS 22.0, GraphPad Prism 6, and Stata 14.0 software. The biological information of intestinal microbiota was analysed with *R* Statistical software. *P* values < 0.05 (two-tail) were considered statistically significant.

RESULTS

Patient characteristics

One hundred and forty-three patients were assessed for eligibility, and 75 patients who fulfilled the inclusion criteria were finally enrolled in the study (Figure 1). No significant differences were found in the clinical data, including age, gender distribution, aetiology, Child-Pugh grade, model for end-stage liver disease (MELD) score, ascites grade, dosage of diuretic, and proportion of patients with SBP and AKI between the rifaximin group (n = 50; 19 patients treated with rifaximin and 31 patients treated with rifaximin plus intravenous antibiotics therapy) and the control group (n = 25) (Table 1).

Rifaximin reduces the body weight significantly and mitigates ascites in cirrhotic patients with refractory ascites

After the 2-wk treatment, the weight of the patients in the rifaximin group (median: 70.00 kg *vs* 69.00 kg) decreased more significantly than that in the control group (median: 70.00 kg *vs* 69.00 kg) (P = 0.011). The ascites subsided significantly in the rifaximin group (18 markedly effective, 21 effective, and 11 invalid) compared with that in the control group (9 markedly effective, 3 effective, and 13 invalid) (P = 0.009).

Rifaximin treatment improves the 6-month survival in cirrhotic patients with refractory ascites

Nine patients in the rifaximin group died within 6 mo, two patients underwent LT, and one underwent transjugular intrahepatic portosystemic shunt during the follow-up. However, nine patients died within 6 mo and one patient was lost to follow-up in the control group (Figure 1). The cumulative survival rate at 6 mo was significantly higher in the rifaximin group than in the control group (subdistribution hazard ratio = 2.53, 95%CI: 1.01-6.38, P = 0.048) (Figure 2).

Two weeks of treatment with rifaximin has no significant effect on liver and kidney function in cirrhotic patients with refractory ascites

After 2 wk of treatment, the Child-Pugh scores of patients decreased significantly in both the rifaximin and control groups (P < 0.001 and 0.015, respectively), while no significant change was noted in the MELD scores (P = 0.202 and 0.189, respectively). No significant difference was noted in the Child-Pugh and MELD scores between the

Table 1 Baseline characteristics of patients, *n* (%)

Characteristic	Rifaximin group (*n* = 50)	Control group (*n* = 25)	*P* value
Age	54.60 ± 9.05	59.04 ± 10.01	0.057
Sex (male/female)	42/8	18/7	0.221
Etiology			
HBV	14 (28)	9 (36)	0.479
HCV	3 (6)	0 (0)	0.546
Alcohol	22 (44)	7 (28)	0.180
HBV/alcohol	7 (14)	3 (12)	1.000
NASH	1 (2)	3 (12)	0.105
AIH	1 (2)	0 (0)	1.000
PBC	0 (0)	1 (4)	0.333
Cryptogenic	2 (4)	2 (8)	0.597
Child-Pugh grade (B/C)	21/29	16/9	0.072
MELD score	10 (6-13)	8 (6-10)	0.094
Furosemide (mg/d)	80 (40-80)	80 (40-80)	0.246
Spironolactone (mg/d)	160 (80-160)	160 (100-160)	0.315
Ascites (grade 1/2)	38/12	20/5	0.978
AKI	3 (6)	2 (8)	1.000
SBP	19 (38)	9 (36)	0.866
Hypertension	7 (14)	5 (20)	0.738
Diabetes mellitus	19 (38)	9 (36)	0.866
Biochemistry			
ALT (U/L)	24.85 (13.75-42.58)	20.50 (16.40-34.95)	0.673
Alb (g/L)	28.40 ± 5.30	27.68 ± 3.79	0.526
TBil (μmol/L)	43.80 (25.88-93.78)	24.70 (18.75-55.55)	**0.039**
Scr (μmol/L)	70.20 (57.00-93.53)	64.20 (53.10-74.35)	0.256
Urea (mmol/L)	7.17 ± 4.70	6.68 ± 3.32	0.641
eGFR (mL/min 1.73 m^2)	95.49 (76.17-114.81)	98.80 (86.80-109.37)	0.897
Coagulation			
PTA (%)	54.00 (45.00-68.50)	64.00 (56.50-74.50)	**0.030**
INR	1.53 ± 0.39	1.37 ± 0.26	0.074
Routine blood test			
WBC (10^9/L)	4.38 (3.41-6.04)	3.87 (3.26-6.78)	0.955
HGB (g/L)	101.22 ± 25.91	98.36 ± 23.03	0.642
PLT (10^9/L)	77 (54-102)	101 (56-172)	0.069

Values are given as the mean ± SD if they follow a normal distribution, otherwise given as medians (interquartile range). HBV: Hepatitis B virus; HCV: Hepatitis C virus; NASH: Nonalcoholic steatohepatitis; AIH: Autoimmune hepatitis; PBC: Primary biliary cirrhosis; AKI: Acute kidney injury; SBP: Spontaneous bacterial peritonitis; eGFR: Estimate glomerular filtration rate; PTA: Prothrombin activity; MELD: Model for end-stage liver disease.

rifaximin and control groups (P = 0.666 and 0.688, respectively). The concentrations of Scr in the rifaximin and control groups were significantly increased after treatment (P = 0.002 and < 0.001, respectively), but no significant difference was found in the change of Scr between the groups (P = 0.258) (Table 2). Analysis of patients with abnormal renal function at baseline (eGFR < 90 mL/min 1.73 m^2) (20 patients in the rifaximin group and 7 patients in the control group) showed that the concentration of Scr in the rifaximin group was slightly lower than that before treatment (P = 0.370), but there was a significant increase in the control group (P = 0.028); no significant difference was noted in the change of Scr between the two groups (P = 0.268) (Figure 3).

Rifaximin improves the systemic inflammatory state of cirrhotic patients with refractory ascites

Finally, 39 patients (26 in the rifaximin group and 13 in the control group) were tested for the markers of inflammation and endotoxin before and after treatment. The

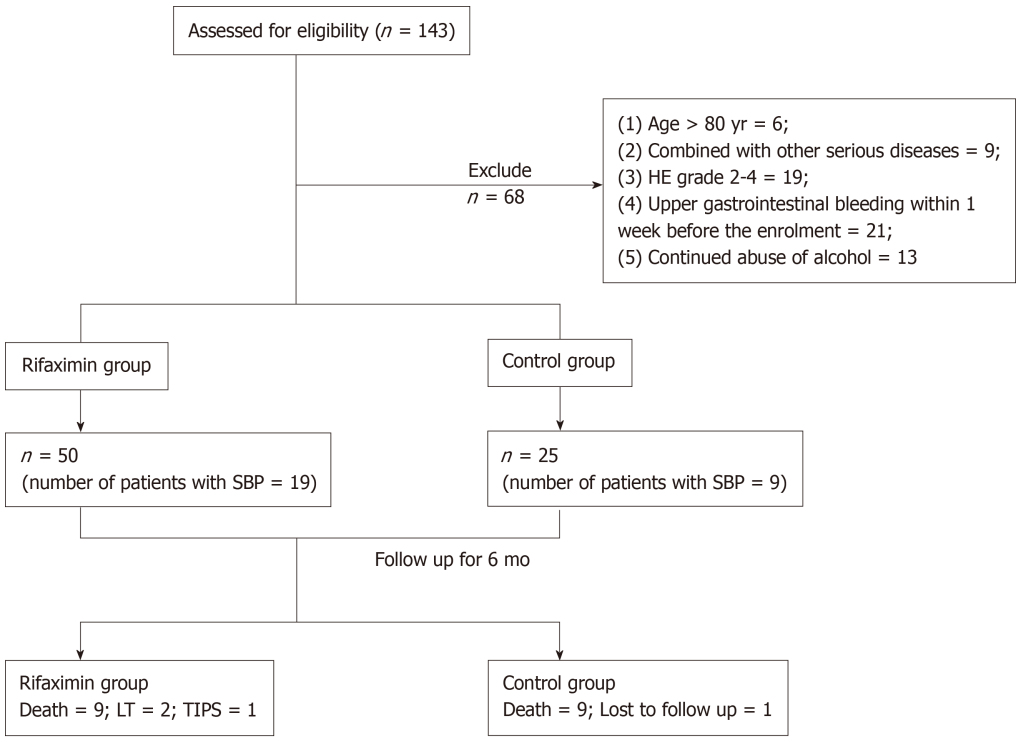

Figure 1 Flow chart for patient selection. SBP: Spontaneous bacterial peritonitis; TIPS: Transjugular intrahepatic portosystemic shunt; LT: Liver transplantation.

concentration of IP-10 decreased significantly in the rifaximin group (187.83 ± 180.08 at baseline *vs* 150.35 ± 126.22 at follow-up) compared with that in the control group (98.53 ± 57.02 at baseline *vs* 228.25 ± 232.65 at follow-up) (P = 0.02). Changes in the concentrations of IL-6, IL-8, TNF-α, monocyte chemoattractant protein-1, and LBP were also analysed, and no differences were observed in these markers after treatment (Table 3). However, Figure 4 shows that the concentrations of TNF-α and LBP in patients treated with rifaximin decreased after treatment but increased in the control group.

Rifaximin affects the characteristics and function of gut microbiota in cirrhotic patients with refractory ascites

A total of 40 stool samples from 20 patients (12 patients treated with rifaximin and 8 patients treated with rifaximin plus intravenous antibiotics) were subjected to bioinformatics analysis after metagenomics sequencing. The diversity Shannon index was calculated using function diversity, the differences before and after treatment were tested using the Wilcoxon test, and the beta diversity was analysed using the non-metric multidimensional scale. Lefse analysis and the Wilcoxon signed-rank test were applied to analyse the changes in the gut microbiota after treatment. The analysis of virulence was performed on all predicted genes using the Virulence Factors Database.

Analysis of composition of gut microbiota: The bacteria in the stools of patients before and after treatment were mainly classified into *Firmicutes*, *Proteobacteria*, *Bacteroidetes*, and *Actinobacteria* at the phylum level, of which the most dominant phylum was *Firmicutes* (41.55% before *vs* 47.16% after treatment). At the genus level, they were mainly classified into *Escherichia*, *Bacteroides*, *Bifidobacterium*, and *Faecalibacterium* (Figure 5).

Analysis of diversity: The Shannon index (P = 0.11 and 0.36), richness (P = 0.055 and 0.11, respectively), and beta diversity (P = 0.824 and 0.455, respectively) of faecal microbiota did not change significantly after treatment with rifaximin and rifaximin plus intravenous antibiotics (Figures 6 and 7).

Analysis of different microbiota in faecal samples: Lefse analysis showed that, at the phylum, class, order, family, and genus levels, no significant change was found in the faecal flora in patients treated with rifaximin. However, in patients treated with rifaximin plus intravenous antibiotics, the abundance of *Verrucomicrobia*, *Verrucomicrobiae*, *Verrucomicrobiales*, *Verrucomicrobiaceae*, and *Akkermansia* significantly

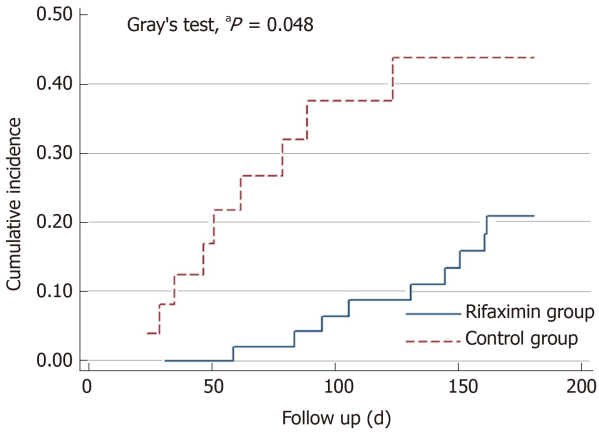

Figure 2 Gray's test showed that the cumulative survival was significantly higher in the rifaximin group than in the control group. $^{a}P < 0.05$ *vs* control group.

decreased, and the abundance of *Actinomycetaceae*, *Enterococcaceae*, *Actinomyces*, *Enterococcus*, and *Coprobacillus* significantly increased. At the species level, the abundance of *Clostridium_ramosum* was significantly increased and that of *Eggerthella_lenta*, *Roseburia_hominis*, and *Eubacterium_hallii* significantly decreased after treatment with rifaximin. However, *Clostrium_nexile*, *Eubacterium_hallii*, *Lachnospiraceae-bacterium4_1_37FAA*, *Lachnospiraceae-bacterium9_1_43BFAA*, *Actinomyces-odontolyticus*, *Lachnospiraceae-bacterium2_1_58FAA*, *Lachnospiraceae-bacterium6_1_63FAA*, *Bifidobacterium-Dentium*, *Alistipes-Onderdonkii*, *Roseburia_hominis*, *Escherichia coli*, *Veillonella_dispar*, and *Leuconostoc_pseudomesenteroides* decreased significantly and the abundance of *Clostridium_ramosum*, *Enterococcus_faecium*, and *Coprobacillus_unclassified* was significantly increased after treatment with rifaximin plus intravenous antibiotics (Figure 8).

Wilcoxon test showed that, at the genus level, the abundance of *Roseburia*, *Haemophilus*, and *Prevotella* was significantly reduced after treatment with rifaximin, while the abundance of *Lachnospiraceae_noname*, *Subdoligranulum*, and *Dorea* decreased and the abundance of *Coprobacillus* increased significantly after treatment with rifaximin plus intravenous antibiotics (Figure 9). At the species level, the abundance of *Roseburia_intestinalis*, *Bacteroides_uniformis*, *Eggerthella_lenta*, and *Haemophilus_parainfluenzae* was significantly reduced, and the relative abundance of *Bacteroidetes_vulgatus* was significantly increased after treatment with rifaximin. Additionally, the abundance of *Bacteroides_dorei* was significantly reduced after treatment with rifaximin plus intravenous antibiotics (Figure 9). The abundance of *Bifidobacterium* and *Lactobacillus* in the intestinal flora, as well as the abundance of *Faecalibacterium_prausnitzii*, decreased after both treatments, although the changes were not significant (Table 4).

Analysis of bacterial virulence: The obtained non-redundant reference gene set was compared with the Virulence Factors Database using DIAMOND (v0.7.9.58), and virulence analysis was performed on all predicted genes. The results are shown in Figure 10. The total expression of virulence factor genes of the intestinal flora in both groups was significantly reduced after treatment.

The ratio of virulence factor gene expression after treatment and before treatment is taken as log2 (fold change), which is calculated as log2 (mean value after treatment/mean value before treatment), and log2 (fold change) < 0 indicated that the virulence factor gene expression was decreased significantly after treatment.

DISCUSSION

The gut microbiota is an important component of the intestinal micro-environment that is involved in the metabolism of various substances, the composition of the mucosal barrier, and the development and maturation of the immune system[17]. There is increasing evidence that a significant difference exists in the gut microbiota between patients with cirrhosis and healthy people[18,19]. Based on the assumption that bacterial overgrowth and translocation cause the systemic inflammatory state, which aggravates the dysfunction of stellate cells and hyperdynamic circulation in patients with cirrhosis, this study suggests that rifaximin can be used to interfere with the

Table 2 Changes in clinical data of patients after treatment in the two groups

	Rifaximin group (*n* = 50)			Control group (*n* = 25)			*P* value
	d0	d15	mean delta	d0	d15	Mean delta	
Weight (kg)	70.00 (60.00-78.75)	69.00 (58.00-74.00)	-3.30	62.00 (55.00-71.25)	59.5 (54.88-59.5)	-1.20	0.011
Cr (μmol/L)	70.20 (57.00-93.53)	78.25 (63.10-92.68)	11.82	9 (8.00-11.00)	73.0 (63.35-95.65)	13.54	0.777
Urea (mmol/L)	7.17±4.70	9.07±6.71	1.90	8 (5.50-10.00)	7.63±3.31	0.95	0.258
eGFR (mL/min 1.73 m^2)	95.49 (76.17-114.81)	93.11 (71.92-108.00)	-5.20	98.80 (86.80-109.37)	92.0 (61.59-99.54)	-9.68	0.136
Child-Pugh score	10 (8.00-11.25)	9 (8.00-10.25)	-0.90	9 (8.00-11.00)	8 (7.50-10.50)	-0.76	0.666
MELD score	10 (6.00-13.00)	11.5 (6.75-15.25)	0.60	8 (5.50-10.00)	8 (6.50-10.00)	0.92	0.688

Delta was defined as the value after treatment minus the value before treatment. eGFR: Estimate glomerular filtration rate; MELD: Model for end-stage liver disease.

process above and improve the haemodynamics by targeting the gut microbiota.

Our study showed that treatment with rifaximin mitigated ascites and improved the survival in cirrhotic patients with refractory ascites. However, 2-wk treatment with rifaximin revealed no significant effect on liver and kidney function. This study also analysed the changes in the concentrations of IL-6, TNF-α, and other inflammatory factors, as well as LBP, in the plasma of cirrhotic patients with refractory ascites. No significant change was noted in the inflammatory factors other than IP-10 after treatment with rifaximin, although the concentrations of TNF-α and LBP showed a declining trend, which is consistent with the results of a previous randomized controlled trial[20]. Previous studies have shown that rifaximin inhibits activation of the NF-κB signalling transduction pathway and downregulates the expression of cytokines and chemokines[21,22]. Studies have also shown that rifaximin can reduce the concentrations of IL-6, TNF-α, and endotoxin in patients with decompensated cirrhosis, thereby exercising the effects of reducing portal pressure and improving haemodynamics[11,12,23]. However, these studies and their follow-up did not set up a controlled trial. Although a case-control study showed that long-term treatment with rifaximin reduced the incidence of esophagogastric and gastric variceal bleeding, SBP, and HRS in patients with decompensated alcoholic cirrhosis and improved their survival rate[13], rifaximin treatment in patients had already been confirmed to be effective before enrolment; thus, there may exist a selection bias. A randomized, double-blind, controlled trial revealed that 4 wk of treatment with rifaximin did not affect the hepatic venous pressure gradient, systemic haemodynamics, GFR, or levels of vasoactive hormones and had no impact on the inflammatory state and only minor effects on BT and intestinal bacterial composition in stable, decompensated cirrhosis[20,24]. Considering the mechanism of action of rifaximin, it may exert effects on patients with poor liver function and severely disordered haemodynamics; hence, a randomized controlled trial performed on a subgroup analysis of patients with Child-Pugh C liver function and elevated LBP at baseline still showed no significant difference[20,24]. Our study performed subgroup analysis in patients with lower eGFR than normal at baseline, and the results suggest a trend of decline in the levels of Scr after treatment with rifaximin but a trend of elevation in patients in the control group, suggesting that rifaximin can show advantages in patients with severely disordered haemodynamics and a high inflammatory state. Regrettably, this study did not assess the effect of long-term treatment with rifaximin on these indicators and did not collect haemodynamic-related data. Thus, further research is needed to assess the effect of long-term treatment with rifaximin on the prognosis of cirrhotic patients with severely disordered haemodynamics and a high inflammatory state.

Studies on irritable bowel syndrome (IBS) have found that rifaximin can inhibit the growth of *Escherichia coli*, *Enterococcus faecalis*, *Staphylococcus aureus*, *Klebsiella*, *Enterobacterium*, and other *non-Enterobacterium*-Gram-negative enterobacteria *in vitro*[25] and increase the abundance of *Lactobacilli* and reduce the number of *Bacillus filiformis*[26]. Thus, rifaximin is considered to inhibit the growth of pathogenic bacteria without affecting the normal composition of gut microbiota. In recent years, rifaximin has been increasingly studied in the prevention and treatment of cirrhosis complications such as SBP and HRS, but the effect of rifaximin in patients with decompensated cirrhosis remains controversial. Studies have shown that rifaximin has minor effects on bacterial composition, inflammation, and BT in stable, decompensated cirrhosis[20,24]. Other studies have shown no significant microbial change besides a modest decrease in *Veillonellaceae* and *Streptococcus*, and an increase

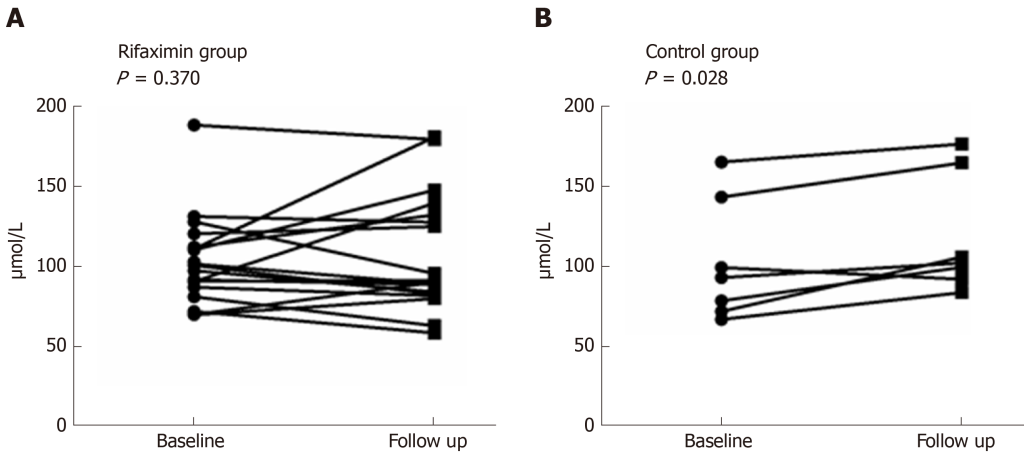

Figure 3 Changes in the concentration of Scr after treatment in patients with renal dysfunction. A: A downtrend in the rifaximin group; B: An uptrend in the control group.

in *Eubacteriaceae* was observed after rifaximin treatment in patients with HE[27-29]. Considering that rifaximin reduces endotoxaemia but has no significant effect on intestinal flora, it is preferred that rifaximin is more likely to exert pharmacological effects through the following pathways: (1) Altering bacterial function and virulence; (2) Improving intestinal barrier function; and (3) Inducing resistance to some flora[28,30]. Studies have confirmed that rifaximin inhibits the adhesion and translocation of bacteria, reduces the virulence of bacteria, and regulates the metabolism of gut microbiota[27,31-33]. Using metagenomic sequencing, this study evaluated the changes in the intestinal flora in cirrhotic patients with refractory ascites after treatment with rifaximin and rifaximin plus intravenous antibiotics. Previously, it was generally believed that the diversity of gut microbiota was decreased in disease conditions, particularly in patients with intestinal diseases, and increased after the disease was relieved[34]. Our study suggested a decline in the richness of gut microbiota in cirrhotic patients with refractory ascites after treatment with rifaximin, probably related to the premise of treatment with antibiotics in this study. In this study, patients with refractory ascites and severely disordered haemodynamics were selected as the research subjects, and the changes in the gut microbiota after treatment with rifaximin are not consistent with the results of previous studies with rifaximin in the complications of cirrhosis such as HE and ascites.

We compared our results with the differences between the structure of gut microbiota in cirrhotic patients and healthy people reported by Qin *et al*[19]: (1) At the genus level, an increase in the abundance of *Haemophilus* and *Prevotella* and a decrease in the abundance of *Roseburia*, *Subdoligranulum*, and *Dorea* were found in patients with cirrhosis by Qin *et al*[19]; we found a decrease in the abundance of *Haemophilus*, *Prevotella*, and *Roseburia* after treatment with rifaximin but a decrease in *Subdoligranulum* and *Dorea* after treatment with rifaximin plus intravenous antibiotics in cirrhotic patients with refractory ascites; and (2) At the species level, a decrease in the abundance of *Haemophilus_parainfluenzae*, *Roseburia_intestinalis*, and *Bacteroides_uniformis* was found in patients with cirrhosis by Qin *et al*[19] as well as in cirrhotic patients with refractory ascites after treatment with rifaximin in our study.

Studies have shown an increase in the concentration of *Bifidobacterium* in the stool of patients with inflammatory bowel disease after rifaximin treatment[35,36]. The abundance of *Lactobacilli* in faecal samples increased one month after treatment with rifaximin in patients with different gastrointestinal diseases such as IBS, inflammatory bowel disease and diverticulosis, but the composition of the gut microbiota did not show any significant change[37]. Another study suggested that the abundance of *Faecalibacterium_prausnitzii* is increased at the end of rifaximin treatment in non-constipation IBS, and the composition of the gut microbiota did not change significantly[38]. *Bifidobacterium* has an intestinal and systemic anti-inflammatory effect[39]; butyrate production by *Faecalibacterium_prausnitzii* was involved in the regulation of proliferation, apoptosis, and differentiation of gastrointestinal epithelial cells, exercising an immunomodulatory effect[40,41]; *Lactobacillus* has anti-inflammatory, immunomodulatory, anti-oxidative, anti-bacterial, and anti-viral properties[30,42]. Our results suggest that the abundance of *Bifidobacterium* and *Lactobacillus* in the gut microbiota is increased after treatment with rifaximin and rifaximin plus intravenous antibiotics in cirrhotic patients with refractory ascites, while the abundance of *Faecalibacterium_prausnitzii* had a slight decrease.

Table 3 Changes in the cytokine and lipopolysaccharide-binding protein levels in patients after treatment in the two groups

	Rifaximin group (*n* = 26)		Control group (*n* = 13)		*P* value
	d0	d15	d0	d15	
IL-6 (pg/mL)	29.73 ± 101.82	8. 93 ± 6.13	27.05 ± 45.70	18.75 ± 39.11	0.644
IL-8 (pg/mL)	45.12 ± 91.71	117.47 ± 359.77	31.51 ± 90.82	42.92 ± 128.15	0.557
TNF-α (pg/mL)	3.62 ± 2.22	3.23 ± 1.31	2.79 ± 0.72	3.07 ± 0.83	0.356
MCP-1 (pg/mL)	93.32 ± 49.00	98.41 ± 61.21	86.71 ± 44.14	79.61 ± 39.87	0.481
IP-10 (pg/mL)	187.83 ± 180.08	150.35 ± 126.22	98.53 ± 57.02	228.25 ± 232.65	0.024
LBP (pg/mL)	6140682.77 ± 3478004.74	5828915.42 ± 3761441.65	5784964.46 ± 2841716.75	9792449.77 ± 8492517.57	0.071

The data are given as the mean ± SD. Interleukin-6, interleukin-8, tumour necrosis factor alpha, and monocyte chemoattractant protein-1 suggest an inflammatory response; interferon-inducible protein 10 activates inflammatory cells and probably affects hepatic stellate cells and cirrhosis; and lipopolysaccharide-binding protein reflects the degree of the inflammatory response caused by endotoxin. IL-6: Interleukin-6; IL-8: Interleukin-8; TNF-α: Tumour necrosis factor alpha; MCP-1: Monocyte chemoattractant protein-1; LBP: Lipopolysaccharide-binding protein. IP-10: Interferon-inducible protein 10.

In conclusion, this study evaluated the effects of rifaximin in cirrhotic patients with refractory ascites with regard to clinical efficacy, plasma inflammatory factors, and changes in the gut microbiota. We concluded that rifaximin may affect the structure and function of the gut microbiota and improve the systemic inflammatory response, thereby improving the clinical symptoms and survival rate in cirrhotic patients with refractory ascites. Studies with a large sample size are still needed to verify our conclusions, and the role of these flora remains to be further explored, since the changes in the gut microbiota in cirrhotic patients with refractory ascites remain unavailable.

Table 4 Changes in the abundance of beneficial bacteria after treatment

Classification	Rifaximin			Rifaximin + antibiotics		
	Before	After	*P* value	Before	After	*P* value
g_Lactobacillus	1.924	3.903	0.791	0.581	2.535	0.547
g_Bifidobacterium	12.567	21.949	0.301	5.036	9.524	0.641
s_Faecalibacterium_prausnitzii	10.448	8.193	0.910	6.590	3.206	0.148

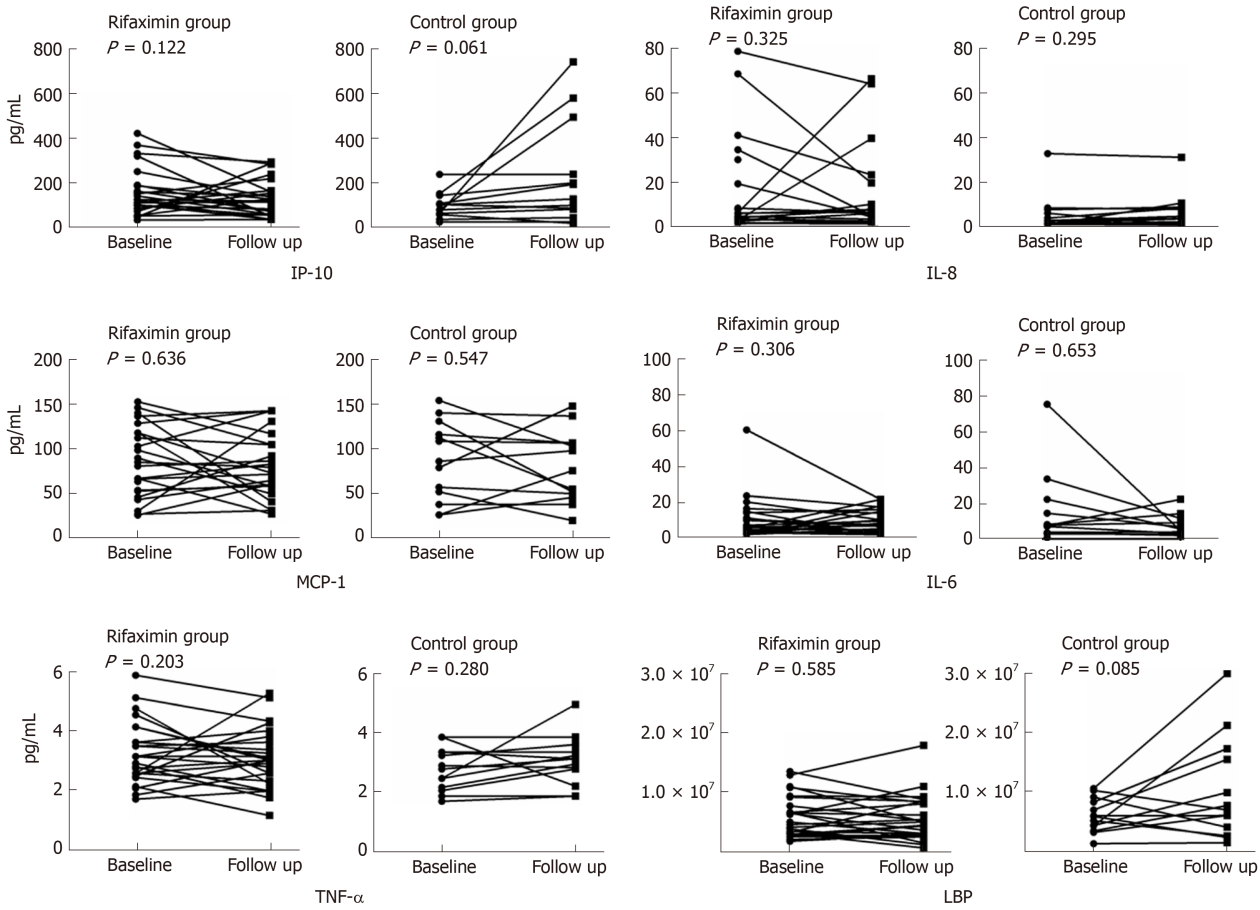

Figure 4 Changes in inflammatory factors and lipopolysaccharide-binding protein after treatment in the two groups. The concentrations of interferon-inducible protein 10, tumour necrosis factor alpha, and lipopolysaccharide-binding protein showed a downtrend in the rifaximin group but uptrend in the control group, and interferon-inducible protein 10 decreased significantly in the rifaximin compared with the control group (Table 3). IL-6: Interleukin-6; IL-8: Interleukin-8; TNF-α: Tumour necrosis factor alpha; MCP-1: Monocyte chemoattractant protein-1; LBP: Lipopolysaccharide-binding protein; IP-10: Interferon-inducible protein 10.

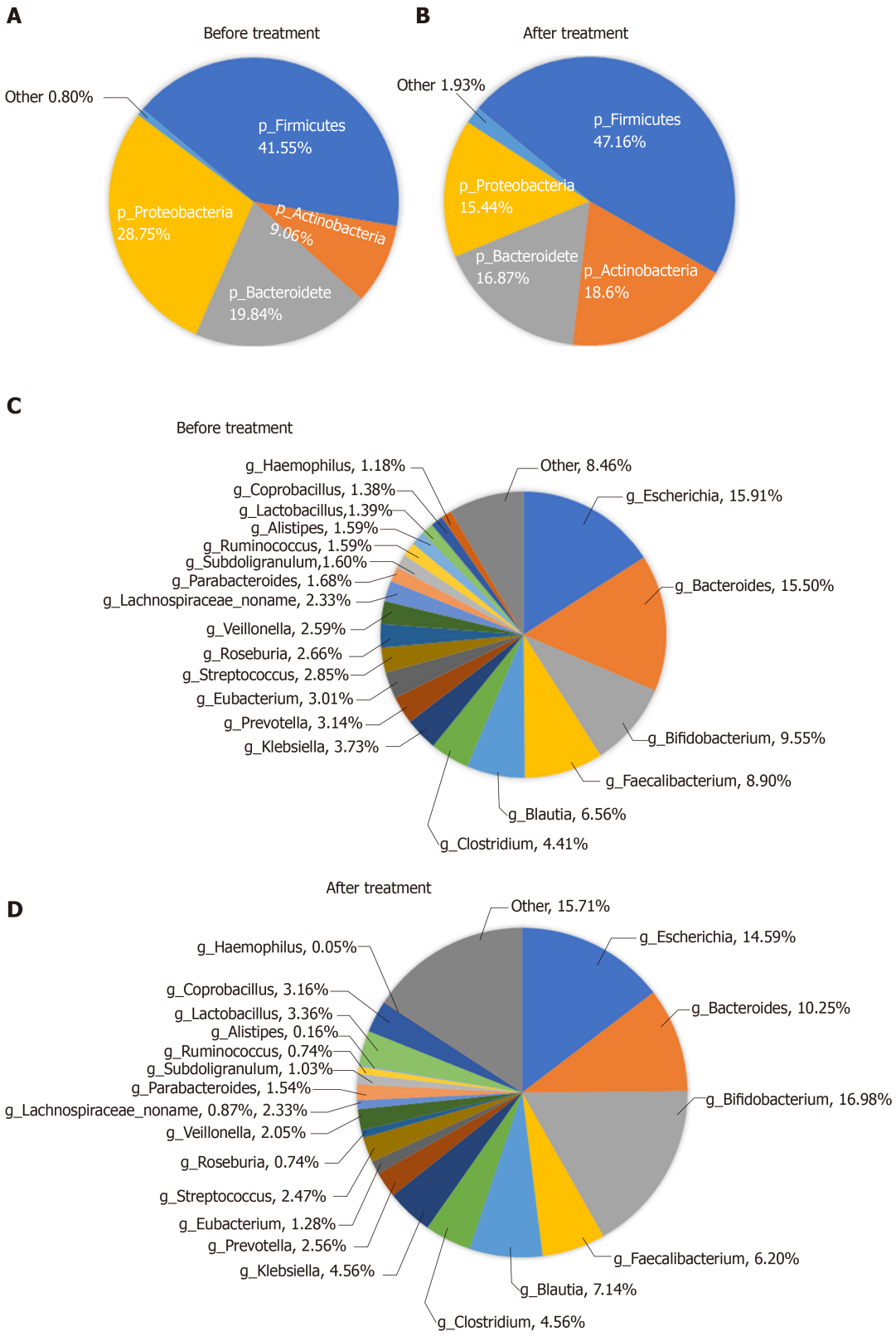

Figure 5 Abundance of the microbiota before and after treatment at the phylum and genus levels. A and B: Phylum level; C and D: Genus level.

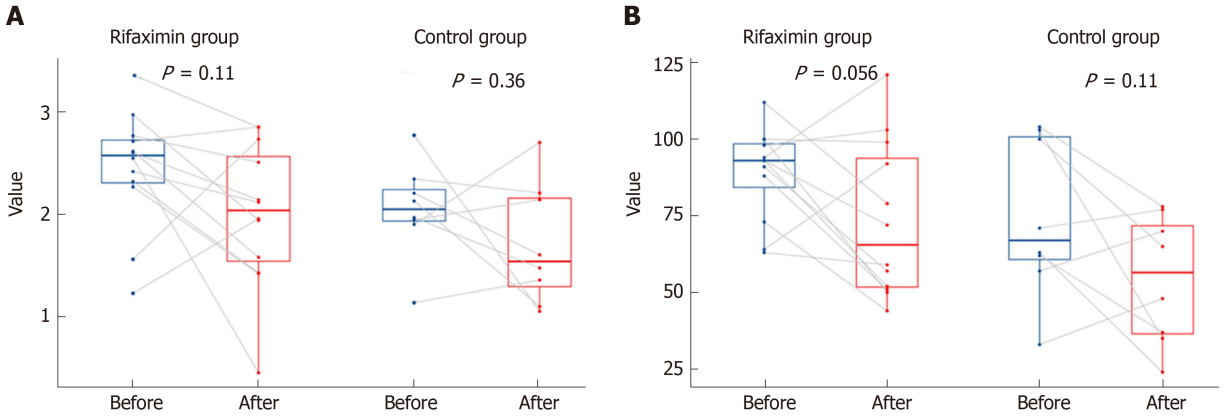

Figure 6 Changes in the Shannon index and Richness in patients of the two groups before and after treatment. A: Changes in the Shannon index in patients of the two groups before and after treatment (no significant decrease); B: Changes in the Richness in patients of the two groups before and after treatment: (no significant decrease).

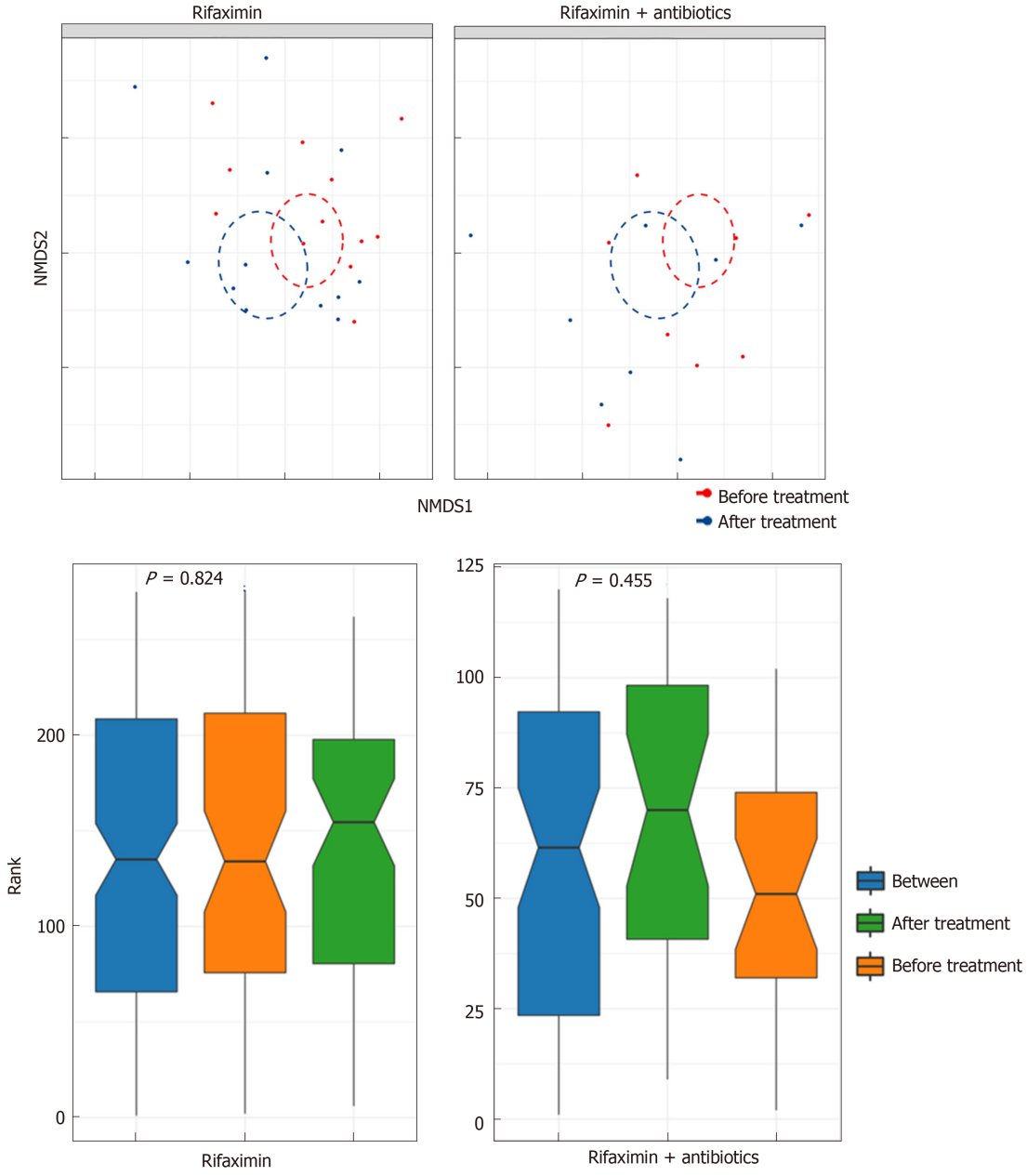

Figure 7 Change in the beta diversity of patients in the two groups before and after treatment.

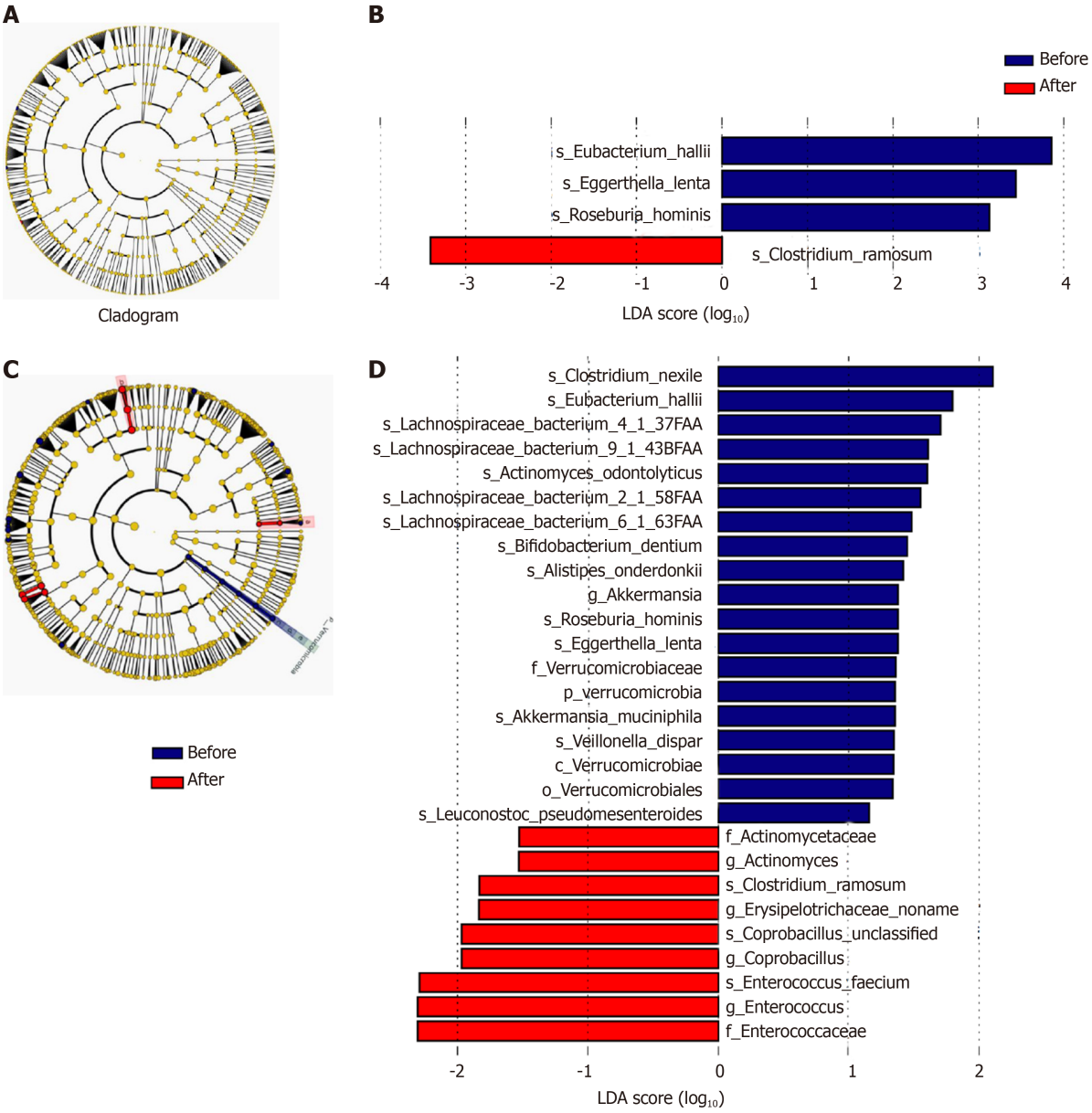

Figure 8 Cladogram and Linear discriminant analysis score of Lefse analysis of patients in the subgroup of rifaximin and rifaximin plus intravenous antibiotics. A and B: Subgroup of rifaximin; C and D: Rifaximin plus intravenous antibiotics. The taxonomic levels are shown in the cladograms, represented by rings with kingdoms at the innermost ring and genera at the outermost ring, the small circles at each classification level represent different classifications at that level, and the diameters represent the relative abundance. Yellow represents no significant difference while blue and red represent significantly different microbiota before and after treatment, respectively. The Linear discriminant analysis score shows significant differences at > 2.0; red and blue represent before and after treatment, respectively, and the length represents the Linear discriminant analysis score, which is the degree of significant difference. LDA: Linear discriminant analysis.

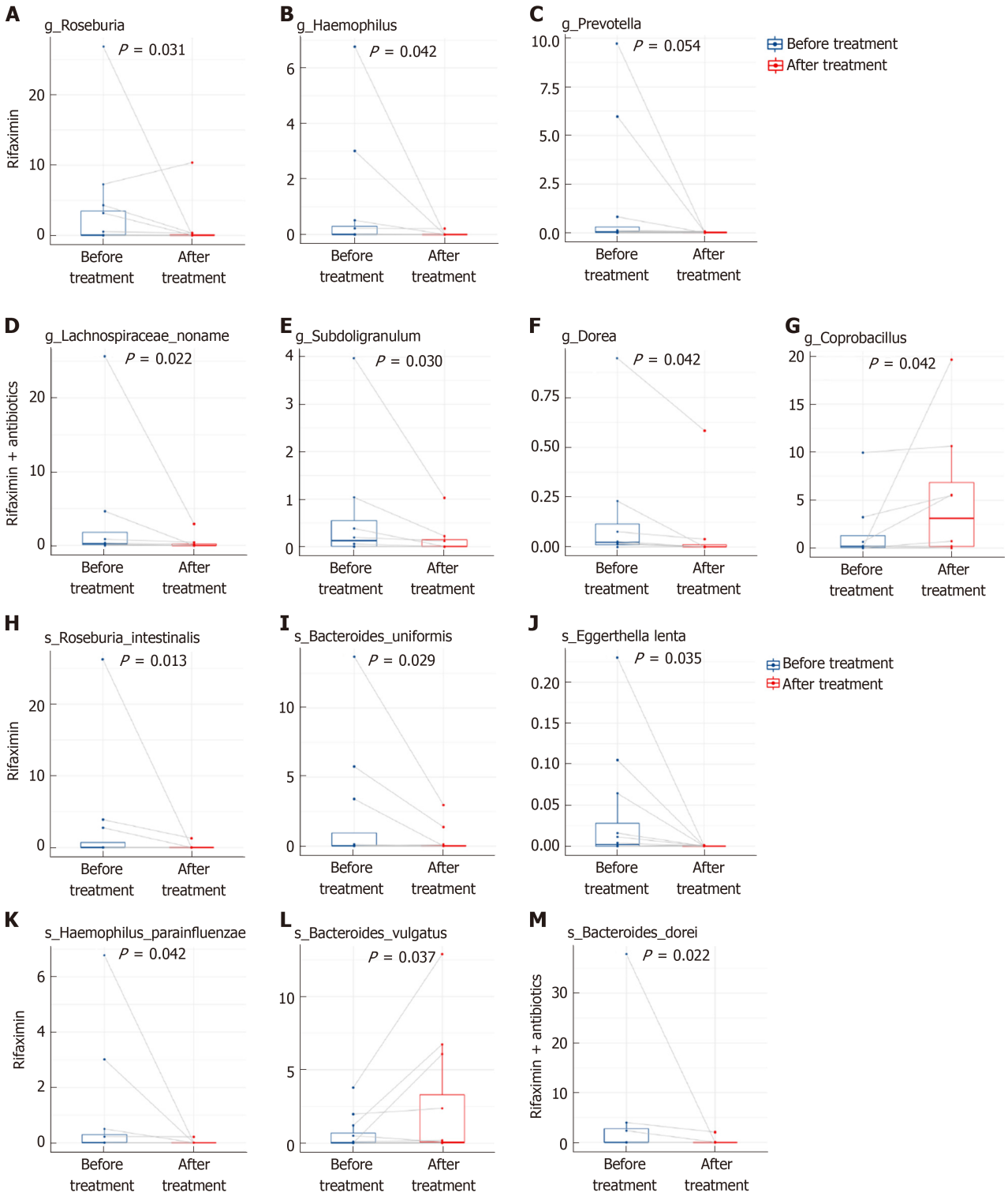

Figure 9 Abundance of microbiota with significant changes at the genus and species levels. A-G: Abundance of microbiota with significant changes at the genus level; H-M: Abundance of microbiota with significant changes at the species level.


A
ysaN type III secretion sytem protein [Yersinia enterocolitica subsp. enterocolitica 8081]
YpsIP31758_3832 putative sensor histidine kinase/response regulator EsrA [Yersinia pseudotuberculosis IP 31758]
YE105_C1176 WbcK protein [Yersinia enterocolitica subsp. palearctica 105.5R(r)]
YE105_C1175 translocase [Yersinia enterocolitica subsp. palearctica 105.5R(r)]
xcpV general secretion pathway protein I [Pseudomonas aeruginosa PAO1]
wlaN beta−1,3 galactosyltransferase [Campylobacter jejuni subsp. jejuni NCTC 11168]
wbpD probable acetyltransferase WbpD [Pseudomonas aeruginosa PAO1]
wbcG putative glycosyltransferase [Yersinia enterocolitica subsp. enterocolitica 8081
vuuB vulnibactin utilization protein [Vibrio vulnificus YJ016]
tssM hypothetical protein [Burkholderia mallei ATCC 23344]
trbE conjugal transfer protein trbE precursor [Legionella longbeachae NSW150]
tonB TonB protein [Neisseria meningitidis Z2491
tbpB transferrin−binding protein 2 precursor [Haemophilus influenzae PittGG]
sugC ABC transporter−−like protein [Mycobacterium vanbaalenii PYR−1]
stgD StgD [Escherichia coli O78:K80:H9 chi7122]
SSU05_0581 CMP−N−acetylneuraminic acid synthetase [Streptococcus suis 05ZYH33]
SSP0067 putative glycosyl transferase [Staphylococcus saprophyticus subsp. saprophyticus ATCC 15305]
srtD sortase [Bacillus cereus ATCC 14579]
spa47 Spa47 [Shigella sonnei Ss046]
sagA SagA [Enterococcus faecium U0317]
rgpX3 polysaccharide biosynthesis protein, putative transporter [Streptococcus thermophilus LMG 18311]
rfpB putative galactosyltransferase [Yersinia enterocolitica subsp. enterocolitica 8081]
rfaC lipooligosaccharide alpha−1,5 heptosyltransferase I [Neisseria meningitidis 8013]
regA two−component regulator sensor kinase [Burkholderia pseudomallei K96243]
pvuA ferric vibrioferrin receptor [Vibrio parahaemolyticus RIMD 2210633]
Psyr_2626 Protein of unknown function DUF323 [Pseudomonas syringae pv. syringae B728a]
PSPTO_2875 ABC transporter, ATP−binding protein [Pseudomonas syringae pv. tomato str. DC3000]
PMI2341 autotransporter [Proteus mirabilis HI4320]
PMI0229 ABC transporter permease [Proteus mirabilis HI4320]
pic serine protease, autotransporter Pic [Shigella flexneri 2a str. 301]
phzG2 probable pyridoxamine 5'−phosphate oxidase [Pseudomonas aeruginosa UCBPP−PA14]
phuW hypothetical protein [Pseudomonas aeruginosa PAO1]
perC/bfpW transcriptional regulator BfpW [Escherichia coli B171]
pce choline binding protein E [Streptococcus pneumoniae TIGR4]
pbtG substrate−binding protein [Proteus mirabilis HI4320]
pbtC decarboxylase [Proteus mirabilis HI4320]
outK general secretion pathway protein K [Pectobacterium atrosepticum SCRI1043]
orbC putative iron transport−related ATP−binding protein [Burkholderia cenocepacia J2315]
oppA oligopeptide ABC transporter substrate−binding protein [Listeria monocytogenes J016]
OG1RF_12303 family 8 polysaccharide lyase [Enterococcus faecalis OG1RF]
NMB1779 hemagglutinin/hemolysin−related protein [Neisseria meningitidis MC58]
mrfB MrfB [Photorhabdus luminescens str. K122]
mps2 linear gramicidin synthetase subunit B [Mycobacterium intracellulare str. MOTT36Y]
mps1 fatty−acid−CoA ligase [Mycobacterium tuberculosis RGTB423]
mce5A Mammalian cell entry related domain protein [Mycobacterium gilvum PYR−GCK]
MAP3760c hypothetical protein [Mycobacterium avium subsp. paratuberculosis K−10]
M3Q_290 hypothetical protein [Acinetobacter baumannii TYTH−1]
lysA diaminopimelate decarboxylase [Mycobacterium abscessus subsp. bolletii 50594]
lpg1062 TPR repeat protein [Legionella pneumophila subsp. pneumophila str. Philadelphia 1]
lpg0756 dTDP−6−deoxy−D−glucose−3,5−epimerase RmlC [Legionella pneumophila subsp. pneumophila str. Philadelphia 1]
lpg0754 acetyltransferase [Legionella pneumophila subsp. pneumophila str. Philadelphia 1]
lisR two−component response regulator [Listeria monocytogenes EGD−e]
lipR Putative acetyl−hydrolase/esterase LipR [Mycobacterium canettii CIPT 140070017]
lgt prolipoprotein diacylglyceryl transferase [Listeria welshimeri serovar 6b str. SLCC5334]
inlB internalin B [Listeria monocytogenes HCC23]
hyl putative hyaluronidase [Streptococcus pyogenes MGAS315]
hurI heme uptake regulator [Bordetella pertussis Tohama I]
hrpY response regulator hrpY [Erwinia amylovora CFBP1430]
hdp1 Haemoglobin binding protein 1 [Listeria monocytogenes EGD−e]
hasE metalloprotease secretion protein [Pseudomonas aeruginosa PAO1]
hasD ABC transporter ATP−binding protein [Pseudomonas fluorescens Pf−5]
gspB platelet binding protein GspB [Streptococcus gordonii str. M99]
glnA1 glutamine synthetase [Mycobacterium tuberculosis RGTB327]
flmD pseudaminic acid biosynthesis−associated protein PseG [Aeromonas hydrophila ML09−119]
exeG general secretion pathway protein G [Aeromonas hydrophila subsp. hydrophila ATCC 7966]
etfB fimbrial chaperon protein [Edwardsiella tarda str. KG8401]
esaA probable membrane protein [Staphylococcus aureus RF122]
enn M protein [Streptococcus pyogenes MGAS10750]
enhC enhanced entry protein EnhC [Legionella pneumophila str. Paris]
EFD32_0765 bacterial regulatory protein, LacI family protein [Enterococcus faecalis D32]
EFAU004_00405 LacI family transcriptional regulator [Enterococcus faecium Aus0004]
ECNA114_2870 hypothetical protein [Escherichia coli NA114]
EC958_4611 hypothetical protein [Escherichia coli O25b:H4−ST131]
EC55989_3325 hypothetical protein [Escherichia coli 55989]
EC55989_3324 hypothetical protein [Escherichia coli 55989]
EC55989_3322 hypothetical protein [Escherichia coli 55989]
devR/dosR Two component transcriptional regulatory protein [Mycobacterium intracellulare str. MOTT36Y]
ctuA putative TonB−denpendent outer membrane receptor [Campylobacter jejuni subsp. jejuni NCTC 11168]
csaN type III secretion system ATPase [Chromobacterium violaceum ATCC 12472]
cpsO glycosyl transferase CpsO(V) [Streptococcus agalactiae 2603V/R]
cps4L UDP−N−acetylglucosamine 2−epimerase [Streptococcus pneumoniae TIGR4]
cps4K capsular polysaccharide biosynthesis protein Cps4K [Streptococcus pneumoniae TIGR4]
cps2L glucose−1−phosphate thymidylyltransferase [Streptococcus pneumoniae D39]
clpV ATP−dependent Clp protease, ATP−binding subunit ClpB [Burkholderia thailandensis E264]
clpP ATP−dependent Clp protease proteolytic subunit [Listeria monocytogenes EGD−e]
CJJ81176_1416 class I glutamine amidotransferase, putative [Campylobacter jejuni subsp. jejuni 81−176]
CJE1280 lipooligosaccharide biosynthesis galactosyltransferase, putative [Campylobacter jejuni RM1221]
cheB−2 chemotaxis−specific methylesterase [Aeromonas salmonicida subsp. salmonicida A449]
CD1546 putative hemolysin−like membrane protein [Clostridium difficile 630]
Cbei_0023 channel protein, hemolysin III family [Clostridium beijerinckii NCIMB 8052]
cadF outer membrane fibronectin−binding protein [Campylobacter fetus subsp. fetus 82−40]
C8J_1332 hypothetical protein [Campylobacter jejuni subsp. jejuni 81116]
C8J_1079 hypothetical protein [Campylobacter jejuni subsp. jejuni 81116]
C8J_1077 hypothetical protein [Campylobacter jejuni subsp. jejuni 81116]
c3400 hypothetical protein [Escherichia coli CFT073]
bscA subfamily M15C metalopeptidase [Burkholderia cenocepacia J2315]
bplG probable sugar transferase [Bordetella avium 197N]
BJAB0868_00098 Nucleoside−diphosphate−sugar pyrophosphorylase involved in lipopolysaccharide biosynthesis/translation initiation factor 2B, gamma/epsilon subunits (eIF−2Bgamma/eIF−2Bepsilon) [Acinetobacter baumannii BJAB0868]
bhuT putative hemin binding protein [Bordetella pertussis Tohama I]
BC5268 Secreted polysaccharide polymerase [Bacillus cereus ATCC 14579]
ACICU_00073 periplasmic protein [Acinetobacter baumannii ACICU]
acfC accessory colonization factor AcfC [Vibrio cholerae O1 biovar El Tor str. N16961]
ABSDF0078 UDP−galactose phosphate transferase (WeeH) [Acinetobacter baumannii SDF]
A1S_0059 glycosyltransferase [Acinetobacter baumannii ATCC 17978]
Name
-5
0
5
Log2FC
Group
After treatment
Before treatment

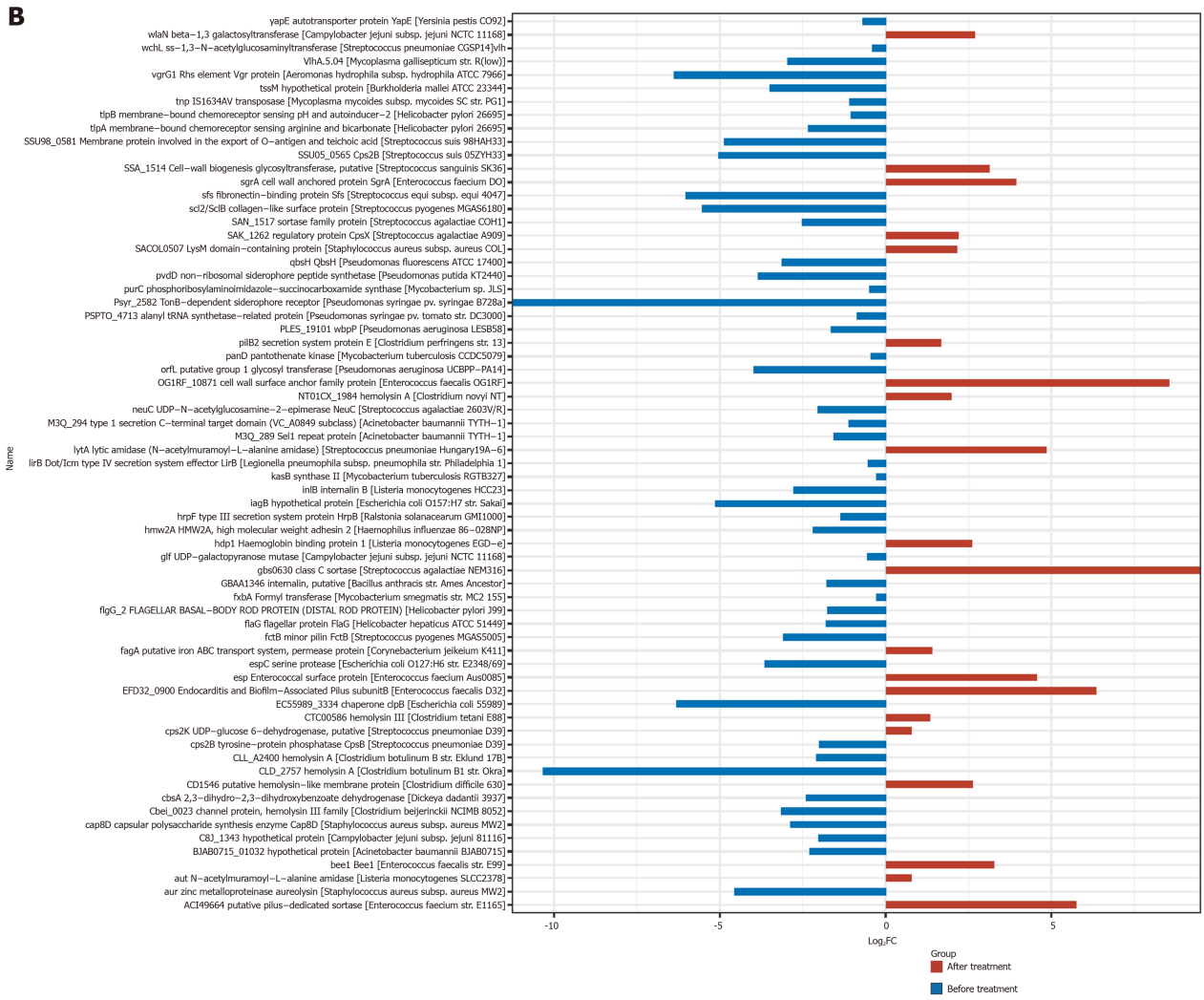

Figure 10 Expression of virulence factor genes before and after treatment with rifaximin and rifaximin plus intravenous antibiotics. A: Treatment with rifaximin; B: Treatment with rifaximin plus intravenous antibiotics.

ARTICLE HIGHLIGHTS

Research background

Patients with refractory ascites have a poor prognosis and there is no effective treatment except for liver transplantation. Rifaximin has been shown to reduce the incidence of hepatic encephalopathy and other complications in patients with cirrhosis. However, few studies have investigated the effect of rifaximin in cirrhotic patients with refractory ascites. And the mechanism of rifaximin in cirrhotic patients with refractory ascites remains unclear.

Research motivation

Previous studies have shown that rifaximin treatment can reduce the concentrations of interleukin-6, tumour necrosis factor alpha, and endotoxin in blood, thus improving systemic haemodynamics and decreasing the hepatic venous pressure gradient in patients with cirrhosis. Rifaximin has been demonstrated to exert positive effects in the prevention and treatment of hepatic encephalopathy and to prevent the development of esophagogastric and gastric variceal bleeding, spontaneous bacterial peritonitis, and hepatorenal syndrome. These provided ideas for the study and treatment in cirrhotic patients with refractory ascites.

Research objectives

The role of the gut-liver axis in the occurrence and development of complications of cirrhosis has aroused great attention. Microbiota dysbiosis and bacterial translocation have been shown to be involved in the progression of cirrhosis. Bacteria and their products are introduced into blood *via* the intestines and then increase the blood levels of endotoxin and inflammatory factors, which in turn accelerate liver fibration and stimulate the production of vasodilator substances. These events cause reduced systemic vascular resistance and an activated sympathetic nervous system and renin-angiotensin-aldosterone system, eventually leading to hyperdynamic circulation, which plays an important role in the pathogenesis of refractory ascites. Therefore,improving the

gut microenvironment may benefit cirrhotic patients with refractory ascites. We conducted this study to explore the effects of rifaximin in cirrhotic patients with refractory ascites.

Research methods

All patients received conventional treatment for refractory ascites, while patients in the rifaximin group received oral rifaximin-α 200 mg four times daily for at least 2 wk. The ascites grade, fasting weight, liver and kidney function, and the inflammatory factors in the plasma were evaluated before and after treatment. In addition, the gut microbiota was determined by metagenomics sequencing (Illumina HiSeq) to analyse the changes in the characteristics of the gut microbiota before and after rifaximin treatment. The patients were followed for 6 mo. This study evaluated the effects of rifaximin in cirrhotic patients with refractory ascites with regard to clinical efficacy, laboratory indicators, inflammatory factors, and intestinal microbiota. The concentrations of interleukin-6, interleukin-8, tumour necrosis factor alpha, monocyte chemoattractant protein-1, interferon-inducible protein 10, and lipopolysaccharide-binding protein were determined with Luminex (Magnetic Luminex Assay; R&D Systems Europe, Ltd., Abingdon OX14 3NB, United Kingdom), which was highly reliable. Intestinal microbiota can be annotated to the level of species and the study of the intestinal microbiota can be deepened to the level of genes and functions using metagenomic sequencing, compared to 16S rDNA sequencing.

Research results

Compared with the control group, the fasting weight of patients decreased and the ascites significantly subsided after treatment with rifaximin. The 6-mo survival rate of patients in the rifaximin group was significantly higher than that in the control group. The concentration of interferon-inducible protein 10 decreased significantly in the rifaximin group compared with that in the control group. The abundance of *Roseburia*, *Haemophilus*, and *Prevotella* was significantly reduced after rifaximin treatment, while the abundance of *Lachnospiraceae_noname*, *Subdoligranulum*, and *Dorea* decreased and the abundance of *Coprobacillus* increased after treatment with rifaximin plus intravenous antibiotics. The gene expression of virulence factors was significantly reduced after treatment in both subgroups treated with rifaximin or rifaximin plus intravenous antibiotics. These findings provide new ideas for study in cirrhotic patients with refractory ascites-targeting the gut microbiota. The functions of these changed intestinal bacteria remain to be explored in the future.

Research conclusions

This study evaluated the clinical efficacy of rifaximin and its effects on intestinal flora characteristics and the systemic inflammatory state in cirrhotic patients with refractory ascites, targeting the gut microbiota. We concluded that rifaximin mitigates ascites and improves survival of cirrhotic patients with refractory ascites, and a possible mechanism is that rifaximin regulates the structure and functions of intestinal bacteria, thus improving the systemic inflammatory state. These provide new ideas for clinical dealing with cirrhotic patients with refractory ascites-targeting the gut microbiota.

Research perspectives

Further research is needed to assess the effect of long-term treatment with rifaximin on the prognosis of cirrhotic patients with severely disordered haemodynamics and a high inflammatory state. Randomized controlled studies with a large sample size are still needed to verify our conclusions, and the role of these floras remains to be further explored, since the changes in the gut microbiota in cirrhotic patients with refractory ascites remain unavailable.

ACKNOWLEDGEMENTS

The authors would like to acknowledge the QuantiHealth Co., Ltd. for metagenomics sequencing.

REFERENCES

1 **Biecker E**. Diagnosis and therapy of ascites in liver cirrhosis. *World J Gastroenterol* 2011; **17**: 1237-1248 [PMID: 21455322 DOI: 10.3748/wjg.v17.i10.1237]
2 **Betrapally NS**, Gillevet PM, Bajaj JS. Gut microbiome and liver disease. *Transl Res* 2017; **179**: 49-59 [PMID: 27477080 DOI: 10.1016/j.trsl.2016.07.005]
3 **Wiest R**, Lawson M, Geuking M. Pathological bacterial translocation in liver cirrhosis. *J Hepatol* 2014; **60**: 197-209 [PMID: 23993913 DOI: 10.1016/j.jhep.2013.07.044]
4 **Møller S**, Hobolth L, Winkler C, Bendtsen F, Christensen E. Determinants of the hyperdynamic circulation and central hypovolaemia in cirrhosis. *Gut* 2011; **60**: 1254-1259 [PMID: 21504996 DOI: 10.1136/gut.2010.235473]
5 **Villanueva C**, Albillos A, Genescà J, Abraldes JG, Calleja JL, Aracil C, Bañares R, Morillas R, Poca M, Peñas B, Augustin S, Garcia-Pagan JC, Pavel O, Bosch J. Development of hyperdynamic circulation and response to β-blockers in compensated cirrhosis with portal hypertension. *Hepatology* 2016; **63**: 197-206 [PMID: 26422126 DOI: 10.1002/hep.28264]
6 **Piano S**, Tonon M, Angeli P. Management of ascites and hepatorenal syndrome. *Hepatol Int* 2018; **12**: 122-134 [PMID: 28836115 DOI: 10.1007/s12072-017-9815-0]
7 **Hoover WW**, Gerlach EH, Hoban DJ, Eliopoulos GM, Pfaller MA, Jones RN. Antimicrobial activity and spectrum of rifaximin, a new topical rifamycin derivative. *Diagn Microbiol Infect Dis* 1993; **16**: 111-118

[PMID: 8385592 DOI: 10.1016/0732-8893(93)90004-q]
8 **Gillis JC**, Brogden RN. Rifaximin. A review of its antibacterial activity, pharmacokinetic properties and therapeutic potential in conditions mediated by gastrointestinal bacteria. *Drugs* 1995; **49**: 467-484 [PMID: 7774516 DOI: 10.2165/00003495-199549030-00009]
9 **Descombe JJ**, Dubourg D, Picard M, Palazzini E. Pharmacokinetic study of rifaximin after oral administration in healthy volunteers. *Int J Clin Pharmacol Res* 1994; **14**: 51-56 [PMID: 7836025]
10 **Ponziani FR**, Gerardi V, Pecere S, D'Aversa F, Lopetuso L, Zocco MA, Pompili M, Gasbarrini A. Effect of rifaximin on gut microbiota composition in advanced liver disease and its complications. *World J Gastroenterol* 2015; **21**: 12322-12333 [PMID: 26604640 DOI: 10.3748/wjg.v21.i43.12322]
11 **Kalambokis GN**, Mouzaki A, Rodi M, Pappas K, Fotopoulos A, Xourgia X, Tsianos EV. Rifaximin improves systemic hemodynamics and renal function in patients with alcohol-related cirrhosis and ascites. *Clin Gastroenterol Hepatol* 2012; **10**: 815-818 [PMID: 22391344 DOI: 10.1016/j.cgh.2012.02.025]
12 **Vlachogiannakos J**, Saveriadis AS, Viazis N, Theodoropoulos I, Foudoulis K, Manolakopoulos S, Raptis S, Karamanolis DG. Intestinal decontamination improves liver haemodynamics in patients with alcohol-related decompensated cirrhosis. *Aliment Pharmacol Ther* 2009; **29**: 992-999 [PMID: 19210289 DOI: 10.1111/j.1365-2036.2009.03958.x]
13 **Vlachogiannakos J**, Viazis N, Vasianopoulou P, Vafiadis I, Karamanolis DG, Ladas SD. Long-term administration of rifaximin improves the prognosis of patients with decompensated alcoholic cirrhosis. *J Gastroenterol Hepatol* 2013; **28**: 450-455 [PMID: 23216382 DOI: 10.1111/jgh.12070]
14 **Chinese Society of Hepatology, Chinese Medical Association**. Guidelines on the management of ascites and complications in cirrhosis. *Zhonghua Gan Zang Bing Za Zhi* 2017; **25**: 664-677 [PMID: 29108189 DOI: 10.3760/cma.j.issn.1007-3418.2017.09.006]
15 **Chinese Society of Hepatology, Chinese Medical Association**. Xu X, Duan Z, Ding H, Li W, Jia J, Wei L, Linghu E, Zhuang H. Chinese guidelines on the management of ascites and its related complications in cirrhosis. *Hepatol Int* 2019; **13**: 1-21 [PMID: 30656520 DOI: 10.1007/s12072-018-09923-2]
16 **Blei AT**, Córdoba J; Practice Parameters Committee of the American College of Gastroenterology. Hepatic Encephalopathy. *Am J Gastroenterol* 2001; **96**: 1968-1976 [PMID: 11467622 DOI: 10.1111/j.1572-0241.2001.03964.x]
17 **Larsson E**, Tremaroli V, Lee YS, Koren O, Nookaew I, Fricker A, Nielsen J, Ley RE, Bäckhed F. Analysis of gut microbial regulation of host gene expression along the length of the gut and regulation of gut microbial ecology through MyD88. *Gut* 2012; **61**: 1124-1131 [PMID: 22115825 DOI: 10.1136/gutjnl-2011-301104]
18 **Chen Y**, Yang F, Lu H, Wang B, Chen Y, Lei D, Wang Y, Zhu B, Li L. Characterization of fecal microbial communities in patients with liver cirrhosis. *Hepatology* 2011; **54**: 562-572 [PMID: 21574172 DOI: 10.1002/hep.24423]
19 **Qin N**, Yang F, Li A, Prifti E, Chen Y, Shao L, Guo J, Le Chatelier E, Yao J, Wu L, Zhou J, Ni S, Liu L, Pons N, Batto JM, Kennedy SP, Leonard P, Yuan C, Ding W, Chen Y, Hu X, Zheng B, Qian G, Xu W, Ehrlich SD, Zheng S, Li L. Alterations of the human gut microbiome in liver cirrhosis. *Nature* 2014; **513**: 59-64 [PMID: 25079328 DOI: 10.1038/nature13568]
20 **Kimer N**, Pedersen JS, Tavenier J, Christensen JE, Busk TM, Hobolth L, Krag A, Al-Soud WA, Mortensen MS, Sørensen SJ, Møller S, Bendtsen F; members of the CoRif study group. Rifaximin has minor effects on bacterial composition, inflammation, and bacterial translocation in cirrhosis: A randomized trial. *J Gastroenterol Hepatol* 2018; **33**: 307-314 [PMID: 28671712 DOI: 10.1111/jgh.13852]
21 **Mencarelli A**, Renga B, Palladino G, Claudio D, Ricci P, Distrutti E, Barbanti M, Baldelli F, Fiorucci S. Inhibition of NF-κB by a PXR-dependent pathway mediates counter-regulatory activities of rifaximin on innate immunity in intestinal epithelial cells. *Eur J Pharmacol* 2011; **668**: 317-324 [PMID: 21806984 DOI: 10.1016/j.ejphar.2011.06.058]
22 **Yang L**, Liu B, Zheng J, Huang J, Zhao Q, Liu J, Su Z, Wang M, Cui Z, Wang T, Zhang W, Li Q, Lu H. Rifaximin Alters Intestinal Microbiota and Prevents Progression of Ankylosing Spondylitis in Mice. *Front Cell Infect Microbiol* 2019; **9**: 44 [PMID: 30886835 DOI: 10.3389/fcimb.2019.00044]
23 **Kalambokis GN**, Tsianos EV. Rifaximin reduces endotoxemia and improves liver function and disease severity in patients with decompensated cirrhosis. *Hepatology* 2012; **55**: 655-656 [PMID: 22030839 DOI: 10.1002/hep.24751]
24 **Kimer N**, Pedersen JS, Busk TM, Gluud LL, Hobolth L, Krag A, Møller S, Bendtsen F; Copenhagen Rifaximin (CoRif) Study Group. Rifaximin has no effect on hemodynamics in decompensated cirrhosis: A randomized, double-blind, placebo-controlled trial. *Hepatology* 2017; **65**: 592-603 [PMID: 27775818 DOI: 10.1002/hep.28898]
25 **Pistiki A**, Galani I, Pyleris E, Barbatzas C, Pimentel M, Giamarellos-Bourboulis EJ. In vitro activity of rifaximin against isolates from patients with small intestinal bacterial overgrowth. *Int J Antimicrob Agents* 2014; **43**: 236-241 [PMID: 24461710 DOI: 10.1016/j.ijantimicag.2013.12.008]
26 **Gao J**, Gillilland MG, Owyang C. Rifaximin, gut microbes and mucosal inflammation: unraveling a complex relationship. *Gut Microbes* 2014; **5**: 571-575 [PMID: 25244596 DOI: 10.4161/gmic.32130]
27 **Bajaj JS**, Heuman DM, Sanyal AJ, Hylemon PB, Sterling RK, Stravitz RT, Fuchs M, Ridlon JM, Daita K, Monteith P, Noble NA, White MB, Fisher A, Sikaroodi M, Rangwala H, Gillevet PM. Modulation of the metabiome by rifaximin in patients with cirrhosis and minimal hepatic encephalopathy. *PLoS One* 2013; **8**: e60042 [PMID: 23565181 DOI: 10.1371/journal.pone.0060042]
28 **Kaji K**, Takaya H, Saikawa S, Furukawa M, Sato S, Kawaratani H, Kitade M, Moriya K, Namisaki T, Akahane T, Mitoro A, Yoshiji H. Rifaximin ameliorates hepatic encephalopathy and endotoxemia without affecting the gut microbiome diversity. *World J Gastroenterol* 2017; **23**: 8355-8366 [PMID: 29307995 DOI: 10.3748/wjg.v23.i47.8355]
29 **Schulz C**, Schütte K, Vilchez-Vargas R, Vasapolli R, Malfertheiner P. Long-Term Effect of Rifaximin with and without Lactulose on the Active Bacterial Assemblages in the Proximal Small Bowel and Faeces in Patients with Minimal Hepatic Encephalopathy. *Dig Dis* 2019; **37**: 161-169 [PMID: 30428474 DOI: 10.1159/000494216]
30 **Ponziani FR**, Zocco MA, D'Aversa F, Pompili M, Gasbarrini A. Eubiotic properties of rifaximin: Disruption of the traditional concepts in gut microbiota modulation. *World J Gastroenterol* 2017; **23**: 4491-4499 [PMID: 28740337 DOI: 10.3748/wjg.v23.i25.4491]
31 **Jiang ZD**, Ke S, Dupont HL. Rifaximin-induced alteration of virulence of diarrhoea-producing Escherichia coli and Shigella sonnei. *Int J Antimicrob Agents* 2010; **35**: 278-281 [PMID: 20045287 DOI: 10.1016/j.ijantimicag.2009.11.013]
32 **Brown EL**, Xue Q, Jiang ZD, Xu Y, Dupont HL. Pretreatment of epithelial cells with rifaximin alters

bacterial attachment and internalization profiles. *Antimicrob Agents Chemother* 2010; **54**: 388-396 [PMID: 19858255 DOI: 10.1128/AAC.00691-09]
33 **Schrodt C**, McHugh EE, Gawinowicz MA, Dupont HL, Brown EL. Rifaximin-mediated changes to the epithelial cell proteome: 2-D gel analysis. *PLoS One* 2013; **8**: e68550 [PMID: 23922656 DOI: 10.1371/journal.pone.0068550]
34 **Matsuoka K**, Kanai T. The gut microbiota and inflammatory bowel disease. *Semin Immunopathol* 2015; **37**: 47-55 [PMID: 25420450 DOI: 10.1007/s00281-014-0454-4]
35 **Brigidi P**, Swennen E, Rizzello F, Bozzolasco M, Matteuzzi D. Effects of rifaximin administration on the intestinal microbiota in patients with ulcerative colitis. *J Chemother* 2002; **14**: 290-295 [PMID: 12120885 DOI: 10.1179/joc.2002.14.3.290]
36 **Maccaferri S**, Vitali B, Klinder A, Kolida S, Ndagijimana M, Laghi L, Calanni F, Brigidi P, Gibson GR, Costabile A. Rifaximin modulates the colonic microbiota of patients with Crohn's disease: an in vitro approach using a continuous culture colonic model system. *J Antimicrob Chemother* 2010; **65**: 2556-2565 [PMID: 20852272 DOI: 10.1093/jac/dkq345]
37 **Ponziani FR**, Scaldaferri F, Petito V, Paroni Sterbini F, Pecere S, Lopetuso LR, Palladini A, Gerardi V, Masucci L, Pompili M, Cammarota G, Sanguinetti M, Gasbarrini A. The Role of Antibiotics in Gut Microbiota Modulation: The Eubiotic Effects of Rifaximin. *Dig Dis* 2016; **34**: 269-278 [PMID: 27027301 DOI: 10.1159/000443361]
38 **Soldi S**, Vasileiadis S, Uggeri F, Campanale M, Morelli L, Fogli MV, Calanni F, Grimaldi M, Gasbarrini A. Modulation of the gut microbiota composition by rifaximin in non-constipated irritable bowel syndrome patients: a molecular approach. *Clin Exp Gastroenterol* 2015; **8**: 309-325 [PMID: 26673000 DOI: 10.2147/CEG.S89999]
39 **Selinger CP**, Bell A, Cairns A, Lockett M, Sebastian S, Haslam N. Probiotic VSL#3 prevents antibiotic-associated diarrhoea in a double-blind, randomized, placebo-controlled clinical trial. *J Hosp Infect* 2013; **84**: 159-165 [PMID: 23618760 DOI: 10.1016/j.jhin.2013.02.019]
40 **Flint HJ**, Scott KP, Duncan SH, Louis P, Forano E. Microbial degradation of complex carbohydrates in the gut. *Gut Microbes* 2012; **3**: 289-306 [PMID: 22572875 DOI: 10.4161/gmic.19897]
41 **Plöger S**, Stumpff F, Penner GB, Schulzke JD, Gäbel G, Martens H, Shen Z, Günzel D, Aschenbach JR. Microbial butyrate and its role for barrier function in the gastrointestinal tract. *Ann N Y Acad Sci* 2012; **1258**: 52-59 [PMID: 22731715 DOI: 10.1111/j.1749-6632.2012.06553.x]
42 **Di Cerbo A**, Palmieri B, Aponte M, Morales-Medina JC, Iannitti T. Mechanisms and therapeutic effectiveness of lactobacilli. *J Clin Pathol* 2016; **69**: 187-203 [PMID: 26578541 DOI: 10.1136/jclinpath-2015-202976]

World Journal of Gastroenterology

Submit a Manuscript: https://www.f6publishing.com

World J Gastroenterol 2020 January 14; 26(2): 219-245

DOI: 10.3748/wjg.v26.i2.219

ISSN 1007-9327 (print) ISSN 2219-2840 (online)

SYSTEMATIC REVIEW

Plasma exchange in patients with acute and acute-on-chronic liver failure: A systematic review

Eunice Xiang-Xuan Tan, Min-Xian Wang, Junxiong Pang, Guan-Huei Lee

ORCID number: Eunice Xiang-Xuan Tan (0000-0002-3757-4986); Min-Xian Wang (0000-0002-7527-1636); Junxiong Pang (0000-0002-9788-701X); Guan-Huei Lee (0000-0002-8652-6403).

Author contributions: Lee GH conceptualized and designed the review; Tan EXX and Lee GH carried out the analysis; Tan EXX drafted the initial manuscript; Wang MX and Pang VJX provided statistical support; all authors reviewed and approved the final manuscript as submitted.

Conflict-of-interest statement: All authors have no conflict(s) of interest to declare in relation to this manuscript.

PRISMA 2009 Checklist statement: A PRISMA checklist was used to guide the development of the systematic review.

Manuscript source: Invited Manuscript

Eunice Xiang-Xuan Tan, Guan-Huei Lee, National University Health System, Singapore 119228, Singapore

Min-Xian Wang, Junxiong Pang, Centre for Infectious Disease Epidemiology and Research, Saw Swee Hock School of Public Health, National University of Singapore, Singapore 119077, Singapore

Guan-Huei Lee, National University of Singapore, Singapore 119077, Singapore

Corresponding author: Guan-Huei Lee, FRCP, MBBS, MRCP, PhD, Assistant Professor, Attending Doctor, Doctor, Senior Consultant, Division of Gastroenterology and Hepatology, National University Hospital, 1E Kent Ridge Rd, Singapore 119228, Singapore. guan_huei_lee@nuhs.edu.sg

Abstract

BACKGROUND

Acute liver failure (ALF) and acute-on-chronic liver (ACLF) carry high short-term mortality rate, and may result from a wide variety of causes. Plasma exchange has been shown in a randomized control trial to improve survival in ALF especially in patients who did not receive a liver transplant. Other cohort studies demonstrated potential improvement in survival in patients with ACLF.

AIM

To assess utility of plasma exchange in liver failure and its effect on mortality in patients who do not undergo liver transplantation.

METHODS

Databases MEDLINE *via* PubMed, and EMBASE were searched and relevant publications up to 30 March, 2019 were assessed. Studies were included if they involved human participants diagnosed with liver failure who underwent plasma exchange, with or without another alternative non-bioartificial liver assist device.

RESULTS

Three hundred twenty four records were reviewed, of which 62 studies were found to be duplicates. Of the 262 records screened, 211 studies were excluded. Fifty-one articles were assessed for eligibility, for which 7 were excluded. Twenty-nine studies were included for ALF only, and 9 studies for ACLF only. Six studies included both ALF and ACLF patients. A total of 44 publications were included. Of the included publications, 2 were randomized controlled trials, 14 cohort studies, 12 case series, 16 case reports. All of three ALF studies which

Received: October 6, 2019
Peer-review started: October 6, 2019
First decision: November 4, 2019
Revised: December 21, 2019
Accepted: January 1, 2020
Article in press: January 1, 2020
Published online: January 14, 2020

P-Reviewer: Sinha R, Williams R, Zheng YW
S-Editor: Wang J
L-Editor: A
E-Editor: Zhang YL

looked at survival rate or survival days reported improvement in outcome with plasma exchange. In two out of four studies where plasma exchange-based liver support systems were compared to standard medical treatment (SMT) for ACLF, a biochemical improvement was seen. Survival in the non-transplanted patients was improved in all four studies in patients with ACLF comparing plasma exchange *vs* SMT. Using the aforementioned studies, plasma exchange based therapy in ACLF compared to SMT improved survival in non-transplanted patients at 30 and 90-d with a pooled OR of 0.60 (95%CI 0.46-0.77, $P < 0.01$).

CONCLUSION
The level of evidence for use of high volume plasma exchange in selected ALF cases is high. Plasma exchange in ACLF improves survival at 30-and 90-d in non-transplanted patients. Further well-designed randomized control trials will need to be carried out to ascertain the optimal duration and amount of plasma exchange required and assess if the use of high volume plasma exchange can be extrapolated to patients with ACLF.

Key words: Acute-on-chronic liver failure; Acute liver failure; Plasmapheresis; Plasma exchange; Liver failure

Core tip: High volume plasmapheresis has been shown to improve survival in non-transplanted patients with acute liver failure. However, there has not been, to date, a review article that summarizes the different plasmapheresis regimens and its effect on mortality and improvement of liver biochemistry. This review article serves as a summary and appraisal of available literature on plasma exchange in liver failure taking into account the volume of plasma exchange, duration of plasmapheresis, and etiology of liver failure in conjunction with the study outcomes of interest and highlights potential areas which might be essential to include in future good quality randomized controlled trials.

Citation: Tan EXX, Wang MX, Pang J, Lee GH. Plasma exchange in patients with acute and acute-on-chronic liver failure: A systematic review. *World J Gastroenterol* 2020; 26(2): 219-245
URL: https://www.wjgnet.com/1007-9327/full/v26/i2/219.htm
DOI: https://dx.doi.org/10.3748/wjg.v26.i2.219

INTRODUCTION

Acute and acute-on-chronic liver (ACLF) carry high short-term mortality rate, and may result from a wide variety of causes. Regardless of its underlying etiology, liver failure at its final stages results in jaundice, hepatic encephalopathy, hepato-renal syndrome, hemodynamic instability, increased susceptibility to severe infections and finally multi-organ failure[1].

Acute liver failure has been defined as a rapid decline in hepatic function characterized by jaundice, coagulopathy, and hepatic encephalopathy in patients with no prior liver disease. There are more overlaps in terminologies for ACLF, and there are currently more than ten definitions of ACLF. The two most widely used definitions are from the Asian Pacific Association for the Study of the Liver (APASL) and the European Association for the Study of the Liver (EASL) Chronic Liver Failure consortium[2]. Besides treating the underlying etiologies and supportive therapy, liver transplantation is the only definitive therapy for those with advanced disease. However, the availability of donor organ limits the availability of the patients that can be saved.

In recent years, there is increasing interest in plasma exchange for the treatment of liver failure. Since Larsen *et al*[3] published the first open randomized control trial of plasma exchange in patients with acute liver failure in 2016, plasmapheresis has been added to the armamentarium. High volume plasma exchange has been included in European guidelines[1] as level I, grade 1 recommendation in management of acute liver failure. Its proposed mechanism is removal of plasma cytokines and drivers of

systemic inflammatory cascade through plasma exchange. Preceding the aforementioned publication, published studies on the use of plasma exchange in the setting of liver failure were mostly retrospective case series or cohort studies. These studies differed greatly in the protocols of plasma exchange. In ACLF, the data is less clear.

The objectives of this review is to provide a summary and analysis of the current evidence for the use of plasmapheresis in patients with ACLF and acute liver failure (ALF) and its effect on mortality particularly in the non-transplanted patients. In addition, the review will summarise the current literature on volume of plasma used during exchange, the duration and frequency of plasma exchange and briefly outline other available apheresis or liver support devices used in liver failure.

MATERIALS AND METHODS

Eligibility criteria

We included studies ranging from case reports to randomized control trials that have been published till 30 March, 2019. We excluded abstracts in this review and have restricted to only studies in English. We excluded studies with insufficient information concerning our outcomes of interest and areas of comparison: *e.g.*, survival, the volume of plasma exchange and type of product exchanged. We included studies with only human participants diagnosed with liver failure who underwent plasma exchange, with or without other alternative liver support systems. There were no restrictions on the dose, duration, and type of plasma exchange (Table 1 for PICOS criteria). A PRISMA checklist was also used to guide the development of the systematic review.

Information sources

A comprehensive search of databases and conference proceedings to identify all relevant studies up to 30 March, 2019 was performed. The following electronic databases were searched: MEDLINE *via* PubMed, and EMBASE. We use both text words and medical subject heading terms. The literature search strategy was adapted to suit each database.

For example, on PubMed we use the combination of the following medical subject heading terms "plasma exchange" or "plasmapheresis" and "liver failure" or "acute liver failure" or "acute on chronic liver failure". Search was limited by "Case reports", "Classical article", "Clinical study", "Clinical trial", "Controlled clinical trial", "Observational study", "Randomized controlled trial", "Review", "Humans", "English", "Core clinical journals" and "MEDLINE". The methods for data collection and analysis were based on the Cochrane Handbook of Systematic Reviews for Interventions. Where clarification of information in published data was required, corresponding authors were contacted through electronic mail for clarification.

Selection of studies, data collection and summary measures

Two review authors (Tan EXX and Lee GH) independently reviewed relevant material identified from the above search. After reading the titles and abstracts of the identified articles, full-text articles of all citations deemed to meet the inclusion criteria were sought. Duplicates were excluded. Each article was independently inspected to verify that they meet the pre-specified inclusion criteria. Study selection process is being summarized in Figure 1. Studies that were included in this systematic review are included in Tables 2-5. We created a case report form specifically for this study for systematic study review/selection and structured data extraction. Relevant study data was independently reviewed selected and extracted. Outcomes of interest such as all-cause mortality, changes in liver biochemistry, and survival in non-transplanted patients were primary outcomes of interest. The volume of plasma exchange used, duration of exchange, and etiology of liver failure were also compared in conjunction with study outcomes of interest.

In addition, pooled odds ratios and its corresponding 95% confidence intervals were respectively calculated for 30- and 90-d mortality in ACLF patients using the random effects model. The data extracted for this calculation includes the number of events (deaths) for the respective time periods and total sample size in the intervention and control arms, and were extracted in duplicate by ET and MXW. The I^2 statistic and Cochran Q test was used to evaluate statistical heterogeneity, where heterogeneity was characterized as minimal (< 25%), low (25%-50%), moderate (50%-75%) or high (> 75%) and was significant if $P < 0.05$. All calculations performed were 2-sided and done through Review Manager 5.3.

Table 1 Participants, interventions, comparisons, outcomes and study design criteria used to define the research question for this systematic review

Variable	Description
Population	Humans diagnosed with liver failure (ALF/ACLF)
Intervention	Plasma exchange with or without other alternative liver support systems; no restrictions on dose, duration and type of plasma exchange
Comparator	Randomized controlled trials/Cohort studies: Standard medical treatment
	Case series/case reports: Nil
Outcome	All-cause mortality, changes in liver biochemistry, and survival in non-transplanted patients
Study design	Randomized Controlled Trials, Cohort studies, Case series, Case reports
Research question	Does plasmapheresis have an effect on all-cause mortality, changes in liver biochemistry, and survival in non-transplanted patients with ALF/ACLF, compared to standard medical treatment?

ALF: Acute liver failure; ACLF: Acute-on-chronic liver failure.

RESULTS

Search results

A total of 324 records were reviewed, of which 62 duplicates studies were removed. Of the 262 records screened, 211 studies were excluded. Fifty-one articles were assessed for eligibility, for which 7 were excluded (Figure 1). Twenty-nine studies were included for ALF only, and 9 studies for ACLF only. Six studies included patients who had both ALF and ACLF. A total of 44 publications were included (Figure 1).

Plasma exchange in ALF

A total of 35 studies included patients with ALF (Table 2, Table 3, and Table 5). Of this, 24 were studies in adults and 11 in the pediatric population (Table 3 and Table 5). In the studies that included adult subjects, 4 also included patients with ACLF. Of the 24 studies in adults, there was 1 randomised controlled trial, 4 cohort studies, 9 case series and 10 case reports. Of the 11 studies with pediatric subjects, there was 1 cohort study, 4 case series and 6 case reports; and 2 of the 11 studies included patients with both ALF and ACLF.

Mortality

There is only one randomized trial to date[3] that assessed transplant-free survival comparing standard medical treatment (SMT) *vs* plasma exchange and SMT in patients with ALF. In the Larsen *et al*[3] study, high volume plasma exchange (HVP) increased survival in non-transplanted patients after three months. However, there was no significant difference in the effect of HVP in patients who received emergency liver transplantation. Of the three studies comparing plasma exchange *vs* SMT or alternative liver support systems, all reported an improvement in survival in patients who did not undergo liver transplant[3,4] or improvement in survival days[5].

Biochemical improvement

All studies that assessed biochemical improvement pre- and post-plasma exchange, found an improvement in biochemical parameters such as coagulopathy, bilirubin, aspartate aminotransferase (AST), alanine aminotransferase or ammonia. However, biochemical improvement did not directly relate to mortality outcome. Even in the patients who did not survive, there was also biochemical improvement post- plasma exchange[5].

Standard vs high volume plasma exchange and other liver assist devices

There is heterogeneity in the amount of plasma exchange a patient gets in ALF amongst the various studies. Two studies[3,6] used plasma exchange at least 15% ideal body weight removal at 1-2 L per hour while in Buckner *et al*[7]'s case series, plasma exchange with 10 L of donor plasma regardless of weight was used. Similar to Buckner *et al*[7], Damsgaard *et al*[8] in a case report used 8-9 L of plasma per session for plasma exchange for a patient with ALF from Wilson's disease, who survived without need for liver transplant. In contrast, in case series by Akdogan *et al*[9], only one-plasma volume was being exchanged daily till patient expired or improved. Majority of studies used approximately 2-4 L of fresh frozen plasma at each plasma

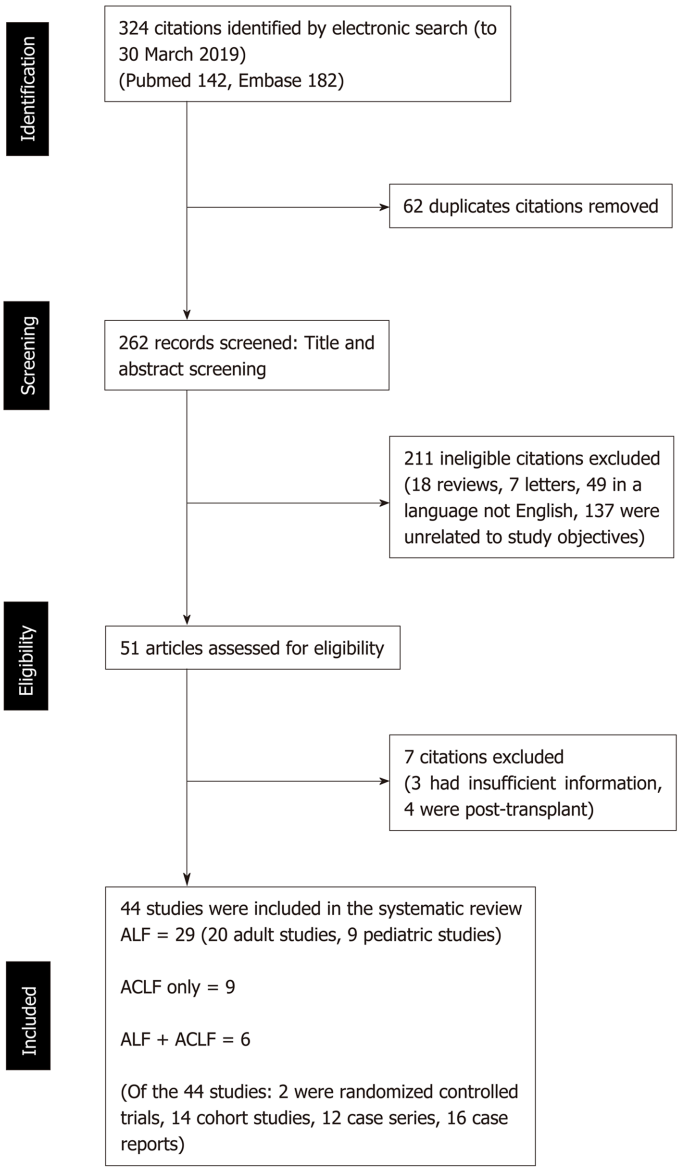

Figure 1 Summary of study selection process.

exchange[4,10-18].

While there are stark differences in amount of plasma exchanged in these aforementioned studies, in the study of the use of plasma exchange in the treatment of acute liver failure, there is only one open randomized controlled trial[3] favoring the use of high volume plasma exchange over standard medical treatment. There are no head to head studies comparing high volume to standard volume plasma exchange. Although most cohort studies or case series that used 2-4 L of plasma and or additional fluid for plasma exchange saw positive results whereby there were reported improvement in biochemical parameters such as bilirubin and coagulopathy[4,5,9,11,12,14-16,18,19], and some of which also reported increased transplant-free survival days[5], at present evidence favor large volume plasma exchange for treatment of ALF[3].

There is currently no clear evidence to support the use of other assist devices in addition to plasma exchange in management of ALF. Several studies[4,10,20] included alternative assist devices to plasma exchange and made comparisons of its efficacy in the treatment of acute liver failure. For example, comparing plasma exchange *vs* plasma exchange + continuous venovenous hemodiafiltration (CVVHDF), Nakae *et al*[10] showed that the latter resulted in a decrease in inflammatory mediators and an increase in citrate compared to the former group. Another study, also by Nakae *et al*[10], reported use of plasmadiafiltration, a blood purification therapy where plasma exchange is performed using a selective membrane plasma separator while the dialysate flows outside the hollow fibers for management of ALF. In that study[21], less

Table 2 Studies included for study of plasmapheresis in acute liver failure in adults

Ref.	Type of study/No. of patients recruited	Study group(s)	Plasma exchange regime	Etiology of liver failure	Results/outcome(s) of interest
Larsen *et al*[3]	Open randomized control trial; *n* = 182 (Plasma exchange + SMT 92, SMT 90)	PE + SMT *vs* SMT	Plasma exchange volume: Volume of plasma exchange was 15% of ideal body weight (representing 8-12 L per day per procedure); patient plasma was removed at a rate of 1-2 L per hour with replacement with fresh frozen plasma in equivalent volume HVP procedure was undertaken on three consecutive days but with no fixed time interval between each treatment Mean number of HVP = 2.4 ± 0.8 Plasma exchange with donor plasma	Predominantly paracetamol (59%), followed by unknown etiology, toxic hepatitis, viral hepatitis, acute Budd Chiari syndrome	HVP increases transplant free survival after 3 mo, and maximal effect of HVP was achieved in patients who did not undergo emergency transplantation Overall hospital survival was 58.7% for patients treated with high volume plasma exchange *vs* 47.8% for control group HR: 0.56 (95%CI: 0.36-0.86), $P < 0.01$ However, HVP prior to transplantation did not improve survival compared with patients who received SMT alone $P = 0.75$ Bilirubin, INR, ALT and ammonia concentration decreased significantly during the first 7 d compared to SMT
Nakae *et al*[10]	Prospective cohort study; *n* = 13	PE *vs* PE + CHDF	Plasma exchange volume: 3.6 to 4.0 L of plasma was exchanged for the same volume of normal FFP, interval between sessions was 48h or more for both treatment methods Plasma exchange with FFP	7 post surgery, 4 fulminant hepatitis, 4 sepsis	Total bilirubin levels were significantly lower after treatment in both arms: Both $P < 0.01$ in both groups No outcomes available on mortality Of note, decreased increase in citrate in patients with PE CHDF compared to PE alone
Hung *et al*[5]	Retrospective cohort study; *n* = 62 (Control 32, PE 30)	PE *vs* control	Average plasma exchange volume: 2916 mL (range, 1875-3750 mL), plasma exchange occurred over 2 h	46.7% HBV, 33.3% Drug induced, 6.7% unknown, 33.3% cirrhosis.	At the end of the first week (week 1), the level of total bilirubin and grading of hepatic encephalopathy in the PE group were significantly lower than those in the control group. At the end of the second week (week 2), there were no differences in the level of total bilirubin and grading of hepatic encephalopathy between the two groups of patients
			Average of 6 rounds of exchange per patient (range, 2-15 rounds) Plasma exchange with FFP	No significant differences in etiology of liver failure between treatment and control groups	Difference in survival rate was not significant 66.7% in PE group *vs* 59.4% in control group Difference in survival days were significant, with 17.63 ± 1.86 in PE group *vs* 8.69 ± 0.86 in control group. $P = 0.01$

Li *et al*[4]	Retrospective cohort study; *n* = 61	PE + HP + CVVHDF, PE + CVVHDF and HP + CVVHDF	Plasma exchange volume: 2000-3000 mL of fresh per session. Flow rate was 80-120 mL/min, the plasma separation rate was 25-30 mL/min, the replacement time was 2.0-3.0 h In the PE + HP + CVVHDF group: After completion of a single plasma exchange, the HP was carried out. After HP, the CVVHDF is carried out Total of 171 exchanges were done	3/61 acute viral hepatitis, 17/61 chronic toxic acute liver failure. 41 cases of non-viral induced liver injury: 5 after cardiac surgery, 7 with drug poisoning, 13 cases after pregnancy childbirth, 1 case mushroom poisoning, 10 cases with severe infection, 5 others	Treatment of the 61 patients using the artificial liver support system yielded a survival rate of 62.3% (38/61), and a viral survival rate of 35.0% (7/20); with the non-viral survival rate being 75.6% (31/41) Biochemically PE + HP + CVVHDF and PE + CVVHDF groups saw improvement in total bilirubin, ALT, PT, Albumin and HP+CVVHDF saw improvement in total and ALT ($P < 0.05$)
Nakamura *et al*[11]	Retrospective case series *n* = 49; Fulminant hepatitis 15; Severe acute hepatitis 14; Healthy controls 20	No comparative arm	Plasma exchange volume: Approximately 2000–4000 mL of fresh-frozen plasma was substituted during each exchange Plasma exchange with FFP	No mention	10/15 fulminant hepatitis and all severe acute hepatitis survived Significant decreases in circulating TNF-a, IL-6, and TGF-ß levels in patients with fulminant hepatitis after a single plasma exchange
Akdogan *et al*[9]	Retrospective case series; *n* = 39 (fulminant hepatic failure)	PE, No comparative arm	Plasma exchange volume: Total plasma volume approximately 1 Plasma exchange continued on a daily basis till clinical response (subjective by ICU team) or patient expired, or transplanted No need for calcium replacement or magnesium replacement Plasma exchange with low volume citrate plasma	Predominantly undetermined (41%), paracetamol (28.5%), acute hepatitis B, autoimmune liver disease, vascular tumor, acute hepatitis A (in presence of cirrhosis)	Improved biochemically (coagulopathy hyperbilirubinemia, AST, Ammonia, Factor V levels): $P < 0.05$ 31% underwent liver transplant, 92% of which survived at 1 year Overall survival 54% (21/39 patients), 37% (10/27) of non-transplanted patients survived
Kondrup *et al*[6]	Case series; *n* = 11	PE, No comparative arm	Plasma exchange volume: 20% body weight plasma exchange intended on three consecutive days, obtained a mean 2.6 exchanges and mean volume 16% body weight Plasma exchange with donor plasma.	6 acetaminophen, 2 non-A/B hepatitis, Halothane, disulfurum toxicity and hepatitis B	5/11 survivors were all acetaminophen toxicity induced ALF All had improved bilirubin after treatment All 4 Grade IV encephalopathy patients all did not survive Those that survived had Grade III encephalopathy or lesser Those that did not survive had a longer duration of coma before initiation of PE (3.5 *vs* 1.8 d)

Freeman *et al*[13]	Case series *n* = 9	PE, No comparative arm	Plasma exchange volume: 3 L of plasma exchange was performed daily until conscious level improved or patient died Plasma exchange fluid: Equal volume of compatible fresh frozen plasma and plasma protein fraction (PPF) usually in the proportion of 2 units FFP:1 PPF	4 acetaminophen, 2 nonA/B hepatitis, 1 hepatitis A, 1 mixed drug overdose, 1 ETOH in 2	7/9 showed improvement in coma grades, 5 achieved normal mental state, 5 were able to discharge from hospital. Of which 3 were paracetamol induced liver failure, 1 was monoamine oxidase/ tricyclic acid induced, 1 was alcohol. Survival 55% Improved biochemistry, bilirubin, coagulation ($P < 0.01$) 1 died of retroperitoneal bleeding
Buckner *et al*[7]	Case series *n* = 4 (1 pediatric)	PE, No comparative arm	Plasma exchange volume: Initial 10 L/day plasma exchange with FFP or fresh/outdated plasma	1 Acute viral hepatitis (pediatric), 2 halothane, 1 hepatitis B viral hepatitis	1 died (pediatric) 1 patient took 37 d to awake from coma 3/4 of patients survived
Liu *et al*[31]	Case series *n* = 2	PE, No comparative arm	Plasma exchange volume: Each treatment lasted for 4-6 h, and the total volume exchanged was approximately 7000 mL (1.5-2x TPV) Plasma exchange fluid: Maximally, 4700 mL of FFP was exchanged in each session, and the rest comprised plasma substitute consisting of 25% human albumin, pentastarch, 0.9% saline, and Ringer's solution. In each session, the plasma substitute was exchanged initially, and FFP was exchanged at the end Duration of PE was based on clinical improvement, both patients had intermittent PE, total 3 sessions	DILI	The two patients with DILI ALF were treated with PE without need for transplant Biochemically improved after PE (AST ALT Bilirubin)
Bilgir *et al*[15]	Case report	PE, No comparative arm	Plasma exchange volume: Each session consists of 15 units of FFP, total 4 sessions Plasma exchange fluid: FFP	L-asparaginase induced ALF	Patient recovered from ALF: However, no biopsy done
Aydemir *et al*[14]	Case report	PE, No comparative arm	Plasma exchange volume: 2500 mL plasma volume removed during each PE session Plasma exchange fluid: Fresh frozen plasma	PTU induced ALF	Patient recovered from ALF: however, no biopsy done
Riveiro-Barciela *et al*[28]	Letter to editor, case report (Ipilimumab)	PE, No comparative arm	Plasma exchange volume: 1500mL of 5% albumin plus 4 units of plasma as replacement fluid, carried out every other day for total 5 treatments Plasma exchange fluid: FFP and 5% albumin	Immunotherapy induced ALF	Patient improved. Liver tests within normal values within one month
Damsgaard *et al*[8]	Case report (ALF in WD)	PE, No comparative arm	Plasma exchange volume: 8-9 L of plasma, total 12 HVP	Fulminant Wilson's disease ALF	Even though WD ALF score was 16, patient survived without need for OLT

			Plasma exchange fluid: Fresh frozen plasma as replacement fluid 1:1		
Göpel *et al*[33]	Case report (Letter to editor)	PE, No comparative arm	Plasma exchange treatment was performed for three consecutive days No mention of volume or type of exchange fluid	Peg-asparaginase induced ALF	Patient improved. Continuous stabilization of fibrinogen and antithrombin 3, an increase of cholinesterase, and a decrease of bilirubin. Clinical signs and symptoms such as jaundice and ascites did also rapidly improve
Lin *et al*[16]	Case report	PE, no comparative arm	Plasma exchange was performed 2 times per week, and 2000 to 2500 mL frozen plasma was used each time	HLH	Patient's condition deteriorated, and he died of multi-organ failure during the 6th week of hospitalization. Autopsy was declined
Chen *et al*[29]	Case report	PE, No comparative arm	Plasma exchange volume: Estimated two times the plasma volume of the patient was exchanged. At most, 40 units of FFP were exchanged, with the remainder of the infused volume consisting of plasma substitutes. The plasma substitutes consisted of 25% human albumin, pentastarch, normal saline, and Ringer's solution	Heat stroke	On day 4 after the admission, the patient received high-volume PE (two plasma volumes exchanged). His consciousness was improved a day after PE The patient was discharged on day 16 after admission without sequelae
Holt *et al*[17]	Case report	PE, No comparative arm	Plasma exchange on post-partum days 3-5. Volume: Average of 3.2 L (1.6 estimated plasma volumes) of FFP replaced per session, followed by a tapering course of prednisone	AFLP *vs* HSV hepatitis associated ALF	After 3 d of TPE the patient's mental status had returned to normal Treatment with TPE was followed by biochemical and clinical improvement but during her recovery herpes simplex virus type 2 (HSV2) infection was diagnosed serologically and confirmed histologically
Shen *et al*[18]	Case report	PE, No comparative arm	Plasma exchange: performed on days 1, 3, and 5, with 3000 mL of plasma exchanged during each session	Occupational Exposure to Tetrachloroethylene	Bilirubin, ammonia, and prothrombin time improved before hospital discharge and patients mental status gradually became normal discharged on day 26 of hospital admission
Pashaei *et al*[30]	Case report	PE, No comparative arm	Plasma exchange volume 2.5L Plasma exchange fluid: FFP	Wilson's disease	36 h after initiation of PE, encephalopathy recovered and there was no renal impairment. Copper, LDH total bilirubin decreased after the treatment

PE: Plasma exchange; SMT: Standard medical treatment; ALF: Acute liver failure; HLH: Hemophagocytic lymphohistiocytosis; FFP: Fresh frozen plasma; INR: International normalised ratio; ALT: Alanine aminotransferase; CVVHDF: Continuous venous-venous hemodiafiltration; CHDF: Continuous hemodiafiltration; HBV: Hepatitis B virus; HSV: Herpes simplex virus; LDH: Lactate dehydrogenase; DILI: Drug induced liver injury; AFLP: Acute fatty liver of pregnancy; DILI: Drug induced liver injury; TPE: Therapeutic plasma exchange.

plasma was used per cycle: 1200 mL fresh frozen plasma (FFP) and 50 mL of 25% albumin per session. However, patients had an average of 8.3 cycles of plasmadiafiltration, which is higher compared to other studies (Table 2). Transplant

Table 3 Studies included in for study of plasmapheresis in acute liver failure in pediatric cohort

Ref.	Type of study / No. of patients recruited	Study group(s)	Plasma exchange regime	Etiology; Age	Results
Pham *et al*[19]	Case series *n* = 10	PE, No comparative arm	Plasma volume: Targeted 1-1.25 plasma volumes Plasma exchange fluid: 77% of procedures were performed with plasma as sole replacement fluid while 23% used the combination of plasma and 5% albumin Median number of TPE: 3.5	Wilsons Disease Age 6-61 yr	Post TPE 9 patients underwent liver transplantation and all 10 patients had at least 6 mo survival Median days from first to OLT was 1-53 d
Chien *et al*[22]	Retrospective case series *n* = 23	PE, No comparative arm	Plasma exchange volume: Plasma exchange was usually performed daily for the first 3 d, and then shifted to every other day or every 3 d according to the patient's condition Plasma exchange volume: 2–4 times the patient's estimated plasma volume Plasma exchange fluid: FFP	60% idiopathic, 17% infection, 8% metabolic and immunologic, 4% toxin Age 0.29-9.25 yr	11 (48%) had native liver recovery (NLR), 9 (39.1%) died without liver transplant, and 3 (12.9%) received liver transplantation The no liver recovery group showed a lower proportion of idiopathic cases, lower peak ammonia level, higher peak alpha fetoprotein (AFP) level, and they had plasma exchange fewer times than the other groups
Ide *et al*[47]	Retrospective case series *n* = 17	PE/CVVHDF, No comparative arm	CVVHDF and PE were applied in all ALF patients PE using 100 mL/kg of FFP per treatment course was implemented once daily for 6 to 8 h until the recovery of coagulopathy	2/17 viral 1/17 mitochondrial 14/17 indeterminate Age 1-11 mo [Median Weight 8.0 (2.7-10 kg)]	All laboratory results relating to liver dysfunction decreased significantly after CVVHDF + PE Overall survival rate 88% with median follow up period of 28 mo
Verma *et al*[23]	Case report	PE, No comparative arm	Plasma exchange volume: 1.5-2 h, 1.2 L plasma exchange in each session, in addition to oral D penicillamine and Zinc	Wilson's disease Age 5 yr (Weight: 15 kg)	Patient improved initially but subsequently deteriorated fter developing renal failure and shock, and died from acute pulmonary hemorrhage.
Morgan *et al*[25]	Case report	PE, No comparative arm	Plasma exchange volume: 1500 mL TPE, 5 single plasma volume over 11 d in addition to trientine Plasma exchange fluid: Plasma	Wilson's disease Age 6 years	Patient had worsening bilirubin, coagulopathy despite treatment and underwent OLT 12 d after beginning TPE
Zhang *et al*[24]	Case report	PE, No comparative arm	Plasma exchange volume: 1200 mL each time, with blood flow velocity of 45–50 mL/min, plasma separation speed of 650–750 mL/h, and a replacement time of approximately 2 h. Total 9 exchanges Plasma exchange fluid: FFP	Wilson's disease Age 7 yr (Weight 21 kg)	CPFA started after PE. The patient had rapid recovery of consciousness, removal of copper and stabilization of serum bilirubin and hemoglobin. 9 d after last PE patient underwent liver transplant.

Yukselmis *et al*[26]	Case report	PE, No comparative arm	Plasma exchange volume: 1.5 times total blood volume then 1 time for the subsequent courses Total 3 sessions PE on top of ostelmavir Plasma exchange fluid: FFP	Viral (Influenza) Age 4 yr (Weight 16 kg)	Patient did not require transplantation in light of clinical improvement and PE resulted in complete recovery
Ponikvar *et al*[27]	Case report	PE+HD, No comparative arm	Plasma exchange volume: 3 volumes of plasma (12% of body weight of 16 kg) per procedure were exchanged (1972 ± 85 mL; range, 1800–2150 mL). FFP was used as the replacement solution. An equal volume of plasma was removed and replaced A total of 13 PEs, 13 HD sessions, and 9 HBO treatments over a period of 1mo. The initial 4 PEs were followed by HD sessions while the other 8 PE treatments were given simultaneously with HD. There was no renal failure; HD was instituted to improve ammonia elimination	Unknown Excluded viruses and metabolic cause Age 3 yr (Weight 16 kg)	Patient did not improve after 1 mo and was referred to a liver transplant center and successfully transplanted. Patient also had hyperbaric oxygen (HBO) during treatment
Harmanci *et al*[48]	Case report / Letter to editor	PE, No comparative arm	Plasma exchange volume: 2.5 L per session Started daily and continued for 7 consecutive days	Wilson's Disease Age 17 yr	Patients mental status improved and was extubated and weaned from mechanical ventilation on the fifth day of hospitalization. The patient did not require liver transplantation. The patient was treated continously with zinc and D-penicillamine

CPFA: Continuous plasma filtration adsorption; HBO: Hyperbaric oxygen; PE: Plasma exchange; SMT: Standard medical treatment; ALF: Acute liver failure; HLH: Hemophagocytic lymphohistiocytosis; FFP: Fresh frozen plasma; INR: International normalised ratio; ALT: Alanine aminotransferase; CVVHDF: Continuous venous-venous hemodiafiltration; CHDF: Continuous hemodiafiltration; HBV: Hepatitis B virus; HSV: Herpes simplex virus; LDH: Lactate dehydrogenase; DILI: Drug induced liver injury; AFLP: Acute fatty liver of pregnancy; DILI: Drug induced liver injury; TPE: Therapeutic plasma exchange; AFP: Alphafetoprotein.

free survival rate was 38.1%, 54.5% in ALF, and 20% in fulminant hepatitis; there was no control arm. Pediatric studies were evaluated separately, and in the included pediatric studies[19,22-27], the amount of plasma exchange per session ranged from 1-4 plasma volumes per exchange.

FFP vs albumin

Most studies used 100% FFP for plasma exchange with the exception of few studies[13,19,21,28-31], where plasma substitutes or albumin were used in conjunction with plasma. For example, in a case series by Liu *et al*[31], Seven liters of fluid was used for plasma exchange, but the first 4.7 L was composed of fresh frozen plasma, while the rest comprised of plasma consisting of 25% human albumin, 0.9% saline and Ringer's solution.

There are by far no studies that use pure albumin as replacement fluid for plasma exchange in ALF. However, Collins *et al*[32] has described in their case report, a patient with fulminant hepatitis from Wilson's disease who underwent single-pass albumin dialysis (SPAD) with improvements in bilirubin. Although of note, the same patient underwent plasma exchange after stopping SPAD in view of serum copper rebound.

Three-day therapy versus intermittent or response guided

As aforementioned, only few[3,6,18,33] studies used a strict consecutive daily or every

Table 4 Studies included for study of plasmapheresis in acute-on-chronic liver failure

Ref.	Type of study/Number of patients recruited	Study group(s)	Characteristics of study population	Plasma exchange regime	Etiology	Results
Meng *et al*[39]	Retrospective cohort study, single center; *n* = 158; PE group: 38; SMT group: 120	PE *vs* SMT	PE group: Higher MELD score Baseline characteristics both groups had 26%-28% of patients with hepatic encephalopathy ACLF definition: ACLF was defined as serum bilirubin ≥ 5 mg/dL and an INR 1.5 or prothrombin activity (PTA) 40 %, complicated within 4 wk by ascites and/or encephalopathy in patients with previously diagnosed or undiagnosed chronic liver diseases	Performed twice a week until patients' condition was stable, additional weekly or biweekly visits were instituted if patients felt deterioration of their condition. Total duration of therapy 2-8 wk Plasma exchange volume not mentioned	Hepatitis B	24/38 (63%) death in the PE group and 82% in SMT group died within 4 wks. By week 12, 71% in PE group and 86% in SMT group died 18% *vs* 14% transplant free survival in 3 mo comparing PE *vs* SMT ($P < 0.01$) Biochemically, there is decreased bilirubin in PE arm cf SMT ($P < 0.01$)
Mao *et al*[38]	Retrospective cohort study, single center PE group: 62 SMT group 131 Not randomised	PE *vs* SMT Baseline characteristics 74%-77% had HE at baseline	ACLF definition: Acute decompensation of liver function in patients with chronic preexisting liver diseases. ACLF is defined as a syndrome with severe jaundice (total bilirubin: 171 mmol/L), coagulopathy (prolonged prothrombin time, prothrombin activity 40%), or hepatic encephalopathy (above grade II)	Plasma exchange volume: 3500 mL at 25-30 mL/min. A total of 3000–4500 mL of fresh frozen plasma (40-60 mL/kg) and 20-40 g of human albumin were supplied Flow rate of blood was adjusted to 60–130 mL/min PE was carried out 2-3 times per week for the first two weeks, then weekly, then stopped based on clinical results	Hepatitis B. Drug hepatitis, Wilson disease, alcoholic liver disease, autoimmune hepatitis excluded	26 survivors and 36 non-survivors were in the PE group, whereas 33 survivors and 98 non-survivors were in the control group after 30 d treatment. Their survival rates were 41.9% and 25.2% for PE and medical therapy, respectively ($P < 0.05$) No mention re: Biochemical improvement

Chen *et al*[42]	Retrospective cohort study multicentre (10) *n* = 250 patients	PE, no comparative arm	ACLF definition: Guidelines for Diagnosis and Treatment of Liver Failure in China (2006): Early stage is defined as a progressively deepening jaundice (Bilirubin level ≥ 171 μmol/L or a daily increase of ≥ 17.1 μmol/L), PTA > 30% but ≤ 40%, and no HE or other complications. Middle-stage disease represents progression of the symptoms of the early stage, including one of the following symptoms: Grades I/II HE, ascites, or a PTA of > 20% but ≤ 30%. In the end-stage disease, the condition deteriorates further with a PTA of ≤ 20% and includes one of the following symptoms: Hepatic-renal syndrome, severe upper gastrointestinal bleeding, serious infection, and grades III/IV HE	Plasma exchange volume: 2500-3500 mL, and the PE rate was 20-25 mL/min Dexamethasone (5 mg) and heparin (2500 U) were injected routinely before PE PE was repeated every 2-4 d	Hepatitis B	Forty-two of the 52 (80.8%) patients in the early stage, seventy-five of the 99 (75.8%) patients in the middle stage and thirty-seven of the 99 (37.4%) patients in the end stage survived for one month after diagnosis Authors concluded that late stage ACLF might benefit from PE as a bridge to definitive treatment-liver transplant
Zhou *et al*[45]	Retrospective, cohort Derivation cohort 113 Validation cohort 68 From the derivation cohort: PE, *n* = 54; PE+PA, *n* = 59	PBA + PE *vs* PE	ACLF was defined as acute liver injury emerging as jaundice and coagulopathy, complicated by ascites and/or encephalopathy within 4 wk in a patient with known or unknown chronic liver disease. The definition of liver failure in ACLF was as follows: Severe jaundice (total serum bilirubin ≥ 5 mg/dL) and coagulopathy (INR ≥ 1.5 or prothrombin activity < 40%) and ascites and/or encephalopathy. Baseline population in this study is 51% cirrhotic	Plasma exchange volume: Approximately 3000 mL of plasma was exchanged per time at a blood flow rate of 20 to 25 mL/min Each patient in the derivation cohort received PE 1 to 4 times	HBV 56.6%, HBV+HEV 31.9% Others 11.5%	The mean overall survival for the derivation cohort was 441 d (95%CI: 379-504), and the 90- and 270-d survival probabilities were 70.3% and 58.3%, respectively The mean survival times of patients treated with PBA plus PE and patients treated with PE were 531 days (95%CI: 455-605) and 343 d (95%CI: 254-432), respectively (*P* = 0.012) Predictors of survival: Age, MELD, Complication, type of ALSS No mention re: Baseline characteristics of PE *vs* PBA

Wan *et al*[44]	Prospective cohort study *n* = 60 TPE 33 DPMAS 27	PE *vs* DPMAS	ACLF was defined as serum bilirubin 5 mg/dL and INR > 1.5 or PTA < 40%, complicated within 4 wk by ascites and/or HE in patients with previously diagnosed or undiagnosed chronic liver diseases Baseline eAg positive greater in TPE group (18% *vs* 7.4%)	Plasma exchange volume: About 3000 mL of plasma exchanged at an exchange rate of 20-30 mL/min at each session. PE was performed 2-3 times/week, lasting 2-3 h every session	HBV	During the study, a total of 42 patients died, with 24 in TPE group and 18 in DPMAS group. The median survival times were 12 wk in TPE group and 11 wk in DPMAS group The 4-wk and 12-wk survival rates in TPE group and DPMAS group were 87.9% and 88.9%, 34.6% and 33.3%, respectively. There was no marked difference in survival between the two groups Bilirubin removal in TPE more efficient compared to DPMAS
Qin *et al*[37]	Open label randomized controlled parallel group single-center study *n* = 234	PE centered ALSS *vs* SMT	Definition of ACLF was according to the Chinese guidelines, Bilirubin ≥ 10 mg/dL, PTA ≤ 40% and cirrhosis and multiorgan failure were not taken as mandatory criteria, according to the Chinese guidelines	PE volume: 3500 mL (40–60 mL/kg) FFP, at 25-30 mL/min ALSS schedule: 3 routine treatments were performed in the first 10 d after inclusion in the study (once per 3–4 d); extra treatments were offered according to the improvement of the patients. The methods of PE-centered ALSS were chosen based on clinical conditions. For patients with coagulopathy, PE was applied; for patients with encephalopathy, PE plus hemoperfusion or continuous hemodiafiltration was used; for patients complicated with HRS or imbalance of water or electrolytes, PE plus continuous hemodiafiltration was used	HBV	Survival rates after 90 d were 60% (62/104) in ALSS-treated patients and 47% (61/130) in the control group. (P < 0.05). The 5-year cumulative survival rates of the ALSS and control groups were 43% (45/104) and 31% (40/130), respectively (P < 0.05) No mention of biochemical improvement
Xia *et al*[40]	Retrospective cohort study *n* = 882 460 NBAL 422 control	NBAL (all had PE) *vs* SMT	ACLF definition: 1 Acute deterioration of pre-existing chronic liver disease 2 Extreme fatigue with severe digestive symptoms, such as obvious anorexia, abdominal distension or nausea and vomiting	All of the patients were treated with PE, and most were treated with one or more additional methods, including 13/26 (50.00%) ALF patients, 16/27 (59.26%) Subacute ALF patients, and 228/407 (56.02%) ACLF patients	For ACLF: 91.24% chronic hepatitis B, 3.69% alcohol abuse, 1.01% autoimmune, 1.01% cholestasis, 3.05% other causes	Clinical outcomes were improved after NBAL treatment. The 30-d survival rates of subacute liver failure (SALF) patients were 63% among those who received NBALs and 21% among those who did not receive NBALs (P < 0.01)

	Of which 49 ALF, 46 SALF and 787 ACLF		3 Progressively worsening jaundice within a short period (serum total bilirubin ≥ 10 mg/dL or a daily elevation ≥ 1 mg/dL) 4 Obvious hemorrhagic tendency with PTA ≤ 40% (PT ≥ 18.3 s or INR > 1.50) The absence of any of the above four criteria precluded a diagnosis of ACLF	The choice of therapy was based on each patient's condition: PE in combination with PP for HE was administered in 12.24% (6/49) of ALF patients, 10.77% (7/65) of SALF patients, and 7.41% (80/1079) of ACLF patients. In patients with HRS, we administered PE with CHDF in 32.65% (16/49) of ALF patients, 23.08% (15/65) sessions of SALF patients and 28.17% (304/1079) sessions of ACLF patients Pts underwent 1-4 times of NBAL each		The 30-day survival rate of acute-on-chronic liver failure (ACLF) patients who received NBALs was 47%, significantly higher than that of the non-NBAL patients ($P < 0.05$) Reported to be effective in biochemical improvement
Li *et al*[49]	Prospective cohort Study PE: 34 PE+UCMSCs: 11 *n* = 45	PE *vs* PE + UCMSCs	ACLF was defined as serum bilirubin ≥ 5 mg/dL and INR ≥ 1.5 or PTA < 40%, complicated within 4 wk by ascites and/or encephalopathy in patients with previously diagnosed or undiagnosed chronic liver disease In PE group: MELD score: 22.5 +/- 1.4, 61.8% cirrhotic	PE volume: About 3000 mL, and the exchange rate of plasma was 20–30 mL/min. Heparin was used as anticoagulant during PE	HBV	The cumulative survival rates at 3 mo in group A and group B were 54.5 % and 29.4 %, respectively (P = 0.015 by log rank test) INR was prominently lower in PE + UCMSCs group than in PE group ($P < 0.05$). At 12 mo, patients in PE+UCMSCs group showed lower levels of AST than patients in PE group ($P < 0.05$). At 24 mo, patients in PE+UCMSCs group had significantly improved levels of albumin, PT and INR than patients in PE group ($P < 0.05$). However, ALT, Total bilirubin, Direct bilirubin, creatinine, white blood cell, Hemoglobin, Platelet and ascites were comparable at each follow-up
Xu *et al*[43]	Retrospective cohort study *n* = 171 PE before LTx: 115 Emergent LTx: 56	PE	Definition of ACLF: Acute hepatic insult manifesting as jaundice and coagulopathy, complicated within 4 wk by ascites and/or encephalopathy in a patient with previously diagnosed or undiagnosed chronic liver disease PE group: MELD score 31+/-6	Total volume exchanged 3300 mL Patients with coagulopathy were indicated for PE, when the patient had HE, PE + hemodiafiltration was used. For patient with hepatorenal syndrome or imbalance of water or electrolytes, PE + continuous hemodiafiltration or MARS was used	HBV	1-yr and 5-yr survival rates in the ALSS-LT group and LT group were 79.2% and 83%, 69.7% and 78.6%

Yao *et al*[41]	Retrospective cohort study *n* = 131 PE group (*n* = 77) DPMAS + PE group (*n* = 54)	PE *vs* DPMAS + PE	Definition of ACLF: Acute hepatic insult manifesting as jaundice and coagulopathy, complicated within 4 wk by ascites and/or encephalopathy in a patient with previously diagnosed or undiagnosed chronic liver disease Baseline characteristics were similar in both groups	PE volume: Fresh frozen plasma was 2200 to 2400 mL per treatment. Duration of single treatment was about 2 h Patients underwent 1-4 times of PE / PE + DPMAS	HBV	The total bilirubin levels immediately after treatment at 24 and 72 h after treatment were markedly decreased in DPMAS + PE group compared to that in PE group (52.3 ± 9.4% *vs* 42.3 ± 7.2%, $P < 0.05$; 24.2 ± 10.0% *vs* 13.5 ± 13.0%, $P < 0.05$; 24.8 ± 13.1% *vs* 14.9 ± 14.9%, $P < 0.05$; respectively). The 28- d survival rates was 62.3% and 72.2% in PE and DPMAS + PE groups ($P = 0.146$). 28- d survival rates were significantly higher in DPMAS + PE group than that in PE group (57.4% *vs* 41.7%, $P = 0.043$) in the intermediate-advanced stage patients
Cheng *et al*[12]	Retrospective, cohort study single tertiary centre *n* = 55; 10 ALF, 45 ACLF	PE, no comparative arm	ACLF definition: acute hepatic insult that manifests as jaundice (serum bilirubin ≥ 5 mg/dL and coagulopathy (INR ≥ 1.5), which is complicated within 4 wk by clinical ascites and/or encephalopathy in a patient with previously diagnosed or undiagnosed chronic liver disease or cirrhosis 79% of patients with ACLF have cirrhosis, 55% have grades III-IV HE	The processed plasma volume was approximately 3000 mL for each session (1-1.5 total plasma volume); the blood flow rate was 100 mL/min; and the PE rate was 25–30 mL/min, with an equivalent volume of replacement fluid using fresh frozen plasma PE occurred daily or every other day till sustained clinical improvement, liver transplantation or no clinical response/death	Hepatitis B (75%) in ACLF group, 6% alcohol, others: HCV, AIH	Biochemical improvements seen after PE: AST/ALT/Bil/INR Average 4-5 sessions of PE in ACLF group, 3-5 sessions in ALF Initial diagnosis to PE is longer in non-survivors in ACLF and ALF though not significant Survival based on etiology of ACLF: 24% HBV, 67% ETOH, 0% HBV + alcohol, 0% HCV 0% HCV + alcohol, 0% AIH

PE: Plasma exchange; SMT: Standard medical treatment; ALF: Acute liver failure; HLH: Hemophagocytic lymphohistiocytosis; FFP: Fresh frozen plasma; INR: International normalised ratio; ALT: Alanine aminotransferase; CVVHDF: Continuous venous-venous hemodiafiltration; CHDF: Continuous hemodiafiltration; HBV: Hepatitis B virus; HSV: Herpes simplex virus; LDH: Lactate dehydrogenase; DILI: Drug induced liver injury; AFLP: Acute fatty liver of pregnancy; DILI: Drug induced liver injury; TPE: Therapeutic plasma exchange; DPMAS: Double plasma molecular adsorption system; AOCLF: Acute on chronic liver failure; PTA: Prothrombin activity; PBA: Plasma bilirubin adsorption; HE: Hepatic encephalopathy; DPMAS: Double plasma adsorption system; ALSS: Artificial liver support system; NBAL: Non-bioartifical liver support; SALF: Subacute liver failure; PP: Plasma perfusion; HRS: Hepatorenal syndrome; PT: Prothrombin time; UCMSCs: Umbilical Cord-Derived Mesenchymal Stem Cell Transplantation.

other day 3-d therapy plasma exchange regime as in the open-RCT by Larsen *et al*[3]. Instead, most studies continued plasma exchange till patient dies, or improves clinically, or receives a liver transplant at a range of intervals from every other day to intermittent (as and when necessary). Buckner *et al*[7] reported an interesting finding in their case series where a patient with halothane toxicity and acute liver failure received plasma exchange with 5-10 L of plasma almost daily for 37 d before she roused from coma. Few studies did not include detailed information on the frequency of plasma exchange[5,29,34].

Etiology specific outcome

Not all studies assessed included etiology of liver failure and its effect on transplant

Table 5 Studies included for use of plasmapheresis in acute liver failure and acute-on-chronic liver failure in adults

Ref	Type of study/No. of patients recruited	Comparative arm	Plasma exchange regime	Etiology	Results
Xia *et al*[40]	n = 882; 460 NBAL 422 control; Of which 49 ALF, 46 SALF and 787 ACLF	NBAL (all had PE) *vs* SMT	All of the patients were treated with PE, and most were treated with one or more additional methods, including 13/26 (50.00%) ALF patients, 16/27 (59.26%) SALF patients, and 228/407 (56.02%) ACLF patients.	For ACLF: 91.24% chronic hepatitis B, 3.69% alcohol abuse, 1.01% autoimmune, 1.01% cholestasis, 3.05% other causes	Clinical outcomes were improved after NBAL treatment. The 30-d survival rates of subacute liver failure (SALF) patients were 63% among those who received NBALs and 21% among those who did not receive NBALs (P < 0.01)
			The choice of therapy was based on each patient's condition: PE in combination with PP for HE was administered in 12.24% (6/49) of ALF patients, 10.77% (7/65) of SALF patients, and 7.41% (80/1079) of ACLF patients. In patients with HRS, we administered PE with CHDF in 32.65% (16/49) of ALF patients, 23.08% (15/65) sessions of SALF patients and 28.17% (304/1079) sessions of ACLF patients	For ALF: 42% drug toxicity, 16% HBV, 10% surgical trauma, 30% unexplained	The 30-day survival rate of acute-on-chronic liver failure (ACLF) patients who received NBALs was 47%, significantly higher than that of the non-NBAL patients (P < 0.05)
			Pts underwent 1-4 times of NBAL	For SALF: 54% drug toxicity, 30% unexplained, 4% Hepatitis E, 11% HBV	Reported to be effective in biochemical improvement
Cheng *et al*[12]	Retrospective, cohort study single tertiary centre; n = 55; 10 ALF, 45 ACLF	PE, no comparative arm	PE volume: About 3000 mL, and the exchange rate of plasma was 20-30 mL/min. Heparin was used as anticoagulant during PE	In ALF group: 50% HBV, 20% drug, others include ischemic hepatopathy, traumatic liver injury, HLH	20% (1/5) of the HBV related ALF survived, 1/2 of drug related ALF survived, and 1/1 of the traumatic liver injury related ALF survived.
					Significant improvements see in levels of serum total bilirubin, AST ALT INR PT. No significant changes in ammonia
Nakae *et al*[21]	Retrospective case series; n = 21; 10 FH; 11 ALF	PDF, no comparative arm	PE volume: 1200mL of normal FFP and 50mL of 25% albumin solution was infused intravenously over 8 h	FH	90 d survival:
				70% Hep B	20% in FH patients
				10% AIH	54.5% in ALF patients
				20% Drug	Overall survival 38.1%
			The PDF session lasted 8h, and the blood flow rate was 100 mL/min. Filtered replacement fluid for was infused at a dialysate flow rate of 600 mL/h and a replacement flow rate of 450 mL/h	ALF	Lower MELD correlated to increased survival
				3/11 Unknown	No patients survived beyond 90 d with MELD > 40
				1/11 GVHD	
				4/11 ETOH	Biochemically: Bilirubin, IL-18 statistially different when compared before and after PDF
				1/11 HBV	
			Fluid removal was performed by reducing the replacement flow rate to 450 mL/h at most	1/11 EBV	
				1/11 Drug	
				5/11 was labelled as AOCLF	

Pu *et al*[34]	Case series (excluding patients who abandoned treatment; *n* = 33); 8 ALF; 3 SALF; 14 ACLF	CHDF followed by sequential PE, No comparative arm	Patients underwent continuous hemofiltration on a daily basis during the daytime followed by sequential treatment with plasma exchange 1800-2400 mL or hemodialysis every 2-3 d	29 patients with hepatitis B virus infection, 1 with Hepatitis E virus infection, and 3 patients with unknown etiology; 18 were male and 15 female; age ranged from 23 to 65	Restoration of consciousness in 6 of 8 cases (75%) in acute liver failure (ALF) group, 3 of 3 cases (100%) in subacute liver failure (SALF) group, and 9 of 14 cases (64.29%) in acute/subacute on chronic liver failure (A/SCLF) group Of all cases, 11 patients restored consciousness after 7 d in a coma. The rate of long-term survival (those who abandoned the treatment were excluded) was 3/7 (42.86%) for ALF group, 2/2 (100%) for SALF group, and 1/11 (9.09%) for A/SCLF group No mention of biochemical changes
Schaefer *et al*[50]	Retrospective cohort study; *n* = 10; 8 had combined PE, HD + MARS 2 had MARS only	PE + HD + MARS *vs* MARS	PE volume: 1.5 plasma volume was exchanged per session within 2–3 h PE was immediately followed by a HD session in six children, using the same extracorporeal circuit with a polysulfone high-flux filter (Fresenius)	Wilson's disease in 2 patients, congenital liver fibrosis, progressive intrahepatic cholestasis, severe combined immunodeficiency, disseminated herpes simplex virus 2 infection, multi-organ failure due to mycoplasma-induced myocarditis, autoimmune hepatitis, fungal sepsis and cetirizine intoxication Age 0.1-18 yr	MARS and PE/HD treatments were well tolerated by all patients. No bleeding episode occurred. 1 patient with multi-organ failure due to mycoplasma-induced myocarditis, 1 with cetirizine intoxication completely recovered. 3 patients were successfully transplanted, five children died with multi-organ failure and sepsis, including the three children treated with Mini-MARS Standard MARS treatment only slightly decreased serum bilirubin (16.3 ± 6.5-13.8 ± 5.9 mg/dL) and ammonia (113 ± 62-99 ± 68 μmol/L) and international normalized ratio (INR) tended to increase (1.5 ± 0.3 and 2 ± 1.1) Mini-MARS did not reduce serum bilirubin, ammonia slightly decreased and INR increased

					PE/HD reduced serum bilirubin (23 ± 8.4-14.7 ± 7 mg/dL), ammonia (120 ± 60–70 ± 40 μmol/L) and INR (2.4 ± 0.8-1.4 ± 0.1, all P < 0.05). Intraindividual comparison showed a slight increase in bilirubin by 2 ± 22% with MARS and a reduction by 37 ± 11% with PE/HD (P < 0.001 *vs* MARS) and a decrease in ammonia of 18% ± 27% and 39% ± 23% (P < 0.05). INR increased during MARS by 26 ± 41% and decreased with PE/HD by 37 ± 20% (P < 0.01)
Singer *et al*[51]	Retroespective case series	No comparative arm, TPE in all patients	Plasma volume removed per exchange was 121 ± 47 mL/kg (2.2 ± 0.6 plasma volume) of FFP	57% FHF, 18% BA, 20% IEM, 5% other of note 43% had CLD	Coagulation profiles after TPE significantly improved compared with mean pre-exchange values
				Age 10 d to 18.4 yr	Spontaneous recovery was observed in three patients; the remaining either underwent transplantation (32/49) or were not considered transplant candidates because of irreversible neurologic insults (11/49) or sepsis (3/49)

PE: Plasma exchange; SMT: Standard medical treatment; ALF: Acute liver failure; HLH: Hemophagocytic lymphohistiocytosis; FFP: Fresh frozen plasma; INR: International normalised ratio; ALT: Alanine aminotransferase; CVVHDF: Continuous venous-venous hemodiafiltration; CHDF: Continuous hemodiafiltration; HBV: Hepatitis B virus; HSV: Herpes simplex virus; LDH: Lactate dehydrogenase; DILI: Drug induced liver injury; AFLP: Acute fatty liver of pregnancy; DILI: Drug induced liver injury; TPE: Therapeutic plasma exchange; BA: Biliary atresia; IEM: Inborn errors of metabolism.

survival. In larger cohort studies, predominant causes of ALF include paracetamol, followed by unknown cause. As already been discussed in previous literature, paracetamol-induced ALF has improved prognosis compared to injury from other causes, for example, viral hepatitis causes. From the earlier studies[6,14] where in two case series survival in ALF patients receiving plasma exchange was 50%-55%, the subgroup of patients who had paracetamol-induced ALF had survival ranging from 83%-100%. However, these are from case series and the level of evidence is not strong. In a Chinese cohort[4] study comparing the efficacy of plasma exchange + hemoperfusion + CVVHDF to plasma exchange + CVVHDF and hemoperfusion + CVVHDF, treatment of the 61 patients using the artificial liver support system yielded a combined survival rate of 62.3% (38/61). When subdivided into viral versus non-viral groups, the viral group survival rate was 35.0% (7/20) while the non-viral group survival rate was 75.6% (31/41).

The use of plasma exchange in patients with fulminant liver failure from Wilson's disease has been reported in case reports and series with encouraging outcomes[8,19,23-25,30,32,35]. EASL guidelines for Wilson's disease[36] recommends that patients with acute liver failure due to Wilsons disease should be treated with liver transplantation when revised King's score is 11 or higher (Grade II-2 B1 Class I, Level B). In one case report[8], a patient who met criteria for requiring liver transplant improved with plasma exchange alone, thereby averting a high-risk liver transplant. In addition, for patients who were subsequently transplanted, plasma exchange temporarily stabilized patients before liver transplant thereby allowing time to source for potential donors for liver transplant[24,25]. Nevertheless, most of the studies that included Wilson's disease are small case series, and the level of evidence remains weak.

Plasma exchange in ACLF

While there is strong evidence to use plasma exchange in ALF to improve survival[3], there has yet to be robust evidence to use plasma exchange in ACLF. Existing studies are mostly cohort studies done in Asia on patients with ACLF of predominantly

hepatitis B viral etiology. Prognosis of patients with ACLF is extremely poor with mortality rates ranging from 30%-70%[2] in the absence of timely liver transplant. As there were very few studies in ACLF that only used plasma exchange solely, this review included all studies that used plasma exchange based-liver support systems in the management of ACLF.

A total of 15 studies of patients with ACLF were included (Tables 4, 5), of which 6 studies included patients with both ACLF and ALF (Table 5). 2 of the studies, which included both ACLF and ALF, were in pediatric patients. The rest of the 13 studies included adult patients only. Of the 13, 1 is a randomised controlled trial, 10 are cohort studies, 2 are case series.

Mortality: Plasma exchange with or without the use of other liver support systems improves survival in non-transplanted in patients with ACLF. An open-label randomized control study by Qin *et al*[37] recruited 234 patients with HBV-related ACLF not suitable for liver transplant and randomized patients to SMT *vs* plasma exchange centered ALSS plus SMT. In this study, survival rates in plasma exchange-based ALSS were significantly higher: 60% *vs* 47% in the control group. Other retrospective cohort studies[38-40] also favored plasma exchange (and or plasma exchange-based non-bioartificial liver support system) to SMT in patients with ACLF from hepatitis B infection. For example, In Yue-Meng *et al*[39], patients with ACLF who had plasma exchange+SMT had increased rate of survival compared to patients who had SMT only: 4-wk mortality was 82% *vs* 63%, $P = 0.001$; 12-wk mortality 86% *vs* 71%, $P = 0.001$).

Similarly, Mao *et al*[38] reported increased 30-day survival in patients with HBV related ACLF where survival rates were 41.9% and 25.2% for plasma exchange and medical therapy respectively ($P < 0.05$). In the same study[38], time from the initial diagnosis to initiation of plasma exchange was found to be longer when in non-survivors compared to survivors, although this was not statistically significant.

Four of the studies[37-40] that reported plasma exchange based liver support system compared to standard medical treatment were analysed for pooled mortality at 30 and 90 d and data was presented in a forest plot (Figure 2). Other studies that had no comparative standard medical treatment arms were excluded from this analysis. Using available published in the aforementioned studies, plasma exchange was superior to SMT for survival in patients with ACLF, at 30-d (OR: 0.38, 95%CI: 0.38-0.88, $P = 0.01$, $I^2 = 44\%$; 3 studies) and at 90-d (OR: 0.54, 95%CI: 0.35-0.84, $P \leq 0.01$, $I^2 = 0$; 2 studies). The pooled mortality at 30 and 90 d is significantly reduced in patients with ACLF who underwent plasma exchange (or plasma exchange based ALSS) *vs* SMT (OR: 0.60, 95%CI: 0.46-0.77, $P < 0.01$, $I^2 = 15\%$; 4 studies).

Several studies compared use of plasma exchange only *vs* plasma exchange together with other liver support system, such as the use of double plasma molecular adsorption system (DPMAS). For example, Yao *et al*[41] reported significantly higher 28-d survival rate in specifically intermediate-advanced stage patients with ACLF who underwent DPMAS + plasma exchange compared to plasma exchange alone (57.4% *vs* 41.7%, $P = 0.043$).

Biochemical improvement: Most studies reporting the effect of plasma exchange-based therapy on patients with ACLF which assessed biochemical improvement pre- and post-plasma exchange found an improvement in biochemical parameters such as coagulopathy, bilirubin, aspartate aminotransferase, alanine aminotransferase, or ammonia[12,39-44], though this was not always associated with clinical improvement. Zhou *et al*[45] reported a predictive model using baseline age, MELD score, number of complications and type of ALSS to predict survival after ALSS in patients with ACLF. In the same study, authors report that plasma bilirubin adsorption (PBA) + plasma exchange compared to plasma exchange only had better 90-day survival 70.3% *vs* 58.3%; although there was no mention if PBA + plasma exchange significantly decreased levels of bilirubin compared to plasma exchange alone. However when DPMAS *vs* plasma exchange was compared in other studies[41,44], increased clearance of bilirubin (as seen in the plasma exchange arm in Wan *et al*[44], and DPMAS + plasma exchange arm in Yao *et al*[41]) was not associated with respective significant improvements in survival. Of note, in the study by Zhou *et al*[45], baseline characteristics of the group of patients who underwent PBA+ plasma exchange *vs* plasma exchange was unavailable, essential information that could have influenced survival outcomes.

Standard *vs* high volume and other liver assist devices: Several studies used solely plasma exchange in management of ACLF. For the studies that included plasma exchange in management of ACLF, a range of 2000-4500 mL of plasma exchange per session[12,37,38,41,43-45] was adopted. There were no studies in ACLF group that used high

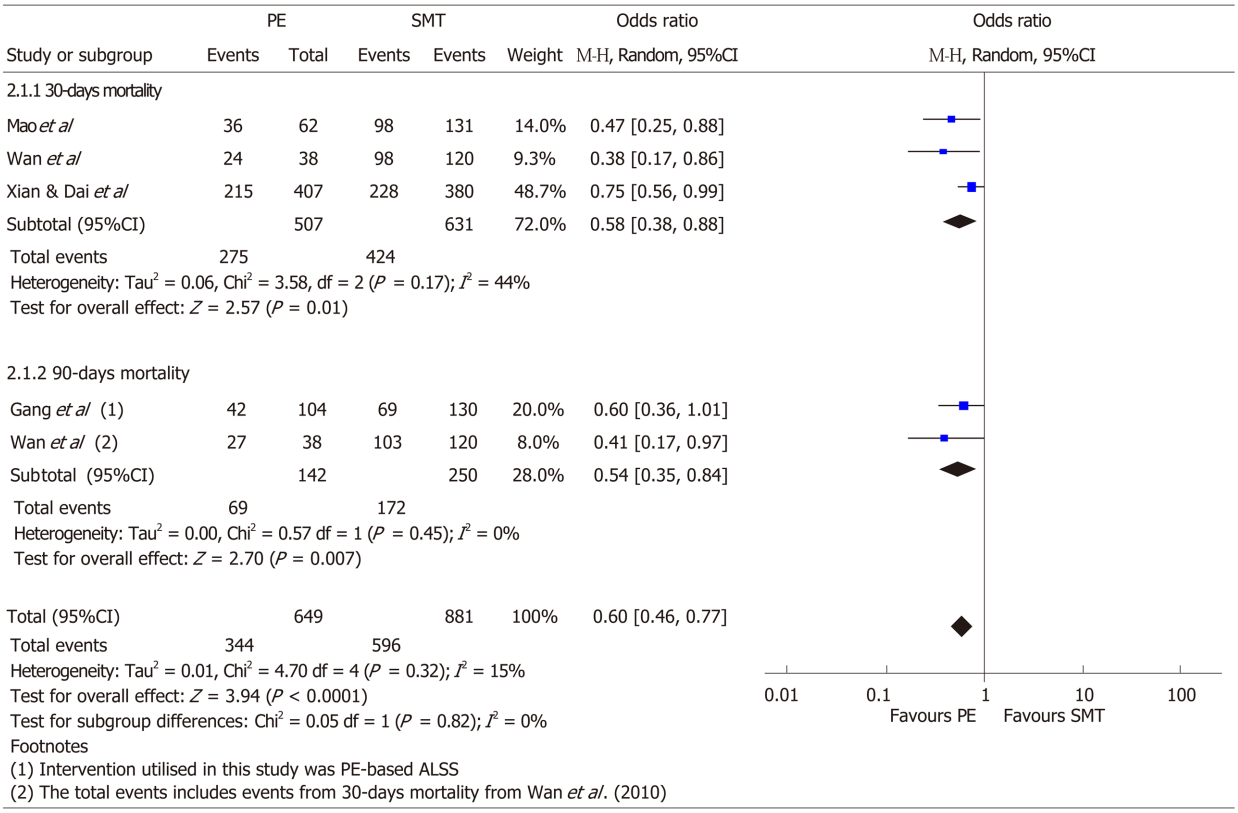

Figure 2 Forest plot for 30- and 90- d mortality in acute-on-chronic liver patients undergoing plasma exchange-based interventions or standard medical treatment. PE: Plasma exchange; SMT: Standard medical treatment.

volume plasma exchange. However, there were more studies in ACLF compared to ALF that use other liver assist devices in conjunction with plasma exchange – for example, DPMAS, PBA, hemofiltration, hemodiafiltration, plasma diafiltration and its combinations. As there is no head to head trial and most studies are retrospective, it is not possible to draw any conclusion as to whether one modality was superior to another.

FFP *vs* albumin: Most studies used FFP for plasma exchange or plasma exchange-based ALSS[12,37-39,41-45]. In addition, Mao *et al*[38] used additional albumin during plasma exchange. Albumin dialysis was not compared with plasma exchange in this review.

Three-day therapy *vs* intermittent or response guided: All studies included for review extended plasma exchange beyond three days wherever relevant based on clinical necessity[12,37-39,41-45]. In addition, most studies do not use daily plasma exchange, and instead, this was performed 2-3 times per week and were response guided, where plasma exchange often was continued till clinical improvement, transplant, or death.

Etiology specific outcome: Of the 13 included studies for plasma exchange in ACLF in adult patients, all were being conducted in Asia where hepatitis B is endemic. Thus, the majority of the patients assessed have HBV related ACLF. In comparison to non-viral causes, ACLF in the presence of viral causes tends to have a poorer survival rate. For example, Cheng *et al*[12] reported a 24% survival in hepatitis B related ACLF *vs* 67% in alcohol-related ACLF in their retrospective cohort study of 45 ACLF and 10 ALF patients. Furthermore, where there were more than two causes for chronic liver injury *e.g.*, HCV and alcohol, HBV and alcohol or in autoimmune hepatitis, mortality was high at 100%. However, this will need to be interpreted with caution as degree fibrosis or severity of cirrhosis of each patient was not available in the published study.

DISCUSSION

Acute liver failure and acute on chronic liver failure carry a high risk of mortality in patients in the absence of a liver transplant, a scarce resource. Liver assist devices, some of which are plasma exchange-based, have been used in patients with ALF or ACLF majority of which reported showing some benefit compared to standard medical treatment. However, there remains an unmet need for good quality prospective trials to be done, to ascertain the ideal volume, type, and duration of plasma exchange in management of ALF. Additional randomized controlled studies are also required to further shed light on the utility for plasma exchange or plasma exchange-based liver support systems for ACLF.

Firstly, while there has been good evidence for the use of high volume plasma exchange in acute liver failure to improve survival, due to the paucity of good-quality studies, at present it is unknown if a lower volume or a longer (or shorter) duration (*i.e.*, beyond the first three consecutive days) of plasma exchange will achieve equal or improved survival in ALF. This is important since donor plasma is a finite resource, and HVP is not without side effects. For example as in the above case series by Freeman *et al*[13] where patients with ALF were treated with standard volume plasma exchange, overall survival was 55% which on surface appears comparable to HVP in Larsen *et al*[3]. Nevertheless, little conclusion can be drawn as case series often seem to show benefit while well-designed clinical randomized controlled trials may fail to fulfil the hopes of initial reports. In addition, as the baseline characteristics of patients could be different from these various studies, no conclusive verdict can be made until further high-quality studies are being carried out comparing high volume plasma exchange *vs* standard volume plasma exchange. There is also insufficient evidence to suggest if plasma exchange with albumin or a combination of albumin and fresh frozen plasma will be non-inferior to high volume plasma exchange in management of ALF.

Furthermore, whether further doses of plasma exchange will benefit a patient with ALF beyond the third exchange will be an important question to answer with future well-designed randomized controlled trials. This is especially important in donor scarce countries, where it may take more than a few days to work up a suitable liver donor for living donor liver transplant. In Buckner *et al*[7], it was reported that one patient who had ALF from halothane toxicity had frequent high volume plasma exchange until she awoke from a coma 37 d later. On the other hand, Chien *et al*[22] reported in a case series of 23 pediatric patients that plasma exchange for more than six times probably offers the little benefit with regard to patient survival in the absence of a timely liver transplant. Mechanistically, Kondrup *et al*[6] has reported that on theoretical assumptions, three courses of plasma exchange on consecutive days would reduce the concentration of "toxins" distributed in extracellular water to 18% of initial concentration at the end of last exchange and an additional course will only theoretically decrease this only to 16%. While this could stand true for patients whose cause of liver failure is from drugs such as paracetamol, the same may not be the case for patients who have liver failure from other causes like autoimmune or viral.

Secondly, there remains insufficient evidence to extrapolate the findings from Larsen *et al*[3] to recommend plasma exchange in patients with ACLF. There is no study to our best knowledge that used consecutive three days of high volume plasma exchange for the management of ACLF. Qin *et al*[37] has reported the use of plasma exchange based ALSS compared to SMT in the only prospective controlled trial to date in patient with HBV-ACLF – however this has not made it to standard practice. Of note, the definition of ACLF in this study follows the Chinese definition hence does not mandate the need for cirrhosis or multi-organ failure. Thus this study population is heterogenous, ranging from patients with no cirrhosis (52%) to patients requiring intensive care and renal replacement therapy. The timing of initiation and type of antiviral was also not standardized which adds limitations and potential bias to the final results. Nevertheless, it is worthwhile to note that the baseline characteristics of both treatment groups were similar and ALSS was found to have improved 90-day and 5-year mortality compared to SMT (60% *vs* 47%, $P = 0.016$; 43% *vs* 31%, $P = 0.013$). These results are promising and thus further randomised controlled trials should be done, ideally with stratification of patients according to different etiologies and grades of ACLF (or acute decompensation in cirrhotics) and assess if there are any differences in response to plasma exchange.

Of the 13 studies on use of plasma exchange based therapy in ACLF in adult patients, 4 studies compared plasma exchange based therapy with SMT. Of the four studies, 3 studies only included patients in HBV-associated ACLF. In the one study that included patients with other etiology of ACLF, HBV-related ACLF was predominant–91.24% of the ACLF study population. Using the aforementioned studies, plasma exchange based therapy in ACLF compared to SMT improved

survival at 30- and 90-d with a pooled OR of 0.60 (95%CI: 0.46-0.77, $P < 0.01$). However, there are limitations in that the number of studies used to generate the pooled OR estimate for mortality comparing plasma exchange *vs* SMT are small due to the limited number of studies reported in literature, hence the risk for bias of each study was not assessed. In addition, the definition of ACLF in these studies do not require the diagnosis of cirrhosis and or more than one organ failure. Moreover, the etiology of ACLF in these groups of patients is HBV related, and thus these findings cannot be extrapolated to ACLF caused by other etiologies.

Thirdly, it will be essential to find out if there is an objective measure of a point of no return whereby plasma exchange or plasma exchange -based ALSS will be futile, whether in ALF or ACLF. For example, Nakae *et al*[21] reported that while overall survival with plasma diafiltration was 54.5% in their study, there were no survivors in the MELD > 40 groups when plasma diafiltration was used in ALF. Chen *et al*[42] also reported a trend where less patients with late-stage ACLF who underwent plasma exchange had transplant-free survival: 80.8% patients in the early stage, 75.8% patients in the middle stage and 37.4% patients in the end-stage survived for one month after diagnosis. Mechanistically, plasma exchange acts by removing plasma cytokines and adhesion molecules, which are the drivers of the systemic inflammatory cascade from the circulation and it is possible that late in the disease course of organ failure that the utility of plasma exchange would exponentially decrease.

Finally, other than using plasma exchange for management of ALF of ACLF, in our literature search there have been reports of other extracorporeal liver support devices could potentially improve outcomes in ALF or ACLF either alone or when used in conjunction with plasma exchange. Examples include molecular adsorbents recirculating system (MARS), Fractionated Plasma Separation, Adsorption and Dialysis device, SPAD. Several of our included studies used modalities like plasma exchange + DPMAS, plasma exchange + CVVHDF, or plasma diafiltration with varying results. Of the above liver devices, MARS has been studied most widely both in ALF and ACLF and its benefits remain modest. For example, a large randomized control trial did not demonstrate benefit in 6-mo survival in patients who had ALF and underwent MARS, although a major limitation of this study was that 75% of enrolled patients received a transplant within 24 h of enrollment, thereby potentially limiting the findings of the study[46]. This will remain to be a major limitation in future studies, especially in areas where donor livers can be quickly obtained. The emerging liver support devices, such as that of bioartificial liver support device which include a bioreactor that contains hepatocytes that can replace the function of the failing liver, *e.g*., the Extracorporeal liver assist device has entered human clinical trials. Other artificial liver support systems that combine detoxification with techniques to attenuate liver injury include the Hepa Wash, Li-Artificial Liver Support, and the University College London-Liver Dialysis Device, which has shown efficacy in animal experiments. More studies will need to be done to allow clinical use of these devices in liver failure.

In summary, the state of art therapy for acute liver failure should include plasma exchange based on the high-quality evidence, especially in patients who do not have a donor liver in sight. Current guidelines by EASL support use of HVP in ALF. While there is an open RCT supporting for plasma exchange-centered ALSS in the management of ACLF[37], and our pooled estimates from four studies favor the use of plasma exchange in ACLF as it is associated with a decreased 30 and 90 d mortality, this has not yet made it to standard practice.

The major limitation of our study is the low number of well-designed high-quality evidence available, as most studies are case series or cohort studies. This is possibly because liver failure is not common, and patients are usually critically ill. Secondly, as most of these studies are cohort studies or case series, we are unable to assess for publication bias *via* a funnel plot. However, publishing bias may exist as published studies are mostly positive studies and negative studies may not be reported. Lastly, the studies that have been included in plasma exchange in ACLF are over-represented by Asian patients, and the definitions of ACLF in each of these studies vary. Furthermore, it is imperative to take into account that the definition of ACLF in most Asian studies do not mandate the need for patients to be cirrhotic and have more than one organ failure, thereby potentially selecting a different group of patients from that seen in the Western ACLF literature. Whether the benefits of HVP in ALF can be extrapolated to patients with ACLF remains uncertain. Due to limited RCTs for ALF, only a subgroup meta-analysis (Figure 2) was explored comparing mortality among non-transplanted ACLF patients who underwent plasma exchange based therapy *vs* SMT.

There are many unanswered questions in this field: For example, the optimal type, duration, frequency, volume and time to plasma exchange one should use for ALF, and ACLF, if at all. Future randomized control trials studying the use of plasma

exchange and or other liver assist devices in liver failure should aim to answer these questions. In addition, future studies should also include the study of biomarkers that can predict the success of therapy. This might further shed light on the optimal duration, volume of plasma exchange and or alternative liver support therapy since there is vast heterogeneity in patients with ALF and ACLF, and perhaps different groups of patients will require different regimes.

ARTICLE HIGHLIGHTS

Research background

Liver failure portends a high mortality without successful liver transplantation. High volume plasma exchange has been included in European guidelines as level I, grade 1 recommendation in management of acute liver failure possibly by removal of plasma cytokines and drivers of systemic inflammatory cascade through plasma exchange. In recent years, there is increasing interest in plasma exchange for the treatment of liver failure, as there is proven improvement in survival in those who do not undergo a liver transplant. Prior to this study, there were several other cohort studies reporting the benefits of plasma exchange in acute liver failure (ALF), however the volume and duration of plasma exchange varies. The evidence for use of high volume plasma (HVP) in acute-on-chronic liver (ACLF) is less robust, but the use of plasmapheresis (not high volume) has been reported in literature.

Research motivation

While there is good evidence to use plasmapheresis in management of acute liver failure especially when there is no liver donor in sight, the optimal volume and duration of plasma exchange is unclear. Donor plasma is a finite resource, and HVP is not without side effects such as hypocalcemia requiring rapid calcium replacement. Several cohort studies showed benefit in standard volume plasmapheresis in management of ALF however no head to head comparisons have been done. Furthermore use of plasma exchange in ACLF, while has been reported to improve survival in literature, has not been widely accepted as standard treatment due to lack of high level evidence.

Research objectives

This study aims to summarize and analyze the current literature for use of plasmapheresis in patients with ACLF and ALF and its effect on mortality particularly in the non-transplanted patients. In addition, the review will summarise the current literature on volume of plasma used during exchange, the duration and frequency of plasma exchange in both ALF and ACLF. It is our hope that this review will serve as a valuable resource by analyzing available literature as well as illustrate the knowledge gaps and unmet needs for future researchers in this field.

Research methods

This systematic review uses guidance from the PRISMA checklist. Databases MEDLINE via PubMed, and EMBASE were searched and relevant publications up to 30 March, 2019 were assessed. Forty-four studies were shortlisted and included in Tables 2-5. In addition, pooled odds ratios and its corresponding 95% confidence intervals were respectively calculated for 30- and 90-d mortality in ACLF patients using the random effects model. We were unable to do this for ALF group due to paucity of studies and lack of critical information from eligible studies.

Research results

There is good evidence for use of high volume plasma exchange in ALF though the optimal duration and volume of plasma exchange at present is uncertain. While high quality randomized control trials are lacking, the use of plasma exchange in ACLF can be considered. Survival in non-transplanted patients was improved in all four studies in patients with ACLF comparing plasma exchange *vs* standard medical therapy (SMT). Using the aforementioned studies, plasma exchange based therapy in ACLF compared to SMT improved survival in non-transplanted patients at 30 and 90-d with a pooled OR of 0.60 (95%CI: 0.46-0.77, $P < 0.01$). There remains insufficient evidence to extrapolate the findings which recommend plasma exchange in patients with ACLF. Whether an individualized plasma exchange regime for each patient with liver failure can be personalised based on biomarkers remains unknown. More head to head trials will need to be done.

Research conclusions

While there has been good evidence for the use of high volume plasma exchange in acute liver failure to improve survival, due to the paucity of good-quality studies, at present it is unknown if a lower volume or a longer (or shorter) duration (*i.e.*, beyond the first three consecutive days) of plasma exchange will achieve equal or improved survival in ALF. In patients with ACLF, plasma exchange based therapy compared to SMT improves survival at 30 and 90-d in non-transplanted patients. The duration of plasma exchange therapy used in most studies in ACLF was clinical response driven and often intermittent; and not with high volume plasmapheresis. The etiology of ACLF was also mostly HBV related; the definitions of ACLF used are varied and not requiring the diagnosis of more than one organ failure and diagnosis of cirrhosis. At present, there is insufficient evidence to extrapolate the use of high volume plasmapheresis to patients with ACLF.

Research perspectives

There are unanswered questions in use of plasma exchange in liver failure: For example, the optimal type, duration, frequency, volume and time to plasma exchange one should use for ALF, and ACLF, if at all. Future randomized control trials studying the use of plasma exchange and or other liver assist devices in liver failure should aim to answer these questions. It is also essential to find out if there is an objective measure of a point of no return whereby plasma exchange or plasma exchange-based ALSS will be futile, whether in ALF or ACLF. Subsequent clinical trials in ACLF or ALF should include study of biomarkers that can predict the success of therapy. This might further shed light on the optimal duration, volume of plasma exchange and or alternative liver support therapy since there is vast heterogeneity in patients with ALF and ACLF and one regime may not fit all. Finally, the definition of ACLF in each study needs to be clearly stated, in order to allow clinicians to assess applicability of study results to their patients.

REFERENCES

1 **European Association for the Study of the Liver**; Clinical practice guidelines panel; Wendon J, Panel members, Cordoba J, Dhawan A, Larsen FS, Manns M, Samuel D, Simpson KJ, Yaron I; EASL Governing Board representative, Bernardi M. EASL Clinical Practical Guidelines on the management of acute (fulminant) liver failure. *J Hepatol* 2017; **66**: 1047-1081 [PMID: 28417882 DOI: 10.1016/j.jhep.2016.12.003]

2 **Hernaez R**, Solà E, Moreau R, Ginès P. Acute-on-chronic liver failure: an update. *Gut* 2017; **66**: 541-553 [PMID: 28053053 DOI: 10.1136/gutjnl-2016-312670]

3 **Larsen FS**, Schmidt LE, Bernsmeier C, Rasmussen A, Isoniemi H, Patel VC, Triantafyllou E, Bernal W, Auzinger G, Shawcross D, Eefsen M, Bjerring PN, Clemmesen JO, Hockerstedt K, Frederiksen HJ, Hansen BA, Antoniades CG, Wendon J. High-volume plasma exchange in patients with acute liver failure: An open randomised controlled trial. *J Hepatol* 2016; **64**: 69-78 [PMID: 26325537 DOI: 10.1016/j.jhep.2015.08.018]

4 **Li M**, Sun J, Li J, Shi Z, Xu J, Lu B, Cheng S, Xu Y, Wang X, Zhang X. Clinical observation on the treatment of acute liver failure by combined non-biological artificial liver. *Exp Ther Med* 2016; **12**: 3873-3876 [PMID: 28105119 DOI: 10.3892/etm.2016.3887]

5 **Hung YM**, Hung GC, Hsu PI, Hung SY, Chou KJ, Chung HM. Short-term survival advantage after plasma exchange in the treatment of acute on chronic liver failure or acute liver failure. *Clin Intensive Care* 2004; **15**: 93–99 [DOI: 10.1080/09563070400003714]

6 **Kondrup J**, Almdal T, Vilstrup H, Tygstrup N. High volume plasma exchange in fulminant hepatic failure. *Int J Artif Organs* 1992; **15**: 669-676 [PMID: 1490760 DOI: 10.1177/039139889201501110]

7 **Buckner CD**, Clift RA, Volwiler W, Donohue DM, Burnell JM, Saunders FC, Thomas ED. Plasma exchange in patients with fulminant hepatic failure. *Arch Intern Med* 1973; **132**: 487-492 [PMID: 4742403 DOI: 10.1001/archinte.1973.03650100011003]

8 **Damsgaard J**, Larsen FS, Ytting H. Reversal of Acute Liver Failure Due to Wilson Disease by a Regimen of High-Volume Plasma Exchange and Penicillamine. *Hepatology* 2019; **69**: 1835-1837 [PMID: 30357869 DOI: 10.1002/hep.30323]

9 **Akdogan M**, Camci C, Gurakar A, Gilcher R, Alamian S, Wright H, Nour B, Sebastian A. The effect of total plasma exchange on fulminant hepatic failure. *J Clin Apher* 2006; **21**: 96-99 [PMID: 16142721 DOI: 10.1002/jca.20064]

10 **Nakae H**, Yonekawa C, Wada H, Asanuma Y, Sato T, Tanaka H. Effectiveness of combining plasma exchange and continuous hemodiafiltration (combined modality therapy in a parallel circuit) in the treatment of patients with acute hepatic failure. *Ther Apher* 2001; **5**: 471-475 [PMID: 11800083 DOI: 10.1046/j.1526-0968.2001.00380.x]

11 **Nakamura T**, Ushiyama C, Suzuki S, Shimada N, Ebihara I, Suzaki M, Takahashi T, Koide H. Effect of plasma exchange on serum tissue inhibitor of metalloproteinase 1 and cytokine concentrations in patients with fulminant hepatitis. *Blood Purif* 2000; **18**: 50-54 [PMID: 10686442 DOI: 10.1159/000014407]

12 **Cheng YL**, Chang CH, Chen WT, Tsai MH, Lee WC, Tu KH, Tian YC, Chen YC, Hung CC, Fang JT, Yang CW, Chang MY. Prognostic factors and treatment effect of standard-volume plasma exchange for acute and acute-on-chronic liver failure: A single-center retrospective study. *Transfus Apher Sci* 2018; **57**: 537-543 [PMID: 29880246 DOI: 10.1016/j.transci.2018.05.030]

13 **Freeman JG**, Matthewson K, Record CO. Plasmapheresis in acute liver failure. *Int J Artif Organs* 1986; **9**: 433-438 [PMID: 3818118 DOI: 10.1177/039139888600900614]

14 **Aydemir S**, Ustundag Y, Bayraktaroglu T, Tekin IO, Peksoy I, Unal AU. Fulminant hepatic failure associated with propylthiouracil: a case report with treatment emphasis on the use of plasmapheresis. *J Clin Apher* 2005; **20**: 235-238 [PMID: 16206173 DOI: 10.1002/jca.20063]

15 **Bilgir O**, Calan M, Bilgir F, Cagliyan G, Arslan O. An experience with plasma exchange treatment of acute lymphoblastic leukemia in a case with fulminant hepatitis related to L-asparaginase. *Transfus Apher Sci* 2013; **49**: 328-330 [PMID: 23871581 DOI: 10.1016/j.transci.2013.06.010]

16 **Lin S**, Li Y, Long J, Liu Q, Yang F, He Y. Acute liver failure caused by hemophagocytic lymphohistiocytosis in adults: A case report and review of the literature. *Medicine (Baltimore)* 2016; **95**: e5431 [PMID: 27893685 DOI: 10.1097/MD.0000000000005431]

17 **Holt EW**, Guy J, Gordon SM, Hofmann JC, Garcia-Kennedy R, Steady SL, Bzowej NH, Frederick RT. Acute liver failure caused by herpes simplex virus in a pregnant patient: is there a potential role for therapeutic plasma exchange? *J Clin Apher* 2013; **28**: 426-429 [PMID: 23857723 DOI: 10.1002/jca.21287]

18 **Shen C**, Zhao CY, Liu F, Wang YD, Wang W. Acute liver failure associated with occupational exposure to tetrachloroethylene. *J Korean Med Sci* 2011; **26**: 138-142 [PMID: 21218043 DOI: 10.3346/jkms.2011.26.1.138]

19 **Pham HP**, Schwartz J, Cooling L, Hofmann JC, Kim HC, Morgan S, Pagano MB, Schneiderman J, Winters JL, Yamada C, Wong EC, Wu Y. Report of the ASFA apheresis registry study on Wilson's disease. *J Clin Apher* 2016; **31**: 11-15 [PMID: 26275240 DOI: 10.1002/jca.21396]

20 **Nakae H**, Igarashi T, Tajimi K. Selective plasma exchange with dialysis in patients with acute liver failure. *Ther Apher Dial* 2012; **16**: 467-471 [PMID: 23046372 DOI: 10.1111/j.1744-9987.2012.01112.x]

21 **Nakae H**, Eguchi Y, Saotome T, Yoshioka T, Yoshimura N, Kishi Y, Naka T, Furuya T. Multicenter study

of plasma diafiltration in patients with acute liver failure. *Ther Apher Dial* 2010; **14**: 444-450 [PMID: 21175541 DOI: 10.1111/j.1744-9987.2010.00864.x]
22 **Chien MM**, Chang MH, Chang KC, Lu FT, Chiu YC, Chen HL, Ni YH, Hsu HY, Wu JF. Prognostic parameters of pediatric acute liver failure and the role of plasma exchange. *Pediatr Neonatol* 2019; **60**: 389-395 [PMID: 30361144 DOI: 10.1016/j.pedneo.2018.09.006]
23 **Verma N**, Pai G, Hari P, Lodha R. Plasma exchange for hemolytic crisis and acute liver failure in Wilson disease. *Indian J Pediatr* 2014; **81**: 498-500 [PMID: 23494839 DOI: 10.1007/s12098-013-0979-x]
24 **Zhang Y**, Li L, Zhang X, Xu W, Guo Q, Zhou J. Plasmapheresis Combined with Continuous Plasma Filtration Adsorption Rescues Severe Acute Liver Failure in Wilson's Disease before Liver Transplantation. *Blood Purif* 2019; **47**: 120-125 [PMID: 30359967 DOI: 10.1159/000493909]
25 **Morgan SM**, Zantek ND. Therapeutic plasma exchange for fulminant hepatic failure secondary to Wilson's disease. *J Clin Apher* 2012; **27**: 282-286 [PMID: 22718095 DOI: 10.1002/jca.21239]
26 **Yükselmiş U**, Girit S, Çağ Y, Özçetin M. A child with acute liver failure associated with influenza A and resolved with plasma exchange treatment. *Hong Kong J Emerg Med* 2018 [DOI: 10.1177/1024907918754441]
27 **Ponikvar R**, Buturović J, Cizman M, Mekjavić I, Kandus A, Premru V, Urbancic A, Zakotnik B, Bren A, Ivanovich P. Hyperbaric oxygenation, plasma exchange, and hemodialysis for treatment of acute liver failure in a 3-year-old child. *Artif Organs* 1998; **22**: 952-957 [PMID: 9821529 DOI: 10.1046/j.1525-1594.1998.06239.x]
28 **Riveiro-Barciela M**, Muñoz-Couselo E, Fernandez-Sojo J, Diaz-Mejia N, Parra-López R, Buti M. Acute liver failure due to immune-mediated hepatitis successfully managed with plasma exchange: New settings call for new treatment strategies? *J Hepatol* 2019; **70**: 564-566 [PMID: 30503040 DOI: 10.1016/j.jhep.2018.10.020]
29 **Chen KJ**, Chen TH, Sue YM, Chen TJ, Cheng CY. High-volume plasma exchange in a patient with acute liver failure due to non-exertional heat stroke in a sauna. *J Clin Apher* 2014; **29**: 281-283 [PMID: 24497379 DOI: 10.1002/jca.21315]
30 **Pashaei MR**, Ajdarkosh H, Daryani NE, Habibollahi P, Beigmohammadi MT. Life saving plasmapheresis for the management of hemolytic crisis and acute liver failure in Wilson's Disease. *Hepat Mon* 2009
31 **Liu CT**, Chen TH, Cheng CY. Successful treatment of drug-induced acute liver failure with high-volume plasma exchange. *J Clin Apher* 2013; **28**: 430-434 [PMID: 23922237 DOI: 10.1002/jca.21291]
32 **Collins KL**, Roberts EA, Adeli K, Bohn D, Harvey EA. Single pass albumin dialysis (SPAD) in fulminant Wilsonian liver failure: a case report. *Pediatr Nephrol* 2008; **23**: 1013-1016 [PMID: 18299897 DOI: 10.1007/s00467-008-0761-x]
33 **Göpel W**, Schnetzke U, Hochhaus A, Scholl S. Functional acute liver failure after treatment with pegylated asparaginase in a patient with acute lymphoblastic leukemia: potential impact of plasmapheresis. *Ann Hematol* 2016; **95**: 1899-1901 [PMID: 27488287 DOI: 10.1007/s00277-016-2773-0]
34 **Pu Y**, Yang D, Mao Y, Zhang Y, Chen K. Therapeutic effects of blood purification in treatment of fulminant hepatic failure. *Braz J Infect Dis* 2013; **17**: 427-430 [PMID: 23810709 DOI: 10.1016/j.bjid.2012.11.008]
35 **Aydinli M**, Harmanci O, Ersoy O, Iskit AT, Ozcebe O, Abbasoglu O, Bayraktar Y. Two unusual cases with Wilson's disease: hepatoma and fulminant hepatitis treated with plasma exchange. *J Natl Med Assoc* 2006; **98**: 1989-1991 [PMID: 17225847]
36 **European Association for Study of Liver**. EASL Clinical Practice Guidelines: Wilson's disease. *J Hepatol* 2012; **56**: 671-685 [PMID: 22340672 DOI: 10.1016/j.jhep.2011.11.007]
37 **Qin G**, Shao JG, Wang B, Shen Y, Zheng J, Liu XJ, Zhang YY, Liu YM, Qin Y, Wang LJ. Artificial liver support system improves short- and long-term outcomes of patients with HBV-associated acute-on-chronic liver failure: a single-center experience. *Medicine (Baltimore)* 2014; **93**: e338 [PMID: 25526495 DOI: 10.1097/MD.0000000000000338]
38 **Mao W**, Ye B, Lin S, Fu Y, Chen Y, Chen Y. Prediction value of model for end-stage liver disease scoring system on prognosis in the acute on chronic liver failure patients with plasma exchange treatment. *ASAIO J* 2010; **56**: 475-478 [PMID: 20613491 DOI: 10.1097/MAT.0b013e3181e6bf13]
39 **Yue-Meng W**, Yang LH, Yang JH, Xu Y, Yang J, Song GB. The effect of plasma exchange on entecavir-treated chronic hepatitis B patients with hepatic de-compensation and acute-on-chronic liver failure. *Hepatol Int* 2016; **10**: 462-469 [PMID: 26482576 DOI: 10.1007/s12072-015-9667-4]
40 **Xia Q**, Dai X, Huang J, Xu X, Yang Q, Liu X, Chen Y, Li L. A single-center experience of non-bioartificial liver support systems among Chinese patients with liver failure. *Int J Artif Organs* 2014; **37**: 442-454 [PMID: 25008954 DOI: 10.5301/ijao.5000341]
41 **Yao J**, Li S, Zhou L, Luo L, Yuan L, Duan Z, Xu J, Chen Y. Therapeutic effect of double plasma molecular adsorption system and sequential half-dose plasma exchange in patients with HBV-related acute-on-chronic liver failure. *J Clin Apher* 2019; **34**: 392-398 [PMID: 30758886 DOI: 10.1002/jca.21690]
42 **Chen JJ**, Huang JR, Yang Q, Xu XW, Liu XL, Hao SR, Wang HF, Han T, Zhang J, Gan JH, Gao ZL, Wang YM, Lin SM, Xie Q, Pan C, Li LJ. Plasma exchange-centered artificial liver support system in hepatitis B virus-related acute-on-chronic liver failure: a nationwide prospective multicenter study in China. *Hepatobiliary Pancreat Dis Int* 2016; **15**: 275-281 [PMID: 27298103 DOI: 10.1016/s1499-3872(16)60084-x]
43 **Xu X**, Liu X, Ling Q, Wei Q, Liu Z, Xu X, Zhou L, Zhang M, Wu J, Huang J, Sheng J, Zheng S, Li L. Artificial liver support system combined with liver transplantation in the treatment of patients with acute-on-chronic liver failure. *PLoS One* 2013; **8**: e58738 [PMID: 23516546 DOI: 10.1371/journal.pone.0058738]
44 **Wan YM**, Li YH, Xu ZY, Yang J, Yang LH, Xu Y, Yang JH. Therapeutic plasma exchange versus double plasma molecular absorption system in hepatitis B virus-infected acute-on-chronic liver failure treated by entercavir: A prospective study. *J Clin Apher* 2017; **32**: 453-461 [PMID: 28304106 DOI: 10.1002/jca.21535]
45 **Zhou PQ**, Zheng SP, Yu M, He SS, Weng ZH. Prognosis of acute-on-chronic liver failure patients treated with artificial liver support system. *World J Gastroenterol* 2015; **21**: 9614-9622 [PMID: 26327769 DOI: 10.3748/wjg.v21.i32.9614]
46 **Saliba F**, Camus C, Durand F, Mathurin P, Letierce A, Delafosse B, Barange K, Perrigault PF, Belnard M, Ichaï P, Samuel D. Albumin dialysis with a noncell artificial liver support device in patients with acute liver failure: a randomized, controlled trial. *Ann Intern Med* 2013; **159**: 522-531 [PMID: 24126646 DOI: 10.7326/0003-4819-159-8-201310150-00005]
47 **Ide K**, Muguruma T, Shinohara M, Toida C, Enomoto Y, Matsumoto S, Aoki K, Fukuda A, Sakamoto S,

Kasahara M. Continuous Veno-Venous Hemodiafiltration and Plasma Exchange in Infantile Acute Liver Failure. *Pediatr Crit Care Med* 2015; **16**: e268-e274 [PMID: 26237654 DOI: 10.1097/PCC.0000000000000511]

48 **Harmanci O**, Buyukasik Y, Bayraktar Y. Successful plasma exchange treatment in hemolytic crisis of Wilson's disease preventing liver transplantation. *Dig Dis Sci* 2006; **51**: 1230 [PMID: 16944016 DOI: 10.1007/s10620-006-8039-2]

49 **Li YH**, Xu Y, Wu HM, Yang J, Yang LH, Yue-Meng W. Umbilical Cord-Derived Mesenchymal Stem Cell Transplantation in Hepatitis B Virus Related Acute-on-Chronic Liver Failure Treated with Plasma Exchange and Entecavir: a 24-Month Prospective Study. *Stem Cell Rev Rep* 2016; **12**: 645-653 [PMID: 27687792 DOI: 10.1007/s12015-016-9683-3]

50 **Schaefer B**, Schaefer F, Engelmann G, Meyburg J, Heckert KH, Zorn M, Schmitt CP. Comparison of Molecular Adsorbents Recirculating System (MARS) dialysis with combined plasma exchange and haemodialysis in children with acute liver failure. *Nephrol Dial Transplant* 2011; **26**: 3633-3639 [PMID: 21421589 DOI: 10.1093/ndt/gfr115]

51 **Singer AL**, Olthoff KM, Kim H, Rand E, Zamir G, Shaked A. Role of plasmapheresis in the management of acute hepatic failure in children. *Ann Surg* 2001; **234**: 418-424 [PMID: 11524594 DOI: 10.1097/00000658-200109000-00015]

World Journal of Gastroenterology

Submit a Manuscript: https://www.f6publishing.com

World J Gastroenterol 2020 January 14; 26(2): 246-265

DOI: 10.3748/wjg.v26.i2.246

ISSN 1007-9327 (print) ISSN 2219-2840 (online)

META-ANALYSIS

Diagnostic and clinical significance of antigen-specific pancreatic antibodies in inflammatory bowel diseases: A meta-analysis

Konstantinos Gkiouras, Maria G Grammatikopoulou, Xenophon Theodoridis, Eirini Pagkalidou, Evangelia Chatzikyriakou, Anna G Apostolidou, Eirini I Rigopoulou, Lazaros I Sakkas, Dimitrios Petrou Bogdanos

ORCID number: Konstantinos Gkiouras (0000-0002-6407-8494); Maria G Grammatikopoulou (0000-0003-4167-6595); Xenophon Theodoridis (0000-0001-9810-7583); Eirini Pagkalidou (0000-0002-8655-7293); Evangelia Chatzikyriakou (0000-0002-5461-3633); Anna G Apostolidou (0000-0001-8012-3454); Eirini I Rigopoulou (0000-0003-1978-4602); Lazaros I Sakkas (0000-0002-7670-3314); Dimitrios Petrou Bogdanos (0000-0002-9697-7902).

Author contributions: Gkiouras K and Bogdanos DP designed research; Gkiouras K contributed to data acquisition, analyzed and interpreted data, drafting the article, final approval; Grammatikopoulou MG contributed to acquisition of data, interpreted data, drafting the manuscript, final approval; Theodoridis X contributed to quality assessment, interpreted data, revising the article, final approval; Pagkalidou E contributed to supervision of the statistical analyses, final approval; Chatzikyriakou E contributed to quality assessment of data, final approval; Apostolidou AG contributed to data acquisition, final approval; Rigopoulou EI and Sakkas LI contributed to data interpretation, drafting manuscript parts, final approval; Bogdanos DP contributed to conception and design of the study, acquisition of data, supervision of all analyses, critical revision, final approval.

Konstantinos Gkiouras, Maria G Grammatikopoulou, Xenophon Theodoridis, Lazaros I Sakkas, Dimitrios Petrou Bogdanos, Department of Rheumatology and Clinical Immunology, Faculty of Medicine, School of Health Sciences, University of Thessaly, Biopolis, Larissa GR41110, Greece

Konstantinos Gkiouras, Maria G Grammatikopoulou, Xenophon Theodoridis, Evangelia Chatzikyriakou, Faculty of Medicine, School of Health Sciences, Aristotle University of Thessaloniki, University Campus, Thessaloniki GR54124, Greece

Maria G Grammatikopoulou, Anna G Apostolidou, Department of Nutritional Sciences and Dietetics, School of Health Sciences, International Hellenic University, Sindos Campus, Thessaloniki GR57400, Greece

Eirini Pagkalidou, Laboratory of Hygiene, Social and Preventive Medicine and Medical Statistics, Faculty of Medicine, School of Health Sciences, Aristotle University of Thessaloniki, University Campus, Thessaloniki GR54124, Greece

Evangelia Chatzikyriakou, Laboratory of Clinical Neurophysiology, AHEPA University Hospital, Faculty of Medicine, Aristotle University of Thessaloniki, University Campus, Thessaloniki GR54124, Greece

Eirini I Rigopoulou, Department of Medicine and Research Laboratory of Internal Medicine, University Hospital of Larissa, Biopolis, Larissa GR41110, Greece

Dimitrios Petrou Bogdanos, Division of Transplantation, Immunology and Mucosal Biology, MRC Centre for Transplantation, King's College London Medical School, London GR41110, United Kingdom

Corresponding author: Dimitrios Petrou Bogdanos, MD, PhD, Assistant Professor, Department of Rheumatology and Clinical Immunology, Faculty of Medicine, School of Health Sciences, University of Thessaly, Biopolis, PO Box 1425, Larissa GR41110, Greece.
bogdanos@med.uth.gr

Abstract

BACKGROUND

Non-invasive criteria are needed for Crohn's disease (CD) diagnosis, with several biomarkers being tested. Results of individual diagnostic test accuracy studies assessing the diagnostic value of pancreatic autoantibodies-to-glycoprotein-2 (anti-GP2) tests for the diagnosis of CD appear promising.

Conflict-of-interest statement: The authors deny any conflict of interest.

PRISMA 2009 Checklist statement: The authors have read the PRISMA 2009 Checklist, and the manuscript was prepared and revised according to the PRISMA 2009 Checklist.

Manuscript source: Invited Manuscript

Received: November 1, 2019
Peer-review started: November 1, 2019
First decision: November 22, 2019
Revised: December 19, 2019
Accepted: January 2, 2020
Article in press: January 2, 2020
Published online: January 14, 2020

P-Reviewer: Mattar MC, Sachar D
S-Editor: Tang JZ
L-Editor: A
E-Editor: Ma YJ

AIM

To systematically review and meta-analyze evidence on the diagnostic accuracy of anti-GP2 tests in patients with suspected/confirmed CD.

METHODS

An electronic search was conducted on PubMed, Cochrane-CENTRAL and grey literature (CRD42019125947). The structured research question in PICPTR format was "Population" including patients with symptoms akin to CD, the "Index test" being anti-GP2 testing, the "Comparator" involved standard CD diagnosis, the "Purpose of test" being diagnostic, "Target disorder" was CD, and the "Reference standard" included standard clinical, radiological, endoscopical, and histological CD diagnostic criteria. Quality was assessed with the Quality Assessment of Diagnostic Accuracy Studies-2 tool and hierarchical models were employed to synthesize the data.

RESULTS

Out of 722 studies retrieved, 15 were meta-analyzed. Thirteen studies had industry-related conflicts-of-interest, and most included healthy donors as controls (spectrum bias). For the combination of IgA and/or IgG anti-GP2 test, the summary sensitivity was 20% (95% confidence interval: 10%-29%) at a median specificity of 97%. If the test was applied in 10000 suspected patients, 9669 would be true negatives and in 26, the diagnosis would be missed. In this hypothetical cohort, the anti-GP2 would fail to produce a diagnosis for 81.3% of the positive cases. Low summary points of sensitivity and high specificity were estimated for the IgG or IgA anti-GP2 test. Analogous results were observed when the analyses were restricted using specific cut-offs, or when ulcerative colitis patients were used as comparators.

CONCLUSION

Anti-GP2 tests demonstrate low sensitivity and high specificity. These results indicate that caution is required before relying on its diagnostic value. Additionally, the need for improving the methodology of diagnostic test accuracy studies is evident.

Key words: Inflammatory bowel disease; Gastrointestinal disease; Evidence-based diagnosis; Sensitivity; Specificity; Ulcerative colitis; Conflicts of interest; Meta-regression; Industry bias

Core tip: The majority of individual studies assessing the diagnostic accuracy of autoantibodies for anti-glycoprotein 2 (anti-GP2) for Crohn's disease (CD) diagnosis either include asymptomatic participants, or patients with symptoms not akin to CD. Most studies carry industry-related conflicts-of-interest, employing non-blinded evaluation of their assays and CD diagnosis preceding anti-GP2 testing. The pooled analyses performed herein using only symptomatic patients as controls, revealed high heterogeneity and low diagnostic accuracy of the anti-GP2, demonstrating low sensitivity and high specificity. Based on the pooled sensitivity and specificity of the anti-GP2 for CD diagnosis, they do not appear to attain the characteristics to be used *per se* as a proper non-invasive diagnostic tool.

Citation: Gkiouras K, Grammatikopoulou MG, Theodoridis X, Pagkalidou E, Chatzikyriakou E, Apostolidou AG, Rigopoulou EI, Sakkas LI, Bogdanos DP. Diagnostic and clinical significance of antigen-specific pancreatic antibodies in inflammatory bowel diseases: A meta-analysis. *World J Gastroenterol* 2020; 26(2): 246-265
URL: https://www.wjgnet.com/1007-9327/full/v26/i2/246.htm
DOI: https://dx.doi.org/10.3748/wjg.v26.i2.246

INTRODUCTION

Pancreatic secretory granule membrane glycoprotein 2 (GP2) consists of a 78kDa glycoprotein[1]. GP2 is synthesized by the acinus cells[1] in the pancreas, and is considered today as the main target of pancreatic autoantibody[2,3]. Recent data indicate that GP2 is a specific receptor on microfold (M) cells of intestinal Peyer's patches[4-6], which consist of the original inflammation site in Crohn's Disease (CD)[2]. With autoreactive responses being important effectors of immune-mediated inflammation, triggering overt inflammatory bowel diseases (IBD)[7], autoantibodies-to-glycoprotein-2 (anti-GP2) have recently been suggested as possible diagnostic markers of CD.

Today, CD differential diagnosis is based on standard clinical, radiological, endoscopical and histological criteria[8,9], and a need for less invasive diagnostic tools has been highlighted, especially given the great number of patients with clinical features mimicking CD[10]. This is why recently, many diagnostic test accuracy (DTA) studies have been conducted, assessing the specificity and sensitivity of various biomarkers against standard CD diagnostic procedures[11], including the anti-GP2.

Despite the fact that a plethora of DTA studies has recently been conducted assessing the sensitivity and specificity of the GP2 autoantibodies for CD's differential diagnosis, synthesis of these studies in the form of a systematic review and meta-analysis would undoubtedly produce more valid results, as compared to individual studies, aiding evidence-based diagnosis[12]. Meta-analyses of DTA studies are important to obtain more valid, summary estimates of the diagnostic accuracy of an index test[13]. One such meta-analysis investigating the diagnostic accuracy of anti-GP2 for CD was published during the year 2017[14], missing however, many of the DTA studies published since then. Additionally, this specific meta-analysis[14] also exhibited few methodological shortcomings, like the improper inclusion of healthy controls in the samples analyzed, although for DTA studies, only patients with symptoms akin to the disease investigated are to be used[15-17].

Given the need for less invasive diagnostic tests (preferably serological) to be used in individuals with clinical suspicion of CD, while identifying the literature gap as per relevant state-of-the-art systematic reviews, the aim of the present systematic review and meta-analysis was to synthetize evidence examining the diagnostic accuracy of anti-GP2 tests in patients with suspected or confirmed CD. The PPPICPTR[18] an adapted PICO for systematic reviews of DTA was applied. In further detail, the PICPTR of the study was Population including patients with gastrointestinal symptoms akin to CD, with the Index test being positive anti-GP2 testing, the Comparator being standard CD diagnosis, the Purpose of test was diagnostic, with the Target disorder being CD, and the Reference standard included the standard clinical, radiological, endoscopical and histological criteria for CD diagnosis[18].

MATERIALS AND METHODS

Literature search

Reporting standards are based on the Preferred Reporting Items for Systematic Reviews and Meta-Analyses of Diagnostic Test Accuracy[19,20]. The protocol of the present systematic review was registered at PROSPERO (CRD42019125947).

A systematic search was conducted using the PubMed and Cochrane CENTRAL databases, until February, 28 2019. The grey literature and websites of companies manufacturing anti-GP2 kits were also explored for possible references using the specific tests. The keywords used in the searches included (anti-glycoprotein 2 antibody), (autoantibodies to glycoprotein 2), (anti-gp2), (autoantibodies), (Crohn's disease), with a combination of MeSH terms wherever possible. In particular, Table 1 details the search strategy used for PubMed and Cochrane-CENTRAL. The keyword "anti-glycoprotein" was used for searches within grey literature sources (Open Grey and National Technical Information Service) and on websites of anti-GP2 manufacturers (Euroimmun, GA Generic Assays, Thermo Fisher, and AMS Biotechnology). Studies were assessed for eligibility independently and in duplicate, by three researchers (Gkiouras K, Grammatikopoulou MG and Bogdanos DP), and any disagreements were resolved by consensus.

Inclusion and exclusion criteria

We imposed no restrictions on the age of the study population, language, or the quality of retrieved DTA studies. Studies assessing anti-GP2 levels to diagnose CD in patients with relevant clinical features were selected. Additionally, studies assessing anti-GP2 levels among IBD patients were also considered eligible. The reference standard to verify CD diagnosis was the standard clinical, radiological, endoscopical and histological criteria for CD diagnosis[8,9,21-25].

Table 1 Search strategy for PubMed and Cochrane-CENTRAL

Database	Key words
PubMed	
No. 1	Anti-glycoprotein 2 antibody
No. 2	"Anti-glycoprotein 2 antibody"
No. 3	Anti-glycoprotein 2 antibody [Text Words]
No. 4	Autoantibodies to glycoprotein 2
No. 5	"Autoantibodies to glycoprotein 2"
No. 6	Autoantibodies to glycoprotein 2 [Text Words]
No. 7	"Glycoprotein 2 autoantibodies"
No. 8	Glycoprotein 2 autoantibodies [Text Words]
No. 9	Autoantibodies (as a MeSH term)
No. 10	OR (No. 1 - No. 9)
No. 11	Crohn's disease
No. 12	Crohn's disease (as a MeSH term)
No. 13	OR (No. 11, No. 12)
No. 14	AND (No. 10, No. 13)
Cochrane-CENTRAL	
No. 1	Anti-glycoprotein 2 antibody
No. 2	Autoantibodies to glycoprotein 2
No. 3	Autoantibodies (as a MeSH term)
No. 4	OR (No. 1 - No. 3)
No. 5	Crohn's disease
No. 6	Crohn's disease (as a MeSH term)
No. 7	OR (No. 5, No. 6)
No. 8	AND (No. 4, No. 7)

No. means order of the keywords entered on PubMed and CENTRAL. OR and AND are Boolean operators used between keywords.

However, studies were excluded when (1) based on animals or non-human samples; (2) not providing sufficient data to construct a 2 × 2 table; (3) presenting duplicate data already reported in other manuscripts; and (4) not reporting the reference CD diagnostic criteria. When two publications had been identified as using overlapping populations, they were counted as a single study[26].

Data extraction

The main outcomes of interest involved sensitivity, specificity and the diagnostic odds ratio[27,28].

Data were extracted by Gkiouras K and Grammatikopoulou MG on prespecified data extraction sheets for DTA studies, as suggested by the Joanna Briggs Institute[29], which were then checked by Bogdanos DP. For studies reporting sensitivity, specificity, positive and negative predictive values and a total number of included patients, 2 × 2 tables of true positives (TP), false positives, false negatives, and true negatives (TN) were calculated, following the instructions of the Oxford Centre for Evidence-Based Medicine[30].

Quality assessment

Quality of included studies was assessed independently and in duplicate by two reviewers (Theodoridis X and Chatzikyriakou E), using the criteria of the Quality Assessment of Diagnostic Accuracy Studies-2 tool[31].

Meta-analysis

Given the great variability regarding the cut-offs used to define disease status in the primary studies[32,33], the hierarchical summary receiver operating characteristic (HSROC) model[34,35] was employed to synthesize data. SROC curves were constructed, but considering that a summary point of sensitivity or specificity among studies using mixed thresholds would be clinically uninterpretable, we chose to estimate summary sensitivity at its median specificity, based on the SROC curves[15,33]. When more than three primary studies reported similar cut-offs, the analysis was

repeated with the hierarchical Bivariate model in order to obtain summary points of sensitivity and specificity[35].

Furthermore, heterogeneity was assessed statistically by including covariates in the HSROC model (meta-regression). Heterogeneity is summarized with the relative diagnostic odds ratios (RDOR) along with their 95% confidence intervals (95%CI). The included covariates involved: Source of funding [state *vs* other (including private or not stated)], diagnostic kit industry conflicts-of-interest (COI) [industry (studies either reporting funding from diagnostic kit manufacturers, or having authors employed in the industry) *vs* other (lack of apparent industry-related COI)], the assay used for detecting autoantibodies (enzyme-linked immunosorbent assay *vs* indirect immunofluorescence), the manufacturers of the anti-GP2 kits (Generic assays *vs* other), blinding of the assay (lacking or not stated *vs* yes), recruitment of consecutive patients (no/not stated *vs* yes), and the percentage of female participants categorized as ≥ 50% *vs* < 50%.

When the complete HSROC models failed to converge and/or returned unstable parameters they were simplified with the symmetric HSROC model or the HSROC model with fixed accuracy, as previously described[36]. Similarly, when the Bivariate model returned unstable parameters, the analysis was repeated with univariate random effects models (UREM), as previously proposed[36]. The fit of the models was assessed with the -2 Loglikelihood test[35]. All analyses were repeated twice, once including DTA studies reporting results from CD cases against all patients with relevant symptoms, and the second time including studies reporting CD cases against ulcerative colitis (UC) cases only. In the analyses combining the result of IgA and/or IgG positive antibodies, studies were included only when reporting relevant results in detail.

Estimates of sensitivities and specificities derived for specific cut-off values were expressed as natural frequencies and summarized in a table[37]. Since the majority of included studies were based in Europe, Germany in particular, and had a case-control design, the estimation of CD prevalence would not have been precise. Subsequently, the prevalence rates used herein were extracted from a recent systematic review[38]. The prevalence rate used was 322 per 100000[38] in a hypothetical cohort of 10000 suspected patients. This figure was selected based on its efficiency to produce logical natural frequencies.

Statistical analyses were carried with the SAS PROC NLMIXED procedure and/or the MetaDAS macro[39] on SAS software (SAS Institute Inc., Cary, NC, United States) and the plots were developed with RevMan[40]. The statistical methods used in this study were reviewed by Dr. Anna-Bettina Haidich, Associate Professor of Medical Statistics and Epidemiology in Aristotle University of Thessaloniki.

RESULTS

Out of 722 DTA studies retrieved in total, 18[41-58] fulfilled the systematic review's protocol criteria. Figure 1 details the selection process of the primary DTA studies. As three studies[44,45,53] did not assess total anti-GP2 but different anti-GP2 isoforms, these were excluded from the meta-analyses, leaving a total of 15 studies[41-43,54-58,46-52].

Study characteristics and quality assessment of studies

Table 2 details the characteristics of the 18 primary DTA studies included in the systematic review. All retrieved studies involved full-text articles, except from the one by Op De Beéck *et al*[48], which was in Letter format. None of the studies reported information on the ethnicity of the samples. The Bonaci-Nicolic *et al*[42] study was the only one lacking ethical permission disclosure, whereas the DTA by Op De Beéck *et al*[48] had reported related ethics in a previous study using part of the same sample[59]. Cummings and associates[44] were the only ones recruiting unrelated participants, whereas seven DTA studies in total included children in their samples. Only five studies assured blinding the assays[43-45,49,51]. Cut-offs used to define positivity in IgA or IgG varied greatly, ranging from 3.7 U/dL to 71.75 U/dL for specific GP2 isoforms.

The quality assessment summary using the QUADAS-2 tool[31] is presented in Figure 2. Risk of bias for the index test was generally unclear since, in most studies, it was unclear if the thresholds used had been prespecified by the kit's manufacturer, or were study-derived[26]. Additionally, many primary DTA studies failed to report whether the anti-GP2 assay was performed with the results of the CD diagnosis being blind[26].

Meta-analysis of the diagnostic accuracy of anti-GP2 (IgG) for CD

A total of 15 studies were included in the pooled analyses for evaluation of the diagnostic accuracy of the anti-GP2 IgG (Figure 3), including a pooled sample of 4365

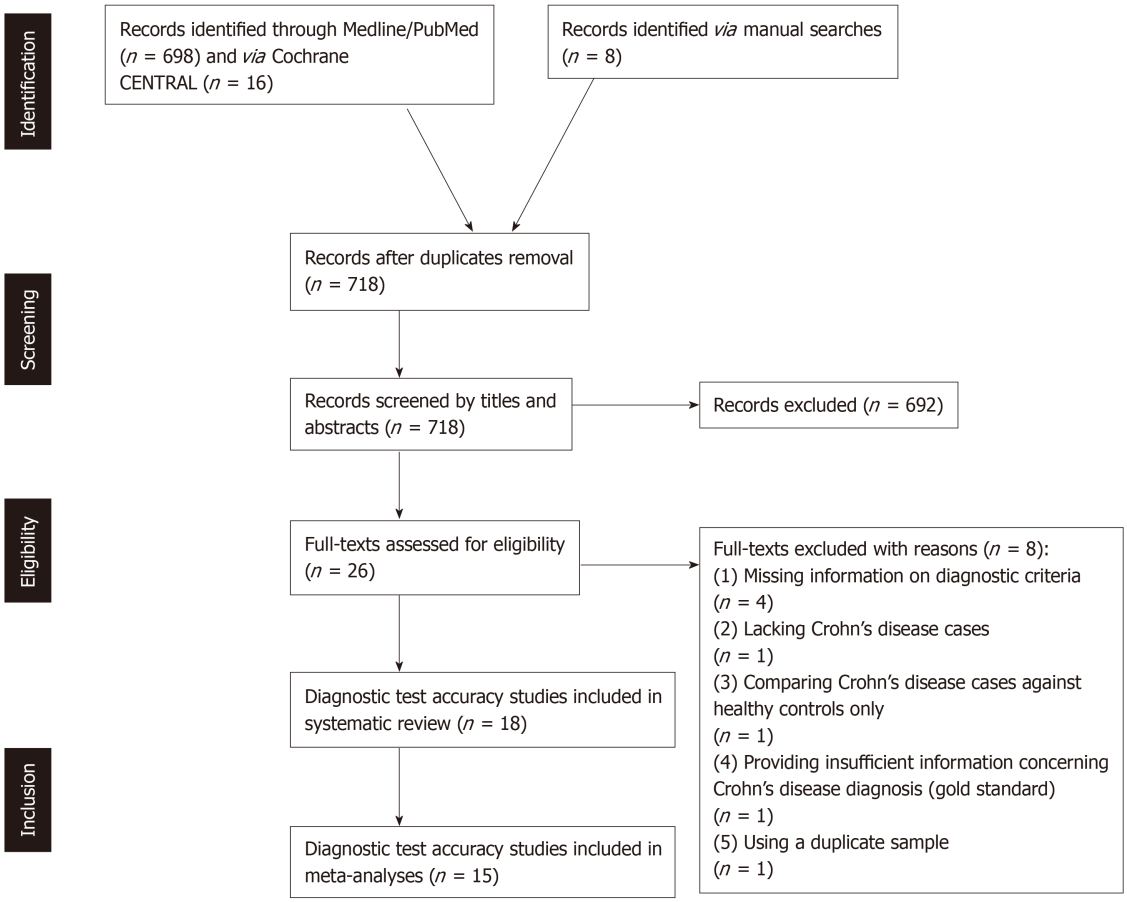

Figure 1 Flowchart of the diagnostic test accuracy studies selection.

patients, with 665 of them being CD cases and 3700 forming the controls group. The diagnostic sensitivity of the anti-GP2 (IgG) for CD ranged between 10% to 43% (Figure 3A), and the specificity ranged from 80 to 100% (Figure 3B). The summary SROC curve is presented in Figure 3C, indicating that on the median specificity of 93%, summary sensitivity reached 27% (95%CI: 20%-34%). With the UREM models (seven DTA studies), it was estimated that at the cut-off level of 20 U/mL, summary sensitivity reached 22% (95%CI: 15%-30%) and specificity was calculated at 93% (95%CI: 91%-95%). At the cut-off of 15 U/mL (three studies, Bivariate model), summary sensitivity was 28% (95%CI: 16%-43%) and specificity reached 92% (95%CI: 84%-96%).

Forest plots of sensitivity and specificity and the summary SROC curve for the diagnostic accuracy of anti-GP2 in patients with CD against those with UC (14 studies, total patients: 3947; CD cases: 640; UC cases: 3307) are presented in Figures 3D-F. A potential outlier study, the one conducted by Bonaci-Nicolic and associates[42], was identified from the forest plot and the space of the SROC curve, indicating the need for refitting the HSROC model accordingly, after excluding this study. Based on the -2 Loglikelihood test ($P < 0.001$), the remaining analyses were carried out without this DTA study[42]. Based on the HSROC model, on the median specificity of 93% summary sensitivity was 30% (95%CI: 24%-36%). With the UREM models, using the cut-off of 20 U/mL (six studies), summary sensitivity was calculated at 24% (95%CI: 17%-33%) and the specificity at 93% (95%CI: 90%-96%). At the cut-off limit of 15 U/mL, summary sensitivity reached 28% (95%CI: 16%-43%) and specificity was estimated at 90% (95%CI: 84%-94%).

Meta-analysis of the diagnostic accuracy of anti-GP2 (IgA) for CD

A total of 14 studies were included in the pooled analysis for the diagnostic accuracy of anti-GP2 IgA, involving 3914 patients in total (CD cases: 380; Control cases: 3534). The reported diagnostic sensitivity ranged from 3% to 37% (Figure 4A) and specificity between 75% to 100% (Figure 4B). Using the HSROC model, the estimated sensitivity on the SROC curve was estimated at 15% (95%CI: 12%-18%) and median specificity reached 97% (Figure 4C). Using the cut-off value of 20 U/mL (seven studies, bivariate

Table 2 Characteristics of the included studies evaluating the diagnostic accuracy of glycoprotein 2 antibodies in crohn's disease

Ref.	Country	Multicenter	Recruitment			CD diagnosis and classification		Assays characteristics					Sample characteristics					Funding
			Year	Site	Consecu-tive	CD diagnosis	Mont-real[81]	Assay	Kit	anti-GP2 form	Blind assay	Positivity cut-off U/dL	N[9]	Unrelat-ed sample	Children included	Sex (% female)	Age (yr)[5]	
Bogdanos *et al*[41]	Germany; United Kingdom	√	NR	Otto-von-Guericke University; UCL Hospital; and Children's hospital Technical University Dresden	NR	Standard clinical, radiological, endoscopical and histological criteria[8,9]	√	ELISA	GA (Dahlewitz /Berlin Germany)	Total	No	IgA 20; IgG 20	CD *n* = 169; UC *n* = 102; HC *n* = 225	NR	√	CD 60.3%; UC 55.9%	CD 36 (8–87)[1]; UC 47 (17-92)[1]	Higher Education Funding Council of England; Biomedical Research Centre, United Kingdom NIHR; and Brandenburg Ministry of Economics; and EU
Bonaci-Nikolic *et al*[42]	Serbia	NR	NR	Clinical Center of Serbia	NR	Clinical, endoscopic, histologic, lab findings[21]	-	ELISA	GA (Dahlewitz /Berlin Germany)	Total	No	IgA 20; IgG 24	CD *n* = 33; UC *n* = 23; GSE *n* = 21; HC *n* = 13	NR	-	CD 42.4%; UC 56.5%; GSE 76.2%; HC 46.1%	CD 35 (19-63)[4]; UC 34 (24-57)[4]; GSE 31 (19-57)[4]; HC 41 (22–55)	None declared
Caneparo *et al*[43]	Italy	-	2008-2014	Policlinico San Donato	NR	Clinical, endoscopic and histological criteria	-	ELISA	GA (Dahlewitz /Berlin Germany)	Total	√	IgA 10; IgG 15	CD *n* = 48 UC *n* = 26 HC *n* = 182	NR	√	CD 47.9%; UC 19.2%	CD 41 (16–65)[4]; UC 39 (17–62)[4]	Regione Piemonte and Letizia Castelli Schubert Foundation
Cummings *et al*[44]	United Kingdom	-	2009-2010	Cleveland Clinic	√	Clinical, endoscopic, radiographic, histopathological criteria[22]	-	ELISA	GA (Dahlewitz /Berlin Germany)	Isoforms GP21 and GP24	√	IgA GP21 14; IgA GP24 3.7; IgG GP21 18; IgG GP24 15	UC *n* = 117	√	-	UC 44.4%	UC 44.3 ± 13.7	Obtained but not disclosed
Degenhardt *et al*[45]	Germany	-	2000-2006	University Medical Center Regensburg	NR	European Crohn and Colitis Organization criteria[23]	√	ELISA	GA (Dahlewitz /Berlin Germany)	Isoform alpha and betta	√		CD *n* = 303; UC *n* = 108; OGD *n* = 72; OPC *n* = 206	NR	√	CD 52.8%; UC 39.8%; ODG 36.1%	CD 36.1 ± 12.5; UC 40.2 ± 12.8; OGD 60.3 ± 13.8	Bundes-ministerium für Bildung & Forschung and Kompetenznetz chronisch entzündliche Darmerkran-kungen

Gross *et al*[46]	Nether-lands	NR	NR	VU University Medical Center Amsterdam	-	Lennard-Jones criteria[24]	-	ELISA	GA (Dahlewitz /Berlin Germany)	Total	No	IgA 20; IgG 20	CD *n* = 38; UC *n* = 40; CeD *n* = 45; GFD *n* = 34; RCD *n* = 15	NR	-	CD 71.1%; UC 52.5%	CD 36.4 ± 11.8; UC 36.5 ± 9.6	CD consortium
Michaels *et al*[47]	Germany	-	2005-2013	University Hospital Schleswig-Holstein	-	Typical clinical, endoscopical, histological and/or radiological findings of CD/UC	√	IIF	Euroim-mun Germany	Total	NR		CD *n* = 224; UC *n* = 136	NR	NR	CD 64.3%; UC 54.4%	CD 392; UC 422	Else-Kröner-Fresenius-Stiftung
Op De Beéck *et al*[48]	Belgium	-	NR	University Hospital Gasthuis-berg, Leuven	NR	Lennard-Jones criteria[24]	-	ELISA	GA (Dahlewitz /Berlin Germany)	Total	NR	IgA 15; IgG 15	CD *n* = 164; UC *n* = 118; OGD *n* = 75	NR	√	CD 58.6%[6]; UC 41.7%[6][59]; ODG NR	CD 42 (17-80)[1,6]; UC 43 (19-78)[1,6][59]; ODG NR	Fund for Scientific Research Flanders and GA GmbH
Papp *et al*[49]	Hungary	-	2005-2010	Institute of Internal Medicine, University of Debrecen	√	Lennard-Jones criteria[24]	√	ELISA	GA (Dahlewitz /Berlin Germany)	Total	√	IgA 20; IgG 20	CD n = 271; UC *n* = 187; HC *n* = 100	NR	-	CD 61.5%; UC 54%	CD 25 (19-33); UC 33 (23-43)	Janos Bolyai Research Scholarship; Debrecen University; and IOIBD Research
Pavlidis *et al*[50]	United Kingdom	-	NR	UCL Hospital	NR	Lennard-Jones criteria[24]	√	ELISA	GA (Dahlewitz /Berlin Germany)	Total	NR	IgG 20	CD *n* = 225; UC *n* = 225	NR	-	CD 56.4%; UC 49.7%	CD 36 ± 14.3; UC 51 ± 15.7	NIHR; Higher Education Funding Council for England; EASL; and INOVA Diagnostics
Pavlidis *et al*[51]	United Kingdom	-	NR	UCL Hospital	√	Lennard-Jones criteria[24]	√	ELISA	Inova Diagnostics (Research use only)	Total	√	IgA 20; IgG 25	CD *n* = 323; UC *n* = 294; OPC *n* = 112; HC *n* = 103	NR	-	CD 54%; UC 47.9%	CD 40 ± 14.3; UC 48.7 ± 15.7	INOVA Diagnostics
Pavlidis *et al*[52]	United Kingdom	-	NR	UCL Hospital	NR	Lennard-Jones criteria[24]	√	IIF	N/A8	Total	NR		CD *n* = 212; UC *n* = 249	NR	-	CD 42.4%; UC 51.4%	CD 42.4 (30-49); UC 51.4 (37-61)	Euroimmun

Röber *et al*[53]	Germany	√	1994-2014	Three children's University hospitals (Dresden, Leipzig, Giessen)	NR	Porto criteria[25]	Paris[82]	ELISA	GP21, GP23: (AMS Biotechnology, Abingdon, United Kingdom); GP22: (CCS GmbH, Hamburg, Germany); GP24: (Thermo Sci, Braunschweig, Germany)	Isoforms 1, 2, 3, 4	NR	IgA GP21 7.02; IgA GP22 7.33; IgA GP23 4.37; IgA GP24 9.01; IgG GP21 33.38; IgG GP22 71.75; IgG GP23 15.89; IgG GP24 23.22	CD *n* = 164; UC *n* = 114; GE *n* = 27; ENDO *n* = 56; HC *n* = 218	NR	√	CD 39.6%; UC 54.3%; GE 52%; ENDO 50%	CD 13 (10-15); UC 14 (11-15); GE 2 (1-5); ENDO 13 (7-16)	None declared
Roggenbuck *et al*[56]	Germany; Greece; Belgium	√	NR	Attikon Hospital, UoA; Otto-von-Guericke University; and University Hospital Leuven	NR	NR. Communication with an author, confirmed the Lennard-Jones criteria[24]	-	ELISA	GA (Dahlewitz/ Berlin Germany)	Total	NR		CD n = 73; CeD *n* = 79; HC *n* = 90	NR		CD 52%; CeD 69.6%	CD 36.5 (30-43)[3]; CeD 24 (12-42)[3]	None declared
Roggenbuck *et al*[55]	Germany	-	NR	Charité Berlin	NR	Lennard-Jones criteria[24]	-	ELISA	GA (Dahlewitz/ Berlin Germany)	Total	NR	IgA 20; IgG 20	CD n = 73; UC n = 49; HC n = 63	NR	-	CD 57.5%; UC 59.1%	CD 41 (20-72)[1]; UC 40 (21-71)[1]	Brandenburg Ministry of Economics and EU
Roggenbuck *et al*[54]	Germany	NR	NR	NR	√	Lennard-Jones criteria[24]	NR	ELISA	GA (Dahlewitz/ Berlin Germany)	Total	NR	IgA 20; IgG 20	CD n = 178; UC n = 100; HC *n* = 162	NR	-	CD 60.7%; UC 54%	CD 39 (18-87)[1]; UC 42 (18-71)[1]	Brandenburg Ministry of Economics and EU
Zhang *et al*[57]	China	-	NR	Peking Union Medical College Hospital	NR	Lennard-Jones criteria[24]	√	ELISA	GA (Dahlewitz/ Berlin Germany)	Total	NR	IgA 20; IgG 20	CD *n* = 35; UC *n* = 35; OGD *n* = 13; HC *n* = 8	NR	√	CD 17%; UC 38%; ODG NR	CD: 17 (13-69)[1]; UC: 38 (18-75)[1]; ODG NR	NNSFC

Zhang *et al*[58]	China	-	NR	Peking Union Medical College Hospital	√	Lennard-Jones criteria[24]	√	ELISA	GA (Dahlewitz/ Berlin Germany)	Total	NR	IgA 10; IgG 15	CD *n* = 171; UC *n* = 208; BD *n* = 71; ITB n = 57; HC *n* = 70	NR	√	CD 33%; UC 43%; BD 38%; ITB 43%	CD 33 (10-85)1; UC 43 (12-77)[1]; BD 38 (10-73)[1]; ITB 43 (14-76)[1]	NNSFC; Chinese Academy of Medical Sciences; and Chinese Key Research & Development Program

[1]Median (minimum–maximum).
[2]Median.
[3]Mean (IQR1–IQR3).
[4]Mean (minimum–maximum).
[5]mean ± standard deviation, or median, IQR.
[6]Not all participants from the Joossens[59] study were included.
[7]Not among participants with Crohn's disease.
[8]Using as substrates IIF chip slides containing sections of unfixed pancreas, recombinantly transformed HEK293 cells-overexpressing GP2[83].
[9]Healthy controls were not included in the sensitivity and specificity analyses herein. Anti-GP2: Glycoprotein 2 antibodies; BD: Behcet's disease; CD: Crohn's disease; CeD: Celiac Disease; EASL: European association for the study of liver; ENDO: Nonspecific gastrointestinal symptoms; ELISA: Enzyme-linked immunosorbent assay; EU: European Union; GA: Generic assays; GE: Acute gastroenteritis; GFD: CeD on gluten-free diet; GP2: Glycoprotein 2; GSE: Gluten-sensitive enteropathy; HC: Healthy controls; IBD: Inflammatory bowel diseases; IIF: Indirect immune-fluorescence; ITB: Intestinal tuberculosis; N/A: Not applicable; NIHR: National Institute for Health Research; NNSFC: National Natural Science Foundation of China; NR: Not reported; OGD: Other gastrointestinal disease; OPC: Other pathological conditions; RCD: Refractory Crohn's disease; UC: Ulcerative Colitis; UCL: University College London; UoA: University of Athens.

Figure 2 Quality assessment of the included studies based on the quality assessment of diagnostic accuracy studies-2 tool[31].

model), summary sensitivity was 16% (95%CI: 9%-26%) and specificity was calculated at 96% (95%CI: 86%-99%).

When UC cases were used as the only comparators (Figures 4D and E; Total patients: 3497; CD cases: 324; UC cases: 3173) the estimated sensitivity on the SROC curve was 11% (95%CI: 3%-20%) at the median specificity of 98% (Figure 4F). However, when the analysis was restricted to studies reporting results at the cut-off of 20 U/mL (eight studies, UREM model), pooled summary sensitivity was calculated at 15% (95%CI: 10%-22%) and specificity reached 98% (95%CI: 96%-99%).

Meta-analysis of the diagnostic accuracy of anti-GP2 (IgA and/or IgG) for CD

A total of five studies were meta-analyzed during the assessment of the diagnostic accuracy of anti-GP2 IgA and/or IgG antibodies, involving a total of 1693 patients (CD cases: 243; Control cases: 1450). The reported diagnostic sensitivity of the anti-GP2 antibody (IgA and/or IgG) for CD ranged between 10% and 34% (Figure 5A), and the reported specificity ranged from 81% to 98% (Figure 5B). The estimated sensitivity was calculated at 20% (95%CI: 10%-29%) at a median specificity of 97% (Figure 5C). At the cut-off value of 20 U/mL (three studies, UREM model), pooled summary sensitivity reached 22% (95%CI: 12%-39%) and pooled summary specificity was computed at 93% (95%CI: 80%-98%).

When UC cases were used as comparators against patients with CD (Figures 5D and E; Total patients: 1541; CD cases: 203; UC cases: 1338), the estimated sensitivity was 20% (95%CI: 4%-35%) at the median specificity of 97% (Figure 5F).

Investigation of heterogeneity

Meta-regression analyses were conducted to explore possible sources of heterogeneity. The results (Table 3) revealed that the assay used to detect the anti-GP2 antibodies was linked with the accuracy of anti-GP2 IgG, both in the pooled patient analysis (RDOR = 4.25, 95%CI: 1.26-14.37), as well as in the analysis using UC cases as

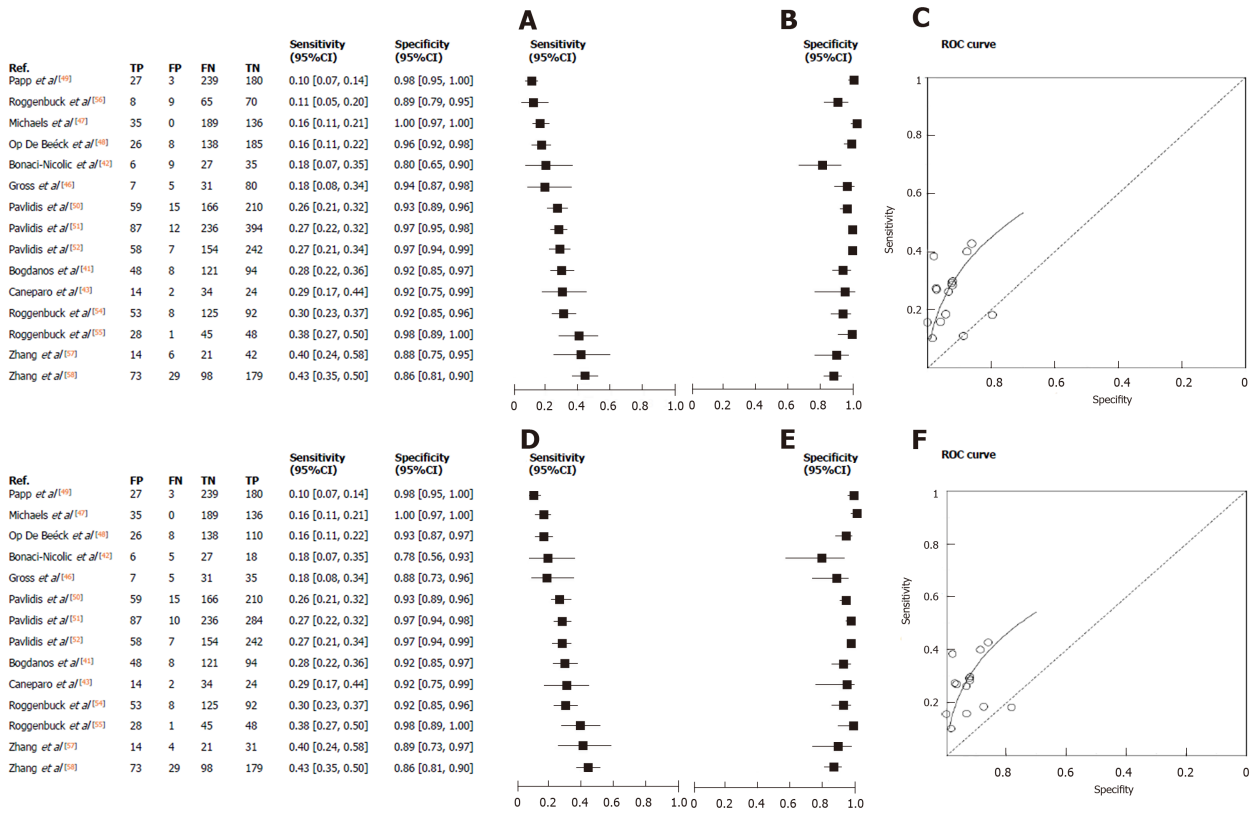

Figure 3 Pooled forest plots. A-C: Pooled forest plots for sensitivity and specificity, and the summary receiver operating characteristic curve of anti-GP2 antibody (IgG positive) for Crohn's Disease against all patients with relevant symptoms. D-F: Pooled forest plots for sensitivity and specificity, and the summary receiver operating characteristic curve of anti-GP2 antibody (IgG positive) for patients with Crohn's Disease against patients with ulcerative colitis. FN: False negative; FP: False positive; ROC: Receiver operating characteristic; TN: True negative; TP: True positive; CI: Confidence interval.

comparators (RDOR = 3.28, 95%CI: 1.33-8.09). However, these results should be interpreted with caution due to the small number of studies included. The rest of the variables failed to demonstrate significant associations. In the analyses for the anti-GP2 IgA antibodies with the CD *vs* the UC cases, the models failed to converge, or returned unstable parameters even with the use of alternative models (see aforementioned Meta-analysis paragraph).

Real-life scenario modeling the present findings

To "measure" the exact effects of using the anti-GP2 assays for the diagnosis of CD according to the results herein and in a hypothetical pragmatic scenario[60], we used the recent data on IBD prevalence[38] (Table 4). When using the combination of IgG and/or IgA anti-GP2 for the diagnosis of CD in a hypothetical cohort of 10000 suspected patients, 9669 will be the TN cases and for 26 CD diagnosis will missed (false negatives) although suffering from CD. In contrary, in the same cohort, 32 patients will suffer from CD and the test will correctly identify only 6 CD cases (TP). Analogous results will be observed if this test is implemented with a cut-off value of 20 U/dL, or in patients suspected only for CD *vs* UC. Likewise, in the analyses of CD *vs* either all symptomatic patients or UC cases only, using the IgG or IgA anti-GP2 tests would result in similarly increased TN and decreased TP cases.

DISCUSSION

The present meta-analysis of DTA studies revealed that the anti-GP2 have a low diagnostic accuracy (low sensitivity and high specificity) in detecting CD true positive cases. In contrast to the published primary DTA research when all relevant DTA studies were pooled together, the autoantibodies did not appear sensitive enough to detect true positive CD cases.

According to Lalkhen *et al*[61] the ideal diagnostic test is never positive in a disease-free patient, and never negative in a patient with the disease. With the low sensitivity

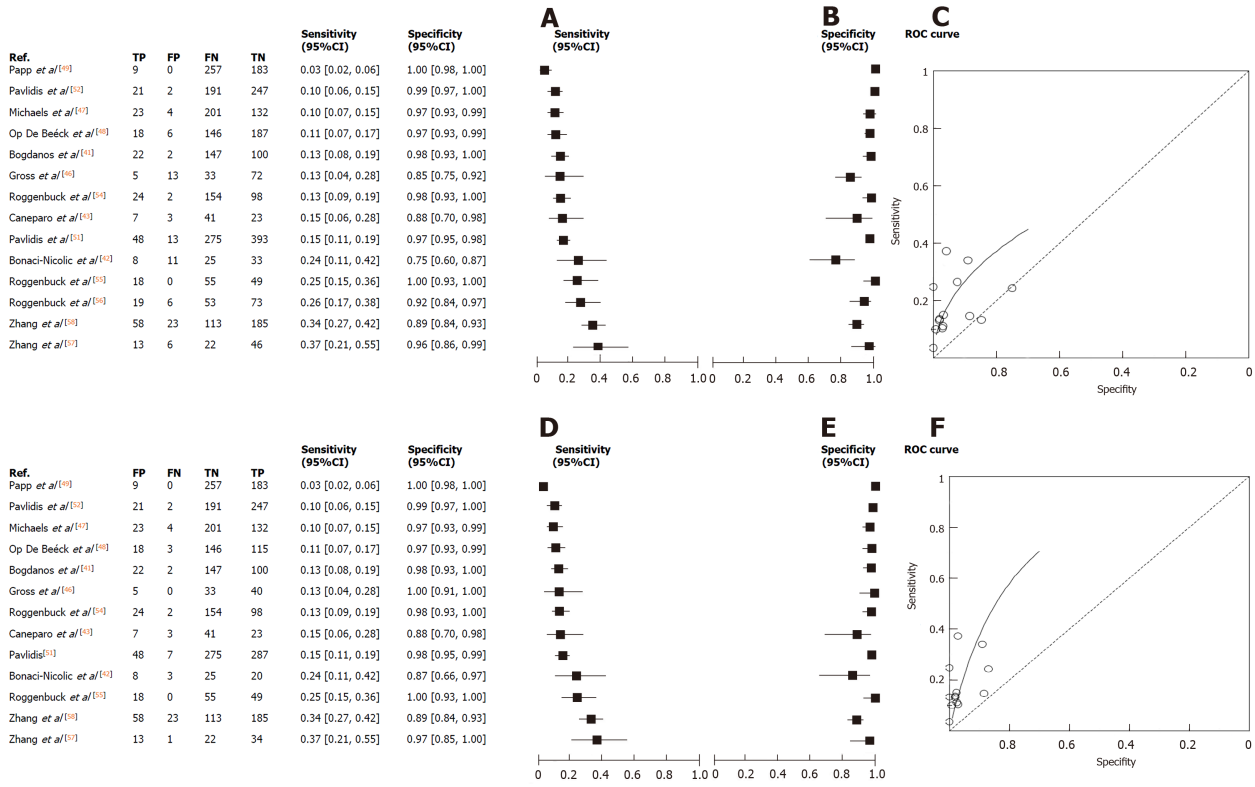

Ref.	TP	FP	FN	TN	Sensitivity (95%CI)	Specificity (95%CI)
Papp *et al*[49]	9	0	257	183	0.03 [0.02, 0.06]	1.00 [0.98, 1.00]
Pavlidis *et al*[52]	21	2	191	247	0.10 [0.06, 0.15]	0.99 [0.97, 1.00]
Michaels *et al*[47]	23	4	201	132	0.10 [0.07, 0.15]	0.97 [0.93, 0.99]
Op De Beéck *et al*[48]	18	6	146	187	0.11 [0.07, 0.17]	0.97 [0.93, 0.99]
Bogdanos *et al*[41]	22	2	147	100	0.13 [0.08, 0.19]	0.98 [0.93, 1.00]
Gross *et al*[46]	5	13	33	72	0.13 [0.04, 0.28]	0.85 [0.75, 0.92]
Roggenbuck *et al*[54]	24	2	154	98	0.13 [0.09, 0.19]	0.98 [0.93, 1.00]
Caneparo *et al*[43]	7	3	41	23	0.15 [0.06, 0.28]	0.88 [0.70, 0.98]
Pavlidis *et al*[51]	48	13	275	393	0.15 [0.11, 0.19]	0.97 [0.95, 0.98]
Bonaci-Nicolic *et al*[42]	8	11	25	33	0.24 [0.11, 0.42]	0.75 [0.60, 0.87]
Roggenbuck *et al*[55]	18	0	55	49	0.25 [0.15, 0.36]	1.00 [0.93, 1.00]
Roggenbuck *et al*[56]	19	6	53	73	0.26 [0.17, 0.38]	0.92 [0.84, 0.97]
Zhang *et al*[58]	58	23	113	185	0.34 [0.27, 0.42]	0.89 [0.84, 0.93]
Zhang *et al*[57]	13	6	22	46	0.37 [0.21, 0.55]	0.96 [0.86, 0.99]

Ref.	FP	FN	TN	TP	Sensitivity (95%CI)	Specificity (95%CI)
Papp *et al*[49]	9	0	257	183	0.03 [0.02, 0.06]	1.00 [0.98, 1.00]
Pavlidis *et al*[52]	21	2	191	247	0.10 [0.06, 0.15]	0.99 [0.97, 1.00]
Michaels *et al*[47]	23	4	201	132	0.10 [0.07, 0.15]	0.97 [0.93, 0.99]
Op De Beéck *et al*[48]	18	3	146	115	0.11 [0.07, 0.17]	0.97 [0.93, 0.99]
Bogdanos *et al*[41]	22	2	147	100	0.13 [0.08, 0.19]	0.98 [0.93, 1.00]
Gross *et al*[46]	5	0	33	40	0.13 [0.04, 0.28]	1.00 [0.91, 1.00]
Roggenbuck *et al*[54]	24	2	154	98	0.13 [0.09, 0.19]	0.98 [0.93, 1.00]
Caneparo *et al*[43]	7	3	41	23	0.15 [0.06, 0.28]	0.88 [0.70, 0.98]
Pavlidis[51]	48	7	275	287	0.15 [0.11, 0.19]	0.98 [0.95, 0.99]
Bonaci-Nicolic *et al*[42]	8	3	25	20	0.24 [0.11, 0.42]	0.87 [0.66, 0.97]
Roggenbuck *et al*[55]	18	0	55	49	0.25 [0.15, 0.36]	1.00 [0.93, 1.00]
Zhang *et al*[58]	58	23	113	185	0.34 [0.27, 0.42]	0.89 [0.84, 0.93]
Zhang *et al*[57]	13	1	22	34	0.37 [0.21, 0.55]	0.97 [0.85, 1.00]

Figure 4 Pooled forest plots. A-C: Pooled forest plots for sensitivity and specificity, and the summary receiver operating characteristic curves of anti-GP2 antibody (IgA positive) for Crohn's Disease against all patients with relevant symptoms; D-F: Pooled forest plots for sensitivity and specificity, and the summary receiver operating characteristic curves of anti-GP2 antibody (IgA positive) for patients with Crohn's Disease against patients with Ulcerative colitis. FN: False negative; FP: False positive; ROC: Receiver operating characteristic; TN: True negative; TP: True positive; CI: Confidence interval.

and high specificity demonstrated herein, it appears that the anti-GP2 fall short in the diagnostic accuracy of CD. According to the rule of thumb suggested by Power[62], in a useful test, the sum of sensitivity + specificity must exceed 1.5, ideally reaching 2.0. In none of the analyses performed herein did the sum of sensitivity + specificity exceed 1.5. When high specificity is detected, the problem of overdiagnosis[62] becomes pivotal. However, low sensitivity and high specificity are ideal characteristics of a screening tool, rather than a diagnostic one[63].

Although different isoforms of the anti-GP2 have been identified since the beginning of the century[64], it is only until very recently that the diagnostic potential of all four isoforms was investigated and compared[53]. According to some researchers, anti-GP2 isoforms 1 and 4 are considered as the best serological markers for CD diagnosis, superior even to the anti-saccharomyces cerevisiae antibodies (ASCA), which are routinely used, despite their poor specificity and insufficient sensitivity[44]. Among the included DTA studies, Papp *et al*[49] reported the use of two different enzyme-linked immunosorbent assay methods employing recombinant human GP2 identified as isoform 4. Degehardt and associates[45] made the distinction between two different isoforms of GP2 synthesized in the pancreas, the larger isoform alpha (analogous to isoforms 1 and 3), and the shorter beta form (analogous to isoforms 1 and 3). However, it is not within the scope of the present paper to further discuss the implications related to antibody reactivities against distinct GP2 isoforms. It should be noted however, that due to the different reported isoforms in the included DTA studies and the small number of studies reporting reactivity against different GP2 isoforms (three)[44,45,53], no analyses could be performed to compare the diagnostic accuracy of different anti-GP2 subtypes. However, when more DTA studies of good methodological quality are published using GP2 isoforms, the diagnostic accuracy of the anti-GP2 might be improved in the respective pooled analyses compared to the total anti-GP2 which was evaluated herein.

One important methodological issue identified in the study involves the inclusion of already diagnosed patients, without securing blinding of the index text. The majority of DTA studies on anti-GP2 were performed on already diagnosed CD patients and only five[43-45,49,51] reported blinding of the assays. This issue results in two forms of bias, being: (1) Partial verification bias[13], as only patients with a positive result on the index test (anti-GP2 assay) have actually undergone the reference

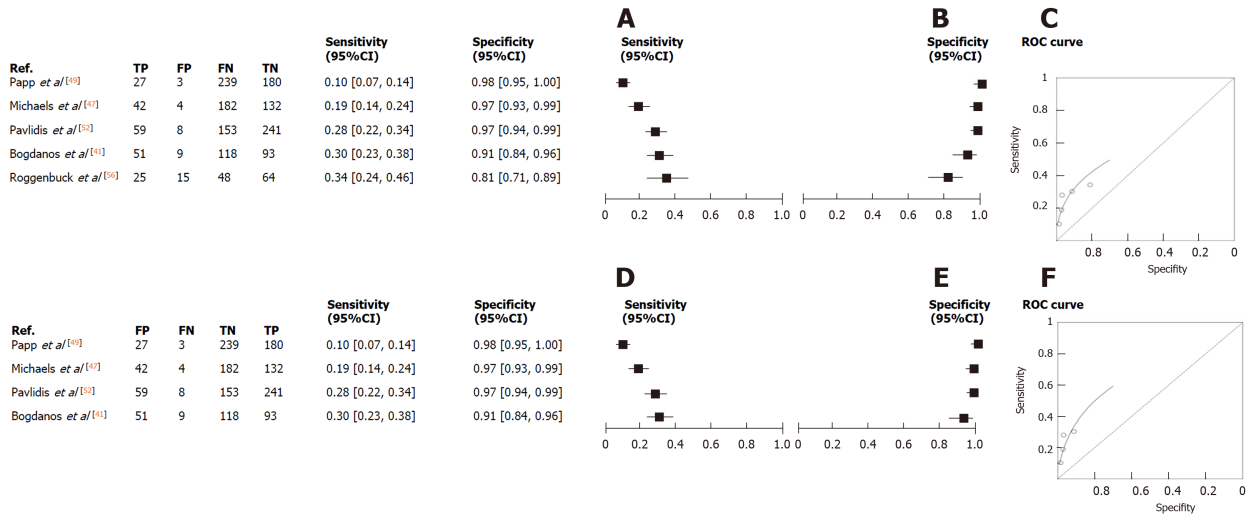

Figure 5 Pooled forest plots. A-C: Pooled forest plots for sensitivity and specificity, and the summary receiver operating characteristic curves of anti-GP2 antibody (IgA and/or IgG positive) for Crohn's Disease against all patients with relevant symptoms; D-F: Pooled forest plots for sensitivity and specificity, and the summary receiver operating characteristic curves of anti-GP2 antibody (IgA and/or IgG positive) for patients with Crohn's Disease against patients with Ulcerative colitis. FN: False negative; FP: False positive; ROC: Receiver operating characteristic; TN: True negative; TP: True positive; CI: Confidence interval.

standard test for CD diagnosis (although in reverse order); and (2) Test review bias[13], as the results of the reference standard are known to reviewers who interpret the index test. Another important limitation of most primary DTA studies involves the inclusion of healthy controls in their samples, either in the form of healthy donors, or as outpatients. This error was even detected in a recently published meta-analysis of anti-GP2 DTA studies[14]. The inclusion of healthy controls, or of patients with a disease having symptoms not akin to CD[15-17] appears to form a systematic error, exhibited by most primary DTA research and has been reported to result in spectrum bias and overestimation of the diagnostic accuracy[15,65]. This was corrected in the present analyses, where CD cases were only compared either against symptomatic patients, or against patients with UC.

When compared to the recently published meta-analysis[14] of anti-GP2 diagnostic accuracy for CD, the sensitivity and specificity previously reported is similar to the one calculated herein, despite pooling healthy controls together in the analyses. Still, authors of that meta-analysis[14] acknowledge several of the limitations of applying the anti-GP2 assay as a diagnostic tool and suggest its use for the differentiation of CD patients from controls, although their definition of controls for DTA studies appears to be arbitrary. According to Al Fattani *et al*[66], evidence from well-designed thorough systematic reviews indicates the importance of attaining a correct methodological design in DTA studies.

Another issue of concern and possible source of bias that may partly explain the systematic error of using healthy controls, or patients with irrelevant symptoms in the control groups, involves the industry-related COI demonstrated among most primary DTA studies. With 13[41,43-45,48,49,51-56,58] out of 18 primary studies included in the systematic review either reporting direct funding by diagnostic kit manufacturers, receiving the kits for gratis, or including authors with kit-industry affiliations, this may partially explain the methodological mistakes detected in most DTA studies, either in the form of guidance throughout the study's implementation, or in the form of statistical or interpretation advice provided by the kit industry. Although comparison between DTA studies with industry-related COI *vs* those lacking any apparent industry-related COI did not differ in terms of anti-GP2 accuracy, further investigation is needed to examine industry-related COI in DTA studies. It is well known that financial competing interests in industry-sponsored research often introduce bias into study design, analyses and interpretation of findings[67], as observed herein. Fairly recently, it was suggested that in several cases the industry might be involved in overdiagnosis, due to underlying financial profits[68,69]. Dakubo *et al*[70] was the first to identify industry financial interests as a major cause of overdiagnosis, however, to our knowledge, COI in DTA research have never been evaluated, nor has the overall influence of the industry. As many of the primary studies included herein failed to report any funding source[42,44,53], it is highly likely that some might have received the diagnostic kits for gratis by the industry without

Table 3 Investigation of heterogeneity (meta-regression)

Covariate		Population	Ig Type	Number of studies	Relative diagnostic odds ratio (95%CI)
Funding type	State *vs* Other	CD *vs* All	IgG	6 *vs* 9	1.91 (0.87-4.21)
			IgA	5 *vs* 9	1.08 (0.38-3.06)
		CD *vs* UC	IgG	5 *vs* 8	1.21 (0.81-1.80)
COI	Industry-related COI *vs* no apparent industry-related COI	CD *vs* All	IgG	7 *vs* 8	0.73 (0.32-1.66)
			IgA	6 *vs* 8	0.53 (0.21-1.30)
		CD *vs* UC	IgG	9 *vs* 4	0.48 (0.19-1.20)
Method	ELISA *vs* IFF	CD *vs* All	IgG	13 *vs* 2	0.84 (0.38-1.85)
			IgA	12 *vs* 2	4.25 (1.26-14.37)
		CD *vs* UC	IgG	11 *vs* 2	1.60 (0.40-6.54)
Blind assay	No/not stated *vs* Yes	CD *vs* All	IgG	12 *vs* 3	3.28 (1.33-8.09)
			IgA	11 *vs* 3	1.77 (0.63-5.00)
		CD *vs* UC	IgG	10 *vs* 3	1.15 (0.32-4.15)
Consecutive sampling	No/not stated *vs* Yes	CD *vs* All	IgG	11 *vs* 4	1.47 (0.65-3.32)
			IgA	10 *vs* 4	1.31 (0.53-3.21)
		CD *vs* UC	IgG	9 *vs* 4	1.88 (0.65-5.38)
Kit manufacturer	GA *vs* All other	CD *vs* All	IgG	12 *vs* 3	1.04 (0.51-2.11)
			IgA	11 *vs* 3	1.28 (0.80-2.03)
		CD *vs* UC	IgG	10 *vs* 3	1.47 (0.48-4.48)
Female participants	≥ 50% *vs* < 50%	CD *vs* All	IgG	11 *vs* 4	1.24 (0.79-1.94)
			IgA	10 *vs* 4	0.75 (0.30-1.93)
		CD *vs* UC	IgG	10 *vs* 3	1.15 (0.54-2.45)

CD: Crohn's disease; CI: Confidence interval; COI: Conflict of interest; GA: Generic assays; ELISA: Enzyme-linked immunosorbent assay; IFF: Indirect immune-fluorescence; Ig: Immunoglobulin; UC: Ulcerative Colitis.

reporting it, or without disclosing relevant academia-industry funding.

The variety of thresholds used in most studies to identify TP CD cases is yet another issue of concern. Given the high number of industry-related COI demonstrated in the primary DTA studies, one might argue that cut-offs are defined arbitrary, based on the expected TP prevalence in order to fulfill the minimum of positive and negative cases set by the College of American Pathologists[71,72]. Thus, it might be wise to report the diagnostic test thresholds in advance, possibly in the form of a published protocol, before initiating a DTA study.

In the present study we explored many potential sources of heterogeneity extensively and only the assay used to detect the anti-GP2 antibodies was associated with heterogeneity affecting the diagnostic accuracy of anti-GP2 IgG. The high degree of clinical heterogeneity exhibited in the primary DTA studies limits the possibility of making strong conclusions regarding the diagnostic performance of anti-GP2 antibodies. Another issue which needs to be taken into account is the performance of this test in combination with other non-invasive tests, such as fecal calprotectin and the ASCA, which are routinely used for the investigation of cases with a clinical suspicion of CD[73-75].

Undoubtedly, diagnostic tests can aid practitioners in the diagnostic process[76]. It appears that identifying a sensitive test without misclassification of many false positives remains a challenge[77], as most tests are imperfect and can only adjust disease probability[12]. Tests with low sensitivity and high specificity, like the anti-GP2, are better for population screening rather than for diagnosing patients[62,63]. Additionally, it appears that given the methodological pitfalls demonstrated in most anti-GP2 DTA research, high quality DTA cohort studies are required, enrolling consecutive patients, presenting clinical and laboratory features akin to CD, where both the assay and the reference diagnosis will be performed in a double-blind manner, preferably without the industry being involved at any step of the process, other than providing the relevant kits. As per CD diagnosis, we would have to agree with the European Crohn and Colitis Organization[78] that based on the currently available data, serological tests should be used as diagnostic adjuvants in parallel to colonoscopy.

In recap, CD differential diagnosis is important[79,80]. Despite the high accuracy

Table 4 Summary of finding table based on a hypothetical scenario[38] of applying glycoprotein 2 antibodies tests on a cohort of 10000 patients

Analysis	Diagnostic cut-off (U/dL)	TP	(Range)	FP	(Range)	TN	(Range)	FN	(Range)
CD *vs* All symptomatic patients (IgG)	Mixed	9	(6-21)	698		9270		23	(21-26)
	20	7	(5-10)	698	(498-897)	9270	(9071-9470)	25	(22-27)
	15	9	(5-14)	797	(399-1,595)	9171	(8373-9569)	23	(18-27)
CD *vs* UC (IgG)	Mixed	10	(8-12)	698		9270		22	(20-24)
	20	8	(5-11)	698	(399-997)	9270	(8971-9569)	24	(21-27)
	15	9	(5-14)	997	(598-1595)	8971	(8373-9370)	23	(18-27)
CD *vs* All symptomatic patients (IgA)	Mixed	5	(4-6)	299		9669		27	(26-28)
	20	5	(3-8)	399	(100-1396)	9569	(8572-9868)	27	(24-29)
CD *vs* UC (IgA)	Mixed	4	(1-6)	199		9769		28	(26-31)
	20	5	(3-7)	199	(100-399)	9769	(9569-9868)	27	(25-27)
CD *vs* All symptomatic patients (IgA and/or IgG)	Mixed	6	(3-9)	299		9669		26	(20-23)
	20	7	(4-12)	698	(199-1994)	9270	(7974-9769)	25	(20-28)
CD *vs* UC (IgA and/or IgG)	Mixed	6	(1-11)	299		9669		26	(21-31)

Mixed diagnostic cut-off includes all cut-offs used as well as studies with unreported cut-offs. A prevalence of 322 per 100000 results in 32 patients with Crohn's disease in this cohort. FN: False negatives; FP: False positives; TN: True negatives; TP: True positives; UC: Ulcerative colitis; Ig: Immunoglobulin.

reported in individual primary DTA studies, and the gaining residence of the anti-GP2 use in CD diagnosis, the present systematic review and meta-analysis revealed that when the anti-GP2 are used as a proxy for the diagnosis of CD the results should be interpreted with caution, due to its relatively low sensitivity and high specificity.

ARTICLE HIGHLIGHTS

Research background

Non-invasive criteria are needed for Crohn's disease (CD) diagnosis, with several biomarkers being tested, including the pancreatic autoantibodies-to-glycoprotein-2 (anti-GP2).

Research motivation

Results of individual diagnostic test accuracy (DTA) studies assessing the diagnostic value of the anti-GP2 for the diagnosis of CD appear promising, however, a systematic review and meta-analysis of the studies is still lacking.

Research objectives

The aim of the present systematic review and meta-analysis was synthesize all evidence on the diagnostic accuracy of anti-GP2 tests in patients with suspected/confirmed CD.

Research methods

An electronic search was conducted on Medline, Cochrane-CENTRAL and grey literature. Quality was assessed with the Quality Assessment of Diagnostic Accuracy Studies-2 tool and hierarchical models were employed to synthesize the data. The hierarchical summary receiver operating characteristic (HSROC) model was employed to synthesize data. SROC curves were constructed and since a summary point of sensitivity or specificity with studies using mixed thresholds would be clinically uninterpretable, the summary sensitivity was estimated at its median specificity, based on the SROC curves. Heterogeneity was assessed statistically by including covariates in the HSROC model (meta-regression) and was summarized with the Relative Diagnostic Odds Ratios.

Research results

Out of 722 studies retrieved, 15 were meta-analyzed. Thirteen studies had industry-related conflicts-of-interest, and most included healthy donors as controls. For the combination of IgA and/or IgG anti-GP2 test, the summary sensitivity was 20% at a median specificity of 97%.

Research conclusions

The anti-GP2 demonstrated low sensitivity and high specificity. These results indicate caution before relying on its diagnostic value. However, the anti-GP2 appear to attain all characteristics of a screening tool rather than a diagnostic one. Therefore, based on the available evidence, the use of the anti-GP2 for CD diagnosis is not warranted. Furthermore, overall quality of DTA studies appears low, with many carrying industry-related, spectrum, test-review and partial verification bias. Thus, the need for improving the methodology of DTA studies is evident.

Research perspectives

The majority of DTA studies are lacking a quality design and should be synthetized with caution. Future research should assess differences between industry-funded and non-industry funded DTA studies.

ACKNOWLEDGEMENTS

All authors appreciate the critical review provided by Assistant Professors Dr. Anna-Bettina Haidich and Dr. Stavros Kalogiannis, as well as the support offered by our friend and colleague Dr. Meletios P Nigdelis, in lending us his voice for the audio core tip! The present study was presented at the 12th International Congress on Autoimmunity (2020) and the 11th Greek Immunology Congress (2019), both held in Athens, Greece.

REFERENCES

1 **Hoops TC**, Ivanov I, Cui Z, Colomer-Gould V, Rindler MJ. Incorporation of the pancreatic membrane protein GP-2 into secretory granules in exocrine but not endocrine cells. *J Biol Chem* 1993; **268**: 25694-25705 [PMID: 7503984]

2 **Roggenbuck D**, Reinhold D, Werner L, Schierack P, Bogdanos DP, Conrad K. Glycoprotein 2 antibodies in Crohn's disease. *Adv Clin Chem* 2013; **60**: 187-208 [PMID: 23724745 DOI: 10.1016/B978-0-12-407681-5.00006-4]

3 **Conrad K**, Hausdorf G, Feist E, Reinhold D, Jungblut P, Porstmann T, Laass M, Henker J, Roggenbuck D. Identification of GP2 as the major autoantigen of pancreatic autoantibodies. Proceedings of the 6th Congress on Autoimmunity; 2008 Sep 9-13; Porto, Portugal. Immunotherapy, 2008

4 **Hase K**, Kawano K, Nochi T, Pontes GS, Fukuda S, Ebisawa M, Kadokura K, Tobe T, Fujimura Y, Kawano S, Yabashi A, Waguri S, Nakato G, Kimura S, Murakami T, Iimura M, Hamura K, Fukuoka S, Lowe AW, Itoh K, Kiyono H, Ohno H. Uptake through glycoprotein 2 of FimH(+) bacteria by M cells initiates mucosal immune response. *Nature* 2009; **462**: 226-230 [PMID: 19907495 DOI: 10.1038/nature08529]

5 **Terahara K**, Yoshida M, Igarashi O, Nochi T, Pontes GS, Hase K, Ohno H, Kurokawa S, Mejima M, Takayama N, Yuki Y, Lowe AW, Kiyono H. Comprehensive gene expression profiling of Peyer's patch M cells, villous M-like cells, and intestinal epithelial cells. *J Immunol* 2008; **180**: 7840-7846 [PMID: 18523247 DOI: 10.4049/jimmunol.180.12.7840]

6 **Ohno H**, Hase K. Glycoprotein 2 (GP2): grabbing the FimH bacteria into M cells for mucosal immunity. *Gut Microbes* 2010; **1**: 407-410 [PMID: 21468225 DOI: 10.4161/gmic.1.6.14078]

7 **Roggenbuck D**, Reinhold D, Schierack P, Bogdanos DP, Conrad K, Laass MW. Crohn's disease specific pancreatic antibodies: clinical and pathophysiological challenges. *Clin Chem Lab Med* 2014; **52**: 483-494 [PMID: 24231127 DOI: 10.1515/cclm-2013-0801]

8 **Stange EF**, Travis SP, Vermeire S, Beglinger C, Kupcinkas L, Geboes K, Barakauskiene A, Villanacci V, Von Herbay A, Warren BF, Gasche C, Tilg H, Schreiber SW, Schölmerich J, Reinisch W; European Crohn's and Colitis Organisation. European evidence based consensus on the diagnosis and management of Crohn's disease: definitions and diagnosis. *Gut* 2006; **55** Suppl 1: i1-15 [PMID: 16481628 DOI: 10.1136/gut.2005.081950a]

9 **IBD Working Group of the European Society for Paediatric Gastroenterology, Hepatology and Nutrition**. Inflammatory bowel disease in children and adolescents: recommendations for diagnosis--the Porto criteria. *J Pediatr Gastroenterol Nutr* 2005; **41**: 1-7 [PMID: 15990620 DOI: 10.1097/01.MPG.0000163736.30261.82]

10 **Marlicz W**, Skonieczna-Żydecka K, Dabos KJ, Łoniewski I, Koulaouzidis A. Emerging concepts in non-invasive monitoring of Crohn's disease. *Therap Adv Gastroenterol* 2018; **11**: 1756284818769076 [PMID: 29707039 DOI: 10.1177/1756284818769076]

11 **Castiglione F**, Mainenti PP, De Palma GD, Testa A, Bucci L, Pesce G, Camera L, Diaferia M, Rea M, Caporaso N, Salvatore M, Rispo A. Noninvasive diagnosis of small bowel Crohn's disease: direct comparison of bowel sonography and magnetic resonance enterography. *Inflamm Bowel Dis* 2013; **19**: 991-998 [PMID: 23429465 DOI: 10.1097/MIB.0b013e3182802b87]

12 **Bianchi MT**, Alexander BM. Evidence based diagnosis: does the language reflect the theory? *BMJ* 2006; **333**: 442-445 [PMID: 16931846 DOI: 10.1136/bmj.38915.558738.55]

13 **Kim KW**, Lee J, Choi SH, Huh J, Park SH. Systematic Review and Meta-Analysis of Studies Evaluating Diagnostic Test Accuracy: A Practical Review for Clinical Researchers-Part I. General Guidance and Tips. *Korean J Radiol* 2015; **16**: 1175-1187 [PMID: 26576106 DOI: 10.3348/kjr.2015.16.6.1175]

14 **Deng C**, Li W, Li J, Zhang S, Li Y. Diagnostic value of the antiglycoprotein-2 antibody for Crohn's disease: a PRISMA-compliant systematic review and meta-analysis. *BMJ Open* 2017; **7**: e014843 [PMID: 28601823 DOI: 10.1136/bmjopen-2016-014843]

15 **Leeflang MM**, Deeks JJ, Gatsonis C, Bossuyt PM; Cochrane Diagnostic Test Accuracy Working Group. Systematic reviews of diagnostic test accuracy. *Ann Intern Med* 2008; **149**: 889-897 [PMID: 19075208 DOI: 10.7326/0003-4819-149-12-200812160-00008]

16 **Rutjes AW**, Reitsma JB, Di Nisio M, Smidt N, van Rijn JC, Bossuyt PM. Evidence of bias and variation in diagnostic accuracy studies. *CMAJ* 2006; **174**: 469-476 [PMID: 16477057 DOI: 10.1503/cmaj.050090]

17 **Lijmer JG**, Mol BW, Heisterkamp S, Bonsel GJ, Prins MH, van der Meulen JH, Bossuyt PM. Empirical evidence of design-related bias in studies of diagnostic tests. *JAMA* 1999; **282**: 1061-1066 [PMID: 10493205 DOI: 10.1001/jama.282.11.1061]

18 **Bae JM**. An overview of systematic reviews of diagnostic tests accuracy. *Epidemiol Health* 2014; **36**: e2014016 [PMID: 25209601 DOI: 10.4178/epih/e2014016]

19 **McGrath TA**, Alabousi M, Skidmore B, Korevaar DA, Bossuyt PMM, Moher D, Thombs B, McInnes MDF. Recommendations for reporting of systematic reviews and meta-analyses of diagnostic test accuracy: a systematic review. *Syst Rev* 2017; **6**: 194 [PMID: 29017574 DOI: 10.1186/s13643-017-0590-8]

20 **McInnes MDF**, Moher D, Thombs BD, McGrath TA, Bossuyt PM; and the PRISMA-DTA Group, Clifford T, Cohen JF, Deeks JJ, Gatsonis C, Hooft L, Hunt HA, Hyde CJ, Korevaar DA, Leeflang MMG, Macaskill P, Reitsma JB, Rodin R, Rutjes AWS, Salameh JP, Stevens A, Takwoingi Y, Tonelli M, Weeks L, Whiting P, Willis BH. Preferred Reporting Items for a Systematic Review and Meta-analysis of Diagnostic Test Accuracy Studies: The PRISMA-DTA Statement. *JAMA* 2018; **319**: 388-396 [PMID: 29362800 DOI: 10.1001/jama.2017.19163]

21 **Hanauer SB**. Inflammatory bowel disease. *N Engl J Med* 1996; **334**: 841-848 [PMID: 8596552 DOI: 10.1056/NEJM199603283341307]

22 **Harbord M**, Annese V, Vavricka SR, Allez M, Barreiro-de Acosta M, Boberg KM, Burisch J, De Vos M, De Vries AM, Dick AD, Juillerat P, Karlsen TH, Koutroubakis I, Lakatos PL, Orchard T, Papay P, Raine T, Reinshagen M, Thaci D, Tilg H, Carbonnel F; European Crohn's and Colitis Organisation. The First European Evidence-based Consensus on Extra-intestinal Manifestations in Inflammatory Bowel Disease. *J Crohns Colitis* 2016; **10**: 239-254 [PMID: 26614685 DOI: 10.1093/ecco-jcc/jjv213]

23 **Dignass A**, Van Assche G, Lindsay JO, Lémann M, Söderholm J, Colombel JF, Danese S, D'Hoore A, Gassull M, Gomollón F, Hommes DW, Michetti P, O'Morain C, Oresland T, Windsor A, Stange EF, Travis SP; European Crohn's and Colitis Organisation (ECCO). The second European evidence-based Consensus on the diagnosis and management of Crohn's disease: Current management. *J Crohns Colitis* 2010; **4**: 28-62 [PMID: 21122489 DOI: 10.1016/j.crohns.2009.12.002]

24 **Lennard-Jones JE**. Classification of inflammatory bowel disease. *Scand J Gastroenterol Suppl* 1989; **170**: 2-6; discussion 16-9 [PMID: 2617184 DOI: 10.3109/00365528909091339]

25 **Levine A**, Koletzko S, Turner D, Escher JC, Cucchiara S, de Ridder L, Kolho KL, Veres G, Russell RK, Paerregaard A, Buderus S, Greer ML, Dias JA, Veereman-Wauters G, Lionetti P, Sladek M, Martin de Carpi J, Staiano A, Ruemmele FM, Wilson DC; European Society of Pediatric Gastroenterology, Hepatology, and Nutrition. ESPGHAN revised porto criteria for the diagnosis of inflammatory bowel disease in children and adolescents. *J Pediatr Gastroenterol Nutr* 2014; **58**: 795-806 [PMID: 24231644 DOI: 10.1097/MPG.0000000000000239]

26 **Taylor KS**, Verbakel JY, Feakins BG, Price CP, Perera R, Bankhead C, Plüddemann A. Diagnostic accuracy of point-of-care natriuretic peptide testing for chronic heart failure in ambulatory care: systematic review and meta-analysis. *BMJ* 2018; **361**: k1450 [PMID: 29785952 DOI: 10.1136/bmj.k1450]

27 **Glas AS**, Lijmer JG, Prins MH, Bonsel GJ, Bossuyt PM. The diagnostic odds ratio: a single indicator of test performance. *J Clin Epidemiol* 2003; **56**: 1129-1135 [PMID: 14615004 DOI: 10.1016/s0895-4356(03)00177-x]

28 **Devillé WL**, Buntinx F, Bouter LM, Montori VM, de Vet HC, van der Windt DA, Bezemer PD. Conducting systematic reviews of diagnostic studies: didactic guidelines. *BMC Med Res Methodol* 2002; **2**: 9 [PMID: 12097142 DOI: 10.1186/1471-2288-2-9]

29 **The Joanna Briggs Institute**. The Joanna Briggs Institute Reviewersâ Manual 2015: The systematic review of studies of diagnostic test accuracy. The Joanna Briggs Institute. 2015; **1**: 46

30 **Taylor KS**. Tip for data extraction in meta-analysis - 1 - Center for Evidence Based Medicine. 2019 Feb 11 [cited 17 March 2019]. Oxford University [Internet]. Available from: https://www.cebm.net/2019/02/tip-for-data-extraction-in-meta-analysis-1/

31 **Whiting PF**, Rutjes AW, Westwood ME, Mallett S, Deeks JJ, Reitsma JB, Leeflang MM, Sterne JA, Bossuyt PM; QUADAS-2 Group. QUADAS-2: a revised tool for the quality assessment of diagnostic accuracy studies. *Ann Intern Med* 2011; **155**: 529-536 [PMID: 22007046 DOI: 10.7326/0003-4819-155-8-201110180-00009]

32 **Dukic V**, Gatsonis C. Meta-analysis of diagnostic test accuracy assessment studies with varying number of thresholds. *Biometrics* 2003; **59**: 936-946 [PMID: 14969472 DOI: 10.1111/j.0006-341X.2003.00108.x]

33 **Takwoingi Y**, Riley RD, Deeks JJ. Meta-analysis of diagnostic accuracy studies in mental health. *Evid Based Ment Health* 2015; **18**: 103-109 [PMID: 26446042 DOI: 10.1136/eb-2015-102228]

34 **Rutter CM**, Gatsonis CA. A hierarchical regression approach to meta-analysis of diagnostic test accuracy evaluations. *Stat Med* 2001; **20**: 2865-2884 [PMID: 11568945 DOI: 10.1002/sim.942]

35 **Macaskill P**. Gatsonis C, Deeks J, Harbord R, Takwoingi Y. Analysing and Presenting Results: Cochrane Handbook for Systematic Reviews of Diagnostic Test Accuracy. Version 1.0. The Cochrane Collaboration, 2010

36 **Takwoingi Y**, Guo B, Riley RD, Deeks JJ. Performance of methods for meta-analysis of diagnostic test accuracy with few studies or sparse data. *Stat Methods Med Res* 2017; **26**: 1896-1911 [PMID: 26116616 DOI: 10.1177/0962280215592269]

37 **Buczinski S**, Gicquel E, Fecteau G, Takwoingi Y, Chigerwe M, Vandeweerd JM. Systematic Review and Meta-Analysis of Diagnostic Accuracy of Serum Refractometry and Brix Refractometry for the Diagnosis of Inadequate Transfer of Passive Immunity in Calves. *J Vet Intern Med* 2018; **32**: 474-483 [PMID: 29210105 DOI: 10.1111/jvim.14893]

38 **Ng SC**, Shi HY, Hamidi N, Underwood FE, Tang W, Benchimol EI, Panaccione R, Ghosh S, Wu JCY, Chan FKL, Sung JJY, Kaplan GG. Worldwide incidence and prevalence of inflammatory bowel disease in the 21st century: a systematic review of population-based studies. *Lancet* 2018; **390**: 2769-2778 [PMID: 29050646 DOI: 10.1016/S0140-6736(17)32448-0]

39 **Takwoingi Y**, Deeks J. MetaDAS: A SAS macro for meta-analysis of diagnostic accuracy studies: User guide, Version 1.3. 30 July 2010. Available from: URL: http://srdta.cochrane.org/ Cited 17 March 2019

40 **The Nordic Cochrane Centre**. Review Manager; 2014. Cochrane Collab. 2014

41 **Bogdanos DP**, Roggenbuck D, Reinhold D, Wex T, Pavlidis P, von Arnim U, Malfertheiner P, Forbes A, Conrad K, Laass MW. Pancreatic-specific autoantibodies to glycoprotein 2 mirror disease location and behaviour in younger patients with Crohn's disease. *BMC Gastroenterol* 2012; **12**: 102 [PMID: 22866900

DOI: 10.1186/1471-230X-12-102]
42 **Bonaci-Nikolic B**, Spuran M, Andrejevic S, Nikolic M. Autoantibodies to GP2, the major zymogen granule membrane glycoprotein, in patients with gluten-sensitive enteropathy: a possible serological trap. *Clin Chim Acta* 2012; **413**: 822-823 [PMID: 22269156 DOI: 10.1016/j.cca.2012.01.005]
43 **Caneparo V**, Pastorelli L, Pisani LF, Bruni B, Prodam F, Boldorini R, Roggenbuck D, Vecchi M, Landolfo S, Gariglio M, De Andrea M. Distinct Anti-IFI16 and Anti-GP2 Antibodies in Inflammatory Bowel Disease and Their Variation with Infliximab Therapy. *Inflamm Bowel Dis* 2016; **22**: 2977-2987 [PMID: 27636380 DOI: 10.1097/MIB.0000000000000926]
44 **Cummings D**, Cruise M, Lopez R, Roggenbuck D, Jairath V, Wang Y, Shen B, Rieder F. Loss of tolerance to glycoprotein 2 isoforms 1 and 4 is associated with Crohn's disease of the pouch. *Aliment Pharmacol Ther* 2018; **48**: 1251-1259 [PMID: 30411391 DOI: 10.1111/apt.15034]
45 **Degenhardt F**, Dirmeier A, Lopez R, Lang S, Kunst C, Roggenbuck D, Reinhold D, Szymczak S, Rogler G, Klebl F, Franke A, Rieder F. Serologic Anti-GP2 Antibodies Are Associated with Genetic Polymorphisms, Fibrostenosis, and Need for Surgical Resection in Crohn's Disease. *Inflamm Bowel Dis* 2016; **22**: 2648-2657 [PMID: 27753692 DOI: 10.1097/MIB.0000000000000936]
46 **Gross S**, Bakker SF, van Bodegraven AA, van Hoogstraten IM, Gelderman KA, Bouma G, Mulder CJ, von Blomberg BM, Bontkes HJ. Increased IgA glycoprotein-2 specific antibody titres in refractory celiac disease. *J Gastrointestin Liver Dis* 2014; **23**: 127-133 [PMID: 24949603 DOI: 10.15403/jgld.2014.1121.232.sg1]
47 **Michaels MA**, Jendrek ST, Korf T, Nitzsche T, Teegen B, Komorowski L, Derer S, Schröder T, Baer F, Lehnert H, Büning J, Fellerman K, Sina C. Pancreatic Autoantibodies Against CUZD1 and GP2 Are Associated with Distinct Clinical Phenotypes of Crohn's Disease. *Inflamm Bowel Dis* 2015; **21**: 2864-2872 [PMID: 26273818 DOI: 10.1097/MIB.0000000000000564]
48 **Op De Beéck K**, Vermeire S, Rutgeerts P, Bossuyt X. Antibodies to GP2, the major zymogen granule membrane glycoprotein, in inflammatory bowel diseases. *Gut* 2012; **61**: 162-164; author reply 164-5 [PMID: 21193445 DOI: 10.1136/gut.2010.233148]
49 **Papp M**, Sipeki N, Tornai T, Altorjay I, Norman GL, Shums Z, Roggenbuck D, Fechner K, Stöcker W, Antal-Szalmas P, Veres G, Lakatos PL. Rediscovery of the Anti-Pancreatic Antibodies and Evaluation of their Prognostic Value in a Prospective Clinical Cohort of Crohn's Patients: The Importance of Specific Target Antigens [GP2 and CUZD1]. *J Crohns Colitis* 2015; **9**: 659-668 [PMID: 25968583 DOI: 10.1093/ecco-jcc/jjv087]
50 **Pavlidis P**, Romanidou O, Roggenbuck D, Mytilinaiou MG, Al-Sulttan F, Liaskos C, Smyk DS, Koutsoumpas AL, Rigopoulou EI, Conrad K, Forbes A, Bogdanos DP. Ileal inflammation may trigger the development of GP2-specific pancreatic autoantibodies in patients with Crohn's disease. *Clin Dev Immunol* 2012; **2012**: 640835 [PMID: 23118780 DOI: 10.1155/2012/640835]
51 **Pavlidis P**, Shums Z, Koutsoumpas AL, Milo J, Papp M, Umemura T, Lakatos PL, Smyk DS, Bogdanos DP, Forbes A, Norman GL. Diagnostic and clinical significance of Crohn's disease-specific anti-MZGP2 pancreatic antibodies by a novel ELISA. *Clin Chim Acta* 2015; **441**: 176-181 [PMID: 25512163 DOI: 10.1016/j.cca.2014.12.010]
52 **Pavlidis P**, Komorowski L, Teegen B, Liaskos C, Koutsoumpas AL, Smyk DS, Perricone C, Mytilinaiou MG, Stocker W, Forbes A, Bogdanos DP. Diagnostic and clinical significance of Crohn's disease-specific pancreatic anti-GP2 and anti-CUZD1 antibodies. *Clin Chem Lab Med* 2016; **54**: 249-256 [PMID: 26351932 DOI: 10.1515/cclm-2015-0376]
53 **Röber N**, Noß L, Goihl A, Reinhold D, Jahn J, de Laffolie J, Johannes W, Flemming GM, Roggenbuck D, Conrad K, Laass MW. Autoantibodies Against Glycoprotein 2 Isoforms in Pediatric Patients with Inflammatory Bowel Disease. *Inflamm Bowel Dis* 2017; **23**: 1624-1636 [PMID: 28691939 DOI: 10.1097/MIB.0000000000001159]
54 **Roggenbuck D**, Reinhold D, Wex T, Goihl A, von Arnim U, Malfertheiner P, Büttner T, Porstmann T, Porstmann S, Liedvogel B, Bogdanos DP, Laass MW, Conrad K. Autoantibodies to GP2, the major zymogen granule membrane glycoprotein, are new markers in Crohn's disease. *Clin Chim Acta* 2011; **412**: 718-724 [PMID: 21195704 DOI: 10.1016/j.cca.2010.12.029]
55 **Roggenbuck D**, Hausdorf G, Martinez-Gamboa L, Reinhold D, Büttner T, Jungblut PR, Porstmann T, Laass MW, Henker J, Büning C, Feist E, Conrad K. Identification of GP2, the major zymogen granule membrane glycoprotein, as the autoantigen of pancreatic antibodies in Crohn's disease. *Gut* 2009; **58**: 1620-1628 [PMID: 19549613 DOI: 10.1136/gut.2008.162495]
56 **Roggenbuck D**, Vermeire S, Hoffman I, Reinhold D, Schierack P, Goihl A, von Arnim U, De Hertogh G, Polymeros D, Bogdanos DP, Bossuyt X. Evidence of Crohn's disease-related anti-glycoprotein 2 antibodies in patients with celiac disease. *Clin Chem Lab Med* 2015; **53**: 1349-1357 [PMID: 25411995 DOI: 10.1515/cclm-2014-0238]
57 **Zhang S**, Wu Z, Luo J, Ding X, Hu C, Li P, Deng C, Zhang F, Qian J, Li Y. Diagnostic Potential of Zymogen Granule Glycoprotein 2 Antibodies as Serologic Biomarkers in Chinese Patients With Crohn Disease. *Medicine (Baltimore)* 2015; **94**: e1654 [PMID: 26496271 DOI: 10.1097/MD.0000000000001654]
58 **Zhang S**, Luo J, Wu Z, Roggenbuck D, Schierack P, Reinhold D, Li J, Zeng X, Zhang F, Qian J, Li Y. Antibodies against glycoprotein 2 display diagnostic advantages over ASCA in distinguishing CD from intestinal tuberculosis and intestinal Behçet's disease. *Clin Transl Gastroenterol* 2018; **9**: e133 [PMID: 29446764 DOI: 10.1038/ctg.2018.1]
59 **Joossens S**, Vermeire S, Van Steen K, Godefridis G, Claessens G, Pierik M, Vlietinck R, Aerts R, Rutgeerts P, Bossuyt X. Pancreatic autoantibodies in inflammatory bowel disease. *Inflamm Bowel Dis* 2004; **10**: 771-777 [PMID: 15626896 DOI: 10.1097/00054725-200411000-00012]
60 **Stafylidou M**, Paschos P, Katsoula A, Malandris K, Ioakim K, Bekiari E, Haidich AB, Akriviadis E, Tsapas A. Performance of Baveno VI and Expanded Baveno VI Criteria for Excluding High-Risk Varices in Patients With Chronic Liver Diseases: A Systematic Review and Meta-analysis. *Clin Gastroenterol Hepatol* 2019; **17**: 1744-1755.e11 [PMID: 31077823 DOI: 10.1016/j.cgh.2019.04.062]
61 **Lalkhen AG**, McCluskey A. Clinical tests: sensitivity and specificity. *Contin Educ Anaesth Crit Care Pain* 2008; **8**: 221-223 [DOI: 10.1093/bjaceaccp/mkn041]
62 **Power M**, Fell G, Wright M. Principles for high-quality, high-value testing. *Evid Based Med* 2013; **18**: 5-10 [PMID: 22740357 DOI: 10.1136/eb-2012-100645]
63 **Trevethan R**. Sensitivity, Specificity, and Predictive Values: Foundations, Pliabilities, and Pitfalls in Research and Practice. *Front Public Health* 2017; **5**: 307 [PMID: 29209603 DOI: 10.3389/fpubh.2017.00307]
64 **Fukuoka S**. Molecular cloning and sequences of cDNAs encoding alpha (large) and beta (small) isoforms

of human pancreatic zymogen granule membrane-associated protein GP2. *Biochim Biophys Acta* 2000; **1491**: 376-380 [PMID: 10760606 DOI: 10.1016/s0167-4781(00)00057-9]

65 **Schmidt RL**, Factor RE. Understanding sources of bias in diagnostic accuracy studies. *Arch Pathol Lab Med* 2013; **137**: 558-565 [PMID: 23544945 DOI: 10.5858/arpa.2012-0198-RA]

66 **Al Fattani AG**, Aljoudi A. Sources of bias in diagnostic accuracy studies. *J Appl Hematol* 2015; **6**: 178 [DOI: 10.4103/1658-5127.171991]

67 **Nature journals tighten rules on non-financial conflicts**. *Nature* 2018; **554**: 6 [PMID: 29388964 DOI: 10.1038/d41586-018-01420-8]

68 **Tulleken C van**. Overdiagnosis and industry influence: how cow's milk protein allergy is extending the reach of infant formula manufacturers. *BMJ* 2018; **363**: k5056 [DOI: 10.1136/bmj.k5056]

69 **Mintzes B**, Swandari S, Fabbri A, Grundy Q, Moynihan R, Bero L. Does industry-sponsored education foster overdiagnosis and overtreatment of depression, osteoporosis and over-active bladder syndrome? An Australian cohort study. *BMJ Open* 2018; **8**: e019027 [PMID: 29440213 DOI: 10.1136/bmjopen-2017-019027]

70 **Dakubo GD**. Cancer biomarkers in body fluids: principles. Ontario, Canada: Springer Nature; 2016; [DOI: 10.1007/978-3-319-01580-4]

71 **Thunnissen E**. How to Validate Predictive Immunohistochemistry Testing in Pathology? A Practical Approach Exploiting the Heterogeneity of Programmed Death Ligand-1 Present in Non-Small Cell Lung Cancer. *Arch Pathol Lab Med* 2019; **143**: 11-12 [PMID: 30307747 DOI: 10.5858/arpa.2018-0410-ED]

72 **Fitzgibbons PL**, Bradley LA, Fatheree LA, Alsabeh R, Fulton RS, Goldsmith JD, Haas TS, Karabakhtsian RG, Loykasek PA, Marolt MJ, Shen SS, Smith AT, Swanson PE; College of American Pathologists Pathology and Laboratory Quality Center. Principles of analytic validation of immunohistochemical assays: Guideline from the College of American Pathologists Pathology and Laboratory Quality Center. *Arch Pathol Lab Med* 2014; **138**: 1432-1443 [PMID: 24646069 DOI: 10.5858/arpa.2013-0610-CP]

73 **Magro F**, Lopes J, Borralho P, Lopes S, Coelho R, Cotter J, Castro FD, Sousa HT, Salgado M, Andrade P, Vieira AI, Figueiredo P, Caldeira P, Sousa A, Duarte MA, Ávila F, Silva J, Moleiro J, Mendes S, Giestas S, Ministro P, Sousa P, Gonçalves R, Gonçalves B, Oliveira A, Rosa I, Rodrigues M, Chagas C, Dias CC, Afonso J, Geboes K, Carneiro F; Portuguese IBD Study Group (GEDII). Comparison of different histological indexes in the assessment of UC activity and their accuracy regarding endoscopic outcomes and faecal calprotectin levels. *Gut* 2019; **68**: 594-603 [PMID: 29437913 DOI: 10.1136/gutjnl-2017-315545]

74 **Frykman PK**, Patel DC, Kim S, Cheng Z, Wester T, Nordenskjöld A, Kawaguchi A, Hui TT, Ehrlich PF, Granström AL, Benliyan F; HAEC Collaborative Research Group (HCRG). Inflammatory Bowel Disease Serological Immune Markers Anti-Saccharomyces cerevisiae Mannan Antibodies and Outer Membrane Porin C are Potential Biomarkers for Hirschsprung-associated Enterocolitis. *J Pediatr Gastroenterol Nutr* 2019; **69**: 176-181 [PMID: 30964819 DOI: 10.1097/MPG.0000000000002358]

75 **Freeman K**, Willis BH, Fraser H, Taylor-Phillips S, Clarke A. Faecal calprotectin to detect inflammatory bowel disease: a systematic review and exploratory meta-analysis of test accuracy. *BMJ Open* 2019; **9**: e027428 [PMID: 30852550 DOI: 10.1136/bmjopen-2018-027428]

76 **Jellema P**, van der Windt DA, Bruinvels DJ, Mallen CD, van Weyenberg SJ, Mulder CJ, de Vet HC. Value of symptoms and additional diagnostic tests for colorectal cancer in primary care: systematic review and meta-analysis. *BMJ* 2010; **340**: c1269 [PMID: 20360221 DOI: 10.1136/bmj.c1269]

77 **Cole SR**, Smith A, Wilson C, Turnbull D, Esterman A, Young GP. An advance notification letter increases participation in colorectal cancer screening. *J Med Screen* 2007; **14**: 73-75 [PMID: 17626705 DOI: 10.1258/096914107781261927]

78 **Gomollón F**, Dignass A, Annese V, Tilg H, Van Assche G, Lindsay JO, Peyrin-Biroulet L, Cullen GJ, Daperno M, Kucharzik T, Rieder F, Almer S, Armuzzi A, Harbord M, Langhorst J, Sans M, Chowers Y, Fiorino G, Juillerat P, Mantzaris GJ, Rizzello F, Vavricka S, Gionchetti P; ECCO. 3rd European Evidence-based Consensus on the Diagnosis and Management of Crohn's Disease 2016: Part 1: Diagnosis and Medical Management. *J Crohns Colitis* 2017; **11**: 3-25 [PMID: 27660341 DOI: 10.1093/ecco-jcc/jjw168]

79 **Kedia S**, Das P, Madhusudhan KS, Dattagupta S, Sharma R, Sahni P, Makharia G, Ahuja V. Differentiating Crohn's disease from intestinal tuberculosis. *World J Gastroenterol* 2019; **25**: 418-432 [PMID: 30700939 DOI: 10.3748/wjg.v25.i4.418]

80 **Zhang TY**, Lin Y, Fan R, Hu SR, Cheng MM, Zhang MC, Hong LW, Zhou XL, Wang ZT, Zhong J. Potential model for differential diagnosis between Crohn's disease and primary intestinal lymphoma. *World J Gastroenterol* 2016; **22**: 9411-9418 [PMID: 27895429 DOI: 10.3748/wjg.v22.i42.9411]

81 **Silverberg MS**, Satsangi J, Ahmad T, Arnott ID, Bernstein CN, Brant SR, Caprilli R, Colombel JF, Gasche C, Geboes K, Jewell DP, Karban A, Loftus EV, Peña AS, Riddell RH, Sachar DB, Schreiber S, Steinhart AH, Targan SR, Vermeire S, Warren BF. Toward an integrated clinical, molecular and serological classification of inflammatory bowel disease: report of a Working Party of the 2005 Montreal World Congress of Gastroenterology. *Can J Gastroenterol* 2005; **19** Suppl A: 5A-36A [PMID: 16151544 DOI: 10.1155/2005/269076]

82 **Levine A**, Griffiths A, Markowitz J, Wilson DC, Turner D, Russell RK, Fell J, Ruemmele FM, Walters T, Sherlock M, Dubinsky M, Hyams JS. Pediatric modification of the Montreal classification for inflammatory bowel disease: the Paris classification. *Inflamm Bowel Dis* 2011; **17**: 1314-1321 [PMID: 21560194 DOI: 10.1002/ibd.21493]

83 **Komorowski L**, Teegen B, Probst C, Aulinger-Stöcker K, Sina C, Fellermann K, Stöcker W. Autoantibodies against exocrine pancreas in Crohn's disease are directed against two antigens: the glycoproteins CUZD1 and GP2. *J Crohns Colitis* 2013; **7**: 780-790 [PMID: 23140841 DOI: 10.1016/j.crohns.2012.10.011]

Published By Baishideng Publishing Group Inc
7041 Koll Center Parkway, Suite 160, Pleasanton, CA 94566, USA
Telephone: +1-925-3991568
E-mail: bpgoffice@wjgnet.com
Help Desk:http://www.f6publishing.com/helpdesk
http://www.wjgnet.com